



***Concentration and derivatization in silicone rubber
traps for mass spectrometric and gas chromatographic
analysis of air and water pollutants***

BY

MARIA JOSÉ FERNANDES-WHALEY

Submitted in partial fulfilment of the requirements for the degree

Doctor of Philosophy

Chemistry

in the Faculty of Natural and Agricultural Science

University of Pretoria

Pretoria

February 2008

***Concentration and derivatization in silicone rubber traps for
mass spectrometric and gas chromatographic analysis of air and
water pollutants***

BY

MARIA JOSÉ FERNANDES-WHALEY

Submitted in partial fulfilment of the requirements for the degree

***Doctor of Philosophy
Chemistry***

in the Faculty of Natural and Agricultural Science
University of Pretoria
Pretoria
South Africa

SUMMARY

Estrogens, alkylphenols and bisphenol-A, enter the environment through waste water systems and waste disposal of manufactured products e.g. detergents, paints, polycarbonates and flame-retardants. These analytes disrupt the endocrine function of living organisms affecting their reproductive health and those of future generations. Gas phase low molecular- mass aldehydes and amines are typically eye, nose, and throat irritants. Formaldehyde is classified as a probable human carcinogen. Given their negative impact on human health it is urgent to monitor pollutants at extremely low levels in both air and water. The aqueous pollutants are often concentrated using solid phase extraction cartridges or liquid-liquid extraction followed by derivatization. Methods that can most effectively and selectively pre-concentrate aldehydes and amines involve *in situ*

derivatization. Unfortunately, the derivatizing reagents as well as their associated solvents or adsorbents, are responsible for problems encountered with these methods.

Polydimethylsiloxane (PDMS) has emerged as the ideal concentration and reaction medium for trace analysis. However the expensive commercial devices such as SPME and SBSE both require the samples to be returned to the laboratory for concentration. Due to the open tubular nature of the PDMS multichannel trap (MCT), developed in our laboratory, it is ideally suited for on-site and on-line sampling. The MCTs have a high analyte capacity owing to the large volume of PDMS available for concentration. The derivatization reaction can be performed *in situ* providing a “one-pot concentration and reaction device”. This allows for reduced risk of contamination of / or losses of the sample and a sampling method that can cater for both air and water samples.

To demonstrate the versatility of the PDMS MCT, two approaches for concentration in PDMS were investigated in this study, namely, 1) the on-line concentration and *in situ* derivatization of volatile polar analytes from air followed by REMPI-TOFMS detection, and 2) the concentration of phenolic lipophilic analytes from water requiring derivatization prior to analysis by GC/MS.

1) Analyte and derivatizing reagent were simultaneously introduced into the PDMS trap using a y-press-fit connector. The reaction occurs *in situ* followed by thermal desorption using a thermal modulator array alone or in conjunction with a thermal desorption unit. The aldehydes and amine derivatives were successfully detected by the REMPI-TOFMS. Reaction efficiencies were determined at room temperature without catalysts. Formaldehyde yielded a low reaction/concentration efficiency of 41 % with phenylhydrazine in PDMS, while acetaldehyde, acrolein and crotonal displayed much improved values of 92, 61 and 74 % respectively. Both propylamine and butylamine yielded 28 % reaction/concentration efficiency with benzaldehyde in the PDMS matrix. Detection limits obtained with this technique were significantly lower than the permissible exposure limits set by the Occupational Safety and Health Administration. It should be noted that the detection limits were not determined by actual measurement but by extrapolation from a larger signal.

2) Aqueous analytes were concentrated in the PDMS MCT using a gravity flow rate of ~50 $\mu\text{l}/\text{min}$. The trap was dried and 5 μl derivatizing reagent added. At room temperature and without the presence of a catalyst, the reaction of alkylphenols with trifluoroacetic acid anhydride in the PDMS matrix was 100% complete after 5 minutes. Bisphenol-A reacted less than 50 % to completion



during this period, but the amount of derivative formed remained constant. This study revealed that extraction efficiencies of the alkylphenols and bisphenol-A off the PDMS trap have poor batch-to-batch repeatability indicating that the PDMS matrix was not homogenous. For two different PDMS batches: *tert*-octylphenol displayed an extraction efficiency of 70 and 79%, nonylphenol displayed 84 and 43% while Bisphenol-A displayed 10 and 26% respectively. The thermally desorbed derivatives were analysed by GC/MS. Despite background contamination in the desorption unit, detection limits were at the ppt level. Detection limits were not determined by actual measurement but by extrapolation from a larger signal.

Real samples were also tested.

Keywords: air pollutants, water pollutants, concentration, *in situ* derivatization, polydimethylsiloxane, PDMS, multichannel traps, thermal desorption, gas chromatography, mass spectrometry, resonance enhanced time-of-flight mass spectrometry.

***Konsentrering en derivatisering in silikoonrubbervalle vir
massaspektrometriese en gaschromatografiese analise van lug-
en waterbesoedelstowwe***

DEUR

MARIA JOSÉ FERNANDES-WHALEY

Voorgelê ter vervulling van 'n gedeelte van die vereiste vir die graad PhD, Chemie
in die Fakulteit Natuur- & Landbouwetenskappe
Universiteit van Pretoria
Pretoria
Suid-Afrika

SAMEVATTING

Estrogene, soos alkielfenole en bisfenol-A, beland in die omgewing deur afvalwatersisteme en die wegdoening van vervaardigde produkte soos wasmiddels, verf, polikarbonate en vlamvertragers. Hierdie analiete ontwig die endokrienfunksie van lewende organismes, en affekteer hul eie voortplantingsgesondheid sowel as dié van hul toekomstige geslagte. Gasfase laemolekulêremassa aldehiede en amiene is tipies oog-, neus- en keel-irritanse. Formaldehyd is geklassifiseer as 'n waaarskynlike menslike karsinogeen. In die lig van hul negatiewe impak op menslike gesondheid is dit dringend noodsaaklik om hierdie besoedelstowwe te moniteer by uiters lae konsentrasies in beide lug en water. Besoedelstowwe in water word dikwels gekonsentreer met soliedefase-ekstraksiepatrone gevolg deur derivatisering. Metodes wat aldehiede en amiene doeltreffend vooraf konsentreer, behels *in situ* derivatisering. Ongelukkig is die derivatiseringsreagense sowel as hul oplosmiddels of adsorbente verantwoordelik vir probleme met hierdie metodes.

Polidimetielsiloksaan (PDMS, silikoon) het ontluik as die ideale konsentrerings- en reaksiedium vir spooranalise. Die duur kommersiële toestelle soos SPME (soliedefase-mikroekstraksie) en SBSE (magnetieseroerder-ekstraksie) vereis egter dat die monsters na die laboratorium gestuur moet word vir konsentrering. As gevolg van die oopbuis geaardheid van die PDMS multikanaalval

(MKV) wat in ons laboratorium ontwikkel is, is dit ideaal geskik vir ter plaatse- en aanlynmonstering. Die MKV's het 'n groot kapasiteit vir analiese as gevolg van die groot volume PDMS beskikbaar vir konsentring. Die derivatiseringsreaksie kan binne-in die val uitgevoer word, wat 'n “eenpot konsentring- en reaksietoestel” tot gevolg het. Dit lei tot 'n verminderde risiko van kontaminasie en/of verlies van die monster, en 'n monsteringsmetode wat geskik is vir beide water- sowel as lugmonsters.

Om die veelsydigheid van die PDMS multikanaalval te demonstreer is twee prosedures ondersoek om stowwe in PDMS te konsentreer, naamlik: 1) aanlyn konsentring en *in situ* derivatisering van vlugtige polêre analiese uit lug, gevolg deur REMPI-TOFMS (resonansversterkte multifotonionisasie - vlugtydmassaspektrometrie) deteksie, en 2) die konsentring van fenoliese lipofiliese analiese uit water, met derivatisering voor analiese met GC-MS (gaschromatografie – massaspektrometrie).

- 1) Analiese en derivatiseringsreagens is tegelykertyd gevoer in 'n PDMS-val met 'n Y-koppelstuk. Die reaksie vind *in situ* plaas, gevolg deur termiese desorpsie met 'n termiese modulatoropstelling alleen, of saam met 'n termiese desorpsie-eenheid. Die aldehiede en amienderivate is suksesvol aangedui met 'n REMPI-TOFMS. Reaksiedoeltreffendhede is bepaal by kamertemperatuur sonder katalisator. Formaldehid het ondoeltreffend gereageer en gekonsentreer (41%) met fenielhidrasien in PDMS, terwyl asetaldehid, akroleien en krotonal baie beter waardes gegee het, nl. 92%, 61% en 74% respektiewelik. Beide propielamien en butielamien het 'n doeltreffendheid van 28% gehad met bensaldehid in die PDMS-matrys. Deteksielimiëte met hierdie tegniek was aansienlik laer as die toelaatbare blootstellingslimiëte van die Beroepsveiligheids- en Gesondheidsadministrasie.
- 2) Waterige analiese is in die PDMS gekonsentreer met 'n swaartekragvloeiempo van ongeveer 50 $\mu\text{l}/\text{min}$. Die val is gedroog en 5 μl derivatiseringsreagens is bygevoeg. By kamertemperatuur en sonder katalisator was die reaksie van alkielfenole met trifluorasynsuuranhidried in die PDMS-matriks 100% volledig na 5 minute. Bisfenol-A het minder as 50% volledig gereageer in hierdie tydperk, maar die hoeveelheid derivaat wat gevorm het, het konstant gebly. Ekstraksiedoeltreffendhede van alkielfenole en bisfenol-A het swak herhaalbaarheid getoon tussen besendings buise, wat aandui dat die PDMS-matriks nie homogeen was nie. Vir twee verskillende klompes PDMS het *ters*-oktielfenol 'n doeltreffendheid getoon van 70% en 79%, nonielfenol 84% en 43%, en bisfenol-A 10% en 26%. Die termiesgedesorbeerde derivate is geanaliseer met GC-MS. Ten spyte van agtergrondkontaminasie in die desorbeerder was deteksielimiëte by die dele-per-triljoenvlak. Regte veldmonsters is ook getoets.



ACKNOWLEDGMENTS

My sincerest gratitude to:

Professor Egmont Rohwer, for his guidance, support, and scientific discussion. For seeing me through all the frustrating times and preparing me for the real world...

Professor Ralf Zimmermann, for his inspiring research approach and the opportunity to work with his group in Germany.

The National Research Fund, the University of Pretoria and the WTZ, Germany for financial support.

Dr Fanie van der Walt, Ms. Yvette Naude and Mr Anthony Hasset, for their good humour and technical assistance with all the instrumentation used throughout this project.

Mr Robin Muir, Mr Juan Taljaard, Mr Gerhard Pretorius and Mr Leon Engelbrecht for technical support and Mr David Masemula, for replacing gas bottles and liquid nitrogen.

Mr Wynand Louw and Ms Betty-Jayne de Vos, at NMISA (formerly CSRI-NML), for affording me the opportunity to complete my research.

My colleagues and friends in research especially; Fabian Muëhlberger, Thomas Adam, André Venter, Anita Botha, Peter Apps, Marcellé Archer, Andreas Landman and Isabel Ferreira for their support and scientific debate on my research.

My Parents and family, who have given me the opportunity to go further and supported me every step of the way.

My parents-in-law, who proof-read this thesis and provided me the opportunity to complete the writing up of this thesis.

My husband Alexander for his continuous love and support.



My babies, Matthew and Kiara for the smiles at the end of the day,

My Lord and Saviour, Jesus Christ,

Thank you

Maria



CONTENTS

	<i>Pages</i>
SUMMARY	i
SAMEVATTING	iv
ACKNOWLEDGEMENTS	vi
CONTENTS	viii
ABBREVIATIONS	xiv
LIST OF TABLES	xvii
LIST OF FIGURES	xx
CHAPTER 1 INTRODUCTION	1
1.1. Organic pollutants and human health	1
1.2. The role of liquid chromatography – mass spectrometry in pollution analyses	3
1.3. Gas chromatography-mass spectrometry and the need for derivatization	6
1.4. Sample enrichment and preparation	7
1.5. Aim of our study	9
1.6. Our approach	10
1.7. Arrangement and presentation	11
CHAPTER 2 CONCENTRATION TECHNIQUES	12
2. Introduction	12
2.1. Adsorption	13
2.1.1. Carbon-based, Alumina, Silica and Porous polymers	13
2.1.2. Solid Phase Extraction (SPE)	14
2.1.3. Cryo-trapping from the gas phase	16
2.2. Absorption – <i>dissolution of analytes from gases and liquids</i>	16
2.2.1. Impingers and bubblers for gaseous samples	17
2.2.2. Denuders for gaseous samples	17



	<i>Pages</i>
2.2.3. Polydimethylsiloxane (PDMS) as dissolution medium	17
2.2.3.1. Open Tubular Traps (OTT)	22
2.2.3.2. The Multichannel Silicone Rubber Trap (MCT)	23
2.2.3.3. Packed Particle Bed Traps (PPBT)	24
2.2.3.4. Solid Phase Microextraction (SPME)	24
2.2.3.5. Stir Bar Sorptive Extraction (SBSE)	28
2.3. Dynamic and static equilibrium	29
2.4. Gas and Liquid phase PDMS extraction	31
2.4.1. Gas Phase Static Sampling	32
2.4.2. Gas Phase Dynamic Sampling	33
2.4.3. Aqueous Phase Static Sampling	36
2.4.4. Aqueous Phase Dynamic Sampling	37
2.4.5. Equilibrium extraction in dynamic sampling	38
2.5. Phase ratio and analyte capacity	39
2.6. Recovery	40
2.6.1. Solvent extraction	40
2.6.2. Thermal desorption	41
CHAPTER 3 DERIVATIZATION	42
3. Introduction	42
3.1. Classification	44
3.1.1. Alkylation	44
3.1.2. Acylation	44
3.1.3. Silylation	45
3.1.4. Schiff bases	46
3.2. Derivatization of aldehydes	46
3.2.1. Hydrazones	46
3.2.2. Oximes	49



	<i>Pages</i>
3.2.3. Cyclization reactions	51
3.3. Derivatization of amines	54
3.3.1. Schiff base formation	54
3.3.2. Acylation	55
3.3.3. Dinitrophenylation	57
3.3.4. Sulphonamide formation	58
3.3.5. Silylation	59
3.3.6. Carbamate formation	59
3.4. Derivatization of alcohols and phenols	60
3.4.1. Acylation	60
3.4.2. Silylation	62
3.4.3. Alkylation	66
3.5. Derivatization and pre-concentration	67
3.5.1. Pre-derivatization	67
3.5.2. <i>In situ</i> derivatization	67
3.5.3. Post-derivatization	68
3.6. Conclusions	68
CHAPTER 4 SAMPLE INTRODUCTION	73
4. Introduction	73
4.1. GC inlets	73
4.2. Thermal desorption units	75
4.2.1. Chrompack®	75
4.2.2. Gerstel® Thermal desorption-cold inlet system (TDU-CIS)	77
4.2.3. Airsense® Enrichment desorption unit (EDU)	78
4.3. Thermal modulator array (TMA)	79
CHAPTER 5 ON-LINE ANALYSIS OF ALDEHYDES AND AMINES USING OPEN TUBULAR AND MULTICHANNEL PDMS TRAPS	81
5.1. Loading the derivatizing reagent into the PDMS MCT by preparative gas chromatography	82
5.2. The approach for on-line concentration and derivatization	85



5.3. Derivatization reaction for “photo-ionization labelling” of amines and aldehydes	88
5.3.1. Initial synthesis of the derivatives	88
5.4. Setup for SPME GC-FID based testing of the PDMS mediated derivatization reactions	91
5.5. On-line derivatization setup	97
5.6. Resonance enhanced time-of-flight mass spectrometry (REMPI-TOFMS)	98
5.6.1. Theory of resonance enhanced multiphoton ionisation (REMPI)	98
5.6.2. Applications of REMPI-TOFMS	99
5.6.3. The REMPI-TOFMS instrumentation	100
5.7. Experimental	100
5.7.1. On-line derivatization setup for REMPI-TOFMS	100
5.7.2. First setup: Direct supply of analytes and reagents through the thermal modulator array (TMA-REMPI-TOFMS)	101
5.7.3. Second setup: Supply of analytes and reagents to an enrichment desorption unit prior to the TMA (EDU-TMA-REMPI-TOFMS)	103
5.8. Results and discussion	105
5.9. Conclusions	110

CHAPTER 6 DETERMINING ENDOCRINE DISRUPTORS FROM WATER BY CONCENTRATION AND DERIVATIZATION IN PDMS MULTICHANNEL TRAPS

6.1. Our approach	111
6.2. Derivatization	112
6.2.1. Initial derivatization reactions involving the estrogens	112
6.2.2. Derivatization of the estrogens with pentafluorobenzoyl chloride (PFBCl)	114
6.2.3. Derivatization of the estrogens with trifluoroacetic acid anhydride (TFAA)	115
6.2.4. Dual derivatization of the estrogens with PFBCl and TFAA	129
6.2.5. Reagent selection for the alkylphenols	132
6.2.6. Derivative confirmation	133
6.3. Extraction	137

	<i>Pages</i>
6.3.1. Predictions based on $K_{o/w}$	137
6.3.2. pH adjustments	139
6.4. Quantitative thermal desorption	142
6.4.1. Optimising desorption conditions	142
6.4.2. The “Christmas tree effect”	144
6.5. Sampling	146
6.5.1. Sampling setup and procedure	146
6.6. Experimental	148
6.6.1. Instrumentation	148
6.6.2. Reagents and materials	149
6.6.3. Extraction efficiency	149
6.6.4. Reaction efficiency	150
6.6.5. Reaction calibration curves	150
6.7. Results and discussion	150
6.7.1. Extraction efficiency	150
6.7.2. Reaction efficiency	152
6.7.3. Reaction calibration curves	155
6.7.4. Minimum detection levels of accumulated mass	156
6.8. Limitations of this method	157
6.8.1. PDMS degradation	157
6.8.2. Desorber contamination	159
6.9. Spiked water samples	160
6.10. Real water samples	160
6.11. Conclusion	168
CHAPTER 7 CONCLUSIONS	169
7.1. On-line analysis of volatile aldehydes and amines from air using PDMS traps	169
7.1.1. Further work	171
7.2. Determining endocrine disruptors from water by concentration and derivatization in PDMS traps	171
7.2.1. Recommendations	172
7.2.2. Further work	173



Pages

REFERENCES

174

APPENDICES

APPENDIX 1 Comparison of various adsorbents	194
APPENDIX 2 Reaction efficiency data	198
APPENDIX 3 Confirmation of the alkylphenol TFA derivatives	200
APPENDIX 4 Significance test for comparing extraction efficiency from two different PDMS batches	205
APPENDIX 5 PDMS MCT trap drying investigation	207
APPENDIX 6 Published article	209



ABBREVIATIONS

AAA	-	acetic acid anhydride
ACGIH	-	American Conference of Governmental Industrial
BEA	-	benzylethanolamine
BPA	-	Bisphenol-A
BSA	-	n-o-bis(trimethylsilyl) acetamide
BSTFA	-	n-o-bis (trimethylsilyl) trifluoroacetamide
C	-	analyte concentration/ alkane carbon number
CIS	-	cooled injection system
CL	-	confidence level
C _o	-	initial analyte concentration in sample
C _{PDMS}	-	PDMS concentration
CW	-	carbowax
C _w	-	water concentration
D _c	-	analyte distribution ratio between 2 phases
D _M	-	diffusion constant (m ² .s ⁻¹) of analyte in mobile phase
DNBS	-	dinitrobenzene sulphonic acid
DNFB	-	dinitrofluorobenzene
DNPH	-	dintirophenylhydrazine
DNSH	-	dansylhydrazine
d _p	-	particle diameter
DVB	-	divinylbenzene
E1	-	estrone
E2	-	17β-estradiol
E3	-	estriol
ECD	-	electron capture detector
EDC	-	endocrine disrupting compound
EDU	-	Airsense® enrichment desorption unit
EE2	-	17α-ethinylestradiol
EI	-	electron impact ionization
ELISA	-	enzyme linked immunosorbent assay
EPA	-	U.S. Environmental Protection Agency
ESI	-	electrospray ionization
F	-	column flow rate
FIA	-	flow injection analysis
FID	-	flame ionization detector/ detection
GC	-	gas chromatography
GWRC	-	Global Water Research Coalition
H	-	plate height
HCHO	-	formaldehyde
HFB-	-	heptafluorobutyl
HFBA	-	heptafluorobutyric acid anhydride
HFBCl	-	heptafluorobutanoyl chloride
HMP	-	hydroxymethylpiperidine
HPLC	-	high performance liquid chromatography
h _r	-	reduced plate height
HSSE	-	headspace sorptive extraction
ITD	-	ion trap detector
k	-	capacity factor



Abbreviations

K	-	equilibrium distribution coefficient
K_a	-	acid in water dissociation constant
K_{fg}	-	SPME fibre/ gas distribution constant
K_{fh}	-	SPME fibre/ headspace distribution constant
K_{fs}	-	distribution coefficient between the SPME fibre and sample
$K_{o/w}$	-	octanol-water partitioning coefficient
L	-	column/ trap length
LASER	-	L ight A mplification by S timulated E mission of R adiation
LC	-	liquid chromatography
LLE	-	liquid-liquid extraction
LOD	-	limit of detection
LOQ	-	limit of quantitation
LPME	-	liquid phase microextraction
LTPRI	-	linear temperature programmed retention index
M	-	neutral molecule
M^*	-	high-energy molecule
m_0	-	total mass of analyte in the sample
MCT	-	multichannel trap
m_{PDMS}	-	analyte mass in PDMS
MPI	-	multiphoton ionization
MS	-	mass spectrometry
MSD	-	mass selective detector
MSTFA	-	n-methyl-n-(trimethylsilyl)-trifluoroacetamide
MTBSTFA	-	n-(<i>tert</i> -butyldimethylsilyl)-n-methyltrifluoroacetamide
N	-	theoretical number of plates
n	-	amount extracted
NCI	-	negative chemical ionization
Nd:YAG	-	neodymium-doped yttrium aluminium garnet
NIOSH	-	National Institute for Occupational Safety and Health
NP	-	4-nonylphenol
NPD	-	nitrogen phosphorous detector
NSD	-	nitrogen specific detector
OSHA	-	Occupational Safety and Health Administration
OTT	-	open tubular trap
p_0	-	column outlet pressure
PA	-	polyacrylate
PAH	-	polyaromatic hydrocarbon
PCB	-	polychlorinated biphenyl
PDMS	-	polydimethylsiloxane
PEL	-	permissible exposure limits
PFBA	-	pentafluorobenzaldehyde
PFBBBr	-	pentafluorobenzylbromide
PFBCl	-	pentafluorobenzoyl chloride
PFBHA	-	pentafluorobenzylhydroxylamine
PFBOH	-	pentafluorobenzoic acid
PFPP-	-	pentafluoropropionyl
PFPA	-	pentafluoropropionic acid anhydride
PFPH	-	pentafluorophenylhydrazine
PTV	-	programmed temperature vaporization
p_i	-	column inlet pressure
p_m	-	flow meter pressure



Abbreviations

ppb	-	part-per-billion
PPBT	-	packed particle bed trap
ppm	-	part-per-million
ppt	-	part-per-trillion
p_w	-	saturated water vapour pressure
REMPI	-	resonance enhanced multiphoton ionization
RI	-	retention index
RIC	-	reconstructed ion chromatogram
SBSE	-	stir bar sorptive extraction
SEP	-	sample enrichment probe
SIBA	-	n-succinimidyl benzoate
SIM	-	selected ion monitoring
SPE	-	solid phase extraction
SPI	-	single photon ionization
SPME	-	solid phase microextraction
T_c	-	column temperature
T	-	absolute temperature
T	-	17 β -testosterone
TCPH	-	trichlorophenylhydrazine
TCT - CP 4020	-	Chrompack® thermal desorption cryotrap unit
TDS	-	thermal desorption system
TDU-CIS	-	Gerstel® thermal desorption unit cooled injection system
TFA	-	trifluoroacetic/acetate
TFAA	-	trifluoroacetic acid anhydride
TIC	-	total ion chromatogram
t_m	-	unretained compound retention time
T_m	-	flow meter temperature
TMA	-	thermal modulator array
TMCS	-	trimethylchlorosilane
TMS	-	trimethylsilyl
TMSI	-	n-trimethylsilylimidazole
TOFMS	-	time-of-flight mass spectrometry
TOP	-	<i>tert</i> -octylphenol
t_r	-	analyte retention time
u	-	linear velocity ($m.s^{-1}$)
UV	-	ultraviolet
V_0	-	void volume
V_b	-	breakthrough volume
V_f	-	volume of the fibre
V_L	-	column stationary phase volume
VOC	-	volatile organic compound
V_{PDMS}	-	PDMS volume
V_r	-	retention volume
V_s	-	sample volume
VUV	-	vacuum ultraviolet
V_w	-	water volume
WHO	-	World health organization
β	-	phase ratio
v	-	reduced velocity in the trap (packed column)
ω	-	base width of analyte peak

LIST OF TABLES

	<i>Pages</i>
Table 3.1 Advantages and disadvantages of analyte derivatization.	43
Table 3.2 Sample preparation, concentration and derivatization techniques used for analysis of endocrine disruptors from various matrices	69
Table 5.1 Comparison of the repeatability of different PFBHA loading techniques.	84
Table 5.2 Summary of the aldehyde and amine permeation gas standards prepared.	92
Table 5.3. Approximation of on-line reaction efficiencies, at room temperature without catalyst, as determined by the SPME set-up (<i>figure 5.9</i>).	96
Table 5.4 Gas standard concentrations and calculated detection limits for the aldehydes and amines studied. Permissible Exposure Limits (PEL) as set by the Occupational Safety and Health Administration (OSHA) are also listed [15]. Detection limit values were not measured values but values determined by extrapolation of the larger measured values to a S/N ratio of 2.	102
Table 6.1 Endocrine disrupting compounds to be analysed by concentration and derivatization in the PDMS MCT.	113
Table 6.2 Comparison of electron-capture detector responses for different testosterone acyl-derivatives [245]. With permission from Preston Publications, IL, U.S.A.	114
Table 6.3 Prediction of analyte recoveries on 3 different PDMS devices, using equation 2.3.	137
Table 6.4. Geometrically calculated parameters for the PDMS MCT.	138
Table 6.5 Predicted retention (V_r) and breakthrough volumes (V_b) for analytes on the PDMS MCT.	139

Table 6.6 Structure of the alkylphenols and bisphenol-A as they ionize in aqueous medium plus their associated ionization constants at 25°C [7, 253]. 141

Table 6.7 Extraction efficiencies obtained for TOP, NP and BPA on 2 different PDMS MCTs. 152

Table 6.8 Minimum Detection Levels. (FID = flame ionization detection, EI-RIC=electron impact reconstructed single ion, EI-SIM=electron impact selected ion monitoring, LOD=limit of detection, LOQ= limit of quantitation, LOC= level of confidence from regression line analysis, LOQ from reagent blanks (5 µl TFAA on PDMS MCT) obtained by taking the average plus three times the standard deviation of the series of measurements). The LOD (s/n =5) was determined by extrapolation from a larger signal and not from actual measurements. 157

Table 6.9 Quantitative results obtained for real samples by external standard calibration, after subtraction of the blank value. Concentration values based on 100% reaction and extraction efficiencies. Corrected concentration values obtained through inclusion of extraction and reaction efficiency factors (PDMS batch 2). TOP (100% reaction, 79 % extraction); NP (100% reaction, 43% extraction) and BPA (37% reaction, 26% extraction) 162

APPENDICES :

Table A.1 A comparison of various adsorbents [48, 69, 70-72, 82, 115, 116] 194

Table A.4 Summary of significance test results [276] 206

LIST OF FIGURES

	<i>Pages</i>
Figure 1.1 Graph showing the analytical domain of GC and LC using polarity versus molecular mass [20]. Copyright Global View Publishing, Pittsburgh, Pennsylvania, U.S.A. Reproduced with permission.	4
Figure 1.2 Chart representing the relative cost of the commercially available chromatographic and MS-hyphenated chromatographic instrumentation based upon data published in ref. 21. Other chromatographic techniques are GC with flame ionization or electron capture detection and HPLC with UV or fluorescence detection.	5
Figure 2.1 Diagram of concentration and recovery techniques commonly used for concentrating analytes from gaseous and aqueous phase samples.	12
Figure 2.2 Use of a SPE device [73].	14
Figure 2.3 Liquid phase extraction devices [81].	16
Figure 2.4 The structure of polydimethylsiloxane (PDMS).	18
Figure 2.5 Thermal desorption run of a blank PDMS MCT.	18
Figure 2.6 Structure of the PDMS methylsiloxane degradation products D3, D4 and D5.	18
Figure 2.7 Increased thermal degradation of PDMS with increasing temperature. Data obtained by desorbing a PDMS MCT for 10 min at each of the indicated desorption temperatures, desorb flow-rate 50 ml/min, cryotrap -100°C, inject for 1 min at 300°C. The respective siloxane degradation peaks were integrated to obtain peak areas (which were plotted on a logarithmic scale) <i>versus</i> desorption temperature.	20

- Figure 2.8 Cross-sections of the various PDMS configurations, with their corresponding PDMS volumes graphically depicted below them [95, 96*].
- OTT: Ultra thick film open tubular trap, consisting of a silicone rubber tube (d_f 145 μm) inserted in a 1 m long wide bore capillary (PDMS volume \sim 105 μl)
- SPME: 100 μm PDMS solid phase microextraction fibre (PDMS volume 0.5 μl *)
- SBSE: Maximum PDMS commercially available 20 mm length x d_f 1.0 mm PDMS film coating a magnetic glass stir bar (PDMS volume 126 μl)
- PPBT: Pulverized silicone rubber particles (PDMS volume 219 μl)
- MCT: 32 silicone rubber tubes (0.63 mm o.d. x 0.3 mm i.d. x 5 cm lengths) arranged in parallel (PDMS volume 250 μl) 21
- Figure 2.9 A polydimethylsiloxane multichannel trap (PDMS MCT). This trap has 32 x \sim 2 cm lengths of PDMS tubes arranged in parallel inside a glass tube. This shorter arrangement is suitable for trapping less volatile analytes which require longer desorption times. 24
- Figure 2.10 The first commercial SPME device from Supelco [49]. 27
- Figure 2.11 Mass profiles over time for the dynamic sampling of a finite sample on a PDMS trap. The analyte mass in the sample reduces as the analyte accumulates in the PDMS, once the analyte reaches its retention volume on the trap it will breakthrough and can be measured at the outlet of the trap. 30
- Figure 2.12 Mass profiles over time for the dynamic sampling of a constant supply of a bulk sample on a PDMS trap. Equilibrium extraction occurs when the analyte concentration entering the trap is the same as the analyte concentration exiting the trap. 31
- Figure 2.13 Recovery as a function of the octanol-water partition coefficient (K_{ow}) of the analyte in 3 different PDMS configurations. The graph was obtained by calculation using equation 2.3 and values for β as stated in section 2.5. 40
- Figure 3.1 Reaction scheme for 2,4-DNPH with an aldehyde [106, 128-134, 137, 138]. 47

Figure 3.2 Reaction scheme for DNSH with an aldehyde [75].	48
Figure 3.3 Reaction scheme for PFPH with an aldehyde [78, 139].	48
Figure 3.4 Reaction scheme for TCPH with an aldehyde [76].	49
Figure 3.5 Reaction scheme for first, benzylhydroxylamine with an aldehyde. Second, methoxy amine with an aldehyde [136].	50
Figure 3.6 Reaction scheme for PFBHA with an aldehyde [140].	51
Figure 3.7 Reaction scheme for ethanolamine with an aldehyde [39, 136].	51
Figure 3.8 Reaction scheme of 2-HMP with an aldehyde [148-151].	52
Figure 3.9 Reaction scheme of cysteamine with an aldehyde [136, 152, 153].	52
Figure 3.10 Reaction scheme for an aldehyde with aqueous ammonia [154].	53
Figure 3.11 Reaction scheme for Dimedon with an aldehyde [155].	53
Figure 3.12 Hantzsch reaction scheme [156, 157].	54
Figure 3.13 Reaction scheme for the condensation of an aldehyde with a primary amine. R = alkyl or aryl substituent [121].	55
Figure 3.14 Reaction scheme for the reaction of a perfluoroacyl anhydride reagent with a primary amine. R = alkyl or aryl substituent, R ₁ = CH ₃ , CF ₃ , C ₂ F ₅ or C ₃ F ₇ [121].	55
Figure 3.15 Reaction scheme for the reaction of an acyl chloride with a primary amine. R = alkyl or aryl substituent, R ₂ = CH ₃ , C(CH ₃) ₃ , CCl ₃ , C ₆ F ₅ , C ₆ H ₄ -NO ₂ , C ₆ H ₃ (NO ₂) ₂ [121].	56
Figure 3.16 Reaction scheme for the reaction of an acyl imidazole with a primary amine. R = alkyl or aryl substituent, R ₁ = CH ₃ , CF ₃ , C ₂ F ₅ or C ₃ F ₇ [121].	56

Figure 3.17 Reaction scheme for the reaction of <i>N</i> -succinimidyl benzoate, SIBA, with a primary amine. R = alkyl or aryl substituent [164].	57
Figure 3.18 Reaction scheme for the reaction of 2, 4-dinitrofluorobenzene (DFNB) with a primary amine. R = alkyl or aryl substituent [121].	57
Figure 3.19 Reaction scheme for the reaction of 2, 4-dinitrobenzenesulphonic acid (DNBS) with a primary amine. R = alkyl or aryl substituent [121].	58
Figure 3.20 Reaction scheme for the sulphonation reaction of benzenesulphonyl chloride with a primary amine. R = alkyl or aryl substituent [121].	58
Figure 3.21 Reaction scheme for the reaction of R ₄ = CH ₃ (BSA) or CF ₃ (BSTFA) with a primary amine, R = alkyl or aryl substituent [121].	59
Figure 3.22 Reaction scheme for the reaction of MTBSTFA with a primary amine [121].	59
Figure 3.23 Reaction scheme for the formation of a carbamate from the reaction of an alkyl chloroformate with a primary amine. R = alkyl or aryl substituent, R ₅ = C ₂ H ₅ , CH ₂ CH(CH ₃) ₂ , C ₅ H ₁₂ , CH ₂ CF ₃ .	60
Figure 3.24 Reaction scheme for the reaction of phenol functional groups with an acyl anhydride to form the ester and carboxylic acid by-product.	61
Figure 3.25 Reaction scheme for the reaction of a phenol functional group with an acyl chloride to form the ester and haloacid by-product.	62
Figure 3.26 Reaction scheme for the formation of phenyl trimethylsilyl ether from the reaction of MSTFA with a phenol.	63
Figure 3.27 Reaction scheme for the formation of phenyl trimethylsilyl ether from the reaction of BSTFA with a phenol.	64

Figure 3.28 Reaction scheme for the formation of phenyl <i>tert</i> -butylsilyl ether from the reaction of MTBSTFA with a phenol.	65
Figure 3.29 Reaction scheme for the formation of phenyl trimethylsilyl ether from the reaction of TMSI with a phenol.	66
Figure 3.30 Reaction scheme for the formation of pentafluorobenzyl ether from the reaction of PFBBBr with a phenol.	66
Figure 4.1 A split / splitless inlet [211]. Copyright Wiley-VCH Verlag GmbH & Co. KGaA. Reproduced with permission	75
Figure 4.2 The 2 main phases in the TCT 4020 thermal desorption unit: A: Desorption Phase B: Injection Phase 1. A: High purity helium carrier gas flow during desorption phase 1. B: High purity helium carrier gas flow during injection phase 2. Glass tube containing ad/absorbent 3. Wide bore fused silica capillary cold trap 4. Heated desorption oven 5. Liquid nitrogen – cooled chamber 6. Ambient desorption oven 7. Ballistically heated cold trap 8. Gas Chromatograph	76
Figure 4.3 Cross section of the Gerstel® TDS-CIS desorption unit [599].	78
Figure 4.4 Gas flow configuration for the Airsense EDU custom-made for the GSF [214]: A: Sampling Phase B: Desorption Phase C: Injection Phase	79
Figure 4.5 Longitudinal section of a Thermal Modulator Array [215].	80

Figure 5.1 Enlarged GC-FID chromatogram obtained from loading PFBHA headspace from the solid reagent onto the PDMS MCT. * PDMS thermal degradation peak, 1: Formaldehyde-Oxime, 2: PFBHA, 3: Dodecane (internal standard used to monitor the completeness of desorption of the analytes off the trap. It was added after derivatization using a glass syringe.)	82
Figure 5.2 The experimental setup using preparative gas chromatography to selectively introduce the PFBHA reagent onto the PDMS MCT.	83
Figure 5.3 Two variations of silicone (PDMS) concentrators namely the thick film open tubular trap (OTT) and the multi-channel silicone rubber trap (MCT).	85
Figure 5.4 Reaction scheme for the derivatization of low molecular mass aldehydes with phenylhydrazine.	86
Figure 5.5 Reaction scheme for the derivatization of low molecular mass alkyl amines with benzaldehyde.	87
Figure 5.6 ITD Mass spectrum of the formaldehyde phenylhydrazone derivative (M^+120).	89
Figure 5.7 ITD Mass spectrum of the acetaldehyde phenylhydrazone derivative (M^+146).	90
Figure 5.8 ITD Mass spectrum of the benzaldehyde propylimine derivative (M^+147). Notice the strong $M+1$ peak as m/z 148 that we ascribe to inadvertent chemical ionisation in the ITD.	90
Figure 5.9 A simulation of the on-line REMPI-TOFMS set-up using SPME to determine approximate reaction efficiencies for the on-line derivatization reactions.	91
Figure 5.10 Graph of mass loss over time for acetaldehyde, acrolein and crotonal. The gradient of the straight line is the permeation rate (g/ min).	92

Figure 5.11 Reaction efficiency results for the on-line derivatization of A; formaldehyde and B; acetaldehyde with phenylhydrazine.

Both graphs display i) the calculated amount of gas standard released over the time interval using their gravimetrically determined permeation rate and ii) the amount of analyte gas trapped using *in situ* derivatization on the SPME fibre as calculated using the internal standard and effective carbon number response for the signal obtained from the GC-FID for the derivative. The graphs on the right hand side represent an enlargement of the left hand side graphs, where the initial accumulation on the SPME fibre appears linear. A comparison of the gradients obtained from the standard and the actual amount of analyte trapped gives an approximation of the reaction/trapping efficiency for this reaction before breakthrough starts occurring in the simple fibre/tube column.

94

Figure 5.12 The GC-FID chromatogram obtained after desorption of a 100 μm PDMS SPME fibre exposed simultaneously for 30 seconds to the permeation gas standards of acetaldehyde, acrolein and crotonal and the phenylhydrazine derivatization reagent. Formaldehyde-phenylhydrazone impurity (5.58 min); Acetal-phenylhydrazone (6.58 & 6.71 min); Propanal-phenylhydrazone (7.36 & 7.45 min); Acrolein-phenylhydrazone (7.68 & 7.75 min) and Crotonal-phenylhydrazone (8.81 & 8.90 min). The double peaks for each derivative, excluding formaldehyde, represent *E-Z* isomers.

95

Figure 5.13 The experimental set-up used for:

A) On-line concentration and derivatization for REMPI-TOFMS using the thermal modulator array (TMA) with a thick film OTT as enrichment and reaction medium

B) On-line concentration and derivatization for REMPI-TOFMS using a multi-channel silicone rubber trap (MCT) in an enrichment and desorption unit (EDU) as enrichment and reaction medium and the thermal modulator array (TMA) with a thick film OTT for analyte modulation.

97

Figure 5.14 (1+1) and (2+1) Multi Photon Ionization processes [234]

98

- Figure 5.15 Mass spectra obtained for the formaldehyde phenylhydrazone derivative using two different ionization techniques. The Electron Impact (EI) mass spectrum was obtained from a prepared derivative on an accurate mass GC-TOFMS. The Resonance Enhanced Multiphoton Ionization (REMPI) mass spectrum was obtained from the on-line concentration and derivatization experiment. 103
- Figure 5.16 REMPI-TOF mass spectra obtained for the on-line concentration and derivatization of A.; acetaldehyde, acrolein and crotonal with phenylhydrazine at 246 nm, and B.; methylamine, ethylamine, propylamine and butylamine with benzaldehyde at 240 nm. 105
- Figure 5.17 Single Photon Ionization (SPI) mass spectrum of the on-line, *in situ* derivatization of Propylamine (m/z 59) and butylamine (m/z 73) with benzaldehyde (m/z 106). The presence of both derivatized (m/z 161 and m/z 147) and underivatized analyte was observed. 106
- Figure 5.18 SPI signal over time, obtained by applying the on-line *in-situ* derivatization TMA set-up to the SPI-TOFMS [32] for the analysis of formaldehyde. The insert shows the mass spectrum obtained as a single shot from the time profile, depicting the formaldehyde-phenylhydrazone derivative. 107
- Figure 6.1. Gas chromatogram and time-of-flight mass spectrum of PFBCl hydrolysis product obtained when performing the method by Kuch and Ballschmiter [193]. 116
- Figure 6.2 GC- (EI) MS: Total ion chromatogram (TIC) of the *in situ* derivatization of estrogens in the PDMS MCT using TFAA. Beneath is the reconstructed ion chromatogram of molecular ions of the estrone (E1-TFA); β -estradiol (E2-di-TFA); estriol (E3-tri-TFA) and testosterone (T-TFA) trifluoroacetate (TFA) derivatives. 118
- Figure 6.3 Electron impact mass spectrum of the estrone-trifluoroacetate (E1-TFA) derivative. Molecular ion (M^+) m/z 366, ($-CF_3$) m/z 69. 119
- Figure 6.4 Electron impact mass spectrum of the 17β -estradiol-trifluoroacetate (E2-di-TFA) derivative. Molecular ion (M^+) m/z 464, ($-CF_3$) m/z 69. 119

- Figure 6.5 Electron impact mass spectrum of the estriol-trifluoroacetate (E3-tri-TFA) derivative. Molecular ion (M^+) m/z 576, ($-CF_3$) m/z 69. 120
- Figure 6.6 Electron impact mass spectrum of the testosterone-trifluoroacetate (T-TFA) derivative. Molecular ion (M^+) m/z 384, ($-CF_3$) m/z 69. 120
- Figure 6.7 Electron impact mass spectrum of the testosterone-ditrifluoroacetate (T-di-TFA) derivative. Molecular ion (M^+) m/z 480, ($-CF_3$) m/z 69. Beneath the mass spectrum is a sketch of the equilibrium between the ketone and enol tautomers of testosterone. 121
- Figure 6.8 The TIC obtained from GC- (NCI) MS of the *in situ* derivatization of estrogens in the PDMS MCT using TFAA, followed by the RIC for m/z 113, indicating all peaks having the trifluoroacetate ion, m/z 488 RIC, indicating the suspected EE2-di-TFA derivative peak eluting at 37 min and m/z 576 RIC indicating the suspected E3-tri-TFA derivative peak eluting at 61 min. 123
- Figure 6.9 The negative chemical ionization-mass spectra (NCI-MS) for one of many peaks in the chromatogram with base peak m/z 113, followed by the NCI-mass spectrum for the suspected EE2-di-TFA derivative (M^- m/z 488) and E3-tri-TFA derivative (M^- m/z 576). 124
- Figure 6.10 The GC- (ITD) MS chromatogram obtained for the reaction of EE2 with TFAA in a glass tube. 5 major compounds, labelled A, B, C, D and E were identified for the derivative. 125
- Figure 6.11. 17α -ethinylestradiol (EE2) undergoing a Wagner Meerwein rearrangement, essentially this is a 1,2- shift between 2 groups on adjacent sp^3 hybridized carbon atoms [247, 248]. 126
- Figure 6.12. The ITD-EI mass spectrum of compound A. The mono-substituted EE2-TFA derivative has undergone a Wagner-Meerwein rearrangement and a water elimination step (dehydration) to form a double bond between the C5 and C6 rings. The base peak m/z 374 is also the molecular ion M^+ . 126

- Figure 6.13. The ITD-EI mass spectrum of compound B. The disubstituted EE2-TFA derivative has lost the 17-alkynyl (C-C) group (-24 amu). 127
- Figure 6.14. The ITD-EI mass spectrum of compound C. The mono-substituted EE2-TFA derivative has undergone a Wagner-Meerwein rearrangement and a water elimination step (dehydration) to form a double bond between the C5 and C6 rings. The methyl group is lost to form base peak m/z 359 and molecular ion at m/z 374. 127
- Figure 6.15. The ITD-EI mass spectrum of compound D. The disubstituted EE2-di-TFA derivative. 128
- Figure 6.16. The ITD-EI mass spectrum of compound E. The disubstituted EE2-di-TFA derivative after a Wagner Meerwein rearrangement. 128
- Figure 6.17 The GC- (EI) MS Reconstructed ion chromatogram (RIC) of m/z 195 corresponding to the pentafluorophenyl carbonyl moiety, for the dual derivatization of estrogens with PFBCl and TFAA. 130
- Figure 6.18 The EI mass spectrum obtained for the derivative formed from the reaction of estrone (E1) with PFBCl and TFAA. Base peak m/z 195 (C_7F_5O) and M^+ m/z 464. 130
- Figure 6.19 The EI Mass Spectrum obtained for the derivative formed from the reaction of 17β -Estradiol (E2) with PFBCl and TFAA. Base peak m/z 195 (C_7F_5O), m/z 69 (CF_3) and M^+ m/z 562. 131
- Figure 6.20 The EI mass spectrum obtained for the derivative formed from the reaction of estriol (E3) with PFBCl and TFAA. Base peak m/z 195 (C_7F_5O), m/z 69 (CF_3) and M^+ m/z 674. 131
- Figure 6.21 The EI mass spectrum obtained for the hydrolysed PFBCl, i.e. Pentafluorobenzoic acid formed from the reaction of the estrogens with PFBCl and TFAA. Base peak m/z 195 (C_7F_5O), and M^+ m/z 212. 132

- Figure 6.22 Reaction mechanism for the derivatization of a primary alcohol with trifluoroacetic acid anhydride (TFAA) to form the corresponding trifluoroacetate derivative and trifluoroacetic acid by-product. 133
- Figure 6.23 Mass spectrum and fragmentation scheme for the main mass spectral fragments obtained for the *tert*-octylphenol TFA derivative. Note the molecular ion (m/z 302) is almost absent. 134
- Figure 6.24 Mass spectrum and fragmentation scheme for the main mass spectral fragments obtained for the 4-*n*-nonylphenol TFA derivative. 135
- Figure 6.25 Mass spectrum and fragmentation scheme for the main mass spectral fragments obtained for the bisphenol-A TFA derivative. 136
- Figure 6.26 Optimisation of thermal desorption temperature of higher boiling alkanes off a 32 PDMS MCT using a Gerstel® TDS-CIS. The injection temperature was maintained at 300°C, while desorption temperature was incremented by 40°C per desorption run. The measurement values are depicted as an x-y scatter plot with data points connected by lines. The optimum desorption temperature was visually determined to be 180°C where the peak area of the analytes appear to reach a plateau. 143
- Figure 6.27 Optimisation of CIS injection time of higher boiling alkanes off a glass baffled inlet liner using a Gerstel® TDS-CIS at 300°C. The measurement values are depicted as an x-y scatter plot with data points connected by lines. The optimum CIS injection time was visually determined to be 5 min for alkanes from C16 to C20, as the peak areas of these analytes appear to reach a plateau at this time. Higher boiling alkanes (C24 to C28) require more than 20 minutes to be desorbed completely off the CIS. A midpoint of 10 min was selected for injection time in this study. 144

- Figure 6.28 Cross-section of a non-polar capillary column showing a large volume splitless injection using (A) a non-polar solvent and (B) a polar solvent. The top figure shows the injection plug entering the column in the mobile phase. Figure A shows how the non-polar solvent “wets” the stationary phase as “like-dissolves-like”. The analytes in the plug begin to partition into the stationary phase and start the chromatographic process resulting in Gaussian peaks eluting from the column. Figure B shows how the polar solvent forms droplets as it does not wet the stationary phase. Each droplet gives rise to its own solvent effect resulting in broad split peaks eluting from the column [255]. 145
- Figure 6.29 Section of two overlaid chromatograms depicting the improvement of chromatographic conditions for a large volume splitless injection. The “Christmas tree effect” of the larger co-eluting peak is replaced by 2 separated, smooth, peaks. 146
- Figure 6.30 The simple setup used in the lab to sample water through the PDMS MCT. 147
- Figure 6.31 Optimum TFAA reagent volume, determined by placing placing 1µl 42 ng/µl TOP, 44 ng/µl NP and 54 ng/µl BPA in acetone on the PDMS trap, the corresponding reagent volumes are added after the solvent has evaporated. The trap is then sealed with glass caps for 10 minutes before thermal desorption and analysis. The optimum TFAA volume of 5 µl was visually determined from the x-y scatter plot as the point where maximum derivative peak area is observed. 153
- Figure 6.32 Reaction efficiencies, determined by placing 1µl 42 ng/µl TOP, 44 ng/µl NP and 54 ng/µl BPA in acetone on the PDMS trap, 5 µl TFAA is added after the solvent has evaporated. The trap is then sealed with glass caps for the duration of the reaction. The measurement values are depicted as an x-y scatter plot with data points connected by lines. The optimum reaction time was visually determined to be 5 min, where the peak areas of the TFA-derivatives appear to reach a plateau. 154
- Figure 6.33 GC-FID calibration curves obtained by the *in situ* reaction of alkylphenols on the PDMS trap. 155

- Figure 6.34 Overlaid chromatogram of 2 PDMS MCTs. The green chromatogram is obtained after the *in situ* derivatization reaction on a “dried” trap. The black chromatogram is obtained after the *in situ* derivatization reaction on a “wet” trap. 158
- Figure 6.35 Reaction equation for the TFA acid by-product in the presence of water. 158
- Figure 6.36 System blank reconstructed ion chromatogram obtained from desorption of an empty glass tube. *Tert*-octylphenol trifluoroacetate derivative (TOP-TFA) m/z 231, $t_R = 21.2$ min; 4-*n*-nonylphenol trifluoroacetate derivative (NP-TFA) m/z 203, $t_R = 25.6$ min; bisphenol-A trifluoroacetate derivative (BPA-TFA) m/z 405, $t_R = 27.2$ min. 160
- Figure 6.37 (A) Total ion chromatogram of the reagent blank.
- Figure 6.37 (B) Total ion chromatogram of a 5 ml MilliQ water sample spiked with 25 ng alkylphenol standard in methanol, sampled through the PDMS MCT (50 μ l/min), dried and allowed to react with 5 μ l trifluoroacetic acid anhydride for 10 min, followed by thermal desorption.
- Figure 6.37 (C) The extracted ion chromatogram of the base peak ions used for quantitation. *Tert*-octylphenol trifluoroacetate derivative (TOP-TFA) m/z 231, $t_R = 21.2$ min; 4-*n*-nonylphenol trifluoroacetate derivative (NP-TFA) m/z 203, $t_R = 25.6$ min; bisphenol-A trifluoroacetate derivative (BPA-TFA) m/z 405, $t_R = 27.2$ min. 163
- Figure 6.38 (A) Total ion chromatogram of the 20 ml Apies River water sample on PDMS MCT M1. Sample extracted at a flow rate of 50 μ l/min, dried and allowed to react with 5 μ l trifluoroacetic acid anhydride for 10 min, followed by thermal desorption.
- Figure 6.38 (B) Extracted ion chromatogram of PDMS degradation peaks m/z 73, 207, 211 and 281.
- Figure 6.38 (C) Extracted ion chromatogram of the base peak ions used for quantitation. *Tert*-octylphenol trifluoroacetate derivative (TOP-TFA) m/z 231, $t_R = 21.2$ min; 4-*n*-nonylphenol trifluoroacetate derivative (NP-TFA) m/z 203, $t_R = 25.6$ min; bisphenol-A trifluoroacetate derivative (BPA-TFA) m/z 405, $t_R = 27.2$ min. 164

Figure 6.39 (A) Total ion chromatogram of the TFAA reagent blank on PDMS MCT M1. 5 μ l trifluoroacetic acid anhydride placed on trap for 10 min, followed by thermal desorption.

Figure 6.39 (B) Extracted ion chromatogram of PDMS degradation peaks m/z 73, 207, 211 and 281. Figure 6.39 (C) Extracted ion chromatogram of the base peak ions used for quantitation. *Tert*-octylphenol trifluoroacetate derivative (TOP-TFA) m/z 231, t_R = 21.2 min; 4-*n*-nonylphenol trifluoroacetate derivative (NP-TFA) m/z 203, t_R = 25.6 min; bisphenol-A trifluoroacetate derivative (BPA-TFA) m/z 405, t_R = 27.2 min.

165

Figure 6.40 (A) Total ion chromatogram of the 20 ml Apies River water sample on PDMS MCT M2. Sample extracted at a flow rate of 50 μ l/min, dried and allowed to react with 5 μ l trifluoroacetic acid anhydride for 10 min, followed by thermal desorption.

Figure 6.40 (B) Extracted ion chromatogram of PDMS degradation peaks m/z 73, 207, 211 and 281.

Figure 6.40 (C) Extracted ion chromatogram of the base peak ions used for quantitation. *Tert*-octylphenol trifluoroacetate derivative (TOP-TFA) m/z 231, t_R = 21.2 min; 4-*n*-nonylphenol trifluoroacetate derivative (NP-TFA) m/z 203, t_R = 25.6 min; bisphenol-A trifluoroacetate derivative (BPA-TFA) m/z 405, t_R = 27.2 min.

166

Figure 6.41 Selected Ion Mode (SIM) chromatogram of the TFAA reagent blank on PDMS MCT M3. Selected ions were m/z 231, 203, 245, 316, 405, 420. 5 μ l trifluoroacetic acid anhydride placed on trap for 10 min, followed by thermal desorption. *Tert*-octylphenol trifluoroacetate derivative (TOP-TFA) m/z 231, t_R = 21.2 min; 4-*n*-nonylphenol trifluoroacetate derivative (NP-TFA) m/z 203, t_R = 25.6 min; bisphenol-A trifluoroacetate derivative (BPA-TFA) m/z 405, t_R = 27.2 min.

167

Figure 6.42 Selected Ion Mode (SIM) chromatogram of the 20 ml UP Sports Centre river water sample on PDMS MCT M3. Sample extracted at a flow rate of 50 μ l/min, dried and allowed to react with 5 μ l trifluoroacetic acid anhydride for 10 min, followed by thermal desorption. Selected ions were m/z 231, 203, 245, 316, 405, 420. *Tert*-octylphenol trifluoroacetate derivative (TOP-TFA) m/z 231, t_R = 21.2 min; 4-*n*-nonylphenol trifluoroacetate derivative (NP-TFA) m/z 203, t_R = 25.6 min; bisphenol-A trifluoroacetate derivative (BPA-TFA) m/z 405, t_R = 27.2 min.

167

APPENDICES:

- Figure A2.1 Reaction efficiency graphs for the on-line derivatization of acrolein and crotonal with phenylhydrazine. The graph displays i) the amount of gas standard released over that time interval as determined by their permeation rate and ii) the amount of analyte gas trapped using *in-situ* derivatization on the SPME fibre as calculated using the internal standard and effective carbon number response for the signal obtained from the GC-FID for the derivative. A comparison of the gradients obtained from the standard and the actual amount of analyte trapped gives an approximation of the reaction/trapping efficiency for this reaction. 199
- Figure A2.2 Reaction efficiency graphs for the on-line derivatization of propylamine and butylamine with benzaldehyde. The graph displays i) the amount of gas standard released over that time interval as determined by their permeation rate and ii) the amount of analyte gas trapped using *in-situ* derivatization on the SPME fibre as calculated using the internal standard and effective carbon number response for the signal obtained from the GC-FID for the derivative. A comparison of the gradients obtained from the standard and the actual amount of analyte trapped gives an approximation of the reaction/trapping efficiency for this reaction. 199
- Figure A3.1
- A) GC-TOFMS chromatogram obtained for the underivatized phenols, TOP $t_R = 17.47$ min, NP $t_R = 20.30$ min and BPA $t_R = 26.25$ min.
- B) GC-TOFMS confirmation chromatogram for the trifluoroacetate derivatives prepared in a vial in acetone as described in section 6.2.6. TOP-TFA $t_R = 15.99$ min, NP-TFA $t_R = 19.00$ min and BPA-TFA $t_R = 20.35$ min. *Notice the absence of underivatized phenols.* 200
- Figure A3.2 GC-TOFMS mass spectrum obtained for the TOP-TFA derivative $t_R = 15.99$ min. M^+ m/z 302, base peak m/z 231. 201
- Figure A3.3 GC-TOFMS mass spectrum obtained for the NP-TFA derivative $t_R = 19.00$ min. M^+ m/z 316, base peak m/z 203. 201

Figure A3.4 GC-TOFMS mass spectrum obtained for the BPA-TFA derivative $t_R = 20.35$ min. M^+ m/z 420, base peak m/z 405.	202
Figure A3.5 Reconstructed ion chromatograms for m/z 231 and m/z 203 representing the TFA derivatives of TOP and NP respectively, along with m/z 135 and m/z 213 representing ions for the corresponding underivatized alkylphenols. The PDMS degradation peaks are indicated by the m/z 73 ion trace.	203
Figure A3.6 Reaction efficiencies, determined by placing $1\mu\text{l}$ $42\text{ ng}/\mu\text{l}$ TOP, $44\text{ ng}/\mu\text{l}$ NP and $54\text{ ng}/\mu\text{l}$ BPA in acetone on the PDMS trap, $5\mu\text{l}$ TFAA is added after the solvent has evaporated. The trap is then sealed with glass caps for the duration of the reaction. The reaction appears to be complete after 5 minutes. See section 6.7.2.	204
Figure A.5 Summary of the drying steps performed in series with the resulting PDMS MCT mass loss achieved from each drying step.	208

Chapter 1

Introduction

1.1. *Organic pollutants and human health*

Over the decades numerous chemicals have been introduced to improve industrial processes, agricultural production, medical treatments, and the manufacture of cosmetic and household care products. Offsetting the convenience of such chemicals has been the increasing concern over potentially adverse effects on human health and the environment arising from their use and disposal.

Industry and society at large have become ever more aware of the harmful nature of natural and synthetic pollutants released into the environment every year. Of particular concern have been the very low levels at which certain pollutants can cause harm. For example, both the man-made and naturally occurring hormonal estrogens, ethinylestradiol (the contraceptive “pill”) and estradiol respectively, which typically enter the environment through waste water systems [1-6], have demonstrated their ability to disrupt the endocrine system of living organisms at the part-per-trillion level (ppt) [1, 2, 4,6, 7]. Such compounds are classified as endocrine disrupting compounds (EDCs).

The World Health Organization has defined an EDC as an exogenous substance or mixture that alters the function(s) of the endocrine system and consequently causes adverse health effects in an organism, or its progeny, or (sub) populations [1, 2, 3, 5]. An EDC priority list has been identified by the Global Water Research Coalition (GWRC) to include hormones, pesticides and herbicides, industrial chemicals such as alkyl phenols, phthalates and polychlorinated biphenyl compounds (PCBs) and heavy metals such as cadmium [5]. Of the organic compounds, the hormones exhibit the highest potency [5].

Bisphenol-A (BPA) and alkylphenols, particularly *tert*-octylphenol (TOP) and 4-nonylphenol (NP) are infamous pollutants found in water [1, 6-9]. TOP and NP are indirectly released into the environment through the anaerobic biological breakdown of non-ionic surfactants namely nonyl- and octylphenol ethoxylates. However, the ethoxylates exhibit neither the toxicity nor the estrogenic effects of their

Chapter 1 - Introduction

breakdown products [10]. Alkylphenol ethoxylates are released into the environment through wastewater, principally from the use of domestic laundry detergents, industrial soap, paints, toiletries and cosmetics [6]. Several isomers of commercial nonylphenol are available, of which 4-nonylphenol is the most common. No standard method currently exists for the sampling, storage and analysis of nonylphenol [9]. Bisphenol-A is used as an intermediate in the production of polycarbonate, epoxy resins and flame-retardants. Low levels of BPA are frequently released into the environment during the manufacturing, processing and use of these products [8].

During an experiment investigating the impact of estrogens on breast cancer cells, it was found that nonylphenol leached from the plastic containers used in the testing laboratory, caused the cancer cells to multiply rapidly [6]. It was established that nonylphenol at concentrations of 50 $\mu\text{g} / \text{L}$ (50 ppb) in water was sufficient to disrupt the reproductive cycle of fish [6]. In addition to decreased sperm counts in male fish, this disruption is also observed when the male fish start to produce *vitellogenin*. This is a female egg yolk protein, used in female ovaries to produce eggs. [6]. The more potent estrogen β -ethinylestradiol produces the same effect at 0.1 ng / L (0.1 ppt) [1, 2, 4, 6, 7].

Recently, it has also been revealed that the exposure of pregnant mothers to BPA leaching from polycarbonate bottles (hard clear plastic used to make baby bottles amongst others) and food cans lined with BPA resins, may have caused harm to their developing fetuses. These resulting children are born underweight; they then become and remain overweight for the rest of their lives [11]

Plant estrogens or phytoestrogens [12] have also been found to interfere with the endocrine system [6, 12, 13]. Various *isoflavones* in clover and *coumestans* found in sunflower oil and seeds and in soy, green and red beans have been identified as having estrogenic activity [6]. This discovery was prompted by sheep in Australia suffering from reproductive problems after eating a certain species of clover [6]. Recently, it was shown that exposure to phytoestrogens, in the form of lavender and tee tree oil used in the manufacture of body creams, caused prepubertal breast development in teenage boys [13].

Not all pollutants are found in aquatic systems. Several are airborne and are equally, if not more, harmful than the compounds already mentioned. Formaldehyde is classified as a probable human carcinogen by the U.S. Environmental Protection Agency (EPA), Occupational Safety and Health

Chapter 1 - Introduction

Administration (OSHA), National Institute for Occupational Safety and Health (NIOSH), as well as by the American Conference of Governmental Industrial Hygienists (ACGIH) [14-16]. Low molecular-mass aldehydes and amines are typically eye, nose, and throat irritants [16-18]. As volatile polar compounds, they are notoriously difficult to analyze, especially as they occur at the part-per-billion level.

Given their negative impact on human health it is urgent to monitor these pollutants at extremely low levels in both air and water.

Trace analysis has been defined as the detection and measurement of analytes below the concentration level of 100 µg per gram of sample, i.e. below 100 part-per-million [19]. Analysis of organic pollutants, at trace levels using liquid chromatography or gas chromatography combined with mass spectrometry has been used extensively over the years to monitor pollution levels. Recently, however, the occurrence of pollutants, which are harmful at the ppt / ppb level, has pushed analytical chemistry into the realm of ultra-trace analysis. Detection at a lower level, i.e., a decrease by an order of magnitude implies an increase of equal magnitude in sample complexity. Successful analysis of ultra-trace analytes requires not only extra sensitivity but also the introduction of an additional step to ensure selectivity prior to the final measurement.

1.2. The role of liquid chromatography – mass spectrometry in pollution analyses

Of the known organic species, 80% of them are analysed by liquid chromatography (LC) and the remaining 20% by gas chromatography (GC) [20]. Only volatile and thermally stable compounds can be analysed by GC and often only those with molecular mass < 800 by gas chromatography / mass spectrometry (GC/MS) [20], figure 1.1. However, GC has the greater separation power than LC and is preferred for the analysis of unknowns in complex samples. As GC/MS is an established technique, extensive unimolecular electron impact (EI) mass spectral libraries exist for the identification of unknowns. Much effort has gone into bringing LC to the same level as GC, especially with the development of liquid chromatography / mass spectrometry (LC/MS) and LC/MS/MS. For the measurement of target analytes at the ppt level, LC/MS/MS has demonstrated equivalent if not better detection limits to those obtained by GC/MS/MS [1].

Chapter 1 - Introduction

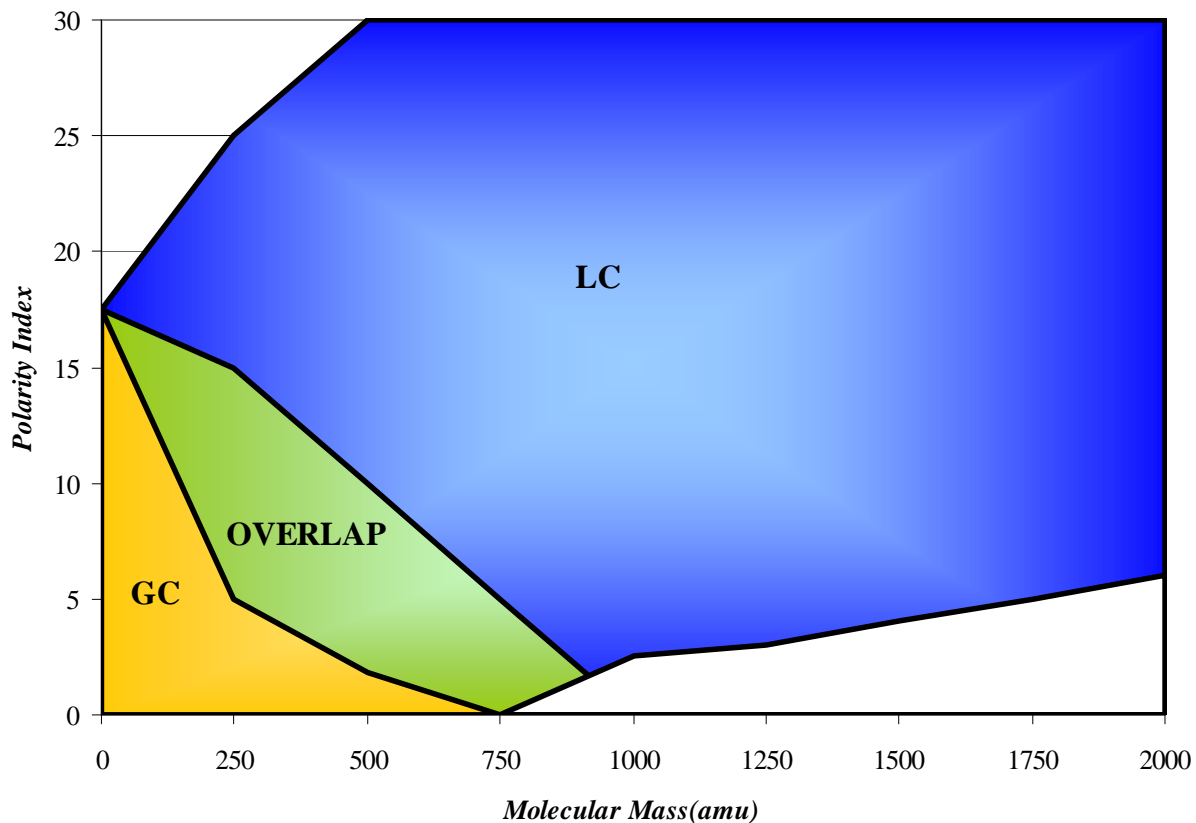


Figure 1.1 Graph showing the analytical domain of GC and LC using polarity versus molecular mass [20]. Copyright Global View Publishing, Pittsburgh, Pennsylvania, U.S.A. Reproduced with permission.

The three most common analytical techniques used for the analysis of estrogens from wastewaters are GC/MS, LC/MS and immunochemical techniques such as ELISA (enzyme linked immunosorbent assays) [21]. Furthermore LC/MS/MS and GC/MS/MS are able to accurately identify and quantify the estrogens at the required detection levels of 0.1 ng / L (ppt) or less [2, 3, 21-25], whereas the immunoassay techniques display measurement variation and can deliver false positives due to non-specific binding of estrogens and estrogen-like compounds to the antibody [3, 21-23, 26, 27].

MS/MS techniques provide added selectivity for very similar compounds. Selectivity is achieved when a certain mass fragment, unique to a particular analyte (or perhaps co-eluting with another) is allowed to move on to the second quadrupole (or TOFMS) for further fragmentation, while the other fragments are deflected. This is an advantage when estrogens having very similar structures cannot be separated effectively by the chromatographic system.

Chapter 1 - Introduction

For the analysis of estrogens in wastewater for example, where both conjugated and non-conjugated estrogens occur, no deconjugation of the estrogens is required since LC can easily separate larger molecules. This contrasts with GC analyses, where deconjugation and derivatization are required.

LC/MS suffers from several limitations, including the fact that only volatile buffers may be used as the LC mobile phase, often making separation of complex mixtures more complicated. In addition, complex samples, e.g. sewage water, often cause matrix effects which results in poor electrospray ionization of the analytes and therefore poorer and less reproducible sensitivity [28]. A general examination of the analytical methods used by GWRC members for monitoring of EDCs in water indicates that the majority of countries still prefer GC/MS [28].

In addition to this, LC/MS/MS is the most costly form of analysis due to the high cost of instrumentation, figure 1.2 [21]. The most common instruments found in the majority of routine analytical laboratories, particularly in South Africa, are those in the lower cost range, namely GC-FID, HPLC-UV, GC/MS and LC/MS (particularly in the pharmaceutical/ drug testing industries).

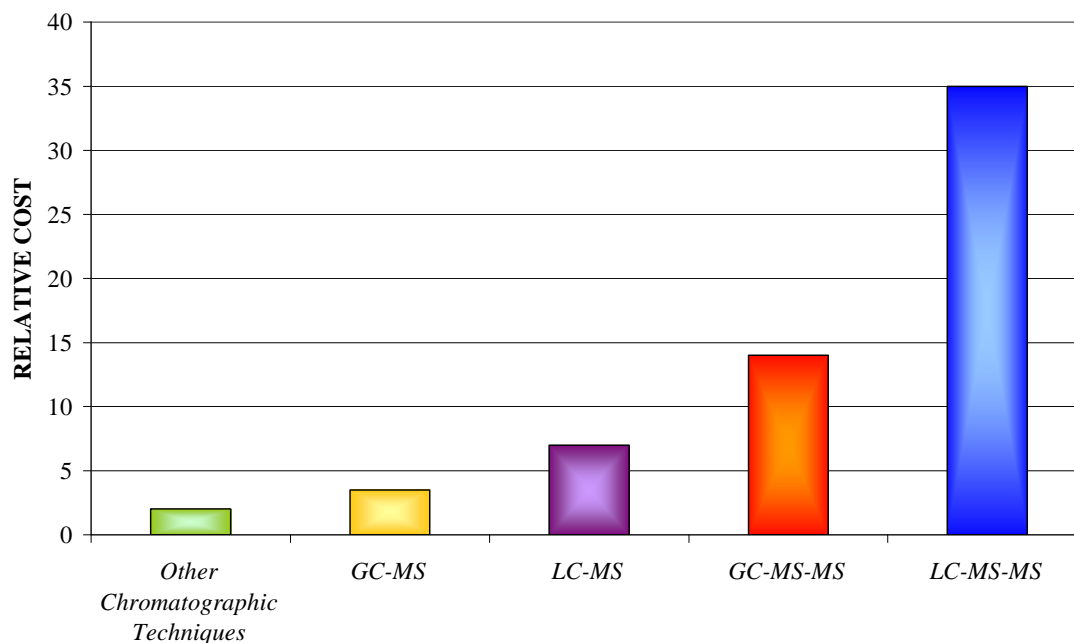


Figure 1.2 Chart representing the relative cost of the commercially available chromatographic and MS-hyphenated chromatographic instrumentation based upon data published in ref.21. Other chromatographic techniques are GC with flame ionisation or electron capture detection and HPLC with UV or fluorescence detection.

1.3. *Gas chromatography-mass spectrometry and the need for derivatization*

The routine use of GC/MS for the analysis of most compounds implies that a number of analytes have to undergo derivatization in order to be amenable to GC analysis. Regardless of the instrument used, some form of pre-concentration of the analytes is required before they can be physically detected by the analytical instrumentation. For extremely complex samples several possibilities are available to improve selectivity and ultimately the sensitivity of the measurement. In some cases, this can be achieved by including some form of derivatization during the sample preparation step. Alternatively, the instrument itself can enhance selectivity. For example, two-dimensional separations using GCxGC/MS can remove interference from the matrix, allowing for minimal sample cleanup [29]. A complex matrix can also be simplified using selective ionization techniques, with or without prior separation by GC or LC. These include negative chemical ionization (NCI) [29, 30] or the lesser known but extremely powerful resonance enhanced multiphoton ionization (REMPI) technique [31-37].

Real-time monitoring of trace organic compounds, such as polyaromatic hydrocarbons (PAHs) and polychlorinated biphenyls (PCBs), in air or process gases is not easily achieved. Measurement usually requires extended pre-concentration, cleanup of sample and instrumental analysis, for example by GC/MS, in a well-equipped analytical laboratory [38-40]. It involves a time-consuming and labour-intensive process that prevents the timely generation of data required for effective pollution-control measures. Recently, several on-line monitoring methods based on direct inlet mass spectrometry (MS) with soft and selective ionization methods have been established. These include chemical ionization MS [41] as well as photo-ionization MS techniques [32-36, 42-46].

One particularly powerful approach for real-time monitoring of aromatic compounds is resonance-enhanced multiphoton ionization time-of-flight mass spectrometry (REMPI-TOFMS). With this technique only aromatic compounds or compounds possessing conjugated systems are ionized before entering the TOFMS, thereby reducing the complexity of the sample matrix. This combination of selectivity and immediate availability of mass spectral information eliminates the time-consuming separation step of gas chromatography. Unfortunately, the relatively simple one colour two-photon REMPI process cannot easily detect compounds such as aliphatic aldehydes and amines that do not possess an aromatic chromophore.

Chapter 1 - Introduction

A fast method for the on-line detection of aldehydes and amines would have several potential applications in the field of process gas analysis, ambient air monitoring or emissions analysis. Furthermore, it would be desirable to benefit from the advantages gained by the REMPI-TOFMS method (i.e., selectivity, sensitivity, and measurement speed) in the detection of these aliphatic compounds.

1.4. Sample enrichment and preparation

Without the use of specialised instrumentation, sample preparation remains the most time-consuming analytical step prior to analysis. Much effort has gone into improving this process. The trend has been to move away from the use of toxic and expensive solvents to extract pollutants to other techniques that require either very few or no solvents at all. This often involves concentration of analytes on adsorbent materials followed by elution with a small volume of solvent, evaporation to 1 ml and injection of 1 μ l into the instrument. Alternatively the adsorbed analytes are thermally desorbed and introduced into the instrument, allowing for quantitative transfer of the entire sample into the instrument and therefore potentially lower detection limits.

Adsorbents are known to have several disadvantages. They possess active sites, which can result in chemical reactions either with the sorbed analytes being analysed or with the reagent used for derivatization. Tenax®, for example, is known to release benzaldehyde as one of its thermal degradation products, making it unsuitable for use in benzaldehyde analysis [47]. Some compounds may be irreversibly adsorbed on the sorbent. This is especially the case when polar compounds adsorb onto carbon sorbents [48]. Additionally, sorbents must undergo several pre-treatment steps before being packed into collection tubes. After the analysis, the sorbent must once again be subjected to several reconditioning and preparation steps before re-use. The entire process therefore becomes time-consuming. The ideal sorbent should be chemically inert, thermally stable and immediately reusable.

Over the last 15 years, polydimethylsiloxane (PDMS) or silicone rubber has gained widespread favour as the ideal liquid-like absorbent for pollutant concentration [47]. Analytes dissolve into the phase as they would in a solution. The silicone absorbent has a larger capacity or concentration range for which the partition isotherm is linear. In contrast, for adsorbents, once all available sites are occupied by a mono-layer, the adsorbent shows less retention for any further analytes entering the trap (non-linear

Chapter 1 - Introduction

partition isotherm). Furthermore, during thermal desorption, degradation of the silicone produces polymethylsiloxane compounds with reproducible retention times. In addition, these polymethylsiloxane compounds are easily distinguished by their electron impact (EI) mass spectral fragments. After thermal desorption, the silicone rubber is ready for use again. Two commercial PDMS devices have already gained widespread use namely solid phase microextraction (SPME) and stir bar sorptive extraction (SBSE - “Twister”) devices. The PDMS multichannel trap (MCT) developed in our laboratory has demonstrated its commercial potential. The use of derivatization in conjunction with PDMS has also been investigated. Unlike our MCT, which can be used in field sampling, the main drawback of the commercial devices is that they require bulky samples to be taken back to the laboratory for further preparation [47, 49].

Typical methods for determining the estrogens, alkylphenols and bisphenol-A are liquid-liquid extraction and solid phase extraction [1, 8, 9]. More recently PDMS has been used to concentrate these analytes from water, usually after conversion to their acetyl esters [50-56]. Typical detected levels of alkylphenols are in the low $\mu\text{g/L}$ range in river water and industrial effluents [57]; in freshwater sediments they are between 1 and 100 000 ng/g [58]. The lowest detection limits obtained for these compounds are at the low ng/L level [1].

The ideal analysis is on-site analysis. A significant reduction in errors is to be expected since the possibility of the sample changing during transport and storage is eliminated. However, a disadvantage at the moment is the poorer performance of the necessarily robust on-site instrumentation [59]. A compromise can be found by combining on-site sampling with off-site analysis since it has been stated by Pawliszyn [59], that analytes are more stable in the extraction phase than in the natural matrix [59]. As such, both the MCT as well as SBSE can be used for off-line concentration and storage of analytes in the PDMS matrix. However, the MCT sample collection procedure requires no electricity and is portable and rugged enough for field sampling, while the SBSE procedure requires a magnetic stirrer plate, for sample enrichment.

The open tubular structure of the MCT allows for the easy movement of air and water through the trap, including particulates. This makes the trap particularly suitable for sampling in the field (e.g. placed in a river) without any additional sample preparation. This also removes the additional complication of transporting large volumes of water and avoids losses resulting from the storage of dilute samples in glass containers. The advantage of the MCT lies in the minimal contact of analytes with container

Chapter 1 - Introduction

materials during sample collection and desorption. This reduces contamination arising from additional sample preparation steps. Any additional derivatization step required (to improve chromatographic elution and obtain additional selectivity and sensitivity) should therefore be performed *in situ*.

The PDMS MCT appears to be the simplest device for solventless sampling, concentration, derivatization and injection of air or water pollutants, as all these processes occur within the trap itself. The resulting chemical simplicity and minimum surface area provides the most inert conditions possible to minimize loss of analytes (including false negatives) and reduce other artifacts (including potential false positives due to sample carry-over) that so often invalidate results in ultra-trace analysis.

1.5. Aim of our study

Sampling methods for analytes in the environment are required that (1) reduce the complexity and cost of the sampling system involved (2) reduce the experimental uncertainties/errors and (3) lower the limit of detection. Versatile sampling methods that can cater for both air and water samples are of special importance.

On this basis, our research was carried out to develop an on-line concentration and derivatization method for low molecular mass aldehydes and alkyl amines, which could fulfil the above requirements using the polydimethylsiloxane (PDMS) open tubular traps and a mobile resonance enhanced multiphoton ionization time-of-flight mass spectrometer (REMPI-TOFMS).

In addition, multichannel silicone rubber traps (MCT) developed in our laboratories [61, 63-68] can be used to determine EDCs from water in combination with gas chromatography – flame ionization detection (GC-FID) and gas chromatography – mass spectrometry (GC/MS). Despite these compounds having a phenolic hydroxyl group, the bulk of the molecules are lipophilic in nature as expressed by their large octanol-water partition coefficients, rendering them ideal for PDMS extraction.

Chapter 1 - Introduction

Our aim was (1) to prepare stable gas standards of volatile aldehydes and amines (2) select and introduce a derivatizing reagent into the PDMS matrix in a convenient repeatable manner (3) demonstrate the efficient pre-concentration of the gaseous and aqueous standards on the reagent-coated PDMS traps (4) quantitatively recover and analyse the contents of the traps (5) demonstrate *in situ* derivatization on the PDMS traps for real samples.

1.6. Our approach

Sorptive extraction of alkylphenols, using SBSE, involves acetylation of the analytes *prior* to extraction. It has, however, been shown that there is no significant increase in the PDMS extraction of alkylphenols from water with or without acetylation. The extraction of bisphenol A, in contrast, improves dramatically with prior derivatization [54].

To demonstrate the versatility of the PDMS MCT, two approaches for concentration in PDMS would be investigated in this study, namely, 1) the on-line concentration and *in situ* derivatization of volatile polar analytes from air followed by REMPI-TOFMS detection, and 2) the concentration of phenolic lipophilic analytes from water requiring derivatization prior to analysis by GC/MS.

To render aldehydes and amines accessible to REMPI-TOFMS detection, a concept would be developed to convert the non-aromatic analytes into specific aromatic derivatives, which would then be detectable by REMPI-TOFMS (“photo-ionization labelling”). Derivatization reactions that in principle can be used for “photo-ionization labelling” are usually performed in liquid solutions. It has recently been demonstrated that a PDMS matrix can also be used as the reaction medium. A PDMS-based device, for example, has been used for *in situ* derivatization of low-molecular-mass aldehydes for GC/MS analysis [60, 61].

The principle of the “photo-ionization labelling” derivatization that would be investigated is as follows; the analytes from the sample gas current (i.e. containing traces of the amines or aldehydes to be analyzed) as well as the derivatization reagent are co-absorbed in a PDMS trap. After a short enrichment phase, the trap is heated. The heating induces both the derivatization reaction itself and the thermal desorption of the formed derivatives. The desorbed derivatives are subsequently transferred to

Chapter 1 - Introduction

the REMPI-TOFMS spectrometer for analysis. This procedure can be repeated at close intervals for on-line analysis.

The concept of using the multichannel PDMS trap as a “one-pot” concentration and derivatization device would be tested for the extraction of alkylphenols from water. Our approach would be first to extract the analytes into the PDMS matrix, and then to derivatize *in situ* in order to convert the hydroxyl functional group to an ester. The ability of the MCT to efficiently extract the alkylphenols directly from water, followed by an efficient conversion to their trifluoroacetate [62] derivatives *in situ* would be investigated.

1.7. Arrangement and presentation

Chapter 2 introduces sample preparation techniques for concentrating analytes from air and water, focussing on pre-concentration devices, particularly those using PDMS. Chapter 3 presents the concept of derivatization as well as the derivatization reactions available for the determination of aldehydes and amines in air, and estrogens/ alkylphenols in water. Various modes of sample introduction into the analytical instrument are summarised in chapter 4. Chapter 5 describes the application of on-line PDMS open tubular trapping with *in situ* derivatization to the determination of low molecular mass aldehydes and alkylamines from air. Chapter 6 discusses initial derivatization studies of estrogens; the application of our multichannel PDMS traps for concentrating and derivatizing alkylphenols and bisphenol-A from water. Conclusions are summarized in chapter 7 and the accredited journal publication of results obtained in chapter 5 appears in the appendix.

Chapter 2

Concentration Techniques

2. Introduction

Samples, which require analysis, are often too dilute, too complex or otherwise incompatible with the chromatographic system. Hence, some form of sample preparation is essential prior to instrumental analysis. Ideally, sample preparation should involve limited effort and expense. Minimal sample preparation will decrease the amount of experimental uncertainty in the results obtained. The diagram in figure 2.1 shows a brief summary of the enrichment and recovery techniques that are most commonly used for concentrating analytes from gaseous and aqueous phase samples.

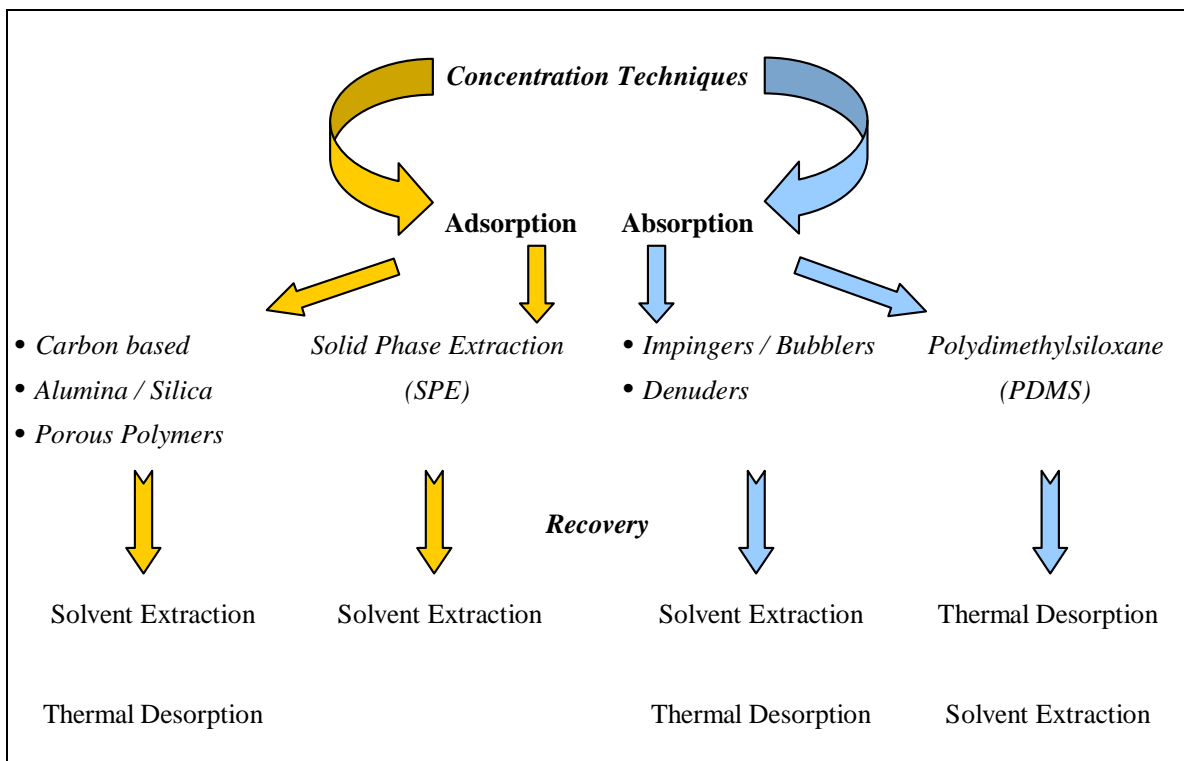


Figure 2.1 Diagram of concentration and recovery techniques most commonly used for concentrating analytes from gaseous and aqueous phase samples.

2.1. Adsorption

Adsorption is a physical process occurring on the surface of adsorbents. As analytes are retained on active surfaces on the sorbent, the amount of adsorption that occurs is related to the available surface area of the sorbent, which in turn is related to the porosity of the sorbent material. The rate of adsorption is determined by the structure both of the micropores and of the molecules moving into the pores [69]. Table 2.1 in Appendix 1 lists the types of adsorbents most commonly used for pre-concentration, as well as their structures, surface areas and pore diameters, uses, advantages and disadvantages.

2.1.1. Carbon-based, alumina, silica and porous polymers

Adsorption tubes are prepared by packing the sorbent into glass tubes of varying sizes depending on the required application. When choosing a sorbent for pre-concentration, it is important to see not only how well compounds are adsorbed, that is their retention, but also how easily they can be recovered. Carbon-based adsorbents are cheap, all purpose pre-concentration sorbents. However, desorption of the adsorbates (particularly polar compounds) may prove difficult and water accumulation is high, making them unsuitable for thermal desorption with cryogenic focusing [48].

Porous polymers are typically used for pre-concentrating high molecular mass and non-volatile compounds such as pesticides. They are popular because they are relatively inert, have large surface areas and are hydrophobic. They also permit the collection of large sample volumes (100 L) at high flow rates [70]. However, general disadvantages of porous polymers include the displacement of VOCs especially by CO₂ [48], and the irreversible adsorption of certain compounds, such as amines [48]. Furthermore oxidation, hydrolysis and polymerisation of the sample may occur [48]. Except for Tenax®, these adsorbents are thermally unstable above 250°C, which makes them unsuitable for thermal desorption as this leads to artefact formation [48]. At the same time, these sorbents are not reusable after solvent desorption. Careful purification of these sorbents, which usually involves soxhlet extraction with high purity solvents, is compulsory before they can be used for trace analysis [48]. Finally, porous polymers are more expensive than the charcoals.

Most solid sorbents are well-suited for trapping specific compounds. In order to trap a wider range of compounds, multi-layered traps, utilising the best features of each adsorbent, have been prepared [71, 72]

Sorbents generally used with solvent extraction include silica gel, activated charcoal, Anasorb 747, carboxens (carbonised porous polymers), porous polymers and carbon molecular sieves. Those used in sampling with thermal desorption include Tenax®, Chromosorb 106, graphitised carbons and carbon molecular sieves [69].

2.1.2. Solid phase extraction (SPE)

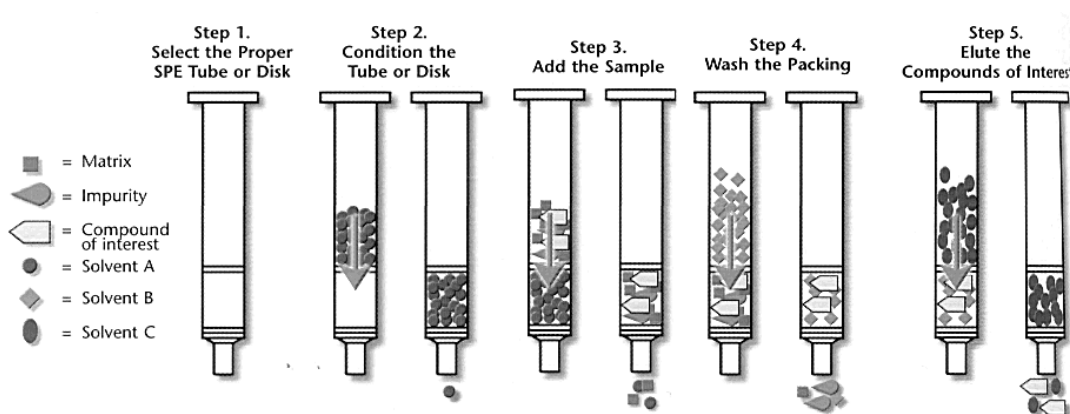


Figure 2.2 Use of a SPE device [73].

Unlike liquid-liquid extraction (LLE), which involves partitioning of the analyte between two immiscible liquid phases, SPE involves partitioning of the analyte between a solid and a liquid phase. The analyte is extracted when its affinity for the solid phase is greater than for the liquid phase. Later, the analyte is removed by extraction with a solvent for which the analyte has a greater affinity. The SPE device is depicted in Figure 2.2. The SPE cartridge consists of a packed adsorbent column between two fritted plastic/metal disks in a polypropylene open syringe barrel [73].

Chapter 2 – Concentration Techniques

The liquid phase is passed through the cartridge by gravity, suction or positive pressure (e.g. gas pressure from a syringe). Retention is caused by the intermolecular forces experienced between the analyte, the active sites on the sorbent-surface and the liquid phase [74].

SPE is not, traditionally, a technique used for pre-concentrating gaseous compounds. It has been used, predominantly, as a reagent coated sorbent [75-77] for derivatization, and for the extraction of derivatized products formed during liquid extraction [78].

Common sorbents used for SPE are based on silica gel with a modified surface. According to the chemical groups bonded to the silica, the phases are classified as non-polar, polar or ion-exchangers. Octadecyl surface phases (C18) are used for the reverse-phase extraction of non-polar compounds in aqueous solution. The shorter octyl phases (C8), are used to extract medium polarity compounds, while silica gel and alumina (Al_2O_3) are used to extract polar compounds [79].

SPE is simple, requires less solvent and less time than LLE, and is easily automated. However, the many steps required to prepare the sorbent and then extract the analyte, as depicted in figure 2.2., can be tedious. Also, the packing quality varies from cartridge to cartridge [78]. Granted, not all modern synthetic phases require sorbent preparation. The synthetic (non-silica based) SPE packings have not demonstrated significant variation between cartridges or batches.

Background contaminants from SPE have been measured at the 2 ng/mL level. They include phthalates and other plasticizers originating from the manufacture of the plastic frits and syringe barrels.

Undecane, originating from the sorbent material (C18), has been measured at 5 ng/mL [80].

To overcome problems encountered with the SPE cartridges, disk devices have been developed, namely, membranes or sorbents that have been packed into circular disks 0.5 mm thick and 4 to 96 mm in diameter. The sample processing rates are faster than those of the traditional SPE columns and the small diameter disks are ideal for processing smaller samples [78].

2.1.3. Cryo-trapping from the gas phase

Gaseous volatile compounds can be trapped at temperatures lying far below their respective boiling points. This is usually achieved by collecting whole air samples through steel tubes or capillaries, which are cooled by using either liquid nitrogen or carbon dioxide. To increase the condensing surface, the tubes are packed with an inert material that possesses a high surface area such as glass-wool or beads. The tubes are then heated ballistically to a suitable injection temperature and the analytes are transferred onto the column. This set-up is not always sufficiently portable for field work, and extra care must be taken when sampling in humid environments as pre-concentrated water will freeze and block the trap [48].

2.2. Absorption – dissolution of analytes from gases and liquids

Absorption is synonymous with dissolution and partitioning. In this process, the analyte is dissolved into a liquid where it is retained until it can be thermally desorbed or preferentially extracted into a different solvent for which the analyte has a greater affinity. This can typically be expressed as a gas-liquid extraction (when a gas phase analyte is involved) or liquid-liquid extraction (when a liquid phase analyte is involved).

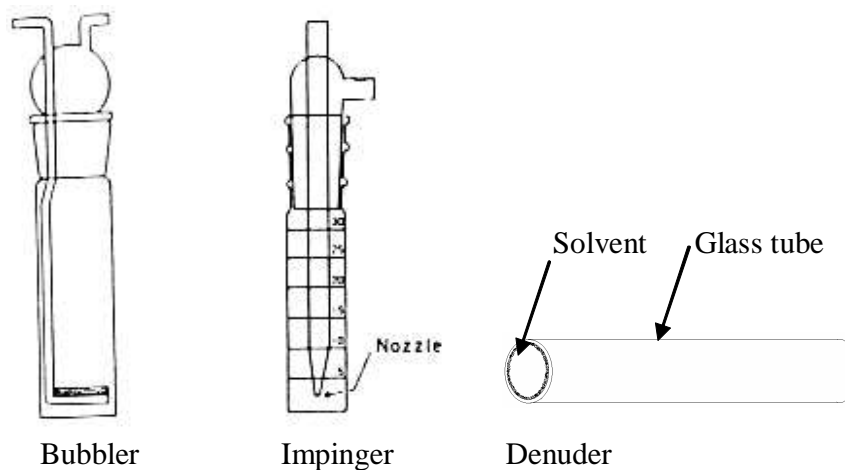


Figure 2.3 Liquid phase extraction devices [81].

2.2.1. Impingers and bubblers for gaseous samples

Special devices such as impingers and bubblers are used to disperse sampled gas in a solvent, see Figure 2.3. The finely divided gas bubbles rise from the bottom of the vessel, allowing for more contact between the gas bubbles and the solvent as the bubbles move toward the surface. In the case of reactive compounds such as formaldehyde, a derivatizing reagent is included with the solvent to improve extraction efficiency and simultaneously provide a more stable compound [81]. Adjusting the temperature of the solvent may also improve extraction. These devices are often used for sampling of gases from industrial stacks and automobile exhausts. However, large sample volumes are generally needed requiring the use of large pumps and extraction devices that are clumsy to wear for personal occupational sampling. Due to the large volumes of solvent used a dilution factor is also present and an additional concentrating step is required [47, 81].

2.2.2. Denuders for gaseous samples

Denuders are open glass tubes that have been coated on the inside with a thin layer of solvent as in Figure 2.3. As air is sucked through the tubes, analyte gas, present in the air, is extracted into the solvent. Unlike impingers and bubblers, higher collection flow-rates may be used. The extract is more concentrated on account of the smaller volume of solvent used [47]. Impingers and denuders have the advantage that any appropriate solvent can be used to trap a desired compound.

2.2.3. Polydimethylsiloxane (PDMS) as dissolution medium

Unlike the previous two techniques, extraction into PDMS can be viewed as dissolution into a “gum-like” phase, as opposed to a liquid phase solvent. Adsorbents, LLE and SPE techniques, are undesirable because they carry contaminants into the final extracted sample, along with the analytes of interest, producing a high background in the analysis. Recently, polydimethylsiloxane (silicone) has emerged as an alternative to adsorbents and organic solvents traditionally used for pre-concentration [49, 60, 63-66, 82-90]. The PDMS structure is depicted in figure 2.4.

Chapter 2 – Concentration Techniques

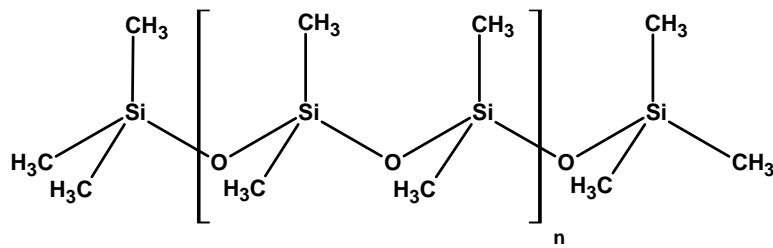


Figure 2.4 The structure of polydimethylsiloxane (PDMS).

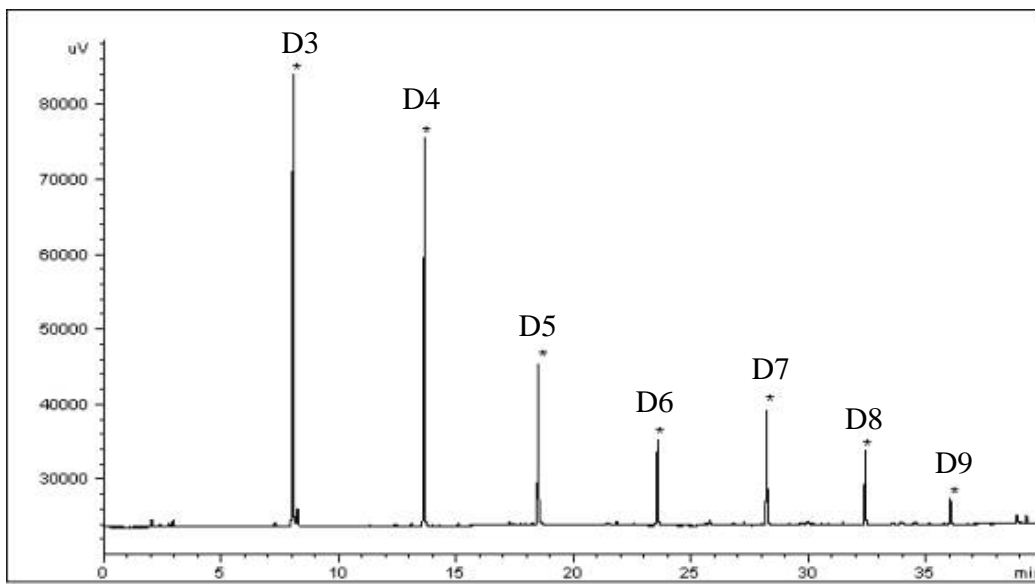


Figure 2.5 Thermal desorption run of a blank PDMS MCT.

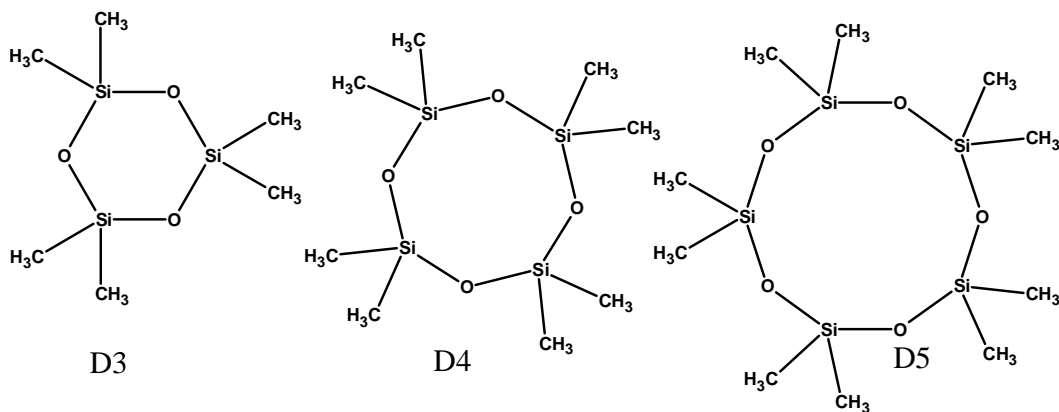


Figure 2.6 Structure of the PDMS methylsiloxane degradation products D3, D4 and D5.

Chapter 2 – Concentration Techniques

Polydimethylsiloxane is a non-polar, homogeneous liquid stationary phase used in GC capillary columns, generally known as SE-30, DB-1 or HP-1 columns. Just as the sample mixture injected onto a GC column will partition between the mobile and stationary phases, leading to a separation of components, so too, will gaseous mixtures in air partition into silicone. As previously discussed, the breakthrough volume of analytes determines their retention in the trap. The trapped contents in the silicone can then be extracted either by using a solvent [91] or by thermal desorption [66, 82].

Apart from being inert, the silicone “fluid” is thermally stable (between 150 and 250°C) under oxygen-free conditions [79]. The advantage of thermally desorbing the silicone lies in the immediate reusability of the material. In addition, all the silicone degradation peaks reveal repeatable retention times (see figure 2.5), as well as characteristic electron impact (EI) mass spectral fragments m/z 73, 207, 211 and 281. The main volatile silicone degradation products are methylcyclosiloxanes, the most abundant of these being hexamethylcyclotrisiloxane (D3) followed by gradually decreasing amounts of the higher molecular mass cyclic siloxanes (D4, D5, D6...) see figure 2.6 [92]. Figure 2.7 demonstrates how desorption temperature impacts on the amount of PDMS degradation that will occur. PDMS degrades significantly at desorption temperatures above 220°C.

As “like-dissolves-like”, polar compounds will have lower retention on a non-polar phase. Modified polymers e.g. polymethylacrylates etc. [49, 83, 93] have therefore been developed in an attempt to increase the polarity of the stationary phase. However, these polymers no longer exhibit a dissolution process, but rather an adsorptive process with all associated disadvantages, particularly high backgrounds during thermal desorption [83]. As opposed to other adsorbents on the market, silicone, has predictable thermal degradation products (by retention time and mass spectral fragments), displays a large linear partition isotherm and is immediately reusable after thermal desorption. Due to these remarkable properties silicone has been widely used as an adsorbent, leading to several possible configurations as described below, and depicted in figure 2.8, 2.9 and 2.10.

Chapter 2 – Concentration Techniques

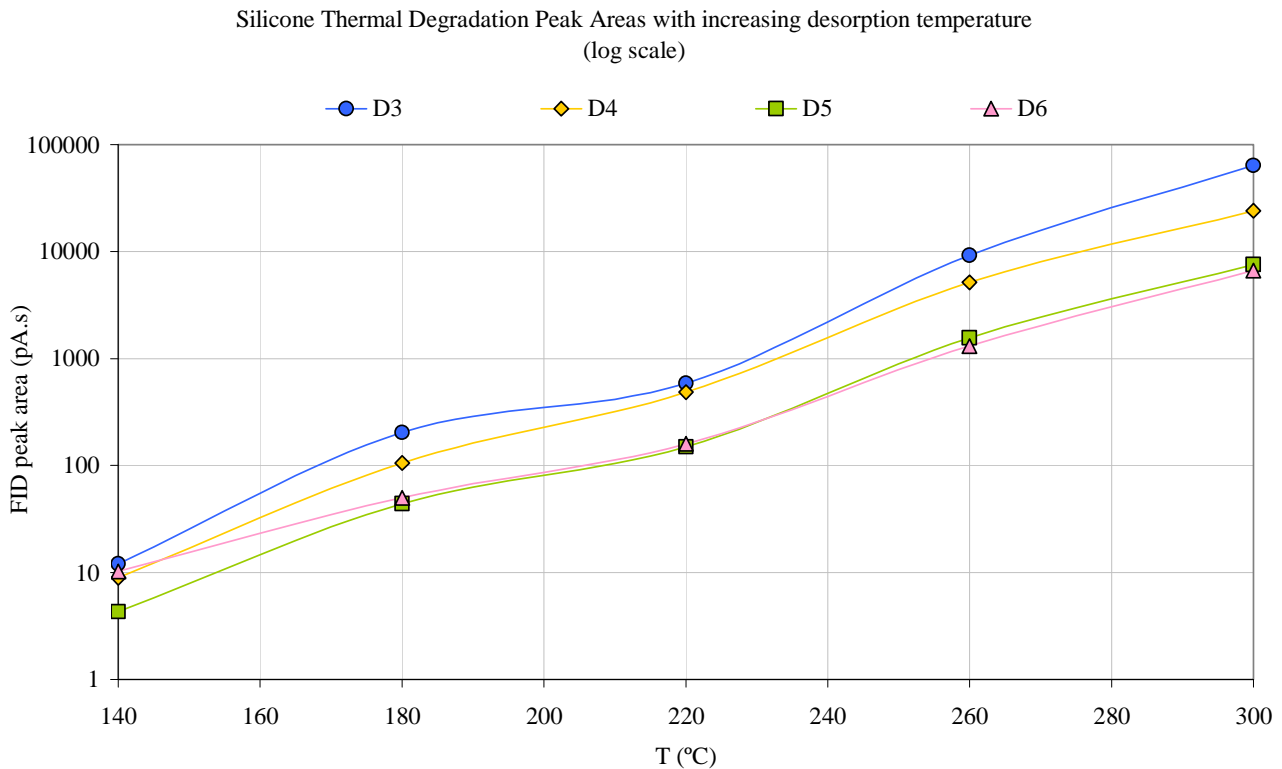


Figure 2.7 Increased thermal degradation of PDMS with increasing temperature.

Data obtained by desorbing a PDMS MCT for 10 min at each of the indicated desorption temperatures, desorb flow-rate 50 ml/min, cryotrap -100°C, inject for 1 min at 300°C. The respective siloxane degradation peaks were integrated to obtain peak areas (which were plotted on a logarithmic scale) versus desorption temperature.

The majority of silicone elastomers incorporate fillers. They act as material extenders but also reinforce the cross-linked polymer matrix. Fumed silica (SiO_2) fillers produce silicone rubbers with high tensile strength, reduced stickiness, increased hardness and elongation capability [94]. Silicone elastomers for medical applications use only fumed silica fillers [94]. According to Baltussen *et al* [95], commercial PDMS tubing contains approximately 40% v/v fumed silica (SiO_2) as filler. The PDMS volumes depicted in figure 2.8 represent the corrected (40% less) PDMS substance available for concentration.

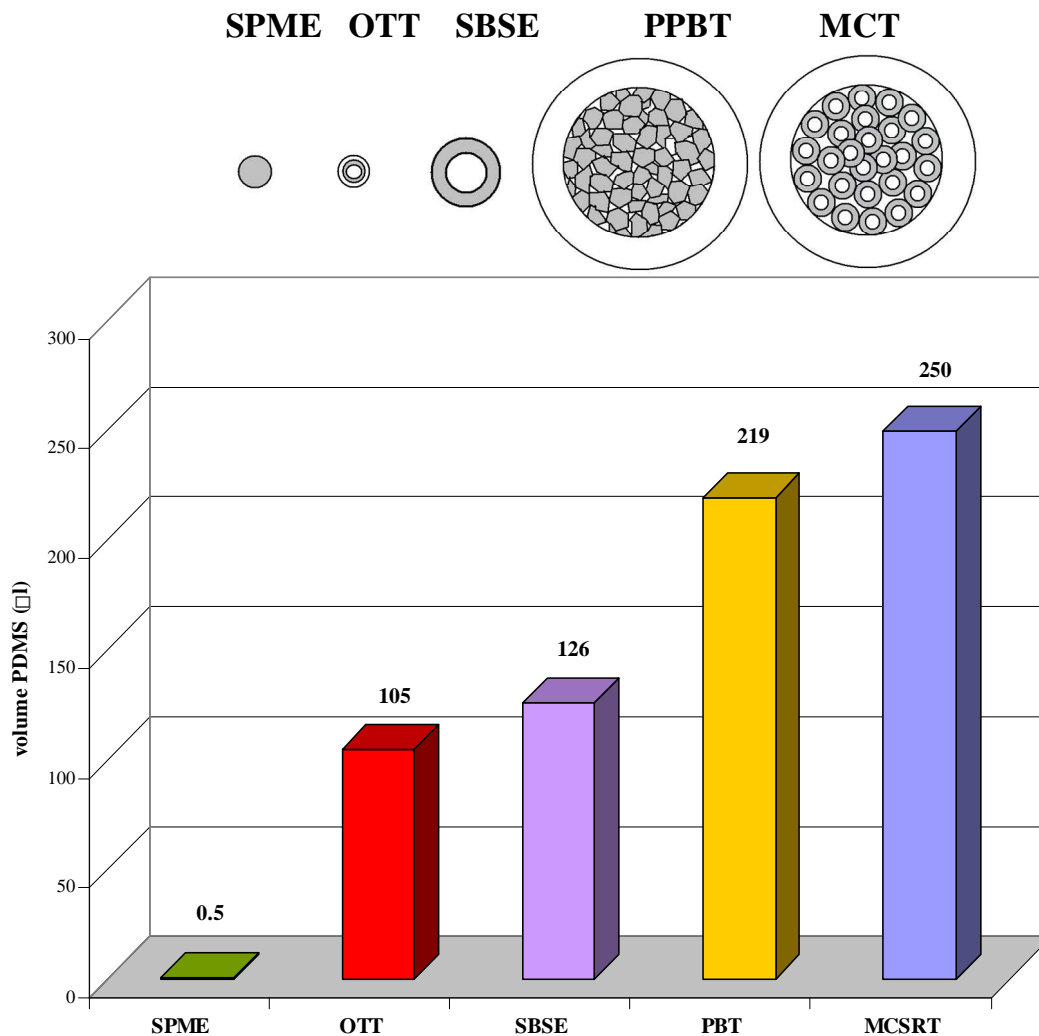


Figure 2.8 Cross-sections of the various PDMS configurations, with their corresponding PDMS volumes graphically depicted below them [95, 96*].

SPME: 100 µm PDMS solid phase microextraction fibre (PDMS volume 0.5 µl*)

OTT: Ultra thick film open tubular trap, consisting of a silicone rubber tube (d_f 145 µm) inserted in a 1 m long wide bore capillary (PDMS volume ~ 105µl)

SBSE: Maximum PDMS commercially available 20 mm length x d_f 1.0 mm PDMS film coating a magnetic glass stir bar (PDMS volume 126 µl)

PPBT: Pulverized silicone rubber particles (PDMS volume 219 µl)

MCT: 32 silicone rubber tubes (0.63 mm o.d. x 0.3 mm i.d. x 5 cm lengths) arranged in parallel (PDMS volume 250 µl)

2.2.3.1. Open tubular traps (OTT)

Grob and Habich [97] introduced the use of OTTs to overcome problems experienced due to incomplete transfer of desorbed analytes from packed column traps onto GC capillary columns. The difference in flow rates obtained when moving from a packed column to a capillary column was eliminated by using the OTT, which has similar dimensions to a capillary column. Different coatings, ranging from activated charcoal to SE30, were used inside the OTTs for the pre-concentration of various compounds [84, 91, 97-98].

This led to the development of ultra thick film OTTs, by Blomberg and Roeraade [85, 86], and Burger *et al* [84, 87]. Blomberg and Roeraade used dynamic coating techniques that require special instrumentation. By comparison, Burger's technique is easier to prepare. A single 1m long silicone rubber tube is inserted into a fused silica capillary, to provide a film thickness of 145 μm . The silicone tube is first stretched and then immersed into liquid nitrogen. In this way it is sufficiently manageable to allow for insertion into the capillary, figure 2.8. The capillary is then fitted into a modified GC where it can be thermally desorbed onto another GC column for analysis. However, the OTTs show limited sampling capacity and can only operate under low sampling flow rates (10 ml/min).

A more modern and user-friendly application of OTT, called in-tube solid phase microextraction (SPME), was developed by Pawliszyn *et al* [100]. In this case a length of open tubular capillary, with an appropriate stationary phase, is housed within the SPME needle assembly, used to pierce the sample vial, figure 2.10 [100, 49]. The entire sampling and desorption steps are automated via a six-port valve. During in-tube sampling the aqueous sample is repeatedly aspirated from the sample vial through the OTT and then dispensed back to the vial by movement of the syringe. Following the extraction step, the six-port valve is switched to desorb the analytes from the OTT by flushing an appropriate solvent, contained in another vial, through the capillary. This flushed volume is taken up in the sample loop and injected into the HPLC or GC system [100-103]. This technique has the advantage of having a variety of stationary phases available to concentrate analytes of varying polarity, and are stable towards solvents used in LC for solvent desorption of the OTT. In-tube SPME has been applied to the analysis of polar thermally labile phenyl urea pesticides on an Omegawax 250 GC capillary column (0.25 mm

i.d., 0.25 μm film thickness). Here the 1.4 ml sample undergoes up to 50 aspirate/dispense steps at a sample flow rate of 63 $\mu\text{L}/\text{min}$. Detection limits for this method were later improved upon, by using a custom made polypyrrole-coated capillary, which showed superior extraction efficiency [103].

2.2.3.2. *The multichannel silicone rubber trap (MCT)*

Ortner and Rohwer developed the multichannel silicone rubber trap [61, 63-68]. It is based on the same principle as the open tubular traps developed by Burger *et al* [87]. However, instead of inserting a single long silicone rubber tube inside a fused silica capillary, the MCT is made more compact by arranging several shorter lengths of silicone rubber tubes in parallel inside a glass tube, depicted in figure 2.8. This makes the trap suitable for desorption in a conventional desorption unit. Due to its open tubular design the MCT exhibits a lower pressure drop than levels associated with packed beds, allowing for higher sampling flow rates of up to 1 L/min, particularly for the collection of non-volatile analytes. To improve the extraction of semi-volatile analytes from the gas phase into the silicone [64, 65] the MCT is operated under low sampling flow rates (15 ml/min) where an increased number of plates (N) is required. For aqueous samples extremely low flow rates of 75 $\mu\text{l}/\text{min}$ are typically used. At this flow rate benzene afforded 11 plates on the 32 multichannel trap [63].

The use of MCT's has already been demonstrated for concentrating semi-volatiles in air and water, and geosmin, low molecular mass amines and aldehydes in air and beer aromas [61, 63-68, 104].

The MCT consists of a glass tube containing several smaller silicone rubber tubes, each 10 cm long, arranged in parallel [61, 63-68, 104] as shown in Figures 2.8. and 2.9. SIL-TEC medical grade silicone tubing for the silicone rubber trap was obtained from Technical Products Inc. (Georgia, U.S.A). It has been shown that the MCT has a very low pressure drop (or flow resistance) with properties similar to the packed PDMS trap described below.



Figure 2.9 A polydimethylsiloxane multichannel trap (PDMS MCT). This trap has 32 x ~2 cm lengths of PDMS tubes arranged in parallel inside a glass tube. This shorter arrangement is suitable for trapping less volatile analytes which require longer desorption times.

2.2.3.3. *Packed particle bed traps (PPBT)*

Baltussen *et al* [82, 83, 88-90] packed a glass tube with equally sized particles of pulverised 100% polydimethylsiloxane, shown in figure 2.8. As this method of packing allows for a low-pressure drop over the trap along with turbulent flow, high sampling flow rates (500 ml/min) can be used. These packed beds have been successfully applied to the analysis of organic acids, PAHs and nitro-PAHs from air [88], for characterisation of natural gas [82], for the monitoring of nicotine in air [90], and of amines, pesticides and PAHs in aqueous samples [83, 89]. An added benefit of these traps is the fact that breakthrough volumes for gas phase analytes can be calculated and predicted through their retention on an SE-30 column [82]. For aqueous samples, the removal of water before thermal desorption and cryo-trapping, is essential. However, all volatile analytes are lost in this process [83, 89].

2.2.3.4. *Solid phase microextraction (SPME)*

The SPME technique developed by Pawliszyn *et al*, is in principle a solventless liquid extraction [49]. The SPME device resembles a syringe. A 1 cm long thin fibre coated with a polymer, normally silicone, is attached to the tip of the syringe plunger, which can be retracted into the syringe barrel, as

Chapter 2 – Concentration Techniques

depicted in figure 2.9 [105]. This device is practical for piercing septa and only exposing the fibre to a hot GC inlet, vial etc.

Unlike the other pre-concentration techniques, which are typically dynamic as they involve a flowing stream of gas passing over the sorbent, SPME is a static sampling technique. The fibre is either exposed to the headspace of a sample or immersed in a liquid sample in a sealed vial for a precise period of time. The analytes will partition into the liquid phase until a distribution-equilibrium is reached. This process usually takes between 2-30 min. Equilibrium can be attained more quickly in headspace SPME than in immersion SPME, as the analytes can diffuse more rapidly towards the fibre. This extraction step is equivalent to one theoretical plate (N). From the equation below [49, 105], it can be seen that the amount extracted (n), is directly proportional to the concentration of the analyte in the sample (C_o).

$$n = \frac{K_{fs} V_f V_s C_o}{K_{fs} V_f + V_s} \quad (2.1)$$

Where K_{fs} is the distribution coefficient between the fibre and sample. V_f is the volume of the fibre, V_s is the sample volume and C_o the initial concentration of the analyte in the sample [49, 105].

Consequently, trace analysis of analytes having a small partition coefficient (K_{fs}) will require sensitive instrumentation.

As for solvent extraction, the extraction efficiency of SPME can be improved by adjusting the pH, temperature, fibre (“solvent”) polarity, fibre thickness, salt content and agitation. Various SPME fibre coatings, of differing thickness, have been developed by forming copolymers with the silicone (e.g. PDMS/DVB for semi non-polars), adding adsorbent material to the coating (e.g. Carbowax/PDMS), or by using a different polymer (e.g. polyacrylate for polar compounds). However, these variations do not exhibit dissolution properties as described for the liquid silicone polymer above [105].

Chapter 2 – Concentration Techniques

When the analyte is too volatile or unstable, derivatization techniques can be used. Derivatization is performed either in the aqueous medium prior to extraction, or by coating the fibre with derivatizing reagent followed by reaction with the analyte (*in situ* derivatization) or, after extraction where analytes in the fibre are derivatized by exposure to the reagent headspace or by direct immersion in the reagent [60, 106]. SPME is suitable for the analysis of large sample volumes, as shown by equation (2.2), taken from (2.1) where $V_s \gg K_{fs}V_f$ [49, 105],

$$n = K_{fs} V_f C_o \quad (2.2)$$

As the amount extracted by the fibre is independent of the sample volume, the thickness of the fibre plays a larger role. Compounds with a low K_{fs} , are efficiently extracted by using a thicker fibre. After extraction, the fibre is conveniently thermally desorbed in a hot GC inlet during the splitless mode. Or in the case of HPLC the elution solvent dissolves / purges the analytes off the fibre [107].

For precision and to save time, reproducible fibre exposure time, desorption time, vial size, sample volume and other sampling parameters are much more important parameters than obtaining full equilibration between fibre and analyte.

This sample preparation technique has become popular because it is simple, rapid and solventless while also demonstrating low detection limits. However, the fibre has proven fragile and is easily destroyed if not handled with care. Also, due to memory effects resulting from the complexity of the sample and desorption conditions used, the fibre may not be reusable. Contaminants arising from the SPME fibre (DVB or CW) have been measured below 2 ng/mL. These include 1, 9- nonanediol and highly bis-substituted phenols (originating from the epoxy glue used to attach the fibre to the stainless steel needle). Bis (2-ethylhexyl) phthalate has been measured between 5 to 20 ng/mL [80]. Under ideal conditions, the fibre assembly can provide 50-100 extractions [105].

Chapter 2 – Concentration Techniques

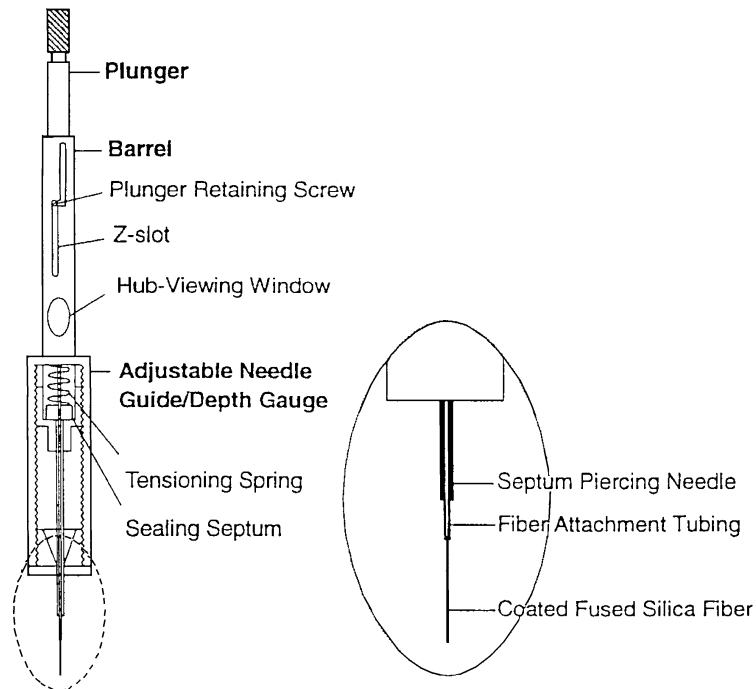


Figure 2.10 The first commercial SPME device from Supelco [49].

As an application of SBSE, headspace sorptive extraction (HSSE) [108, 109], uses a small glass rod coated with a large amount of polydimethylsiloxane (50 mg). As is the case for the SPME fibre, the rod is exposed to headspace samples. However, it is then thermally desorbed in an automated thermal desorber. The HSSE technique shows increased sensitivity over SPME, as the volume of absorbent (V_f) is much larger.

Another new, though similar approach called a sample enrichment probe (SEP) was developed by Burger *et al* [110]. A 15-mm sheath of PDMS tubing is stretched over a stainless steel rod (13 cm x 1.5 mm). The PDMS is evened out by rolling the PDMS-coated rod between glass plates. The resulting volume of PDMS is larger than for SPME and similar to HSSE. However, the probe is desorbed in a GC inlet, removing the need for an expensive thermal desorption unit. The probe is custom-made with matching thread to fit the septum cap of a Carlo Erba® GC. Sampling bottles are adapted to fit the probe. The carrier gas is switched on shortly after desorption has occurred. A thick film column is used to aid focussing of the desorbed analytes [110]. A comparison between SPME and the SEP for

extraction of the headspace volatile compounds in Rooibos tea has demonstrated the superior extraction properties of the SEP relative to SPME [110].

2.2.4. Stir bar sorptive extraction (SBSE)

Stir bar sorptive extraction (SBSE), introduced by Sandra and co-workers, consists of a glass stir bar coated with 50-300 μl PDMS [95]. The stir bar is placed inside an aqueous sample where the analytes may partition into the PDMS whilst being stirred. Depending on the sample volume and the stirring speed, equilibration times are expected to lie between 30 to 60 minutes.

The amount of analyte recovered is described by the equation:

$$\frac{m_{PDMS}}{m_0} = \frac{\left(\frac{K_{O/W}}{\beta}\right)}{1 + \left(\frac{K_{O/W}}{\beta}\right)} \quad (2.3)$$

Where m_{PDMS} is the mass of analyte in the stir bar, m_0 is the total mass of analyte in the sample, $K_{O/W}$ is the octanol-water partition coefficient for the analyte and β is the phase ratio ($\beta = V_w / V_{PDMS}$) [95].

The stir bar is then removed and may undergo either thermal or solvent desorption [95, 111]. SBSE has also been applied to biological fluids and heterogeneous matrices such as fruit pulp [112, 113] in addition to several other applications mentioned in chapter 3. Unlike SPME, a thermal desorption unit with cryogenic focussing is required to thermally desorb the stir bars. However, the SBSE has a much higher analyte capacity, owing to the larger volume of PDMS available for concentration, and can therefore reach much lower detection levels than SPME.

2.3. *Dynamic and static equilibrium*

SPME, SBSE and HSSE are static sampling techniques; OTT, PPBT and MCT are dynamic sampling techniques [114]. In the case of static sampling the sample and the extractant are in contact with each other the whole time. The analytes first have to diffuse towards the extractant and then partition into it until an equilibrium is reached between the 2 phases. To encourage diffusion of analytes towards the extractant the sample is agitated through stirring, mixing or sonication [114]. Selection of the extractant is based on the “like-dissolves-like” principle, described in the section entitled solvent extraction below.

During dynamic sampling the sample is introduced to the extractant over time i.e. not all at once. This is comparable to a chromatographic system where the extractant is the stationary phase and the sample is the mobile phase [114].

The sample enters the trap at an optimum flow rate that provides the “column” with the maximum number of plates. The various analytes in the sample partition into the PDMS with an effectiveness determined by their distribution coefficients (for gaseous analytes $K_{\text{PDMS/GAS}}$ obtained from GC retention indices; for aqueous analytes : $K_{\text{PDMS/W}} \approx K_{o/w}$). At a given point in time, a certain analyte will have partitioned entirely into the PDMS, while the sample (“mobile phase”) continues to move through the “column”. The continued movement of the sample (behaving as the “mobile phase”) through the column will cause the retained analyte in the PDMS to start eluting off the “column” once it has exceeded its retention volume on the trap. When the analyte starts to leave the trap it has reached its breakthrough volume. Depending on which analyte is of interest in the sample, sampling is generally stopped when 5 % or less of the initial analyte concentration has broken through. The process is called breakthrough sampling. Figure 2.11 demonstrates the extraction of analyte from a finite sample onto a PDMS trap.

Chapter 2 – Concentration Techniques

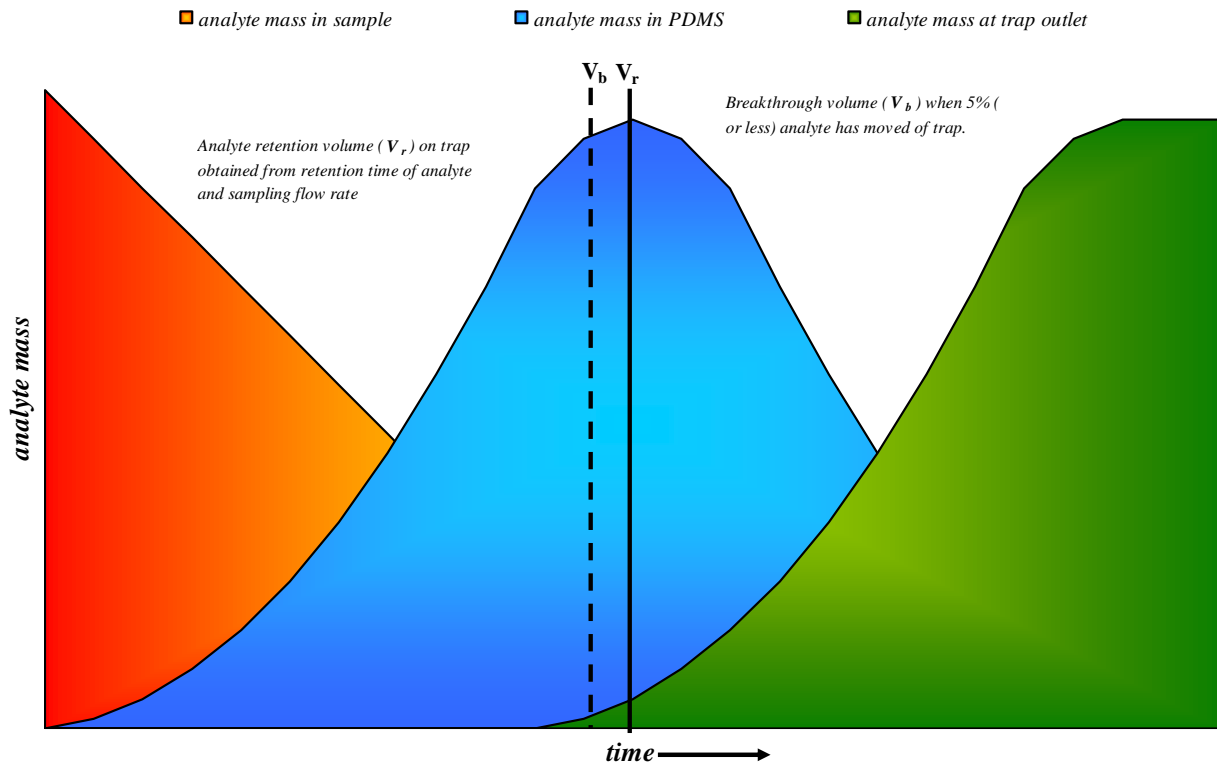


Figure 2.11 Mass profiles over time for the dynamic sampling of a finite sample on a PDMS trap. The analyte mass in the sample reduces as the analyte accumulates in the PDMS, before the analyte reaches its retention volume on the trap it will breakthrough and can be measured at the outlet of the trap.

When an unlimited amount of sample is available, then dynamic equilibrium sampling is an option. In this case, sampling continues beyond the breakthrough volume of the selected analyte of interest. Equilibrium extraction occurs at the point where the analyte concentration in the sample equals the analyte concentration exiting the trap. The process is depicted in figure 2.12. This process requires a much longer period of time.

Determination of extraction efficiencies / recoveries using PDMS static and dynamic sampling in the gas and aqueous phases are described below.

Chapter 2 – Concentration Techniques

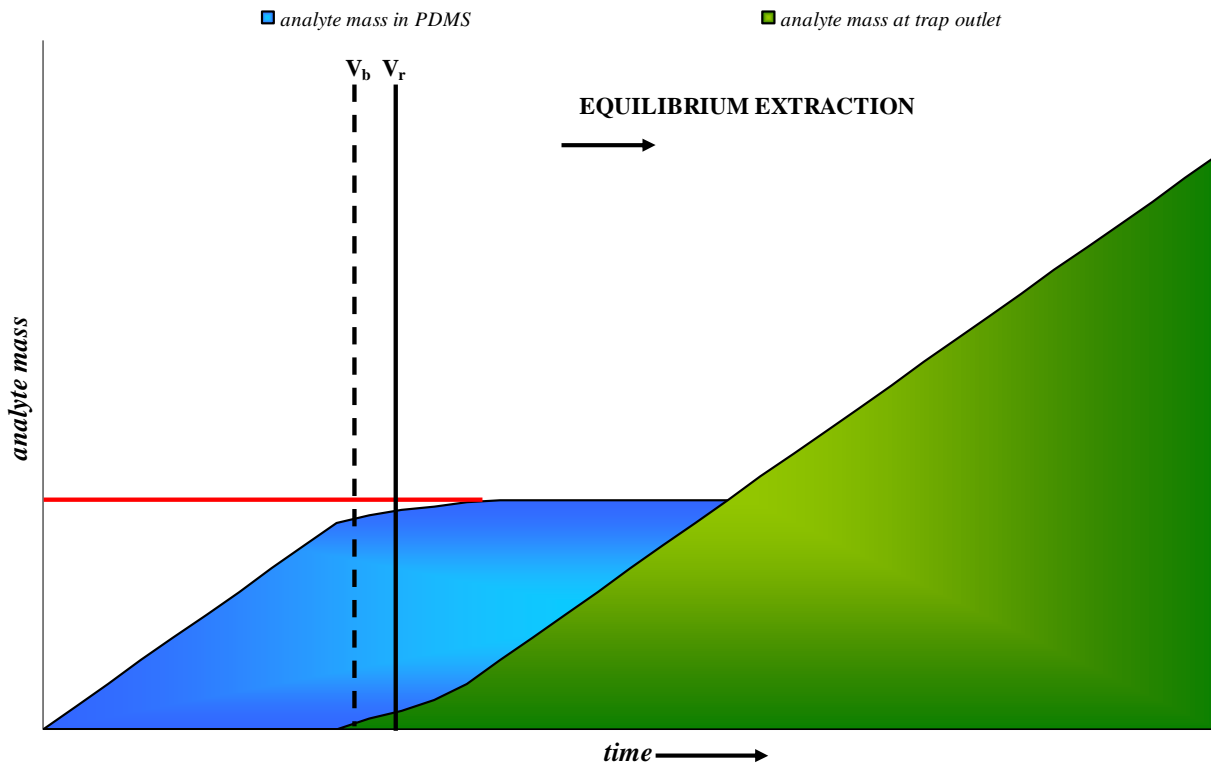


Figure 2.12 Mass profiles over time for the dynamic sampling of a constant supply of a bulk sample on a PDMS trap. Equilibrium extraction occurs when the analyte concentration entering the trap is the same as the analyte concentration exiting the trap.

2.4. Gas and Liquid phase PDMS extraction

In brief, the partitioning between analytes in the gas phase and PDMS can be predicted by the retention of analytes in a PDMS capillary column and a carrier gas (dominated largely by the volatility of the analyte), while the partitioning of analytes in water into PDMS can be predicted by the octanol-water partition coefficients of the analytes. Account is taken of the fact that octanol is slightly more polar than PDMS and that $K_{\text{PDMS}/\text{W}}$ is not equal to $K_{\text{o/w}}$.

2.4.1. Gas Phase Static Sampling

The maximum amount of analyte extracted by a SPME fibre is given by equation 2.1.

$$n = \frac{K_{fs} V_f V_s C_o}{K_{fs} V_f + V_s} \quad (2.1)$$

K_{fs} , the fibre coating/ sample distribution constant, which plays a large role in the extraction efficiency of the fibre, can be predicted using isothermal GC retention times for a given analyte, on a column that has an identical stationary phase and temperature to the SPME fibre, e.g. PDMS fibre with SE30 column at sampling temperature[49].

For a gaseous sample the correlation between K_{fs} and retention time is described by the following:

$$K_{fh} = K_{fg} = (t_r - t_m) \times F \times \frac{T}{T_m} \times \frac{p_m - p_w}{p_m} \times \frac{3}{2} \times \frac{(p_i / p_o)^2 - 1}{(p_i / p_o)^3 - 1} \times \frac{1}{V_L} \quad (2.4)$$

Where K_{fh} and K_{fg} , are the respective fibre/ headspace and fibre/gas distribution constants, t_r and t_m , are the retention times for the analyte and unretained compound respectively. F is the column flow rate; T_c and T_m are the respective temperatures of the column and flow meter; p_m , p_w , p_i and p_o are the pressures of the flow meter, saturated water vapour, column inlet and outlet, respectively. V_L , is the volume of stationary phase present in the capillary column [49].

Another alternative to determine K_{fh} at the sampling temperature – often room temperature, is to use the linear temperature programmed retention index system (LTPRI) available from published tables [49].

Chapter 2 – Concentration Techniques

For PDMS:

$$\log K_{fh} = \log K_{fg} = 0.00415 \times \text{LTPRI} - 0.188 \quad (2.5)$$

If the LTPRI is not available for a particular analyte, it can be determined experimentally from a GC run from the definition below:

$$\text{LTPRI} = (100 \times N) + \left[100 \times \frac{t_{R(A)} - t_{R(N)}}{t_{R(N-1)} - t_{R(N)}} \right] \quad (2.6)$$

N, is the number of carbon atoms for the n-alkane; $t_{R(A)}$, $t_{R(N)}$ and $t_{R(N-1)}$ are the retention times for the analyte, n-alkane and n-1 alkane, respectively [49].

2.4.2. Gas Phase Dynamic Sampling

Breakthrough volume is a measure of the retention of an analyte on a sorbent i.e. retention capability. Tubes packed with ad/absorbents can be regarded as chromatographic columns operating under frontal analysis conditions with a constant concentration of analyte. The analyte will continue to be ad/absorbed in the trap until it reaches its breakthrough volume (V_b). This is usually when 5% or less of the initial concentration of the analyte has started to elute from the trap. The maximum sampling volume or breakthrough volume (V_b), is described by Raymond and Guiochon [115] as:

$$V_b = V_r \times \left(1 - \left(\frac{2}{\sqrt{N}} \right) \right) \quad (2.7)$$

Where V_r is the retention volume and N the number of plates of the trapping column. However, for short “columns” with a low number of plates (N), Lövkvist and Jönsson [96], have suggested a more realistic model for breakthrough volume. This can be described by:

Chapter 2 – Concentration Techniques

$$V_b = V_r \times \left(a_0 + \left(\frac{a_1}{N} \right) + \left(\frac{a_2}{N^2} \right) \right)^{-1/2} \quad (2.8)$$

Where a_0 , a_1 and a_2 are coefficients for different values of the breakthrough level b described as [96]:

b = total amount of analyte eluted from trap / total amount of analyte sampled

b can vary from 0.1, 1, 2 to 10%, the popular value being 5%.

Baltussen *et al* [47, 82] have applied this theory for breakthrough volume at 5%, to their PPBT's, giving:

$$V_b = V_0 \times (1+k) \times \left(0.9025 + \left(\frac{5.360}{N} \right) + \left(\frac{4.603}{N^2} \right) \right)^{-1/2} \quad (2.9)$$

Where V_0 is the trap dead volume and k the capacity factor.

The capacity factor k can be calculated by:

$$k = \frac{K}{\beta} \quad (2.10)$$

Where β is the phase ratio and K the equilibrium distribution coefficient that for an alkane in PDMS at any temperature can be calculated as follows:

$$K = \exp \left(\frac{950 + 905 \times C}{1.987 \times T} - 0.59 \times C - 1.8 \right) \quad (2.11)$$

T is the absolute temperature and C the carbon number of the alkane.

Chapter 2 – Concentration Techniques

To determine K for non-alkanes an alternative formula was derived by Baltussen *et al* [47, 82], using Kovats Retention Indices (RI) defined as follows:

$$RI = 100 \times \frac{\log(t'_A) - \log(t'_z)}{\log(t'_{z+1}) - \log(t'_z)} + 100 \times Z = 100 \times \frac{\log(K_A) - \log(K_z)}{\log(K_{z+1}) - \log(K_z)} + 100 \times Z \quad (2.12)$$

Where Z is the number of carbons in the *n*-alkane eluting just before the compound of interest (A), t'_i is the net retention time and K_i is the equilibrium constant of the component *i*.

This definition can be rearranged to give:

$$\log(K_A) = \log(K_z) + \left(\frac{RI}{100} - Z \right) \times (\log(K_{z+1}) - \log(K_z)) \quad (2.13)$$

The RI values of analytes at a specific trapping temperature are available as published data sets [47], K_{Z+1} and K_Z can be calculated using Equation 2.11.

To solve equation 2.9, the plate number N needs to be determined using the Knox equation for packed columns [47]:

$$h_r = 3\nu^{1/3} + \frac{1.5}{\nu} + 0.05\nu \quad (2.14)$$

h_r , is the reduced plate height and ν the reduced velocity in the trap (packed column) which are defined as follows [47]:

$$h_r = \frac{H}{d_p} = \frac{L}{N \times d_p} \quad (2.15)$$

$$\nu = \frac{u \times d_p}{D_M} \quad (2.16)$$

Chapter 2 – Concentration Techniques

Where H is the plate height (m), d_p is the diameter (m) of the particles used to pack the trap, L , the length of the trap “column”, u , the linear velocity ($\text{m}\cdot\text{s}^{-1}$) in the trap and D_M is the diffusion constant ($\text{m}^2\cdot\text{s}^{-1}$) of the analyte in the mobile phase. It should be noted that these equations are only valid if the pressure drop over the trap is negligibly small [47, 82, 114].

2.4.3. Aqueous Phase Static Sampling

The extraction efficiency of analytes from aqueous phase samples into PDMS is largely determined by the partition coefficient between water and PDMS. These coefficients can be determined through a laborious process. Alternatively the octanol-water partition coefficient $K_{o/w}$, which correlates well to PDMS-water partitioning, can be used to predict the extraction of aqueous analytes into PDMS [95, 114].

$$K_{O/W} \approx K_{PDMS/W} = \frac{C_{PDMS}}{C_W} = \frac{m_{PDMS}}{m_W} \times \frac{V_W}{V_{PDMS}} \quad (2.17)$$

Since the phase ration β is described by:

$$\beta = \frac{V_W}{V_{PDMS}} \quad (2.18)$$

Equation 2.17 can be rewritten to give:

$$\frac{K_{O/W}}{\beta} = \frac{m_{PDMS}}{m_W} = \frac{m_{PDMS}}{m_0 - m_{PDMS}} \quad (2.19)$$

Where m_0 is the total amount of analyte present in the sample.

Chapter 2 – Concentration Techniques

After rearranging equation 2.19, the extraction efficiency or recovery can then be described by equation 2.3:

$$\frac{m_{PDMS}}{m_0} = \frac{\left(\frac{K_{O/W}}{\beta}\right)}{1 + \left(\frac{K_{O/W}}{\beta}\right)} \quad (2.3)$$

2.4.4. Aqueous Phase Dynamic Sampling

The retention volume of an analyte from water on a dynamic sampling trap can be determined from the equation:

$$V_r = V_0 \left(1 + \frac{K_{O/W}}{\beta}\right) \quad (2.20)$$

Where V_r and V_0 are the trap's retention and void volumes respectively.

If V_r is known, then the breakthrough volume can be determined from Lövkvist and Jönsson's equation:

$$V_b = V_r \left(0.9025 + \frac{5.360}{N} + \frac{4.603}{N^2}\right)^{-1/2} \quad (2.21)$$

Where V_b represents a breakthrough volume at 5% sample concentration at the trap outlet and N , the number of plates in the trap.

For the PPBT, developed by Baltussen *et al* [114], the Knox equation is used to determine N as described in equations 2.14 and 2.15.

Chapter 2 – Concentration Techniques

For the MCT, developed by Rohwer et al [63-68], N is experimentally determined from:

$$N = 16 \left(\frac{V_r}{\omega} \right)^2 \quad (2.22)$$

where ω is the base width of the analyte peak (obtained from elution analysis) between the peak tangents [66].

2.4.5. Equilibrium extraction in dynamic sampling

As indicated above, with an unlimited supply of sample, it is possible to stop sampling well past the breakthrough volumes of the analytes [114]. At this point the analytes are in complete equilibrium with the PDMS, i.e. the concentration of analyte entering the PDMS is equivalent to the concentration of analyte leaving the PDMS. The analyte concentration (C) in the sample can therefore be described by the following equation (for K values significantly larger than 1):

$$C = \frac{m_{PDMS}}{V_r} = \frac{m_{PDMS}}{V_0 \times \left(1 + \frac{K}{\beta} \right)} \approx \frac{m_{PDMS}}{V_{PDMS} \times K} \quad (2.23)$$

where m_{PDMS} is the mass of analyte absorbed in the PDMS, V_r , V_0 and V_{PDMS} are the retention, void and PDMS volumes respectively. K is the equilibrium distribution coefficient and β the phase ratio [114].

2.5. Phase ratio and analyte capacity

From equation 2.3,

$$\frac{m_{PDMS}}{m_0} = \frac{\left(\frac{K_{O/W}}{\beta}\right)}{1 + \left(\frac{K_{O/W}}{\beta}\right)}$$

it can be seen that for static sampling from aqueous phases, the phase ratio, β , plays a critical role in the recovery of analyte. The phase ratio β , is defined as the ratio of sample to trapping phase i.e. V_w / V_{PDMS} .

Figure 2.11 represents graphically equation 2.3 for 3 different PDMS configurations (for a 10 ml water sample). SPME has the largest phase ratio (20 000), followed by SBSE (100) and the MCT (40). This implies that in order to get good recoveries SPME requires very large $K_{O/W}$'s. Figure 2.11 shows that SPME never reaches 100% recoveries, even with extremely large $K_{O/W}$, whereas SBSE and the MCT achieve ~ 100% recovery for $K > 1000$. Although the MCT is not a static sampling technique, when operating under equilibrium extraction conditions (sampling beyond the breakthrough volumes) it is essentially operating near static equilibrium sampling conditions. The MCT displays improved recoveries compared with SBSE at the $K_{O/W} < 1000$. For example, for a $K_{O/W}$ of 100, the MCT can obtain recoveries of 70% while the SBSE obtains only 50%.

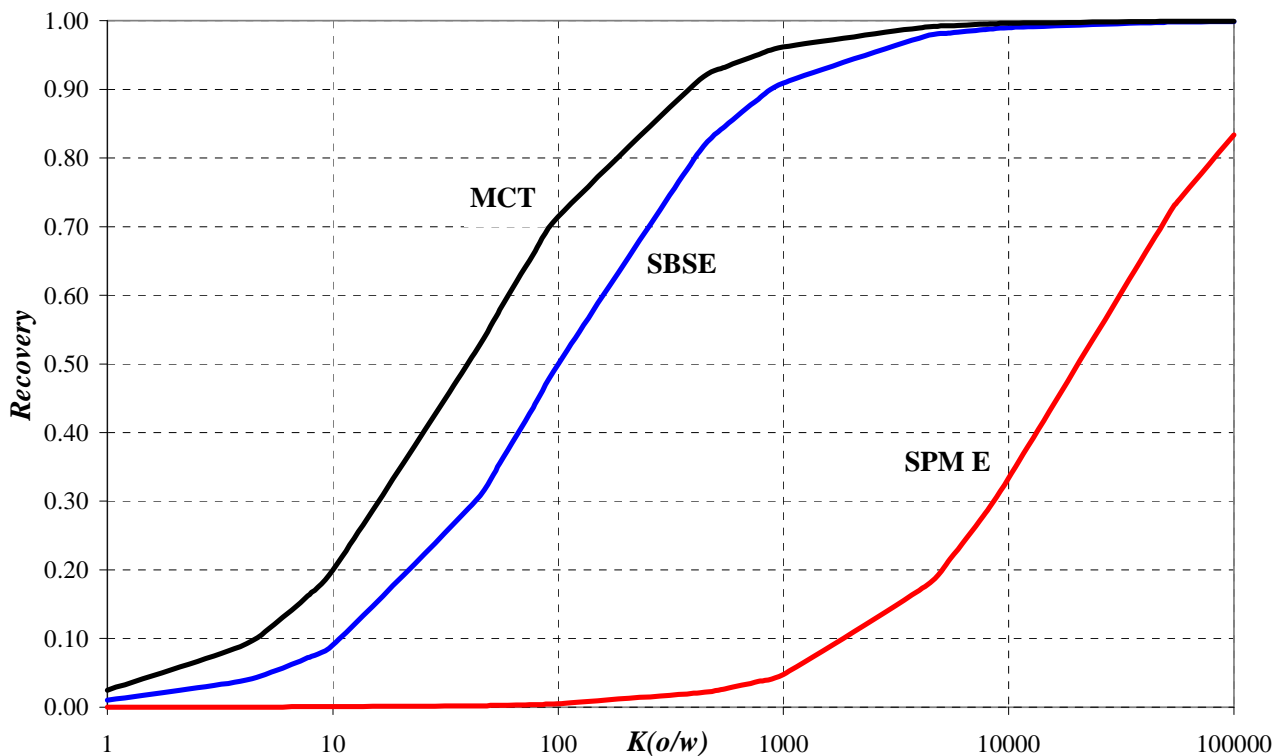


Figure 2.13 Recovery as a function of the octanol-water partition coefficient (K_{ow}) of the analyte in 3 different PDMS configurations. The graph was obtained by calculation using equation 2.3 and values for β as stated in section 2.5.

2.6. Recovery

2.6.1. Solvent Extraction

This technique is otherwise known as liquid-liquid extraction [81, 116]. A solvent can be used to isolate analytes from a liquid sample or from a solid, in our case the sorbents. The technique relies on a distribution of the analyte between two immiscible liquid phases. For acids and bases the distribution coefficient ($K = C_{\text{solvent}} / C_{\text{sample}}$) is easily affected by the pH of the solution. In this way the extraction can be made more selective. In general, the principle that “like-dissolves-like” is applied. Polar analytes will dissolve into polar solvents and non-polar analytes into non-polar solvents.

Chapter 2 – Concentration Techniques

The sample solution is shaken up with an equal amount of solvent in a separation funnel. When the 2 phases separate, the desired fraction is collected. The extraction efficiency increases with the number of extractions. Because the final fraction still contains a large amount of solvent, an extra step is required to concentrate the extract before it can be analysed. Analytes with small K 's or large sample volumes require continuous extraction or counter current extraction to achieve a complete separation [81, 116]. Overall, this is a simple but time-consuming technique. The general trend is to move away from these methods. In addition, the large volumes of high purity solvents required for such extractions have proven toxic and expensive.

Recently, these disadvantages have been minimised with the introduction of liquid-liquid micro-extractions. Typically, 1 ml of solvent is added to 10ml of sample in a vial. The extract can then be injected without further pre-concentration.

2.6.2. Thermal Desorption

Thermal desorption is the process through which the analytes on a sorbent are removed by heat energy. During this process, the analytes are transferred onto the chromatographic column. However, it is common to have a refocusing step before transfer onto the column. Usually, a second trap is cooled, using either liquid nitrogen or CO₂ gas, to sub-ambient temperatures ranging from 0°C to –100°C. This second trap is heated ballistically after desorption, in order to transfer the analytes in a narrow plug onto the column. A description of the instrument used for thermal desorption is given in chapter 4.

Thermal desorption has several advantages over solvent extraction, principally the removal of the dilution effect. With solvent extraction only a small fraction of the entire extract is injected for analysis. In addition, thermal desorption requires no expensive high purity solvents or labour to perform the liquid extractions as automated thermal desorption units allow for desorption of several traps overnight. Disadvantages include the occasional blocking of the cryogenic trap, although this can be prevented by avoiding the use of hydrophilic sorbents. Furthermore, instrumentation and use of large quantities of liquid nitrogen are expensive [47, 48].

Chapter 3

Derivatization

3. Introduction

In analytical chemistry, derivatization is the process of chemically modifying a compound to produce a new compound that has properties that are suitable for instrumental analysis.

Whether gas or liquid chromatography is used for the analysis of analytes, at some point or another derivatization of certain analytes will be required. In the case of gas chromatography it is most often a matter of improving the chromatographic properties of the analyte. Gas chromatographic analysis of compounds, having functional groups with “acidic” hydrogens such as -COOH, -OH, -NH₂, -NH and -SH, are of great concern. These functional groups tend to form intermolecular hydrogen bonds, which affect the volatility and thermal stability of the compound. Moreover they will often interact unfavourably with active sites in the GC inlet and with the stationary phase of a poorly deactivated capillary column. Strong interactions between the “acidic” hydrogen and silanol groups on the inner surface of the capillary column result in nonlinear adsorption effects. These effects manifest themselves as tailing peaks in the chromatogram. Integration of these chromatographic peaks particularly at trace levels yields results with poor precision. As a result, several methods exist to convert most analyte functional groups such as carbonyls, carboxylic acids and alcohols into their less interactive Schiff bases and esters. In addition, this process also improves the physical, chemical and thermal stability of the analytes before GC analysis [107, 117-119].

In both LC and GC, derivatization is used to improve the detection properties of the analyte towards a specific detector. Careful selection of derivatizing reagents allows, for example, the introduction of a fluorescent chromophore onto an analyte permitting sensitive HPLC- fluorescent detection of the analyte. Halogenated derivatives deliver increased detection by electron capture, negative chemical ionization and selected ion mass spectrometric detection. Halogenation has the additional benefit of providing heavier ions in the mass spectrum, without changing the volatility (and therefore the GC retention) of the analyte. This provides mass selectivity in GC-MS runs. Also a reagent that reacts

Chapter 3 - Derivatization

selectively with one particular functional group in the presence of others, will decrease the sample complexity whilst simultaneously improving the sensitivity of the analysis [107, 117-119].

Ideally, a good derivatization reagent should provide a single derivative with a high and reproducible yield. Apart from the formation of the derivative, the reagent should not cause any restructuring of the original analyte e.g. formation of enols or dehydration reactions. The derivative should be distinguishable and separable from the starting materials. The reaction should proceed rapidly at room temperature and not require complicated laboratory techniques. It should be selective and avoid the use of hazardous reagents or harsh reaction conditions [107, 117-119].

It would appear that the advantages of derivatization should appeal to everyone undertaking analyte detection. However, derivatization is generally only used as a final resort, as it is always preferable to limit the amount of sample preparation to a minimum so that no additional contamination or errors are introduced into the analyses. Table 3.1 below summarizes the advantages and disadvantages of analyte derivatization.

In this chapter, emphasis is placed on the derivatization of aldehydes, amines and phenol and alkyl-hydroxylated compounds, as these are the types of analytes investigated in this study.

Table 3.1 Advantages and disadvantages of analyte derivatization.

<i>Advantages</i>	<i>Disadvantages</i>
Improved detection properties of the analyte i.e. increased sensitivity	Additional sample preparation steps, solvents and reagents required
Improved mass selectivity as derivatives yield higher masses in the mass spectrum	Incomplete analyte conversion
Improved physical (volatility), chemical (polarity and acidity) and thermal properties of the analyte	Potential sample contamination from impurities in the reagents and solvents used
Selective conversion of analytes decreases complexity of the sample matrix	Sample losses due to additional use of glassware etc.

3.1. Classification

In general derivatization reactions can be classified either according to the functional group that needs to be converted, for example carboxylic acids (-COOH) and alcohols (-OH), or by the nature of the resulting derivative, for example, a silyl (-SiR₃), alkyl (-R) or acylated (-COR) derivative [107, 117-119]. Each type of derivative, if appropriately selected for an application, has its own benefits. A brief summary of the 3 main derivative categories is described below.

3.1.1. Alkylation

Alkylation is the replacement of the “acidic” or “active” hydrogen in carboxylic acids (R-COOH), alcohols (R-OH), thiols (R-SH), and amines (R-NH₂) with an aliphatic alkyl or aryl group. The general rule of thumb is that “as the acidity of the active hydrogen decreases, the strength of the alkylating reagent must be increased”. Although this implies that the selectivity and applicability of the method becomes more limited as the reagents and conditions become harsher [120-125].

Alkylation has largely been applied to the conversion of organic acids into esters, particularly methyl esters. This process is sometimes referred to as esterification. In a typical reaction esterification involves the condensation of the carboxyl group of an acid and the hydroxyl group of an alcohol, with the resulting elimination of water [120-125].

Trimethylsilyl derivatives of carboxylic acids are more easily formed than the alkyl derivatives. However, they offer limited stability compared to the alkyl esters which can, if required, be isolated and stored for extended periods of time [120-125].

3.1.2. Acylation

Acylation involves the replacement of the “acidic” hydrogens on alcohols (-OH), thiols (-SH), and amino (-NH) groups with an acyl group to form esters, thioesters and amides respectively. Insertion of perfluoracyl groups is very popular as these also permit electron capture detection (ECD) and

Chapter 3 - Derivatization

thus negative chemical ionization mass spectrometry (NCI-MS) as well. In addition, the carbonyl groups adjacent to halogenated carbons enhance the response of the ECD. An extra benefit of acylation is the formation of fragmentation-directing derivatives for GC-MS analysis.

Perfluoroacylation reagents can be classified into three main groups: fluoro acid anhydrides, acyl chlorides and fluoracylimidazoles [121, 122].

The fluorinated anhydride derivatives of alcohols, phenols and amines are both stable and highly volatile. However, these derivatives produce acidic by-products, which must be removed prior to instrumental analysis. Typically, an organic base such as triethylamine is used to drive the reaction to completion whilst consuming the acidic by-products. However, it is critical that a pH less than 6 is used during the reaction and extraction steps, as the unprotonated base will catalyze the hydrolysis of the just-formed derivatives [126].

The fluoracylimidazoles react readily with hydroxyl groups and secondary or tertiary amines to form acyl derivatives. In this case the imidazole by-product is relatively inert and does not require removal prior to analyses [126].

3.1.3. Silylation

Silylation is the most widely used derivatization technique, as it can convert nearly all functional groups hydroxyls, carboxylic acids, amines, thiols and phosphates into silyl derivatives. In this case the “acidic” hydrogen on the analyte is replaced with an alkylsilyl group, most frequently, trimethylsilyl (-SiMe₃).

Silylation reagents and their derivatives react rapidly with water and thus require extremely anhydrous reaction conditions. The *tert*-butyl dimethylsilyl derivatives are slightly less sensitive to moisture due to their bulky nature, although this also means that their formation requires more time.

Trimethylchlorosilane (TMCS), together with trimethylsilyl-imidazole (TMSI) or *tert*-butyldimethylchlorosilane (TBCS) and *tert*-butyldimethylsilyl-imidazole (TBSI), are usually added as catalysts to enhance derivatization.

Chapter 3 - Derivatization

TMS derivatives are notorious for the formation of silylation artefacts [127]. Very pure solvents should be used to avoid the formation of excessive peaks in the final chromatogram. Under certain conditions functional groups such as aldehydes, amides, carboxylic acids, esters and ketones will form additional silyl derivatives and by-products. The silylation reagent often reacts with itself, other inorganic/organic reagents and/or organic solvents to yield artefacts [127].

Silylation reagents can accumulate in the analytical system. The silyl imidazole reagents form inert by-products that should neither accumulate nor damage the analytical system. Extra care should be taken not to avoid introducing silylation reagents into systems that contain “active” hydrogens e.g. Carbowax® columns [121, 122].

3.1.4. Schiff bases

The formation of a Schiff base occurs when a carbonyl functional group (on aldehydes and ketones) condenses with an amine functional group to release water. Depending on which analyte is to be derivatized, one group will be the reagent the other the target analyte. This reaction is extremely selective as only the carbonyl or amine group will be converted.

3.2. Derivatization of aldehydes

As the low molecular mass aldehydes acetaldehyde, acrolein, crotonal, propanal, butanal and particularly formaldehyde were selected for this study, a review of only the derivatization techniques most commonly used for determining these aldehydes, will be described below.

3.2.1. Hydrazones

2,4-DINITROPHENYLHYDRAZINE (DNPH)

In other studies formaldehyde has been collected in an impinger [128] and bubbler [129] containing DNPH, on DNPH coated sorbents [130-132], DNPH coated glass fibre [133], sintered glass [134] and

PDMS SPME fibre [106]. HCHO reacts *in situ* with the DNPH solution to form the 2,4-dinitrophenylhydrazone chromophore which can be determined using HPLC with UV detection or GC-ECD/MS/FID/TSD [106, 131, 133]. The reaction takes place under strongly acidic conditions. Although this reagent has been used with GC analysis, removal of excess DNPH is required prior to injection to avoid column and detector deterioration [38, 39, 133]. Frequent cleaning of the inlet liner [135].

High oven temperatures are required because of the low volatility of the derivative [136]. Hence, HPLC-UV is favoured for this method, being both sensitive and easy to implement [38, 39, 135]. This technique is employed as a standard method for formaldehyde determination by the EPA, (EPA-TO11)[14], and NIOSH, (Method 2016)[16]. To accommodate the poor resolution and detection of an HPLC, a new detection method using diode array ultraviolet spectroscopy and atmospheric pressure negative chemical ionization mass spectrometry for liquid chromatography was introduced. The set-up showed a significant increase in resolution (34 carbonyls) and sensitivity in the ppb range [137]. Figure 3.1 shows the reaction scheme.

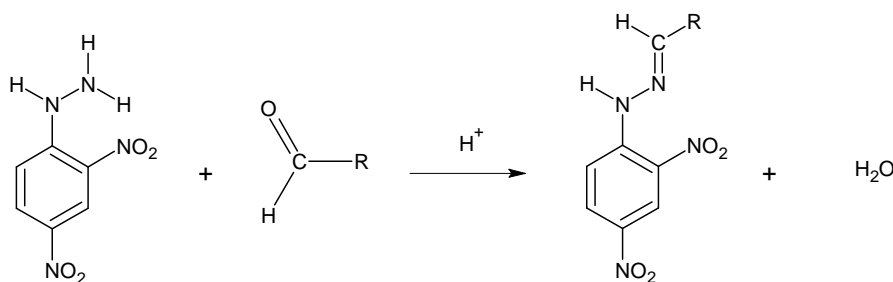


Figure 3.1 Reaction scheme for 2,4-DNPH with an aldehyde [106, 128-134, 137, 138].

DANSYLHYDRAZINE (DNSH) – (1-dimethyl-aminonaphthalene-5-sulfonylhydrazine)

Schmied *et al*, developed a method for determining aldehydes and ketones simultaneously by derivatization on silica gel coated with DNSH. The reaction scheme is shown in figure 3.2. This reaction is highly efficient and allows for collection flow rates of 2 L/min. After collection, the hydrazones are extracted and separated by HPLC with fluorescence detection. DNSH is purified before each use. Detection limits are in the picogram range [75].

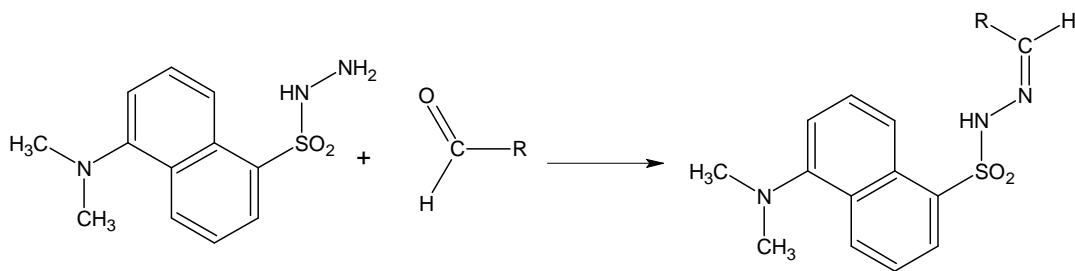


Figure 3.2 Reaction scheme for DNSH with an aldehyde [75].

O- (2,3,4,5,6-PENTAFLUOROPHENYL) HYDRAZINE (PFPH)

The hydrazine's detectability using ECD is enhanced by the pentafluoro-moiety. To date, the reagent has only been used in the study of lipid peroxidation in which volatile carbonyl compounds are formed [78, 139]. Stashenko *et al* [78], heated a vegetable oil sample in a test tube and added PFPH solution. After the carbonyls reacted at room temperature with the PFPH, they were extracted into non-polar phases using either LLE or SPE. The extracts were analysed by GC-FID/ECD/MS-SIM. Detection limits of 10^{-14} and 10^{-12} mol/ml per aldehyde were obtained using ECD and MS-SIM respectively. More recently, using the same concept, Pawliszyn used a SPME fibre to pre-concentrate carbonyls using *in situ* derivatization on a PFPH coated PDMS/DVB fibre which, following desorption in the GC inlet, was analysed by GC with ECD to obtain a detection limit of 10-90 fmol [60, 139]. The reaction scheme is shown in figure 3.3 below.

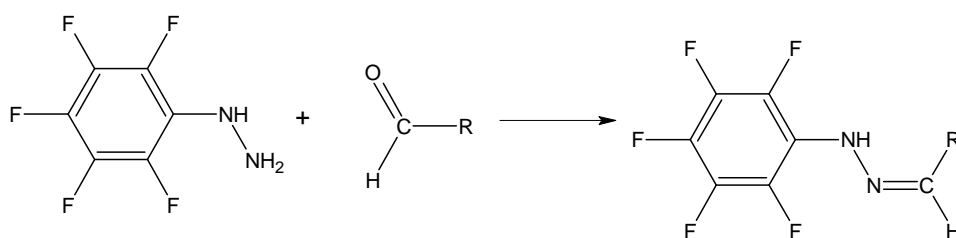


Figure 3.3 Reaction scheme for PFPH with an aldehyde [78, 139].

2,4,6-TRICHLOROPHENYLHYDRAZINE (TCPH)

This reagent was introduced to reduce the problems experienced using 2,4-DNPH and GC analysis. An octadecyl silica cartridge impregnated with TCPH is used to collect HCHO. Thereafter the cartridge is held at 100°C for 6 min to allow for complete reaction. The cartridge is eluted with acetonitrile followed by GC-ECD analysis. Detection limits are determined by the blank. In the case of HCHO the

Chapter 3 - Derivatization

limit of detection is 0.1 ppb, while other carbonyls have even lower limits. An ozone scavenger has been used to eliminate the interference of ozone at concentrations above 300 ppb [76]. The reaction scheme is shown in figure 3.4 below.

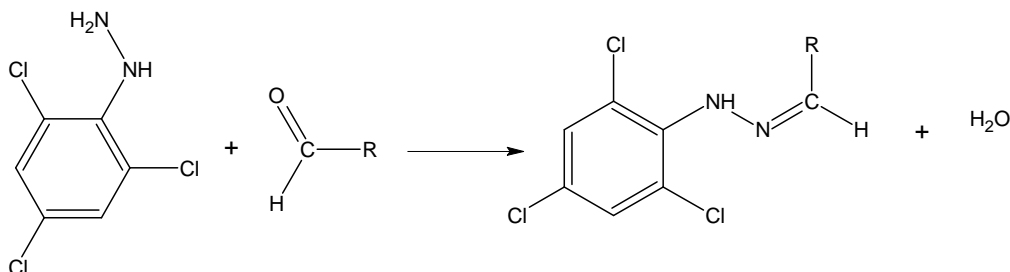


Figure 3.4 Reaction scheme for TCPH with an aldehyde [76].

3.2.2. Oximes

Oximes are ideal for GC analysis due to their volatility, providing a possibility to obtain a good separation, while the reaction conditions are mild, unlike those for hydrazone formation [136]. Typical amine reagents used in HCHO derivatization reactions followed by GC analysis are discussed below.

BENZYLHYDROXYLAMINE AND METHOXYAMINE

Benzylhydroxylamine and methoxyamine can be applied to automobile exhaust and stationary source analysis. The reagents are not suitable for ambient air measurements since their reaction with low molecular mass aldehydes yield volatile products. Detection limits have therefore not been reported for benzyloximes. Figure 3.5 shows the reaction schemes for benzylhydroxylamine with an aldehyde, and for methoxyamine with an aldehyde. The carbonyls were collected on silica gel, eluted with water, derivatized with benzylhydroxylamine and analysed by GC-NPD. Derivatives were well separated and could be detected to the picogram level [136]. O-Methyloximes provided detection limits of 40 ppb for aldehydes in air. For the determination of unsaturated aldehydes, particularly acrolein and crotonal, their respective O-methyloximes and benzyloximes are brominated and analysed using GC-ECD. The brominated acrolein methyloxime was detected at 0.5 ppb in a 40 L air sample [136].

Chapter 3 - Derivatization

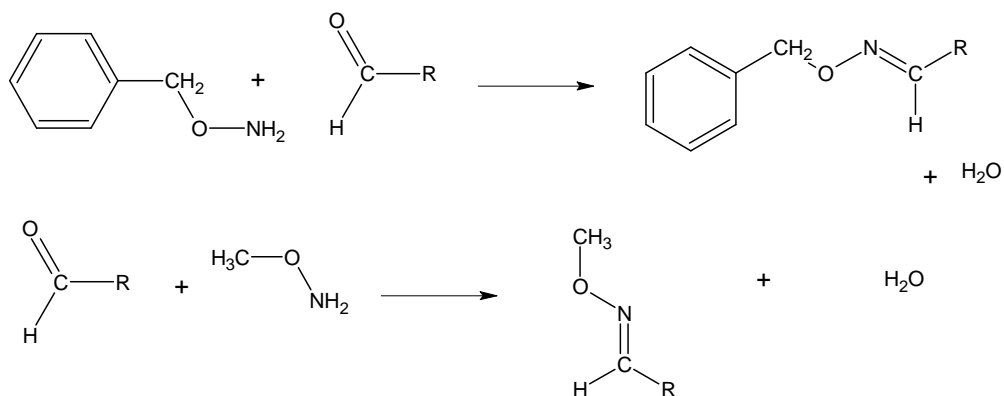


Figure 3.5 Reaction scheme for first, benzylhydroxylamine with an aldehyde. Second, methoxy amine with an aldehyde [136].

O-(2,3,4,5,6-PENTAFLUOROBENZYL) HYDROXYLAMINE (PFBHA)

This reagent is ideal for the determination of trace amounts of volatile aldehydes in air samples [136]. The oximes that are formed are volatile and stable to high temperatures allowing for GC analysis. All the oximes have a common base peak of m/z 181, which allows for easy identification with Mass Spectrometry [140]. The reagent has typically been used for determining aldehydes in drinking water with electron-capture detection (ECD) [141] (EPA method 556) and mass spectrometry (MS) [140] as well as in beer [142], cognac [143] and vegetable oils [144]. Recently PFBHA has also been used for indoor air and headspace sample analysis. C-18 silica gel cartridges coated with PFBHA were used to determine aldehydes in air emitted by vegetation as terpene oxidation products. After elution of the derivatives with hexane, a 50 L air sample provided a detection limit of 2 ppb using GC-MS [77]. Wu and Que Hee [145] developed a dynamic personal air sampler consisting of Tenax-GC solid sorbent coated with PFBHA. The formed PFBHA derivatives were eluted from the sorbent with hexane and analysed by GC-MS. The detection limit for acrolein was 0.025 ppm. Later, Wu and Que Hee [146] developed a passive sampler by applying the same concept. Martos and Pawliszyn introduced the use of a SPME PDMS/DVB fibre, for the *in situ* derivatization of HCHO. The headspace of an aqueous PFBHA solution coats the fibre, which is then exposed to the HCHO atmosphere or headspace of a sample. The fibre is then desorbed in the inlet of a GC oven. The technique is excellent for grab sampling and time weighted averaging for indoor air. Detection limits were as low as 15 ppb using GC-FID [60, 147]. Figure 3.6 shows the reaction scheme.

Chapter 3 - Derivatization

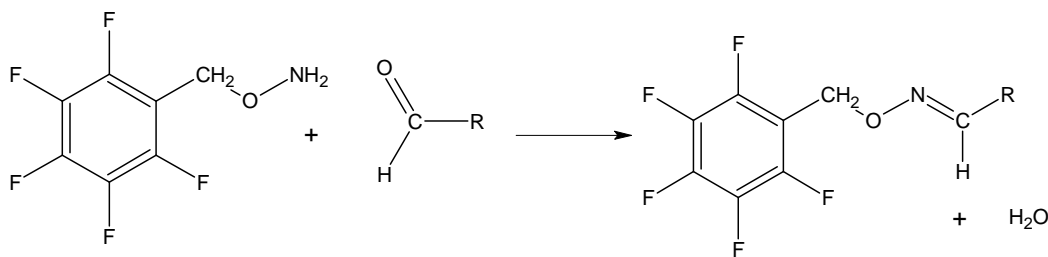


Figure 3.6 Reaction scheme for PFBHA with an aldehyde [140].

3.2.3. Cyclization Reactions

N - (BENZYLETHANOL) AMINE (BEA) -COATED SORBENT TUBE METHOD

Formaldehyde and most carbonyl compounds react rapidly with secondary aminoethanols to form the cyclic oxazolidine derivative, as shown in figure 3.7. Formaldehyde was collected on BEA coated Chromosorb® sorbent. The derivative was extracted with isooctane and separated using GC-FID. Detection was in the range of 0.55-4.71 mg/m^3 [136]. The method lacks sensitivity due to the low sampling rate required to ensure derivative formation, and high blank levels. Thus, the reagent is unsuitable for ambient air analysis. The use of a nitrogen specific detector enhances sensitivity slightly. Acid gases/mists will react with the BEA and convert it to the ammonium salt, resulting in lower BEA reagent availability [39].

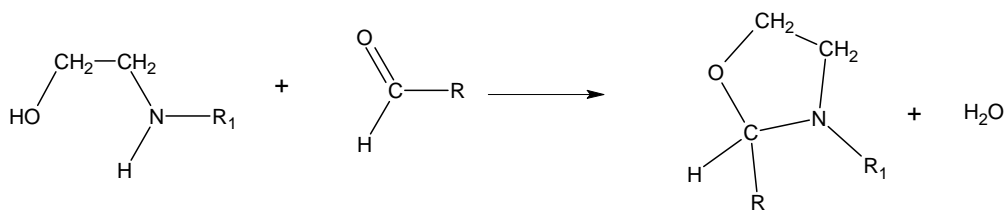


Figure 3.7 Reaction scheme for ethanolamine with an aldehyde [39, 136].

2-HYDROXYMETHYLPIPERIDINE (HMP)

Kennedy, *et al.* determined acrolein in air by pre-concentration on a XAD-2 sorbent tube coated with 2-HMP. Acrolein forms a bicyclo-oxazoline, which can then be determined by gas chromatography - nitrogen specific detection (GC-NSD) in the 0.13-1.5 mg/m³ range [148]. Formaldehyde can also be determined by conversion to hexahydrooxazolo [3,4- α] pyridine in a denuder tube coated with 2-HMP (with a back-up tenax sorbent tube). Figure 3.8 shows the reaction scheme. Recovery is achieved by thermal desorption followed by GC-MS analysis for which the limit of detection is in the range of 0.03 to 0.51 mg/m³ [149]. NIOSH uses this technique for the determination of formaldehyde and acrolein in air (Method 2541) with a detection range of 0.3-20 mg/m³ [150], as well as aldehyde screening (Method 2539)[151] using GC -FID/MS detection.

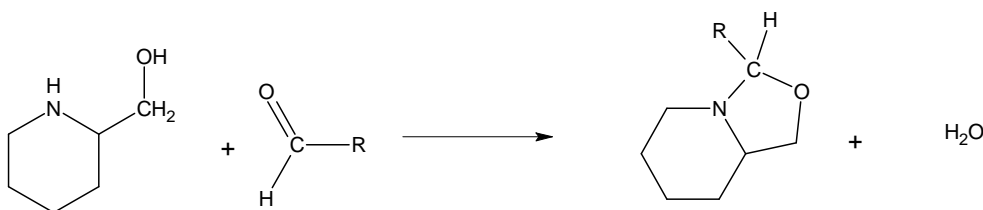


Figure 3.8 Reaction scheme of 2-HMP with an aldehyde [148-151].

CYSTEAMINE (2-AMINOETHANETHIOL)

Cysteamine reacts readily with carbonyl compounds at room temperature and neutral pH. However, it does not react with β -unsaturated aldehydes such as acrolein and crotonaldehyde. Unlike certain derivatizing reagents, no *cis-trans* isomers of the reaction product are formed making quantitation easier [136]. This reagent has been used in the determination of volatile carbonyl compounds in cigarette smoke [152] and automobile exhausts [153]. The smoke/exhaust is collected in a vessel containing an aqueous solution of cysteamine. The carbonyl compound is converted to the thiazolidine as shown in figure 3.9, followed by analysis with GC with NPD. Detection limits are in the picogram range.

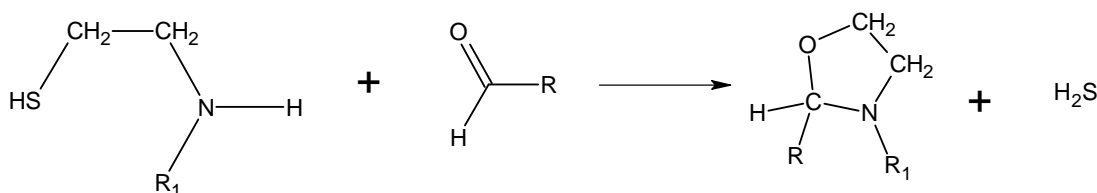


Figure 3.9 Reaction scheme of cysteamine with an aldehyde [136, 152, 153].

AMMONIA

Formaldehyde is collected on a silica gel sorption cartridge coated with polyethylene glycol (PEG-400), to increase the polarity of the adsorbent. The pre-concentrated HCHO is extracted using aqueous ammonia, with which HCHO reacts exclusively to form a hexamethylenetetramine, as shown in figure 3.10, which is then analysed using GC-FID. Detection limits fall in the same range as for the use of 2,4-DNPH, but with the use of thermionic detection, the limit can be improved [154].

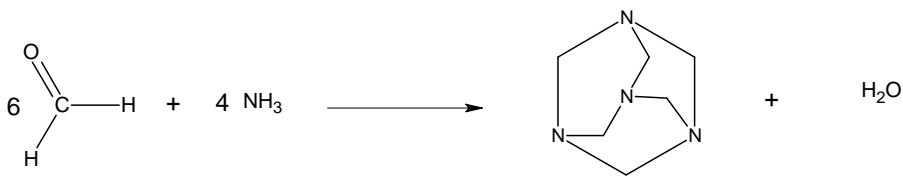


Figure 3.10 Reaction scheme for an aldehyde with aqueous ammonia [154].

ACETYLACETONE OR DIMEDONE (5,5-DIMETHYL-1,3-CYCLOHEXANDION)

Aldehydes in air were determined by pumping air through a bubbler to which dimedone, ethanol and piperidine were added. An extensive sample workup consisting of washing, refluxing for 20 minutes, a triple extraction and drying produces an extract, which is analysed by GC-ECD. This method, unlike the 2,4-DNPH for GC method, can separate *o*-, *m*- and *p*-tolualdehyde as well as acrolein, propanal and acetone which are poorly separated by HPLC. The detection limit for acrolein was 80 pg and for benzaldehyde 17 pg [155]. Figure 3.11 shows the reaction scheme.

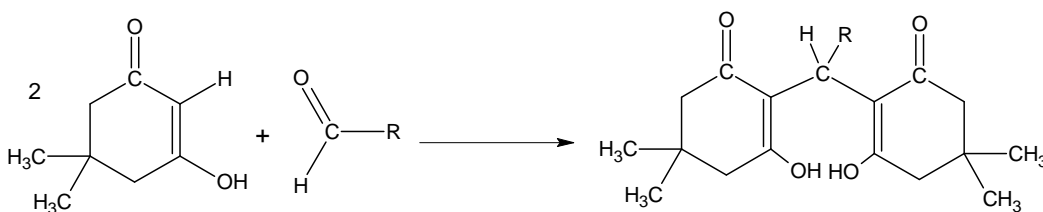


Figure 3.11 Reaction scheme for Dimedon with an aldehyde [155].

The reaction of the dimedone reagent with HCHO in the presence of ammonia is otherwise known as the Hantzsch reaction. The reaction scheme is shown in figure 3.12. Formaldehyde has been simultaneously derivatized in, and extracted by supercritical fluid using the Hantzsch reaction [156].

Chapter 3 - Derivatization

LC-MS has also been used to determine the derivatives of the Hantzsch reaction. An advantage of this reaction is that only the product exhibits fluorescent properties. Problems with increasing fluorescence in the reagent blank, however, were experienced [157].

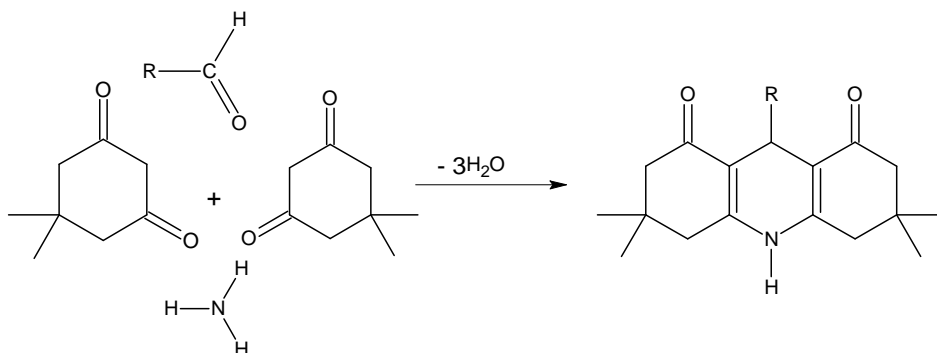


Figure 3.12 Hantzsch reaction scheme [156, 157].

3.3. Derivatization of amines

Emphasis is placed in this study on the derivatization of primary alkyl amines, as these were selected for investigation. Further information on the derivatization reactions for the determination of amines by gas chromatography and their applications in environmental analysis can be obtained from a useful review by Kataoka [121].

3.3.1. Schiff base formation

Traditionally, benzaldehyde has mainly been used for Schiff base condensations with primary amines. Benzaldehyde imines form with high yields after 10-30 min slight warming [121, 158].

Pentafluorobenzaldehyde (PFBA) has been used to derivatize small alkyl amines in water (pH 10), followed by headspace SPME (polyacrylate fibre) of the imine derivatives and GC/FID analysis [159].

The derivatives were formed after 20 min at 80°C. The limits of detection were determined by the reagent blank and fell between 26-0.4 ng /ml.

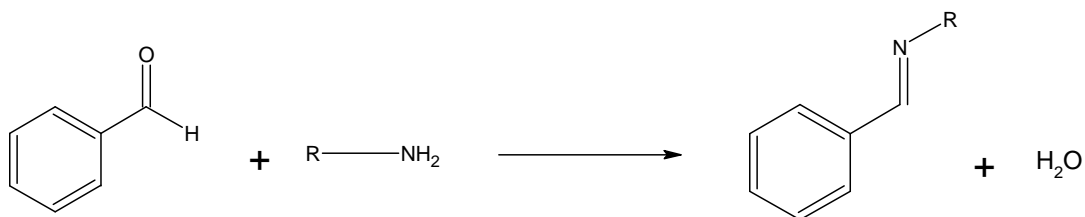


Figure 3.13 Reaction scheme for the condensation of an aldehyde with a primary amine. R = alkyl or aryl substituent [121].

3.3.2. Acylation

PERFLUOROACYLANHYDRIDES

Heptafluorobutyric acid anhydride (HFBA) has been used to derivatize the primary amine on tocainide, an antiarrhythmic drug [160]. The derivative yield was 92% in toluene with a reagent concentration of only 0.01% v/v. However, the authors found that an excess of HFBA, and similarly for trifluoro- and propionic acid anhydride [161], degraded the formed derivatives [160]. A combination of HFBA and heptafluorobutanoyl chloride (HFBCl) 2:8 v/v, has been used to derivatize amphetamine-like drugs from urine [162]. A headspace *in situ* SPME derivatization reaction was used, as the rate at which the water hydrolyzed the reagent was much faster than the rate of the acylation reaction of the amines with the reagent. A glass insert, with 12 holes, containing the derivatizing reagents, was placed in the vial containing the urine sample. The SPME fibre was exposed to the headspace above the glass insert. While the vial was heated, the volatile amphetamine-like drugs diffused into the insert where they were simultaneously derivatized and absorbed by the PDMS SPME fibre. The detection limits of this method were in the range of 0.016–0.193 ng/ml [162].

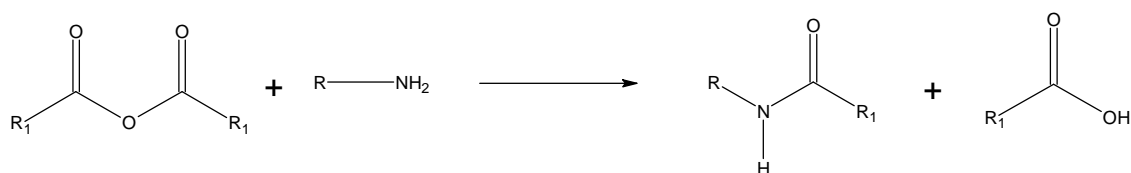


Figure 3.14 Reaction scheme for the reaction of a perfluoroacyl anhydride reagent with a primary amine. R = alkyl or aryl substituent, R₁ = CH₃, CF₃, C₂F₅ or C₃F₇ [121].

ACYL CHLORIDE

Amphetamine in buffered human urine has been extracted *in situ* using a pentafluorobenzoyl chloride (PFBCl)-coated PDMS SPME fibre, followed by GC/ECD or GC/MS analysis [163]. However, excess PFBCl was required since most of the PFBCl loaded on to the fibre reacted with the water and matrix compounds in the sample. An interfering matrix compound caused the limit of detection to vary between 100 pg/ml and 250 pg/ml for reagent loading times of 1 min and 5 min respectively [163].

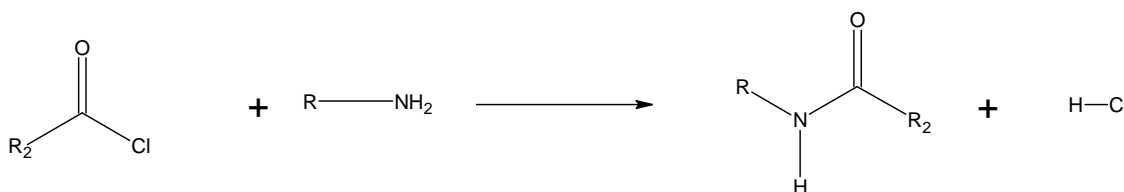


Figure 3.15 Reaction scheme for the reaction of an acyl chloride with a primary amine. R = alkyl or aryl substituent, R₂ = CH₃, C(CH₃)₃, CCl₃, C₆F₅, C₆H₄-NO₂, C₆H₃(NO₂)₂ [121].

ACYL IMIDAZOLE

The acyl imidazoles have a very high reactivity due to the delocalization of the nitrogen's electrons into the heterocyclic ring [158]. The imidazole by-product from the reaction is volatile and does not interfere with the GC analysis. Heptafluorobutyl (HFB) imidazole has been used as derivatization reagent for analysis of drugs with a primary or secondary amine functional group [121]. HFB, PFP and TFA – imidazole derivatization reactions usually occur in a fairly non-polar organic solvent and require a certain amount of heating which is dependant on the size of the amine-bearing compound [158].

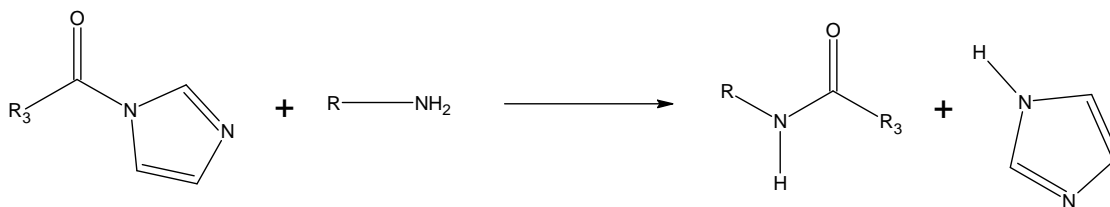


Figure 3.16 Reaction scheme for the reaction of an acyl imidazole with a primary amine. R = alkyl or aryl substituent, R₁ = CH₃, CF₃, C₂F₅ or C₃F₇ [121].

Chapter 3 - Derivatization

***N*-SUCCINIMIDYL BENZOATE (SIBA)**

Primary alkyl amines in water have been derivatized with a newly developed reagent called SIBA. SIBA was added to the buffered aqueous solution and heated at 60°C for 20 min. The formed derivatives were extracted with a SPME fibre coated with polyphenylmethylsiloxane. The fibre was exposed for 1 hour to the vial headspace, while the vial contents were magnetically stirred and held at 80°C [164]. Detection limits of the derivatized amines were 0.13–7.2 nmol/l for analysis by GC-FID [164].

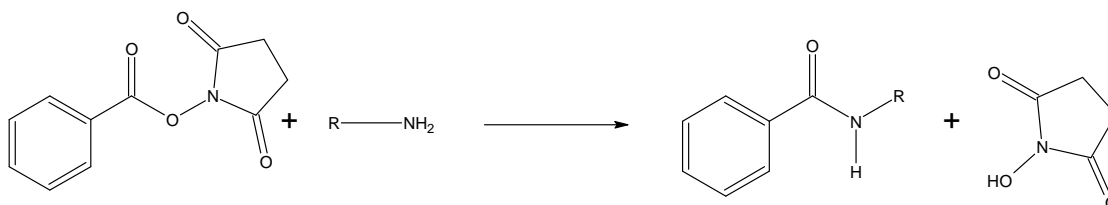


Figure 3.17 Reaction scheme for the reaction of *N*-succinimidyl benzoate, SIBA, with a primary amine. R = alkyl or aryl substituent [164].

3.3.3. Dinitrophenylation

2,4-dinitrofluorobenzene (DNFB), better known as Sanger's reagent, has been used to derivatize primary alkyl amines in wastewater for GC/MS analysis [165]. The determination limits were in the range of 1 µg/L [165]. The reaction is fairly tedious, occurring in a basic medium for 60 min at room temperature, then for another 60 min at 90°C to hydrolyze the excess DNFB. In addition, 3 wash steps are required to remove 2,4-dinitrophenol, one of the hydrolysis products of the DNFB, to prevent any damage to the GC column [165]. DNFB has also been used as a pre-column reagent to derivatize paromomycin in human plasma and urine for analysis by HPLC-UV [166]. Amphetamine enantiomers were resolved and identified by HPLC - circular dichroism spectroscopic analysis, after DNFB derivatization [167].



Figure 3.18 Reaction scheme for the reaction of 2, 4-dinitrofluorobenzene (DNFB) with a primary amine. R = alkyl or aryl substituent [121].

Chapter 3 - Derivatization

2, 4-Dinitrobenzene sulphonic acid (DNBS) is water soluble, while the DNB derivatives are not, allowing for an easy separation of excess reagent before analysis. DNBS reacts only with amino groups, unlike DNFB which reacts with amines, thiols, imidazoles and hydroxyls. However, longer reaction times and strongly alkaline reaction conditions are required by DNBS [121].



Figure 3.19 Reaction scheme for the reaction of 2, 4-dinitrobenzenesulphonic acid (DNBS) with a primary amine. R = alkyl or aryl substituent [121].

3.3.4. Sulphonamide formation

An alkaline aqueous mixture of primary, secondary and tertiary amines can be separated by a one-pot selective derivatization and extraction procedure described by Hinsberg *et. al.* [121] Benzenesulphonyl chloride and *p*-toluenesulphonyl chloride are two reagents that react selectively with primary and secondary amines. Separation is achieved when the hexane extraction removes the water-insoluble sulphonamide derivative of the secondary amine and not the water-soluble primary amine derivative. The tertiary amine remains unchanged [121].

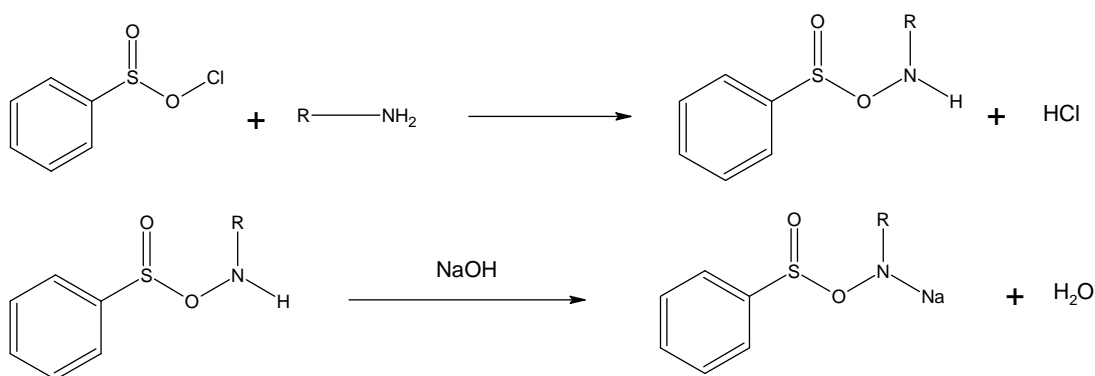


Figure 3.20 Reaction scheme for the sulphonation reaction of benzenesulphonyl chloride with a primary amine. R = alkyl or aryl substituent [121].

3.3.5. Silylation

Silylation of amines generally requires strong silylation reagents and harsh reaction conditions [121, 122]. BSA, BSTFA and MTBSTFA have been used to silylate primary and secondary amines. However, in addition to the associated disadvantages mentioned above, these reagents also react with hydroxyl and carboxylic acid groups [121, 122].

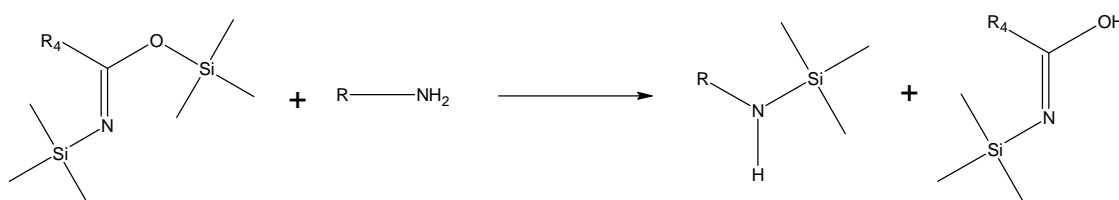


Figure 3.21 Reaction scheme for the reaction of $R_4 = \text{CH}_3$ (BSA) or CF_3 (BSTFA) with a primary amine, $R =$ alkyl or aryl substituent [121].

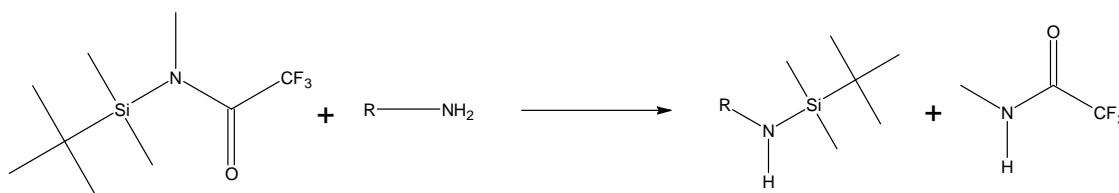


Figure 3.22 Reaction scheme for the reaction of MTBSTFA with a primary amine [121].

3.3.6. Carbamate formation

2-(9-anthryl) ethyl chloroformate has been used, in an automated process, as a precolumn derivatization agent for determining amino acids. Both primary and secondary amines were converted to stable carbamate derivatives before being analysed by HPLC. The reaction occurred at room temperature in a buffered aqueous medium, after removal of excess reagent prior to injection. The anthracene chromophore provided lower UV and fluorescence detection limits of 0.5 pmol and 0.06 pmol, respectively, than the better-known 9-fluorenylmethyl chloroformate [168, 169]. For GC analysis, smaller molecular tags are used for carbamate formation, typically the methyl, ethyl and isobutyl chloroformates [112, 169]. Trichloro- and pentafluorobenzyl chloroformates have also been developed for ECD detection [169].

Chapter 3 - Derivatization

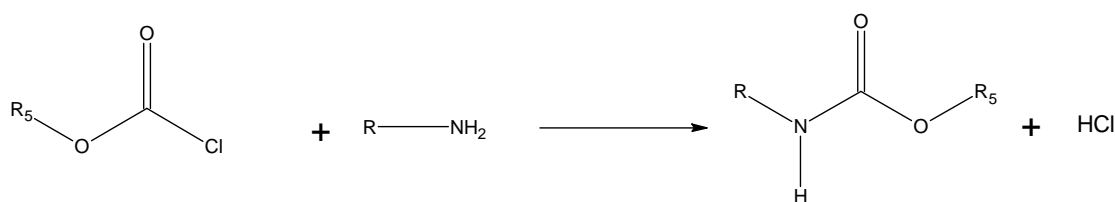


Figure 3.23 Reaction scheme for the formation of a carbamate from the reaction of an alkyl chloroformate with a primary amine. R= alkyl or aryl substituent, R₅ = C₂H₅, CH₂CH(CH₃)₂, C₅H₁₂, CH₂CF₃.

3.4. Derivatization of alcohols and phenols

3.4.1. Acylation

ACYL ACID ANHYDRIDES

Acetic acid anhydride (AAA) is by the far the most popular reagent for derivatizing phenols. The stable methyl ester derivatives form rapidly under aqueous alkaline conditions followed by extraction into an organic solvent or polymeric sorbent [122, 170].

AAA has been used to derivatize chlorophenols in tap water for analysis by plasma atomic emission detector [171], pentachlorophenol in leather using supercritical fluid extraction [172], phenol and methylphenol isomers in soil [173], bisphenol A in river water using liquid phase microextraction (LPME) [174] and alkylphenols in water by FIA and membrane introduction mass spectrometry [175].

There are several applications of *in situ* derivatization using AAA. These use stir bar sorptive extraction (SBSE) to extract and concentrate the formed derivatives followed by thermal desorption GC/MS analysis. Using this method, the following have been determined; estrone, 17 β -estradiol and 17 α -ethinylestradiol [55, 176], alkylphenols and bisphenol-A in human urine samples [51] and in river water [54, 177], chlorophenols in river and tap water as well as human urine [178], hydroxy-PAH's in water [179], phenols in human urine [112], lake and ground water [180]. Detection levels were typically at the

Chapter 3 - Derivatization

ppt level. 17α -Ethinylestradiol was extracted and derivatized by SBSE with AAA and BSTFA to convert both the phenolic and sterically hindered alkyl hydroxyl group. A multishot desorption of 5 stir bars resulted in a detection limit of 0.1 ng/L [181].

For improved detection trifluoroacetic (TFA) [182]-, pentafluoropropionic (PFP) and heptafluorobutyric (HFB) acid anhydrides have frequently been used [122]. Several haloacyl anhydrides were tested for the determination of 21 endocrine disrupting compounds, of which TFAA and HFBA proved most useful [62]. Unlike most other derivatization reactions described in the relevant literature, these reactions all proceeded to completion within 5 min [62].

Estrone, 17β -estradiol and 17α -ethinylestradiol have been concentrated and cleaned from sewage water using SPE. The extract was derivatized with PFPAA and analyzed by GC-MS (SIM). Detection limits were in the range of 5 - 10 ng/L [21, 183]. Estrone, 17β -estradiol, estriol, nonylphenol and bisphenol-A were determined from sediments. After ultrasonic extraction and silica gel fractionation, the extract was derivatized with PFPAA and analyzed by GC-MS (SIM). Detection limits were in the range of 0.1 – 1.5 ng/g [184].

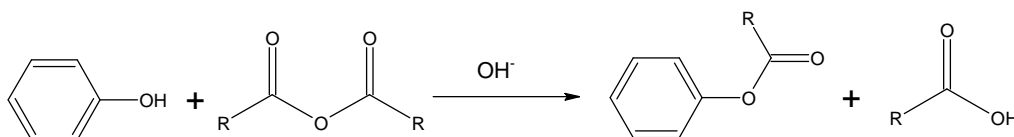


Figure 3.24 Reaction scheme for the reaction of phenol functional groups with an acyl anhydride to form the ester and carboxylic acid by-product.

ACYL HALIDES

Pentafluorobenzoyl chloride (PFBCl) has become a very popular acylation reagent for phenols. PFBCl has been used to determine phenols [185, 186] and chlorophenols in water, wastewater and sludge by GC/ECD [187]. The PFB esters could be detected down to 1 pg [186].

Chapter 3 - Derivatization

PDMS/ DVB SPME of chlorophenols in tap water has been achieved *via in situ* derivatization of the analytes in the fibre with PFBCl [188]. PFBCl headspace was loaded onto the PDMS/DVB fibre for 20 min at 40°C followed by immersion for 10 min at 40°C into the buffered aqueous solution containing the chlorophenols. The SPME fibre was then desorbed for 3 min at 260°C in the GC inlet [188]. Limits of detection of 0.005 – 0.8 µg/L were obtained from GC/ECD analysis [188].

The following have been determined as their PFB derivatives by GC/NCI-MS: Alkylphenols in cod at the low µg/kg level [189]; alkylphenols in produced water from offshore oil installations at the low ng/L level [190]; and β-estradiol in bovine urine (LOD 287 pg/ml) [191]. The estrogens estrone, 17β-estradiol, estriol and 17α-ethinylestradiol have been determined in various waste and drinking waters. The samples were cleaned and concentrated by SPE followed by evaporation and derivatization with PFBCl. Remarkable detection limits 0.03 – 0.2 ng/L were reached for each estrogen [192, 193].

Perfluorooctanoyl chloride has been used to derivatize fatty alcohols in order to move the molecular ions into the higher mass ranges of 600-700 m/z [194]. Reaction times of 2 min were obtained using microwave irradiation [194].

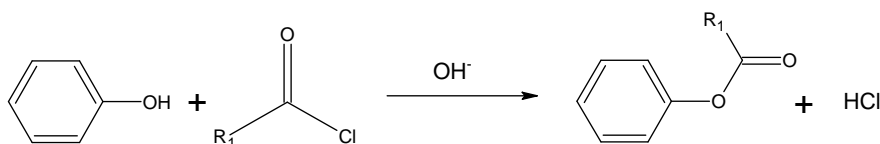


Figure 3.25 Reaction scheme for the reaction of a phenol functional group with an acyl chloride to form the ester and haloacid by-product.

3.4.2. Silylation

Silylation reactions are typically used for improving the volatility and thermal stability of the analytes. Most silylations occur on the phenol / alcohol groups of large bulky molecules, for example steroids. Investigation into the use of various catalysts and solvents for different applications is generally

Chapter 3 - Derivatization

required since yields fluctuate according to these parameters [195, 196]. The most commonly used reagents described in the relevant literature are highlighted below.

***N*-METHYL-*N*-(TRIMETHYLSILYL)-TRIFLUOROACETAMIDE (MSTFA)**

Estrogens from water have been extracted using a polyacrylate SPME fibre followed by headspace derivatization using MSTFA [197, 198]. MSTFA, unlike other reagents, is capable of converting both phenolic and aliphatic alcohols into their TMS ethers. Conversion of both groups occurred at 60°C after 30 min. Detection limits of 0.2-3 ng/L were obtained [198].

Natural and synthetic estrogens in water samples were determined using SPE and derivatization with MSTFA, followed by analysis using GC/MS or GC/MS/MS. Quantification limits were found to lie between 1 and 3 ng/L [199].

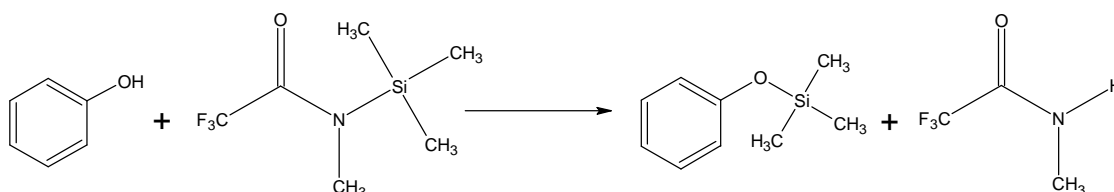


Figure 3.26 Reaction scheme for the formation of phenyl trimethylsilyl ether from the reaction of MSTFA with a phenol.

***N*-*O*-BIS (TRIMETHYLSILYL) TRIFLUOROACETAMIDE (BSTFA)**

Li *et al* investigated the simultaneous silylation of alkylphenols, chlorophenols and bisphenol-A for GC/MS analysis using BSTFA. Optimum quantitative reaction conditions for BSTFA were found in acetone at room temperature. Removal of excess BSTFA through hydrolysis provided enhanced long-term stability of the formed trimethylsilyl derivatives eliminating one of the drawbacks of BSTFA [200].

Chapter 3 - Derivatization

Alkylphenols in water have been determined by SBSE and in-tube silylation using BSTFA by Kawaguchi *et al* [55]. Detection limits were at the sub ppt level. A dual derivatization “multishot” technique using SBSE, *in situ* acylation with AAA and in-tube silylation with BSTFA, was tested for the analysis of 17 β -estradiol in river water, also by Kawaguchi *et al* [181]. AAA forms the methyl acetate ester on the phenolic group while the BSTFA forms the trimethylsilyl ester on the aliphatic alcohol. A detection limit of 0.1 pg/ml was obtained for this method [181]. SPE of estrogens in river water followed by derivatization using PFBBBr and BSTFA, to form the PFB-TMS derivatives, and analysis by GC-NCI/MS provided detection limits of 0.10 to 0.28 ng/L [30].

Alkylphenols and steroid hormones in biological samples and water has been determined by polyacrylate (PA) SPME and headspace BSTFA derivatization [201, 202]. Limits of quantitation were in the low ppb range lower levels than this were not possible due to matrix effects [201, 202]. The SPME fibres are destroyed by direct contact with the liquid BSTFA [201]. The same technique was previously also used to determine hydroxy - PAHs in urine samples with method detection limits in the range of 0.01–0.1 ng/mL [203]. Headspace PA SPME followed by BSTFA derivatization was used to determine bisphenol-A from plastic containers [52], and *tert*-octylphenol, nonylphenol and bisphenol-A from underground and seawater [197]. Detection by GC-MS (SIM) provided detection limits of 0.4 ng/L [52] and 100 ng/L [197] respectively.

BSTFA has also been used to derivatize alkylphenols and bisphenol-A from seawater samples after extraction by porous polysulfone hollow fibre membrane (PS-HFM). Detection limits ranged between 0.07 and 2.34 ng/L [50]. The estrogens: estrone, 17 β -estradiol, estriol and 17 α -ethinylestradiol have been determined in river water. The samples were cleaned and concentrated by SPE followed by evaporation and derivatization with BSTFA and 1% Trimethylchlorosilane (TMCS). Detection by GC – ITD/MS provided detection limits in the range of 5 ng/L for each estrogen [196].

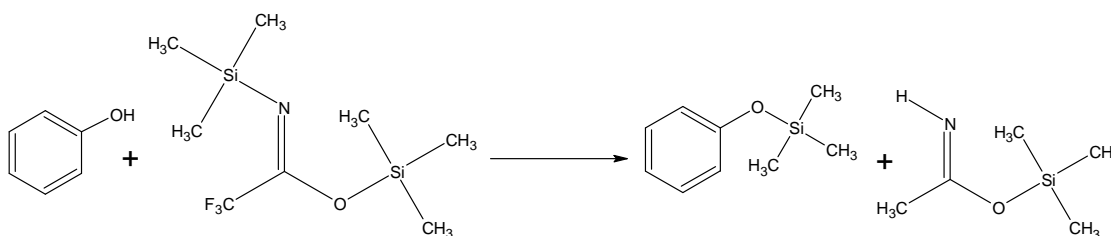


Figure 3.27 Reaction scheme for the formation of phenyl trimethylsilyl ether from the reaction of BSTFA with a phenol.

***N* - (*tert* - BUTYLDIMETHYLSILYL)-*N*-METHYLTRIFLUOROACETAMIDE
(MTBSTFA)**

MTBSTFA has been used to derivatize hydrolysed lipids [204]. The *tert*-butylsilyl esters provided higher resolution and sensitivity than the corresponding methyl esters on a GC/FID [204].

Both MSTFA and MTBSTFA have been used to determine 19-norandrosterone in human urine [205]. Despite the *tert*-butylsilyl derivative having a slightly lower sensitivity than the trimethylsilyl derivative, the *tert*-butylsilyl derivative eluted much later and the molecular ion fell in the higher mass range allowing for unambiguous identification of the steroid [205].

More than 50 substituted phenols have been detected at the ng/L level from environmental samples having high matrix content [206]. After SPE, the phenols were derivatized using MTBSTFA. The characteristic ion $[M-57]^+$ resulting from *tert*-butyl cleavage, allowed for very low detection by GC/EI-MS in the SIM mode [206].

Endocrine disrupting estrogens in water have been derivatized using MTBSTFA and analyzed by GC tandem MS and GC/MS [207, 208]. Detection limits were 1 ng/L and 4 – 6 ng/L, respectively [207, 208].

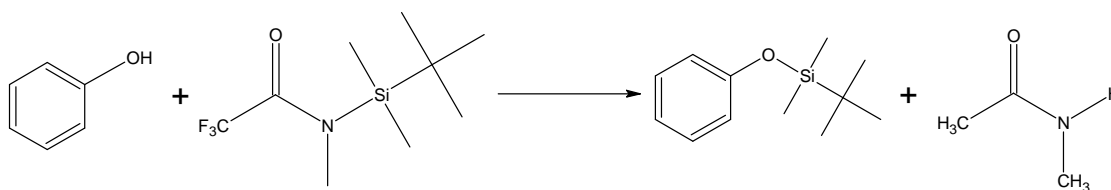


Figure 3.28 Reaction scheme for the formation of phenyl *tert*-butylsilyl ether from the reaction of MTBSTFA with a phenol.

Chapter 3 - Derivatization

N-TRIMETHYLSILYLIMIDAZOLE (TMSI)

Fine *et al*, determined estrogens in ground water and swine lagoon samples using NCI-GC/MS/MS, after derivatization of the phenolic groups with pentafluorobenzylbromide (PFBBr), and of the hydroxyl groups with TMSI [209]. Limits of quantitation of 1 ng/L and 40 ng/L were obtained for the 2 samples respectively [209].

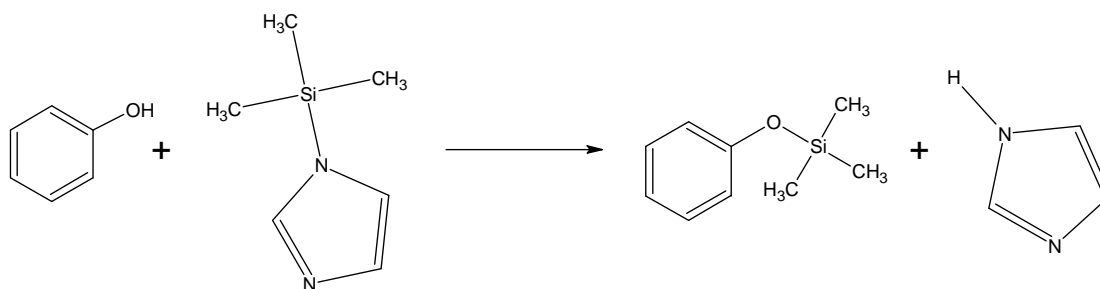


Figure 3.29 Reaction scheme for the formation of phenyl trimethylsilyl ether from the reaction of TMSI with a phenol.

3.4.3. Alkylation

Pentafluorobenzylbromide is often used as alkylation reagent for hydroxyl and phenol groups [62]. Alkylation reactions are more often used for the conversion of carboxylic acids into their esters than for the conversion of alcohols into ethers, as the reactions tend to be tedious reactions [62, 210]. PFBBr has been used to convert hydroxy PAHs from urban aerosols, into their corresponding PFB ethers, for analysis by GC/ECD and GC/MS [210]. Detection limits of 0.01 and 3.3 pg in ECD and (NCI)-SIM-MS were respectively obtained [210]. The estrogens: estrone, 17 β -estradiol, estriol and 17 α -ethinylestradiol have been determined in river, ground and swine lagoon water. Trimethylsilyl-imidazole (TMSI) was used as catalyst and acid scavenger. The detection limit fell in the range of 0.1 – 40 ng/L [30, 209].

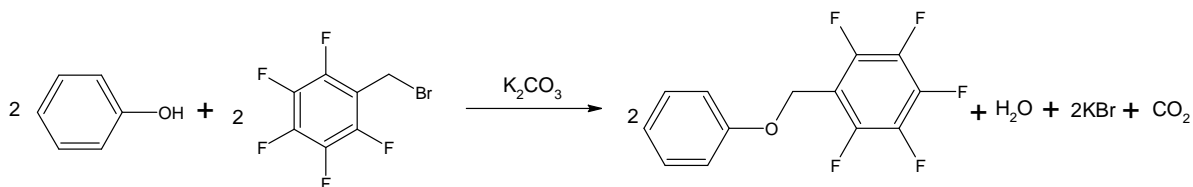


Figure 3.30 Reaction scheme for the formation of pentafluorobenzyl ether from the reaction of PFBBr with a phenol.

3.5. Derivatization and pre-concentration

Table 3.2 summarises the sample preparation, concentration and derivatization techniques used for the analysis of endocrine disruptors from various matrices. It also lists the detection limits obtained by GC/MS and LC/MS/MS (where no derivatization was utilized). Excellent detection limits are obtained when GC- (NCI) MS, after derivatization with PFBCl, is used. Pre-concentration using SPME or SBSE appears to yield similar results using only GC- (EI) MS.

When pre-concentration techniques are used for analytes requiring derivatization, it is necessary to determine the most suitable time to perform the derivatization reaction. The principal objective is to obtain maximum selective concentration and consequently maximum sensitivity.

3.5.1. Pre-derivatization

Derivatization is often performed before extraction if it will significantly enhance the partitioning of the analyte into the extraction medium. For example, in order for *aqueous* polar analytes to be extracted by SBSE, a non-polar concentration medium (100 % PDMS), they must be converted into their corresponding non-polar derivatives before they will partition into the PDMS. Phenols are first derivatized in a buffered aqueous medium using AAA, to form their corresponding methyl esters, prior to SBSE. The following have been determined using this technique: alkylphenols and bisphenol-A in human urine samples [51] and in river water [54, 177], chlorophenols in river and tap water as well as human urine [178], hydroxy-PAH's in water [179], phenols in human urine [112], lake and ground water [180]. Very low detection limits, typically at the ppt level have been achieved, as detection is enhanced through selective extraction of non-polar derivatives into the stir bar.

3.5.2. In situ derivatization

In situ derivatization is frequently used when working at ultra trace levels where all possible sample losses due to use of additional extra glassware need to be avoided. It is not necessarily required that the extraction medium have the same polarity as the analyte, since the analyte is converted while simultaneously being extracted. For example, the derivatization reagent PFBHA headspace is dissolved

Chapter 3 - Derivatization

into the PDMS of the multichannel silicone rubber trap, simultaneously derivatizing airborne low molecular mass aldehydes and concentrating their corresponding hydroxylamine derivatives within the PDMS [61]. Similarly, a SPME fibre has been simultaneously exposed to the headspace of the derivatizing reagent (HFBCl) and analytes (amphetamine-type drugs), allowing the analytes to be derivatized in and extracted into the fibre [162].

3.5.3. Post-derivatization

Post derivatization can only occur if the concentrating medium and analyte have similar polarity. In this case only the detection properties of the analytes are enhanced prior to analysis, since partitioning into the concentrating medium is not affected by the derivatization reaction. SPME benefits the most from this type of extraction because it has an assortment of fibres with different polarity. This means that it can extract a wide range of analytes without requiring derivatization prior to extraction. However, the extracted analytes can still be made amenable to GC analysis by derivatization prior to or during desorption in the GC inlet. Alkylphenols and steroid hormones in biological samples and water have been determined by extraction onto a polyacrylate SPME fibre followed by headspace BSTFA derivatization [201, 202].

3.6. Conclusions

From the above review above it is apparent that every reagent has its own inherent set of advantages and disadvantages. Selection of a reagent should therefore be undertaken in a manner that ensures that the majority of analysis requirements are met, particularly in terms of enhancing the selectivity and sensitivity of the reaction and the analyses.

Table 3.2 Sample preparation, concentration and derivatization techniques used for analysis of endocrine disruptors from various matrices

Analytes	Matrix	Sample preparation	Preconcentration	Derivatization	Instrumental analysis	LOD (LOQ) ng/ L (ppt)	Year	Reference
E1, E2, E3, EE2	Ground. River and sewage water	SPE	SPE & evaporation	PFBCl	GC- (NCI) MS	0.2, 0.03, 0.06, 0.05	2001	[192]
E1, E2, EE2	Surface & drinking water	SPE	SPE & evaporation	PFBCl	GC- (NCI) MS	0.05-0.15	2001	[193]
E1, E2, E3, EE2	Human urine	pH adjustment & enzyme hydrolysis	LLE & evaporation	PFBCl	GC- (NCI) MS	100	2000	[247]
TOP, NP	Sea water	Anion exchange SPE	SPE & evaporation	PFBCl	GC- (NCI) MS	103, 102	2004	[190]
E1, E2, E3, EE2	River water	SPE	SPE & evaporation	PFBBBr, TMSI	GC- (NCI) MS	0.1 – 0.28	2001	[30]
E1, E2, E3, EE2	Ground & swine lagoon water	Centrifuge & filter	SPE	PFBBBr, TMSI	GC – (NCI) MS/MS	(1 (ground)) (40 (swine))	2003	[209]
E1, E2, E3, EE2	River water	SPE	SPE & evaporation	BSTFA + 1% TMCS	GC- (ITD) MS	(5)	2003	[196]
BPA	Plastic containers		Headspace PA SPME	BSTFA + 1 % TMCS	GC- (EI) MS (SIM)	0.4	2005	[52]
TOP, NP, BPA	Sea water		Hollow fibre SPME	BSTFA	GC- (EI) MS (SIM)	0.07 – 2.34	2005	[50]
E1, E2, EE2, TOP, BPA	Waste water	SPE		BSTFA	GC- (EI) MS (SIM)	4.0-26.5	2004	[262]
TOP, NP, BPA	Sea water	Silyl SPE & derivative kit	SPE	BSTFA	GC- (EI) MS (SIM)	100, 190, 138	2001	[200]

Analytes	Matrix	Sample preparation	Preconcentration	Derivatization	Instrumental analysis	LOD (LOQ) ng/ L (ppt)	Year	Reference
OP, NP, E1, E2, DES	River water & blood serum		In-sample PA SPME	BSTFA	GC- (EI) MS (SIM)	2 – 378 (8 – 1261)	2006	[202]
TOP, NP, BPA	Underground & sea		Headspace PA SPME	BSTFA	GC- (EI) MS (SIM)	100	2001	[197]
E1, E2, E3, EE2	River & sewage water	SPE	SPE & evaporation	MSTFA	GC- (EI) MS (SIM)	(1-3)	2004	[199]
E2, EE2	Surface	SPE		MTBSTFA	GC- (EI) MS (SIM)	50-300	2000	[208]
E1, E2, EE2	Reservoir, river & waste water	SPE		MTBSTFA & 1% TBDMCS	GC- (EI) MS/MS	1	2000	[207]
E1, E2, EE2	Surface & waste water	SPE	HPLC fraction	Sil A reagent	GC- (EI) MS/MS	0.1-2.4	1999	[263]
EE2	River water		SBSE	AAA & BSTFA	TD-GC- (EI) MS (SIM)	0.5 (2) 0.1 multishot	2006	[181]
E1, E2, EE2	River water		Multishot 5 x SBSE	AAA	TD-GC- (EI) MS (SIM)	0.2, 0.5, 1	2004	[55, 176]
TOP, NP, BPA	Human urine	Protein precipitation & centrifuge	SBSE	AAA	GC- (EI) MS (SIM)	10, 50, 20	2005	[51]
TOP, NP, BPA	River water		SBSE	AAA	TD-GC- (EI) MS (SIM)	0.1 – 3.2	2004	[54]
BPA	River water		LPME	AAA	GC- (EI) MS (SIM)	2 (10)	2006	[174]
TOP, NP, BPA	River water		SBSE	AAA	GC- (EI) MS (SIM)	0.5, 5, 2	2004	[177]
E1, E2, E3, NP, BPA	Sediment	Ultra-sonic extraction, silica gel fractionation		PFPAA	GC- (EI) MS (SIM)	0.6, 0.8, 1.5, 0.2, 0.1 ng/g	2006	[184]
E1, E2, EE2	Sewage water	SPE		PFPAA	GC- (EI) MS (SIM)	5-10	1998	[21, 183]

Analytes	Matrix	Sample preparation	Preconcentration	Derivatization	Instrumental analysis	LOD (LOQ) ng/ L (ppt)	Year	Reference
NP, NPEO	Tap & river water		Headspace CW-DVB SPME	Dimethylsulphate/NaOH	GC- (EI) MS (SIM)	20-1500	2002	[264]
E1, E2, EE2	Sewage water	SPE	HPLC fraction		GC-MS	0.5-1	2001	[21, 265]
NP, BPA, EE2	Sewage water		Hollow fibre membrane extraction		GC- (EI) MS (SIM)	100, 300, 20	2003	[266]
NP, BPA, EE2	Waste water		Automated PA SPME		GC- (EI) MS (SIM)	800, 1000, 40	2003	[267]
E1, E2, EE2	Sewage water	SPE	HPLC fraction & LLE		GC- (EI) MS (SIM)	0.2	1998	[21, 268]
E1, E2, EE2, TOP, BPA	Waste water	SPE			GC- (EI) MS/MS	2.5-27.5	2004	[262]
EE2	River water		Molecularly imprinted polymers		LC/MS	1.8 (5.4)	2006	[269]
E1, E2, E3, EE2	River water	SPE	SPE & evaporation		LC- (ESI) MS (SIM)	0.1- 0.2	2005	[270]
E1, E2, EE2, TOP, NP, BPA	River & waste water		PA SPME		HPLC-UV-ED	300-1100 (UV) 60 – 80 (ED)	2002	[271]
E1, E2, E3, EE2	Sewage, surface & drinking water	SPE	SPE & evaporation		LC-DAD-MS (APCI, ESI±)	50-500 (DAD) 2-500 (ESI) 20-5000 (APCI)	2000	[272]
E1, E2, E3, EE2, DES	River water & sediment	On- & Off-line SPE			LC- DAD- (ESI) MS (SIM)	< 1	2001	[273]

Analytes	Matrix	Sample preparation	Preconcentration	Derivatization	Instrumental analysis	LOD (LOQ) ng/ L (ppt)	Year	Reference
TOP, NP, BPA	Mineral water & soda beverages	SPE	SPE & evaporation		LC- (ESI) MS/MS (MRM)	(0.04, 0.03, 0.2)	2005	[8]
E1, E2, E3, EE2, DES	Surface & waste water	0.2 µm nylon filtration	In-tube SPME (PLOT capillary)		LC- (ESI) MS/MS	2.7 – 11.7	2005	[274]
E1, E2, E3, EE2, DES	River & Sewage water	0.45µm filtration	On-line SPE		LC- (ESI) MS/MS (SRM)	(0.02 – 1.02)	2004	[275]
E1, E2, E3, EE2	River & sewage water	SPE	SPE & evaporation		LC- (ESI) MS/MS	(0.008- 0.9)	2000	[276]
EE2	River & Sewage water	Glass fibre filtration			Chemiluminescence ELISA	0.2±0.1 (1.4±0.8)	2005	[26]
E1	Sewage plant water	SPE	SPE & evaporation		ELISA	1.25	2004	[27]

Abbreviations:

(E1) Estrone; (E2) 17β-Estradiol; (E3) Estriol; (EE2) 17α-Ethinylestradiol; (DES) Diethylstilbestrol; (TOP) *tert*-octylphenol; (OP) Octylphenol; (NP) 4-n-nonylphenol; (NPEO) Nonylphenoethoxylate; (BPA) Bisphenol-A; (GC) Gas Chromatography; (LC) Liquid Chromatography; (HPLC) High Performance Liquid Chromatography; (MS) Mass Spectrometry; (EI) Electron Impact Ionization; (NCI) Negative Chemical Ionization; (ITD) Ion Trap Detector; (SIM) Selected Ion Monitoring; (TD) Thermal Desorption; (ESI±) Positive/Negative Electrospray Ionization; (APCI) Atmospheric Pressure Chemical Ionization; (SRM) Selected Reaction Monitoring; (MRM) Multiple Reaction Monitoring; (UV) Ultraviolet; (ED) Electrochemical Detection; (SPE) Solid Phase Extraction; (LPME) Liquid Phase Microextraction; (LLE) Liquid-liquid extraction; (SPME) Solid Phase Microextraction; (SBSE) Stir Bar Sorptive Extraction; (PA) Polyacrylate; (CW-DVB) Carbowax-Divinylbenzene; (PLOT) Packed Layer Open Tubular; (PFBCl) Pentafluorobenzoyl chloride; (PFBBBr) Pentafluorobenzylbromide; (TMSI) Trimethylsilyl-imidazole; (BSTFA) Bis(trimethylsilyl)trifluoroacetamide; (TMCS) Trimethylchlorosilane; (MSTFA) Methyl(trimethylsilyl)trifluoroacetamide; (MTBSTFA) Methyl(*tert*-butyldimethylsilyl) methyltrifluoroacetamide; (TBDCMS) *tert*-butyldichloromethylsilane; (AAA) Acetic acid anhydride; (PFPA) Pentafluoropropionic acid anhydride; (NaOH) Sodium hydroxide
 Additional reviews can be obtained from [1-3, 21, 23-25, 243]

Chapter 4

Sample Introduction

4. Introduction

Volatile organic compounds, which have been pre-concentrated in a solvent or on ad/absorbents, need to be quantitatively transferred as a narrow injection band into the GC capillary column. A brief description of the various inlet techniques used during this study is presented below. The GC inlet was used to introduce prepared derivatives for confirmation using GC/MS and for desorption of SPME fibres. The Chrompack® and Gerstel® Thermal desorbers were used to desorb traps in the off-line concentration of alkylphenols from water, and the Airsense® EDU and thermal modulator array were used for the on-line concentration and derivatization of aldehydes and amines for introduction into a Resonance Enhanced Multi Photon Ionization Time of Flight Mass Spectrometer (REMPI-TOFMS).

4.1. GC inlets

By far the most common sample introduction technique for GC analysis is the split / splitless injector, figure 4.1. In general, the syringe is inserted through a leak tight rubber septum, where the injected sample is released into the heated zone of a glass inlet liner. An incoming stream of carrier gas pushes the vaporised sample into the GC capillary column, maintained at least 50°C lower than the inlet temperature. The sample is injected instantaneously so that, in combination with the high temperature of the inlet, e.g. 250°C, the volatilised components in the sample are focussed onto the cooler column, e.g. at 40°C, as a narrow injection band.

When the sample is too concentrated or injected as a large volume, split injection is used. At a preset split-ratio only a small proportion of sample, usually a few nanolitres, is transferred onto the column. The presence of a high gas flow rate through the inlet ensures that the reduced sample vapour rapidly enters the column as a narrow solute band [211, 212]. Split injection is not suitable for trace analysis and discrimination effects based on boiling point of analytes do occur [212, 255]

When sample components are present in trace amounts the entire sample can be transferred onto the column by splitless injection, thereby improving detection limits [211]. However, for a splitless



injection the injection volume should not exceed the internal volume of the splitless inlet liner [212]. This will cause the expanded vaporised sample to escape from the inlet chamber through the septum purge, split outlet or into the carrier gas inlet, resulting in sample losses and future memory effects [211,212]. It usually takes between 10-40 seconds for the vaporized sample to enter the column. The split valve must be opened when the transfer is almost complete in order to purge the remaining sample out of the inlet [212]. A low initial column temperature will ensure that condensation and re-concentration of the sample occurs in the column. Cold trapping and the solvent effect are two re-concentration mechanisms often used with splitless injections [212, 255].

Large volume splitless injection techniques were introduced to overcome the limitations of splitless injections on a normal split/splitless inlet. The most popular large volume splitless injection techniques use either a programmed thermal vaporization inlet (PTV) with solvent splitting [212, 255] or the on-column retention technique developed by Grob *et al* [212, 255]. The cold inlet system (CIS) described below is essentially operating as a PTV (with a solvent splitting option available). The on-column retention technique uses an on-column liner packed with an appropriate packing material (often glass wool or other poor heat conductors) [212]. The sample is injected into the inlet where the sample liquid is deposited on the cooler packing. As the solvent evaporates it maintains the inlet vaporizing chamber temperature at the solvent's boiling point until evaporation is almost complete. The solvent vapour exits through the septum purge (which is wide open) or it is allowed to expand to outside the vaporizing chamber hence the term "overflow" technique. The injector temperature is then raised and the solutes evaporate and are transferred onto the column by the carrier gas [212].

When SPME is used for pre-concentration, the fibre is typically desorbed in a split / splitless inlet. The SPME fibre is protected by the syringe barrel, which is used to pierce through the rubber septum. The fibre is exposed once the syringe barrel is inside the inlet. Here, it is essential that the fibre is exposed in the heated zone of the inlet; this is usually towards the centre of the inlet as the ends are generally cooler. Desorption usually occurs in the splitless mode for 2-5 min depending on the nature of the desorbed analytes and the desorption temperature. The fibre is then retracted into the syringe barrel and removed from the inlet, while the split flow is opened and the desorbed analytes are transferred onto the cooler GC column.

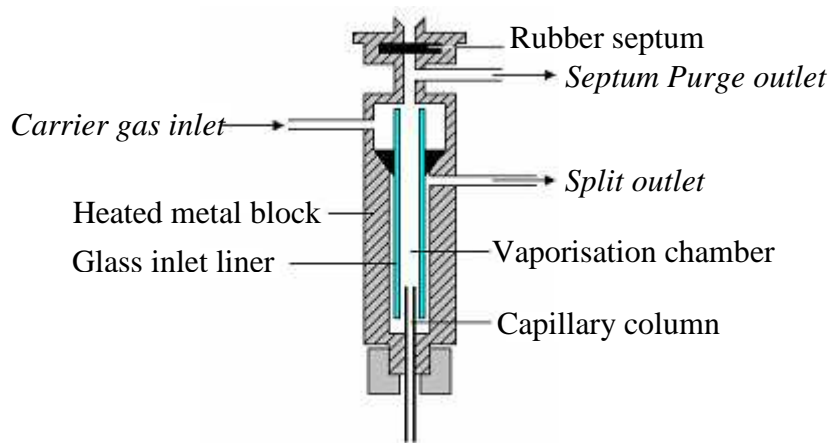


Figure 4.1 A split / splitless inlet [211]. Copyright Wiley-VCH Verlag GmbH & Co. KGaA. Reproduced with permission.

4.2. Thermal Desorption Units

4.2.1. Chrompack®

A Chrompack® 4020 desorption unit was initially used in our study, Figure 4.2[213]. A glass tube, either empty or packed with sorbent, is placed in the desorption oven, where it is heated while the carrier gas transfers the volatiles from the tube onto a cold trap.

The cold trap consists of a fused silica capillary, 30 cm long with an internal diameter of 0.53 mm, which is coated with a thick film of non-polar stationary phase to increase its capacity. During desorption, the cold trap is cooled and maintained at sub-ambient temperatures ranging from 0°C to -100°C by using liquid nitrogen. Upon completion of desorption the cooling flow is stopped. A metal capillary tube, which surrounds the fused silica cold trap, is heated ohmically. This ensures a ballistic temperature increase from, for example -100°C to 250°C within 1 minute. Within that time, the carrier gas transfers the contents of the cold trap and refocuses it onto the GC capillary column, which is at a lower temperature. Figure 4.2 shows the 2 main phases, namely desorption and injection, in the TCT - CP 4020 [213].

This system is no longer manufactured as it has several flaws, namely: insertion of the glass trap tubes into the desorption oven requires tightening of the Swagelok® nut and graphite ferrule at the base of the glass tube. To obtain leak tight connections often leads to over tightening and breakage of the glass trap tubes. The thermal gradient across the cold trap during the injection phase is such

that there are cold spots at the inlet and outlet ends of the capillary trap, which lead to incomplete transfer and tailing of higher boiling analytes. The software has a default injection time of 1min at a maximum temperature of 300°C. Trying to override the injection time manually, in order to obtain complete transfer, leads to a malfunction of the heating element and thermocouple.

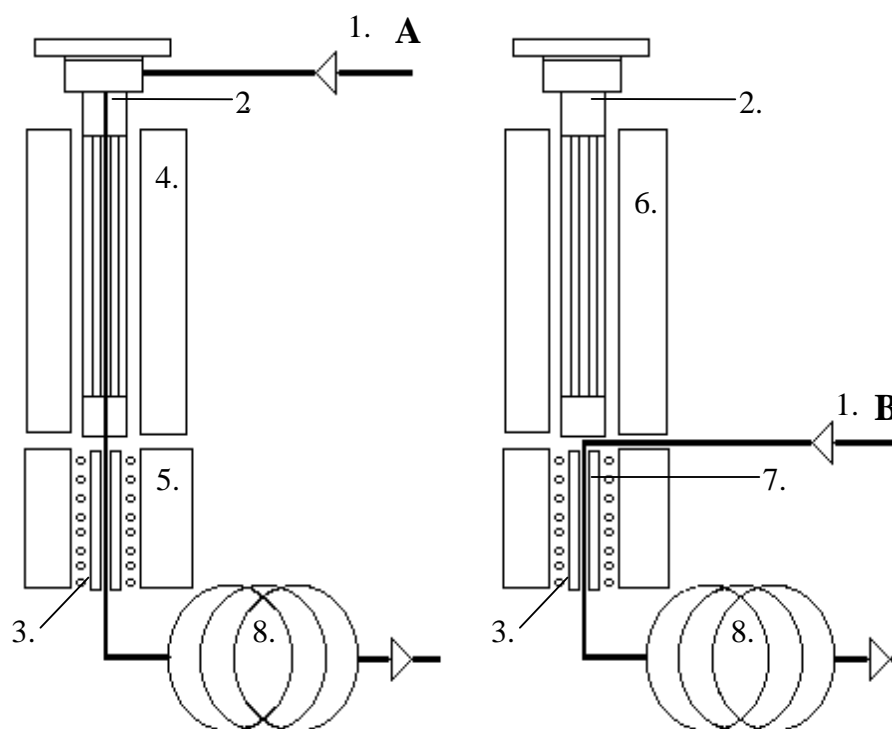


Figure 4.2 The 2 main phases in the TCT 4020 thermal desorption unit:

A: Desorption Phase

B: Injection Phase

1. A: High purity helium carrier gas flow during desorption phase

1. B: High purity helium carrier gas flow during injection phase

2. Glass tube containing ad/absorbent

3. Wide-bore fused silica capillary cold trap

4. Heated desorption oven

5. Liquid nitrogen – cooled chamber

6. Ambient desorption oven

7. Ballistically heated cold trap

8. Gas Chromatograph

4.2.2. Gerstel® Thermal Desorption System – Cold Inlet System (TDS-CIS)

Figure 4.3 shows a cross section of the Gerstel® desorption unit. The Thermal Desorption System (TDS 2) is connected to the Cooled Injection System (CIS 4) by way of a 15 cm long stainless steel capillary transfer line, maintained at a temperature of at most 400°C. High temperature o-rings and a lock-tight mechanism, provide a leak-tight seal as desorption tubes are inserted horizontally into the TDS oven. The tubes may be cooled while excess solvents, residual water and oxygen are removed from the tubes by the carrier gas, prior to desorption.

Desorbed analytes are trapped in the CIS at -100°C or lower. The CIS doubles up as a cryogenic trap and a GC inlet. Analytes are focussed in the inlet liner, in our case a glass baffled liner, before being transferred onto the GC column as a narrow band. Various inlet liners are available for different applications, allowing for greater flexibility when trapping analytes and protection of the column [214].

This desorption unit is a vast improvement on the Chrompack® desorption unit. A short stainless steel transfer line is heated uniformly across the length of the tube; thus, as depicted in figure 4.3[214] no cold or hot spots should occur in the system. The software allows one to programme different desorption and injection temperature gradients from ambient temperatures up to maximum 400°C. Operation of the TDS in split / splitless sampling modes provides a wide dynamic range. High desorption flow rates with splitless transfer allows for lower detection limits. In addition, the manual TDS can be converted into an automated system able to desorb up to twenty tubes.

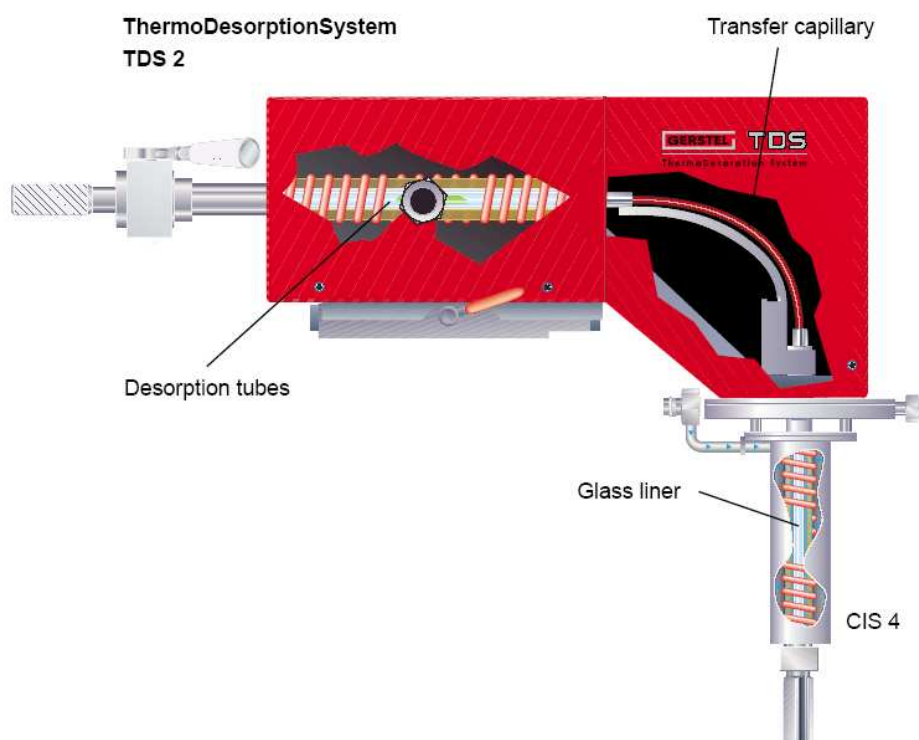


Figure 4.3 Cross section of the Gerstel® TDS-CIS desorption unit [214].

4.2.3. *Airsense® Enrichment Desorption Unit (EDU)*

The EDU system used in this study was a unique trap and thermal desorption system developed by Airsense Analytics (Airsense Analytics, Schwerin, Germany) for the Institute of Ecological Chemistry, GSF. The design allows for the on-line concentration of exhaust gases from various combustion sources. Gaseous substances are trapped at sampling temperatures (ambient or less) on, for example, Tenax adsorption tubes and analyzed after thermal desorption. Temperatures of the adsorbent during sampling and desorption phases can be adjusted via settings within the related software EDU. For increasing the speed of analysis, very small tubes, with inner diameters of 1.5 mm, filled with Tenax-TA can be used. Peltier cooling is used in order to achieve sampling temperatures of 4°C. After sampling, the tubes are desorbed by resistive heating. With this flash desorption, temperature increments of 200°C are possible in just 4 s. By sucking air through a cold adsorption tube, the analytes are trapped. In the case of sampling hot gases, it is also possible to dilute the sampling gas to reduce the temperature of the gas. After sampling, a post sampling step can be introduced to remove unappealing gases and vapours (e.g. moisture). To extract analytes off the trap, thermal desorption is performed. For injection, the gas flow is reversed and led into the detection system. Afterward, the tube is cleaned by heating it to a higher temperature than the desorption temperature and flushing the tube with cleaned air. After cooling to near ambient temperatures, the trap is ready for the next measurement [215].

For on-line real-time analytical applications, however, analyte focusing can also be important, not for the enhancement of the chromatographic resolution, but for time resolution and sensitivity (as is the case for on-line REMPI-TOFMS). Analyte focusing can be achieved, by repetitive thermal modulation. In this study, the EDU was used in combination with a segmented thermal modulator array (TMA), described below.

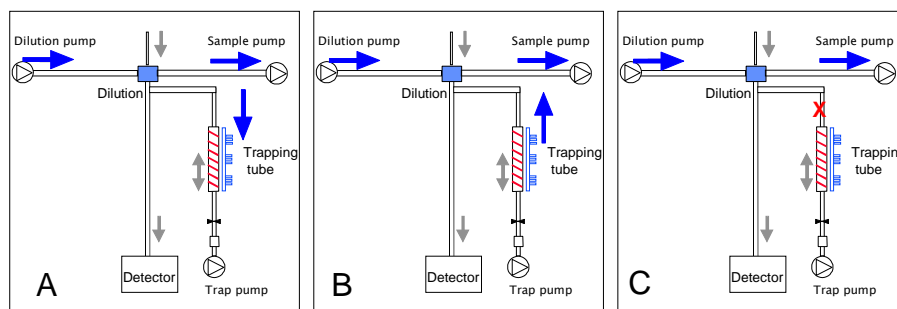


Figure 4.4 Gas flow configuration for the Airsense EDU custom-made for the GSF [215]:

- A: Sampling Phase**
- B: Desorption Phase**
- C: Injection Phase**

4.3. Thermal Modulator Array (TMA)

The segmented thermal modulator array [216] was developed by Ben Burger and co-workers. The modulator houses a narrow-bore capillary coated on the inside with a thick film of PDMS (capillary trap). This capillary represents the concentrating /derivatizing device such as the open tubular traps (OTT) described in chapter 2.

Modulators have predominantly been developed for use as an interface between two columns in comprehensive two-dimensional gas chromatography [217]. Their function is to rapidly focus fractions of effluent from the first column onto the head of the second column. In this study, a segmented thermal modulator array, developed by Ben Burger *et al* [216] was used to transfer and focus the effluent from the capillary trap or EDU, into the REMPI-TOFMS. In principle, the sorption and desorption of effluent from the stationary phase in the modulator capillary can be controlled by careful manipulation of the temperature of the capillary. The thermal modulator array uses rapid resistive heating of consecutive segments of a stainless steel tube surrounding the

capillary to focus the effluent inside the modulator capillary. This ensures a “sweeping” heat motion without disadvantageous cold spots or moveable parts, typical of other modulators [218-223]. The segmented heating of the effluent in the capillary speeds up the chromatographic process in the capillary column, “compressing” zones from the rear and providing a focused chromatographic band that enters the REMPI-TOFMS. Although not providing the shortest injection pulse widths, the TMA is simple and compact; it does not require cryogenic cooling and can operate unattended, making it suitable for on-line analysis with the REMPI-TOFMS.

In greater detail, in this study the modulator capillary consisted of a fused-silica capillary column (0.2 mm i.d.) coated with non-polar phase PS-255 (3- μm film, DB-1 equivalent). A capillary of 20 cm length was used with 5 cm of the stationary phase stripped off at both ends, as described in reference 216. A stainless steel capillary (105 mm x 0.6 mm o.d. x 0.35 mm i.d.) was converted to function as a modulator [216]. An electronic sequencer was used to provide current to the modulator in steps from 1 to 10 A at 5 V with a time duration of 10-2500 ms. To maintain reasonable flow rates and operate at atmospheric pressure, jet restrictors yielding a flow rate of between 0.6 and 1.0 mL/min were prepared from fused silica capillaries, according to the method described in reference 36 from an uncoated capillary (30 cm x 0.32 mm i.d.). The restrictor was coupled to the modulator capillary by a suitable press-fit. All transfer capillaries and connection points were either directly heated to 150 °C, by a heating mantle or surrounded by a copper tube, which was then heated by a heating mantle.

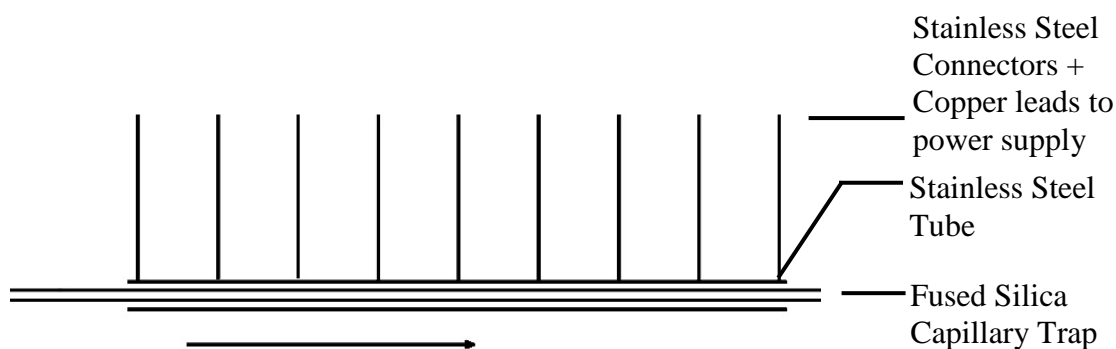


Figure 4.5 Longitudinal section of a Thermal Modulator Array [216].



Chapter 5

On-line analysis of aldehydes and amines using Open Tubular and Multichannel PDMS traps

The bulk of the work presented in this chapter is the result of a collaborative study between the University of Pretoria, South Africa, and the Institute for Ecological Chemistry, GSF Research Centre, Germany. The German partner was interested in extending the analysis range of its home-built REMPI-TOFMS instrument. Not only should aromatic compounds be detected by the REMPI-TOFMS but also non-aromatics such as aliphatic aldehydes and amines. This could be achieved through the use of PDMS MCT newly developed by the South African partner, which had been used to demonstrate the *in situ* derivatization of low molecular mass aldehydes, using O- (2, 3, 4, 5, 6)-Pentafluorobenzylhydroxylamine (PFBHA) [61], effectively attaching an aromatic tag to an aliphatic compound (see Chapter 3, section 3.2.2).

Problems were anticipated with low level formaldehyde measurements, since formaldehyde is a ubiquitous compound and is frequently present in the reagent blank. Hence, the initial work described below is a continuation of my MSc project, where an attempt was made to decrease the formaldehyde content in the PFBHA derivatizing reagent used. The detection limit for formaldehyde using *in situ* derivatization on the MCT was severely constrained by the lack of a good reagent blank (*see section 6.3 MSc Thesis* [61]).

5.1. Loading the derivatizing reagent into the PDMS MCT by preparative gas chromatography

The aim in this experiment was to find a simple, repeatable and efficient method for loading excess PFBHA vapour into the PDMS MCT. Initial methods for saturating the silicone rubber included: loading the dynamic headspace of PFBHA from an aqueous solution of PFBHA in an impinger-type device and loading the dynamic headspace of PFBHA from the pure reagent packed in a glass tube (*see section 6.3 MSc Thesis [61]*). In the process of saturating the PDMS with PFBHA, the presence of HCHO-oxime impurity in the reagent was observed. Therefore, in addition to the above techniques, a method to remove the HCHO-oxime impurity before loading the PFBHA had to be determined. Figure 5.1 illustrates a typical reagent blank for PFBHA.

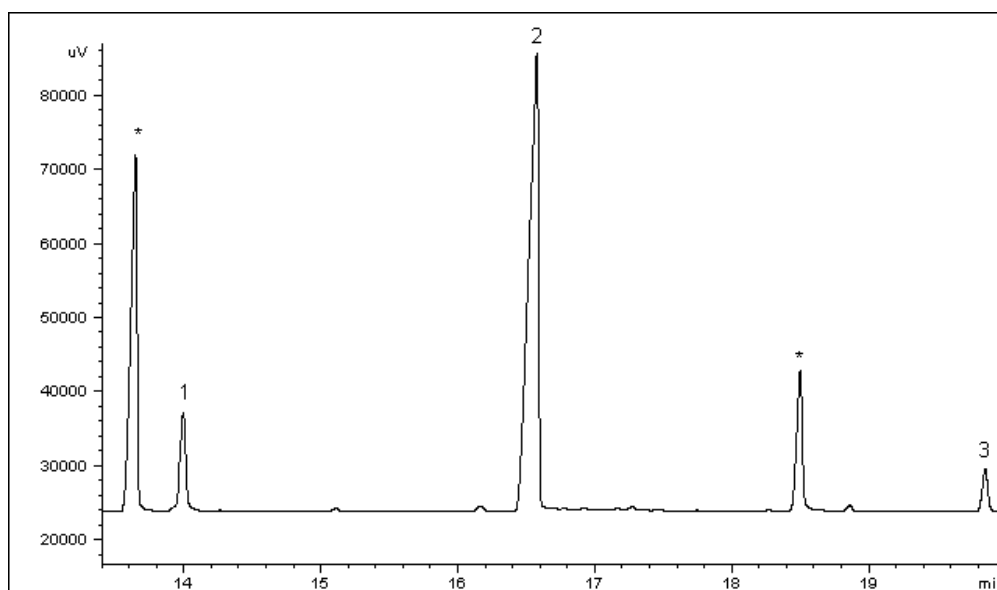


Figure 5.1 Enlarged GC-FID chromatogram obtained by loading PFBHA headspace from the solid reagent into the PDMS MCT. * PDMS thermal degradation peak, 1: Formaldehyde-Oxime, 2: PFBHA, 3: Dodecane (internal standard used to monitor the completeness of desorption of the analytes off the trap. It was added after derivatization using a glass syringe.)

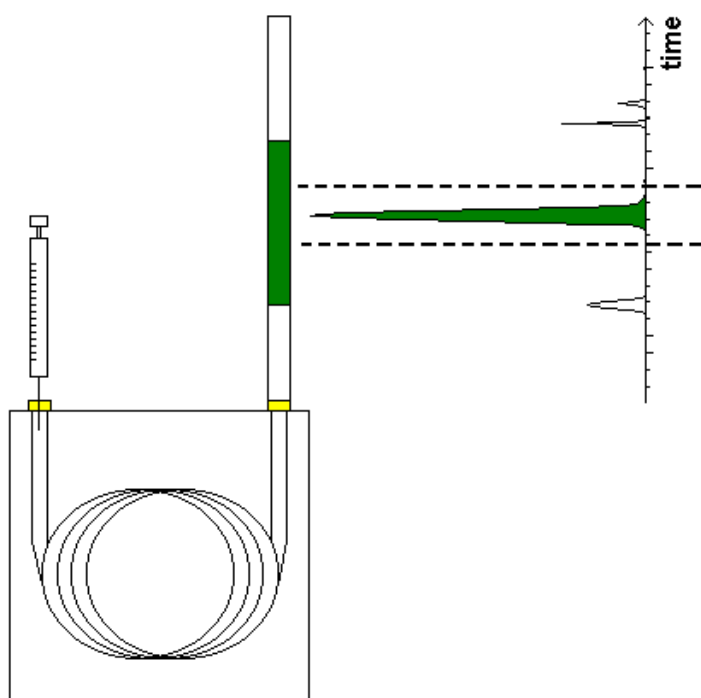


Figure 5.2 The experimental setup using preparative gas chromatography to selectively introduce the PFBHA reagent into the PDMS MCT.

Preparative chromatography using a polar packed column (OV-225) was used in the investigation. With this technique only the PFBHA peak was collected at its respective elution time by fitting the PDMS MCT with a Teflon® connection over the unlit FID detector. A Carlo Erba Fractovap 4200 GC was used for this procedure. The PFBHA was dissolved in hexane (17 g/L). One microlitre of the solution was injected into the GC and the chromatographic data collected. The retention time of the overloaded PFBHA peak was read from the chromatogram. The flame was then switched off and the separation repeated on the GC. The PDMS MCT was then pressed tightly on the unlit FID detector 30 seconds prior to the PFBHA peak retention time (time is monitored with a stop watch), for 1 minute. This collection procedure is sufficient to exclude the formaldehyde derivative peak eluting near the PFBHA peak. The setup is shown in figure 5.2.

For each loading technique, several measurements were made to determine the repeatability of the PFBHA and formaldehyde-oxime amounts loaded onto the trap. Loading the PFBHA headspace from an aqueous solution of PFBHA was performed for 5 min at a flow rate of 10 ml/min. Two sets of measurements were adopted for the collection of PFBHA headspace from the pure reagent, one for 5 min at a flow rate of 10 ml/min, and the other for 10 min at a flow rate of 5 ml/min.



Table 5.1 shows a comparison of the results obtained using the different loading techniques. As expected, the preparative chromatography method is the most promising as it introduces the lowest percentage of formaldehyde-oxime impurity relative to the amount of PFBHA loaded. The repeatability of the amount of HCHO impurity present is also much higher for this method. Unfortunately, even with chromatographic separation of the impurity and PFBHA, some impurity is still present after desorption.

Table 5.1 Comparison of the repeatability of different PFBHA loading techniques.

	PFBHA (aq) 1 min at 10 ml/min	PFBHA (s) 5 min at 10 ml/min	PFBHA (s) 10 min at 5 ml/min	PFBHA (g) Preparative chromatography
%RSD PFBHA peak area	27	96	23	43
%RSD HCHO-oxime peak area	101	62	26	11
% HCHO- oxime relative to PFBHA	12	8	14	2
n	10	4	5	4

We suspect that this HCHO amount recorded after separation must be present in the lab air or in the desorption unit. Similar contamination problems have also been experienced by other users of PFBHA [141, 140, 225, 226]. (Our lab air was not tested using a different analytical technique. Formaldehyde is found in buildings where particleboard (used in flooring and furniture) and hardwood plywood panelling has been treated with urea-formaldehyde based resins. Tobacco smoke, combustion gases from gas appliances, disinfectants and water based paints all release formaldehyde indoors. It is also possible that the air is contaminated in the laboratory by the formaldehyde gas standard, formed by the thermal depolymerisation of paraformaldehyde at 90°C Although the exhaust of the formaldehyde permeation gas standard was vented to the outside of the laboratory through an extraction duct, the removal procedure may not have been as effective.

The thermal desorption unit could have residual unreacted formaldehyde present in the system. It was shown in my MSc thesis that the trapping efficiency of a PFBHA coated PDMS MCT for formaldehyde is 75% for a concentration of 6 ppm and 95 % for a concentration of 0.1 ppm. It was assumed that unreacted formaldehyde flies through the trap and none remains underivatized inside the PDMS MCT prior to desorption.)

5.2. The approach for on-line concentration and derivatization

Potential derivatization reactions were first investigated for the conversion of aldehydes and amines into REMPI-TOFMS detectable compounds. The “on-line” reaction and concentration had to be simulated to determine the suitability of the reagent and PDMS for on-line analysis. Once these factors were determined the method could be tested on the on-line REMPI-TOFMS instrument.

As the Solid-Phase Microextraction (SPME) device has a comparable PDMS volume to the PDMS capillary trap that would be used for on-line sampling, the proof of principle (i.e. of efficient PDMS-mediated derivatization) was tested using SPME with GC/MS and GC-FID analysis. The low volume PDMS devices that would be used for the on-line analysis are depicted in figure 5.3.

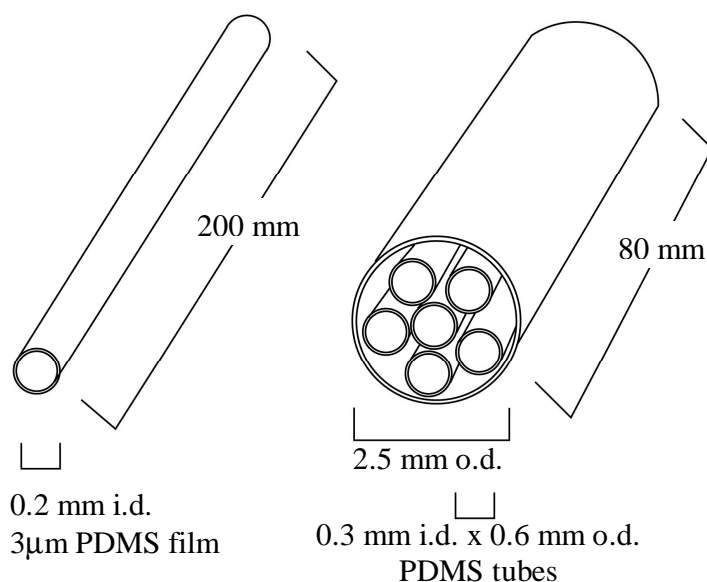


Figure 5.3 Two variations of silicone (PDMS) concentrators namely the thick film open tubular trap (OTT) and the multi-channel silicone rubber trap (MCT).

Chapter 5 – On-line analysis of aldehydes and amines

Reagents investigated were phenylhydrazine to form the phenylhydrazone derivative with the aldehydes and benzaldehyde for the derivatization of amines to form the respective benzaldehyde alkylimine derivatives. The derivatization reaction schemes for aldehydes and amines are depicted in figures 5.4 and 5.5 respectively.

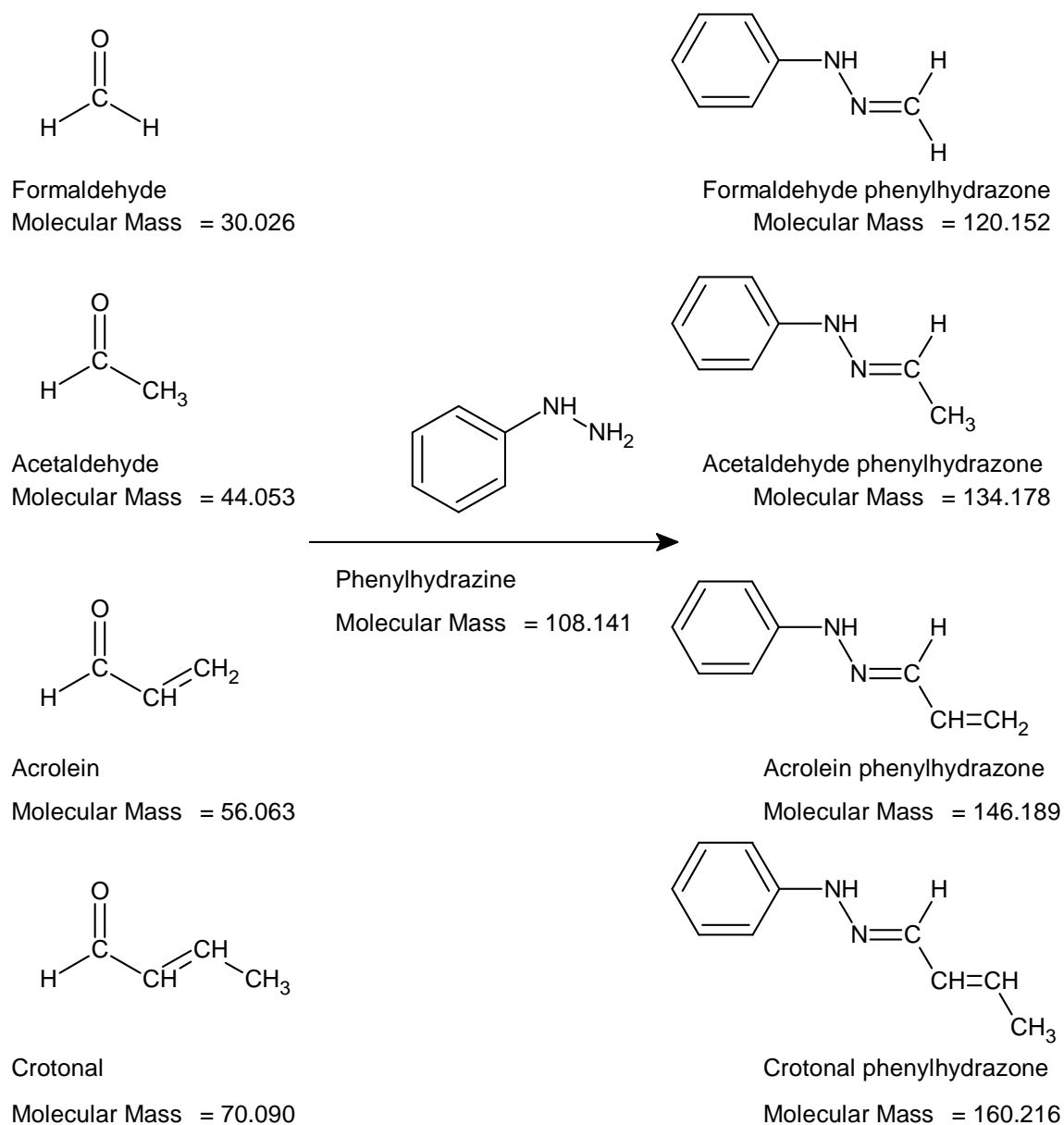


Figure 5.4 Reaction scheme for the derivatization of low molecular mass aldehydes with phenylhydrazine.

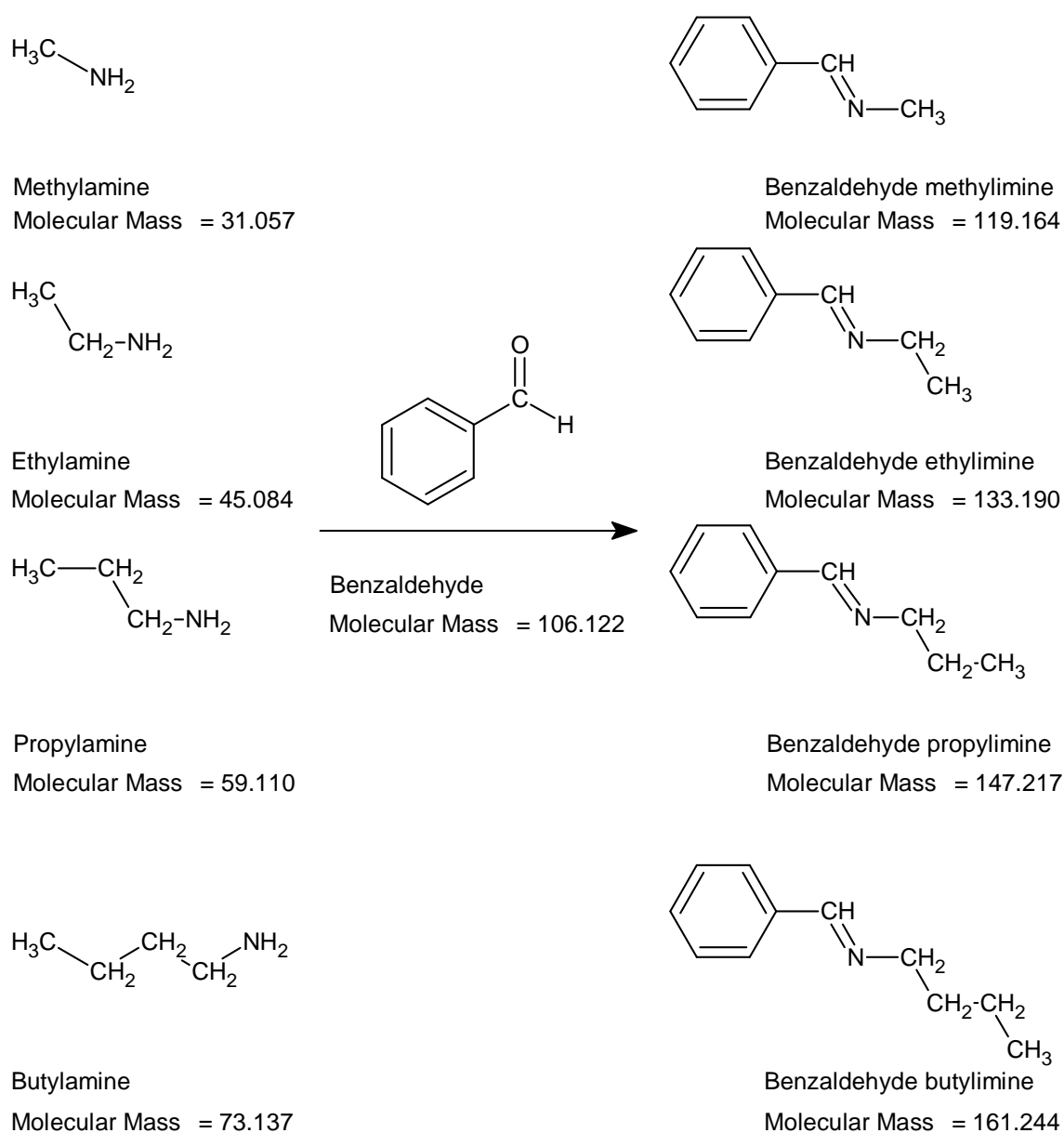


Figure 5.5 Reaction scheme for the derivatization of low molecular mass alkyl amines with benzaldehyde.



5.3. Derivatization Reaction for “Photo-ionization Labelling” of Amines and Aldehydes.

Schemes for the derivatization reagents, analytes, and products formed are shown in Figures 5.4 and 5.5. These reagents were selected to introduce a REMPI-active chromophore to the analyte structure. Substituted rings, such as pentafluorinated benzaldehyde, were discarded in this case as they pose the risk of reducing the REMPI efficiency. In addition, in order for the reaction to occur efficiently, both reagents had to possess a significant vapour pressure to ensure that the reagent would be present in excess in the gas phase.

5.3.1. Initial synthesis of the derivatives

Since commercial standards and library mass spectra of the derivatives were not available the derivatives had to be prepared. Three derivatives were prepared, namely the formaldehyde and acrolein phenylhydrazones and benzaldehyde propylimine. The derivatives were prepared using slightly altered methods to those described in Vogel’s Handbook of Practical Organic Chemistry [227]. Mass spectra obtained from these derivatives were compared with derivative mass spectra obtained by *in situ* derivatization on the SPME fibre and with those obtained by the REMPI-TOFMS.

The phenylhydrazone derivatives were prepared by adding approximately 0.8 g sodium acetate to 400 µl phenylhydrazine in 5 ml water. 500 µl of the aldehyde in 500 µl of ethanol was added to this solution. *Caution: As phenylhydrazine is highly poisonous and formaldehyde is a potential carcinogen, it is essential always to wear gloves and avoid inhalation when working with these reagents.* The reaction mixture was shaken until it became clear adding where necessary extra ethanol. The reaction mixture was warmed in a water bath at ~40°C for 10 to 15 minutes and then allowed to cool. The crystalline derivative was then filtered and recrystallized from dilute ethanol in water. The crystals were dissolved in dichloromethane. 0.4 µl of this solution was injected splitless into the GC- (ITD) MS for analysis. Figures 5.6 and 5.7 present the ITD mass spectra obtained for the formaldehyde and acrolein phenylhydrazone derivatives.



The benzaldehyde propylimine derivative was prepared by dissolving 325 μl propylamine in 500 μl methanol. 400 μl of benzaldehyde was added to this solution. The reaction mixture was heated to 80°C for 35 minutes and allowed to crystallize overnight. The product was recrystallized in ethanol. The crystals were dissolved in dichloromethane. 0.4 μl of this solution was injected splitless into the GC-(ITD) MS for analysis. Figure 5.8 shows the ITD mass spectra obtained for the benzaldehyde propylimine derivative.

Each of the derivatives displays an abundant molecular ion (M^+). In addition, because ions are held in the ion trap and collide with mass neutrals before mass separation, a strong $M+1$ peak is sometimes observed as a result of self-chemical ionization protonation. Benzene (m/z 77) and the tropyllium (m/z 91) mass fragments were also present in the mass spectra obtained.

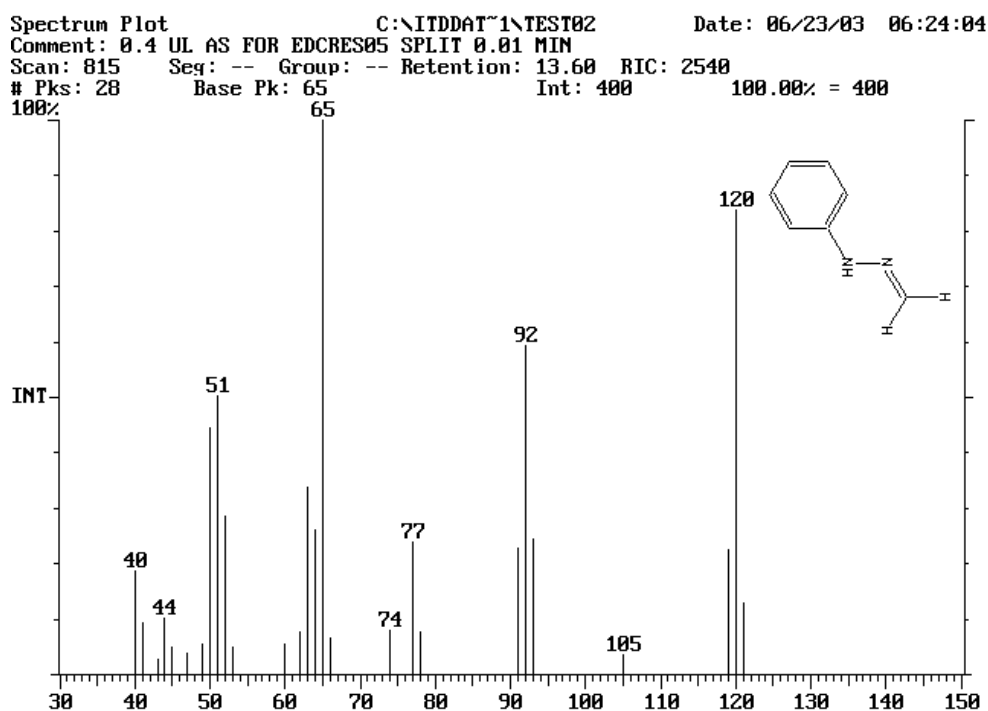


Figure 5.6 ITD Mass spectrum of the formaldehyde phenylhydrazone derivative (M^+120).

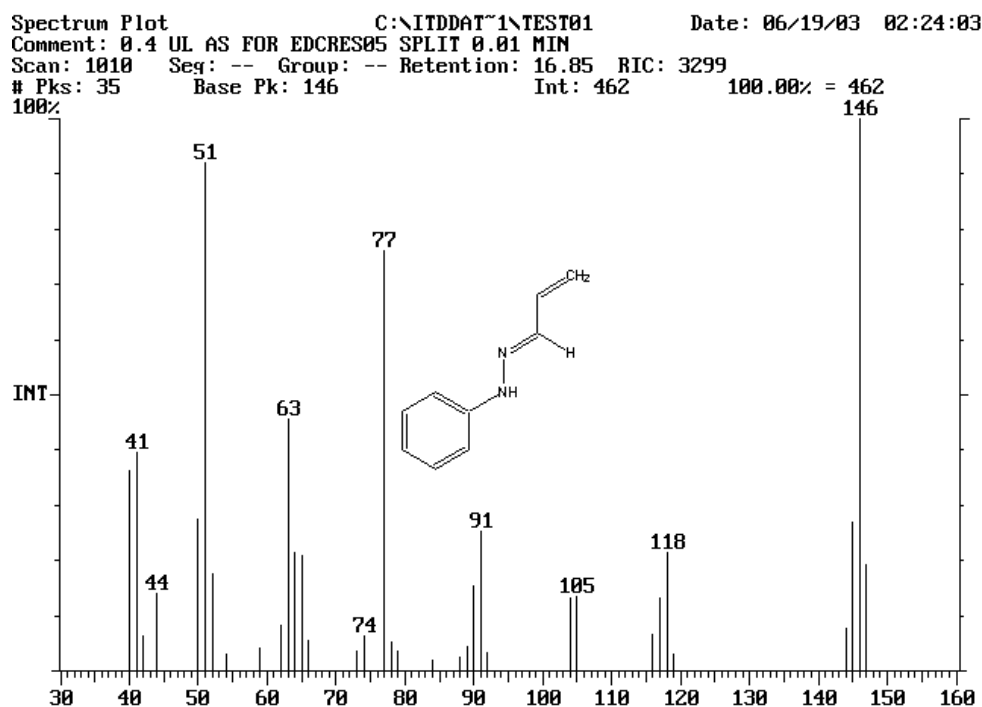


Figure 5.7 ITD Mass spectrum of the acrolein phenylhydrazone derivative (M^+ 146).

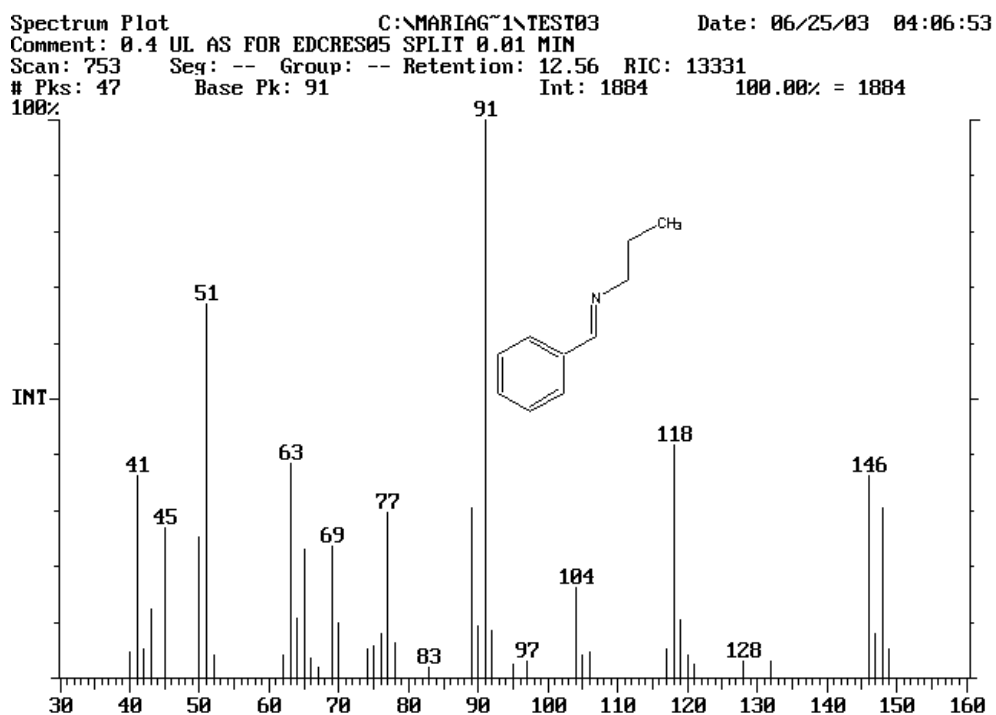


Figure 5.8 ITD Mass spectrum of the benzaldehyde propylimine derivative (M^+ 147). Notice the strong $M+1$ peak as m/z 148 that we ascribe to inadvertent chemical ionisation in the ITD.

5.4. Setup for SPME GC-FID-Based Testing of the PDMS mediated derivatization reactions

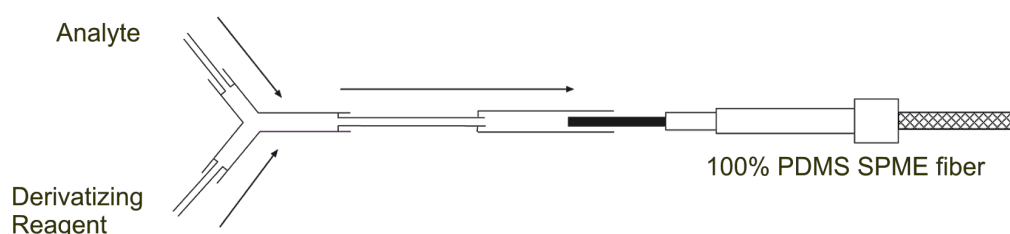


Figure 5.9 A simulation of the on-line REMPI-TOFMS set-up using SPME to determine approximate reaction efficiencies for the on-line derivatization reactions.

Simple reaction tests were performed to determine whether the selected derivatization reaction would take place in the PDMS and to estimate how efficiently the arrangement would trap the analyte. Figure 5.9 shows the on-line setup used to determine the approximate reaction efficiency for the various derivatization reactions.

Stable gaseous concentrations of the analytes were obtained by preparing permeation gas standards of the respective aldehydes and amines. Gas standard preparation and measurement has been described in my MSc thesis and in the literature [228, 229]. Two sets of gas standards were prepared: the first set was prepared in South Africa and used to determine the reaction efficiencies of the analytes; the second set was prepared in Germany to test the on-line REMPI-TOFMS technique. Concentrations provided by the gas standards are listed in Table 5.2. Figure 5.10 illustrates how the permeation rate is obtained. Plotting a graph of mass loss over time for each analyte should provide a straight line of which the gradient (mass-loss/ time) is the permeation rate. Unfortunately the formaldehyde gas standard, which is formed by the thermal depolymerization of paraformaldehyde at 80°C [61], was depleted before the REMPI-TOFMS experiments could be performed. The headspace from formaldehyde (stabilized with methanol in water) was then used as the formaldehyde gas source. This concentration was rather high and could not be determined in the framework of the experiments presented here.

Table 5.2 Summary of the aldehyde and amine permeation gas standards prepared.

Compound:	Pretoria			Munich		
	Permeation Rate			Permeation Rate		
	(ng/ min):	R ²	n	(ng/ min):	R ²	n
Formaldehyde	40	0.9979		60	0.9962	3
Acetaldehyde	70	0.9355	6	20	0.9823	3
Propanal	~	~	~	10	0.9989	4
Acrolein	8	0.9909	4	90	0.9984	4
Crotonal	40	0.9804	6	80	0.999	4
Diethylamine	~	~	~	200	0.9999	4
n-Propylamine	600	0.9998		100	0.9997	4
n-Butylamine	70	0.9935		40	0.9999	4

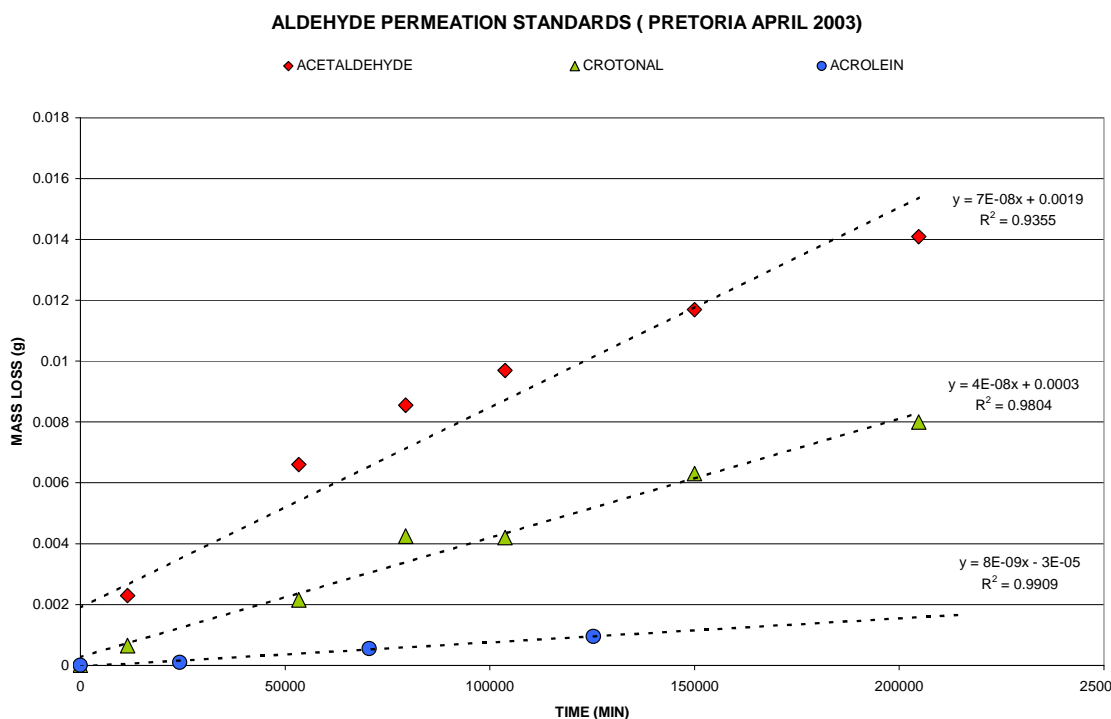


Figure 5.10 Graph of mass loss over time for acetaldehyde, acrolein and crotonal. The gradient of the straight line is the permeation rate (g/ min).



The gas standards were purged with nitrogen gas at a flow rate of 4 mL/ min. The gas standards provide a known concentration of analyte gas into the glass Y press-fit connector [230] (obtained from Chromatography Research Supplies, Inc., Louisville, KY) via an uncoated length of fused-silica capillary. Similarly, the derivatizing reagent, also being purged with nitrogen gas at 4 mL/min, was introduced at the other end of the Y press-fit connector. A 1-mL portion of the derivatizing reagent was placed in a 2 mL vial and sealed with a crimp cap. Two holes were pierced in the septum of the vial. A length of uncoated fused-silica capillary was pushed through each hole in the septum. One capillary was connected to the nitrogen gas, the other to the Y press-fit connector. Leading from the combined exit of the Y press-fit connector was another length of uncoated fused-silica capillary. The measured flow rate at this point was 8 mL/min, similar to the flows obtained from the REMPI-TOFMS vacuum. The exiting capillary was sealed into another glass press-fit connector, the opposite end of which was modified to house the exposed SPME fibre.

The SPME device consisted of a 100 μm PDMS-coated fibre [49] that was exposed over increasing time intervals to the on-line arrangement shown in figure 5.9. The SPME assembly and 100- μm PDMS fibres were obtained from Supelco (Bellefonte, PA). The fibre was desorbed in the heated inlet of a Varian 3300 GC at 150°C for 1 min. Quantitation was performed by flame ionization detection (FID) using undecane as internal standard and (calculated) effective carbon number responses of the derivatives, for which commercial standards are not available [61, 231, 232]. 1 μl of a 20ng/ μl undecane in CS_2 standard was injected, 2 minutes after desorption of the SPME fibre.

Thermal desorption of the SPME fibre is performed simply and quickly in the heated inlet of the GC oven; however, desorption of the silicone trap requires a desorption unit with some form of cooling in order to focus the desorbed contents onto the GC column. This is usually a longer process [61]. When the above procedure is carried out in GC-FID or GC/MS, the low initial temperature of the GC oven also acts to focus or concentrate the derivatized analyte in a short band. For real-time on-line applications, in the absence of such a focusing mechanism in the direct coupling of the trap to the TOFMS, another concentration device is required to enhance detectability. The reaction efficiency graphs shown in Figure 5.11 for the on-line derivatization of formaldehyde and acetaldehyde with phenylhydrazine display the increasing mass accumulation of derivative on the SPME fibre over time. Additional graphs for acrolein, crotonal, propylamine and butylamine can be found in the appendix.

Chapter 5 – On-line analysis of aldehydes and amines

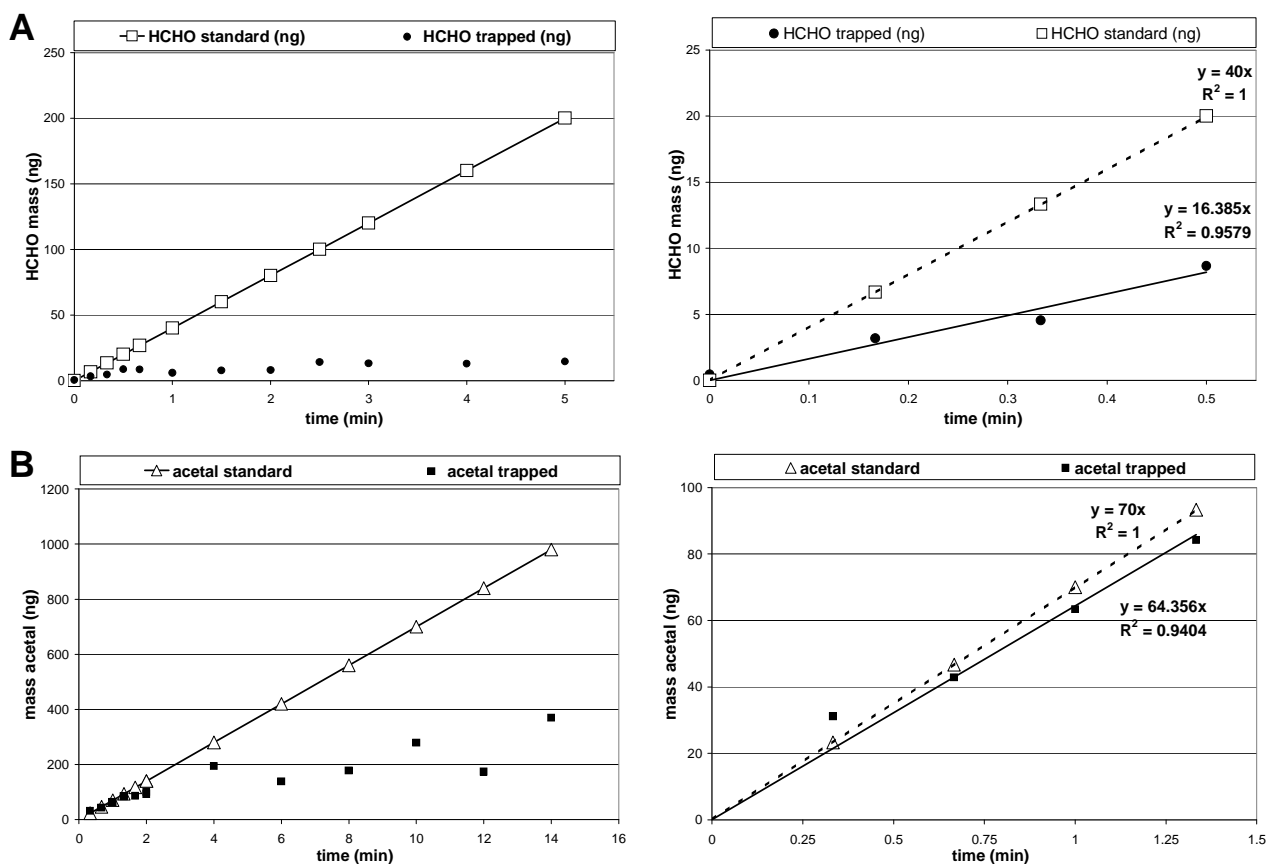


Figure 5.11 Reaction efficiency results for the on-line derivatization of A; formaldehyde and B; acetaldehyde with phenylhydrazine.

Both graphs display i) the calculated amount of gas standard released over the time interval using their gravimetrically determined permeation rate and ii) the amount of analyte gas trapped using *in situ* derivatization on the SPME fibre as calculated using the internal standard and effective carbon number response for the signal obtained from the GC-FID for the derivative. The graphs on the right hand side represent an enlargement of the left hand side graphs, where the initial accumulation on the SPME fibre appears linear. A comparison of the gradients obtained from the standard and the actual amount of analyte trapped gives an approximation of the reaction/trapping efficiency for this reaction before breakthrough starts to occur in the simple fibre/tube column.

Figure 5.12 depicts a GC-FID chromatogram of acetaldehyde, acrolein and crotonal (determined simultaneously). Formaldehyde gas was determined separately. As stated earlier, formaldehyde gas was prepared in an oven, while the remaining standards were in a glass tube at room temperature. Apart from formaldehyde, all the aldehydes form *E-Z* isomers (across the nitrogen-carbon double bond) and appear as two peaks in the chromatogram. Both peaks were integrated for quantitation purposes.

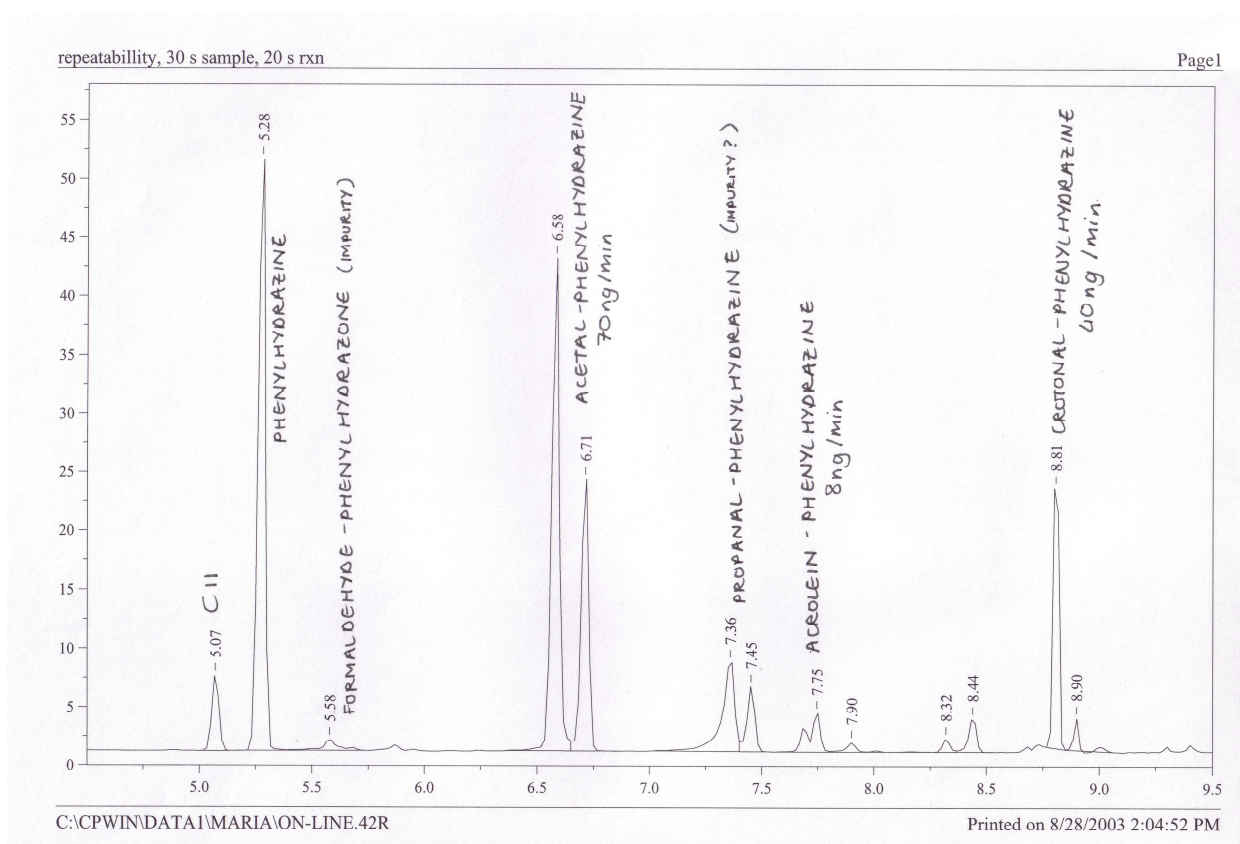


Figure 5.12 The GC-FID chromatogram obtained after desorption of a 100 μm PDMS SPME fibre exposed simultaneously for 30 seconds to the permeation gas standards of acetaldehyde, acrolein and crotonal and the phenylhydrazine derivatization reagent. Formaldehyde-phenylhydrazone impurity (5.58 min); Acetal-phenylhydrazone (6.58 & 6.71 min); Propanal-phenylhydrazone (7.36 & 7.45 min); Acrolein-phenylhydrazone (7.68 & 7.75 min) and Crotonal-phenylhydrazone (8.81 & 8.90 min). The double peaks for each derivative, excluding formaldehyde, represent *E-Z* isomers.



In figure 5.11, both graphs display (i) the amount of gas standard released over the time interval determined by their permeation rate, and (ii) the amount of analyte gas trapped using *in situ* derivatization on the SPME fibre, as calculated using an internal standard and the effective carbon number response for the signals obtained from the GC-FID for the desorbed derivatives [61, 232, 233]. The graphs on the right represent an enlargement of the graphs on the left, where the initial accumulation on the SPME fibre appears linear. A comparison of the initial gradients obtained from the analyte standard and the actual amount of analyte trapped gives an approximation of the reaction/trapping efficiency for this reaction [61]. The flattening off of the accumulation curves over time is the result of increased loss or “breakthrough” of the reaction product from the SPME fibre concentrator.

The reaction efficiency data, shown in Table 5.3 were obtained at room temperature using the arrangement, as shown in Figure 5.9. In Table 5.3, approximate reaction efficiencies of 28% for the reaction of propylamine and butylamine with benzaldehyde, 41% for the formaldehyde reaction with phenylhydrazine, and around 70% for the aldehydes with phenylhydrazine are indicated.

Table 5.3. Approximation of on-line reaction efficiencies, at room temperature without catalyst, as determined by the SPME set-up (figure 5.9).

Compound	Reagent	%Reaction efficiency	R ² (n)
Formaldehyde	Phenylhydrazine	41	0.9579 (4)
Acetaldehyde	Phenylhydrazine	92	0.9404 (4)
Acrolein	Phenylhydrazine	61	0.9990 (4)
Crotonal	Phenylhydrazine	74	0.9251 (4)
Propylamine	Benzaldehyde	28	0.9570 (4)
Butylamine	Benzaldehyde	28	0.9205 (4)

5.5. On-line derivatization setup

In Germany, an experimental on-line derivatization setup was built and coupled to the REMPI-TOFMS system. Two different variants were used for the derivatization procedure. In the first setup, a thermal modulator array (TMA) [216] with a fused-silica open tubular trap (OTT) (3- μm silicone film, DB-1 equivalent) was used to absorb, derivatize, desorb, and refocus the analytes. The second setup consisted of an enrichment desorption unit (EDU; Airsense Analytics, Schwerin, Germany) [234] with a PDMS MCT [61, 65, 66] as PDMS medium for derivatization followed by the above-mentioned arrangement with the TMA [216]. These experimental setups are shown in Figure 5.13 (A and B respectively). The TMA and EDU are described in chapter 4.

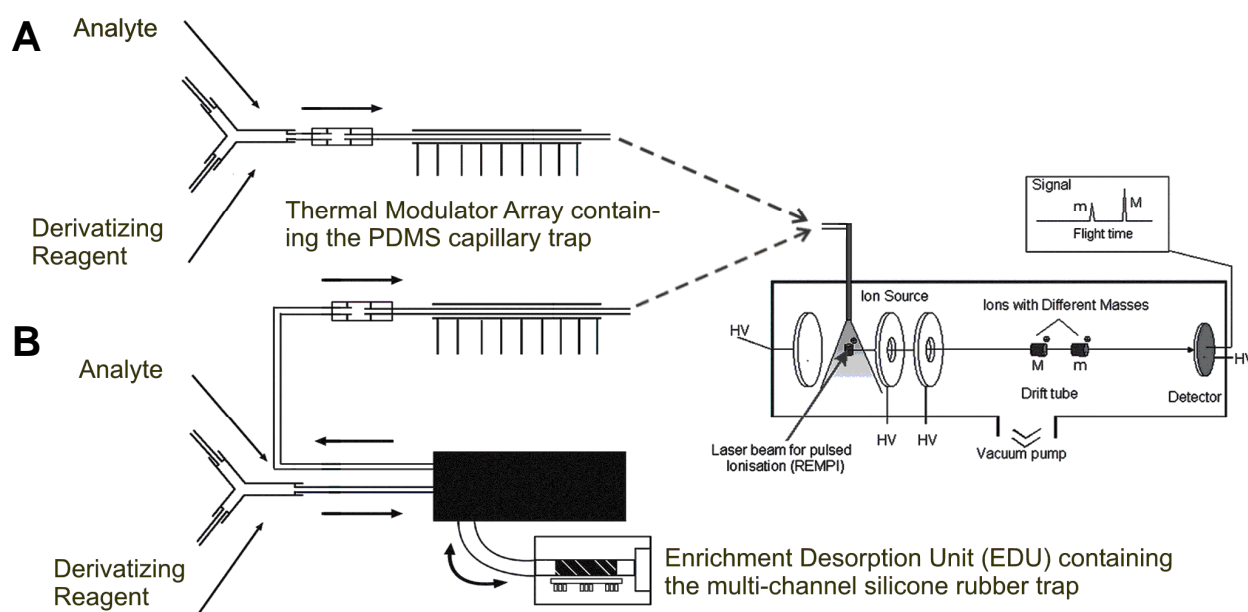


Figure 5.13 The experimental set-up used for:

A) On-line concentration and derivatization for REMPI-TOFMS using the thermal modulator array (TMA) with a thick film OTT as enrichment and reaction medium

B) On-line concentration and derivatization for REMPI-TOFMS using a multi-channel silicone rubber trap (MCT) in an enrichment and desorption unit (EDU) as enrichment and reaction medium and the thermal modulator array (TMA) with a thick film OTT for analyte modulation.

5.6. Resonance Enhanced Time of Flight Mass Spectrometry (REMPI-TOFMS)

5.6.1. Theory of Resonance-Enhanced Multi Photon Ionization (REMPI)

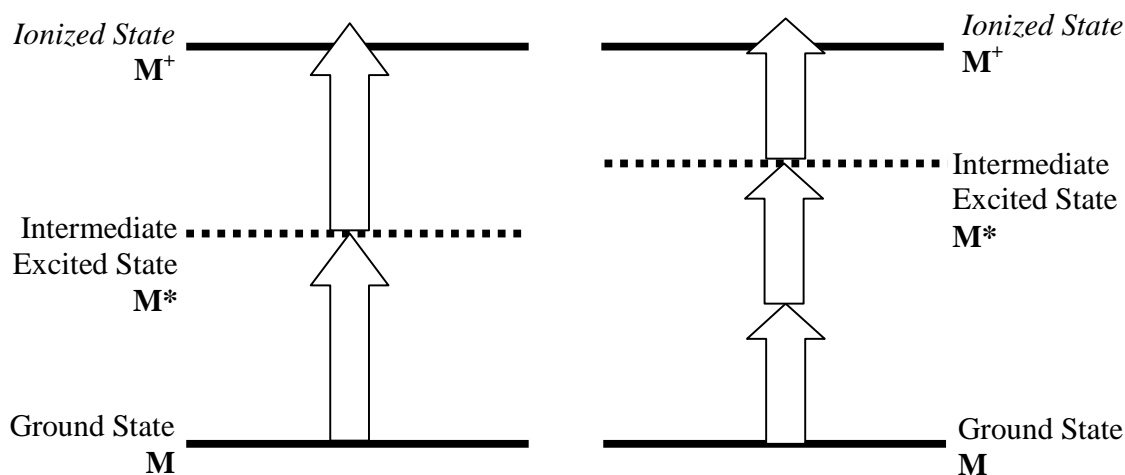


Figure 5.14 (1+1) and (2+1) Multi Photon Ionization processes [235]

The most familiar gas phase ionization technique is Electron Impact (EI) Ionization. High-energy electrons, usually 70 eV, bombard molecules as they enter the ionization chamber. Most molecules are ionized at this energy as they have ionization energies well below 70 eV. EI is also known as a hard ionization technique because it causes massive fragmentation of the ionized molecules. Less familiar (but well accepted) ionization techniques, particularly for on-line processes, are those using laser ionization, such as Single Photon Ionization (SPI) and Resonance Enhanced Multiphoton Ionization (REMPI). These are known as soft ionization techniques as lower energy photons are used to selectively ionize molecules resulting in very little to no fragmentation of the molecules [32, 235].

In laser ionization, a neutral molecule (M) is excited to a higher energy level through absorption of a UV photon, forming a high-energy neutral molecule (M*). Through the absorption of a second photon the molecule's ionization threshold is reached. The neutral molecule loses an electron to form the ionized molecule (M⁺). This is more commonly known as a (1+1) multiphoton ionization (MPI) process [235]. However, due to the critical energies required to reach the intermediate and ionization thresholds of small molecules, a higher order MPI process is frequently used, such as the (2+1) MPI process [235],



figure 5.14. Since each molecule has its own characteristic UV absorption spectrum, selective ionization of a molecule can be achieved through careful selection of a laser wavelength, at which the molecule undergoes selective absorption and (by resonant MPI) selective ionization [234]. 5

The REMPI process is based on a two-UV-photon absorption/ionization utilizing excited intermediate states (i.e. UV absorption bands), for resonance enhancement. Most aromatic compounds exhibit strong absorption bands in the 220-300-nm region. This wavelength region is easily accessible by commercial laser systems. REMPI is therefore a soft ionization source for selectively ionizing molecules with conjugated systems such as aromatic compounds and alkenes. However, increasing the laser intensity to obtain higher ionization yields will cause fragmentation of the molecule to occur [235]. After ionization, the charged molecules move into the TOFMS where separation is based on the differing masses of the ionized molecules that travel down the flight tube at differing speeds.

By comparison, with regards to ionization selectivity, the SPI technique lies between EI and REMPI [32]. In SPI, vacuum ultraviolet (VUV) photons are used. They have a much lower energy of 10.5 eV compared to EI electrons. This energy per photon is, however, high enough to cause ionization of selected molecules. In this case the VUV photons provide a single photon absorption/ ionization process where only molecules having a lower ionization potential than 10.5 eV, will be ionized [32].

5.6.2. Applications of REMPI-TOFMS

The home-built REMPI-TOFMS at the GSF, has been used for the on-line monitoring of dioxin surrogates and other aromatic trace species in waste incinerator emissions [32, 33], characterization of the formation of phenolic compounds during coffee roasting [34, 35], and puff-resolved analysis of toxic aromatic compound release during the cigarette smoking process [36] as well as the characterization of wood combustion [37]. In addition to the analysis of gaseous matrices, solid matrices can also be handled in a two-step process, using laser desorption followed by REMPI of the volatilized compounds [236-240].



5.6.3. The REMPI-TOFMS instrumentation

The resonance-enhanced multiphoton ionization time-of-flight mass spectrometer used for this application is a home-built system housed at the GSF, Oberschlesheim, Germany. The REMPI-TOFMS contains a pulsed Nd:YAG laser (Quanta-Ray INDI 50; Spectra Physics, Stratford, CT). The initial 1064-nm laser beam (repetition rate 10 Hz, pulse duration 10 ns) is frequency tripled, and the resulting wavelength of 355 nm is used to pump a β -BBO crystal of a thermally stabilized type II OPO laser system (GWU-Lasertechnik, Germany) to generate wavelength-tunable laser pulses in the range of 220 nm to 2.5 μ m. The generated laser pulses ($\sim 10^6$ W cm⁻²) are directed into the ionization chamber of the TOF (Kaessdorf Instruments, Germany) underneath the jet capillary inlet by optical elements. Molecular ions formed are accelerated and extracted into the flight tube of the reflectron TOFMS.

Mass spectra were recorded via a transient recorder PC card (Aquiris, Switzerland, 250 MHz, 1 GS/s, 128 k) whereby data processing is done by LabView (National Instruments, Austin, TX)-based home-written software. Wavelengths of 244 and 246 nm were selected for REMPI-TOFMS analysis of the formaldehyde- and acrolein-phenylhydrazone derivatives, respectively, and 240 nm for the benzaldehyde alkylimine derivatives. Spectroscopic investigations showed that for the REMPI-TOFMS setup used, these wavelengths are very efficient.

5.7. Experimental

5.7.1. On-Line Derivatization Setup for REMPI-TOFMS

Figure 5.13 (A) and (B) show the on-line derivatization REMPI-TOFMS setups. Unlike the arrangement for initial testing using SPME (see figure 5.9), the gas standards and reagents were not purged with nitrogen gas. In this case, the mass spectrometer vacuum provides the flow into the REMPI-TOFMS. On-line *in situ* derivatization was investigated using two different PDMS enrichment desorption devices, namely:



- (i) a thermal modulator array (TMA) with a PDMS thick-film capillary OTT and
- (ii) an enrichment desorption unit with a PDMS MCT .

Two setup variants were tested. In the first setup, only the TMA (i) with a PDMS thick-film OTT was used, whereas in the second setup, the EDU with a PDMS MCT (ii) was applied in combination with the TMA with a PDMS thick-film OTT (i). The two experimental setups are described in more detail below.

5.7.2. First Setup: Direct Supply of Analytes and Reagents through the Thermal Modulator Array (TMA-REMPI-TOFMS)

The centrepiece of the derivatization setup is the segmented thermal modulator array (TMA) [216]. The modulator houses a narrow-bore capillary coated on the inside with a thick film of PDMS (capillary trap). This capillary represents the concentrating / derivatizing device. The amount of PDMS within the capillary is comparable to the amount of PDMS forming the SPME fibre.

The modulator capillary consisted of a fused-silica capillary column (0.2 mm i.d.) coated with non-polar phase PS-255 (3 µm film, DB-1 equivalent). A capillary of 20 cm length was used with 5 cm of the stationary phase stripped off on either end, as described in reference [216]. A stainless steel capillary (105 mm x 0.6 mm o.d. x 0.35 mm i.d.) was converted to a modulator [216]. An electronic sequencer was used to provide current to the modulator in steps from 1 to 10 A at 5 V with a time duration of 10-2500 ms. To maintain reasonable flow rates and operate at atmospheric pressure, jet restrictors yielding a flow rate of between 0.6 and 1.0 mL/min were prepared according to the method described in reference 676 from an uncoated capillary (30 cm x 0.32 mm i.d.). The restrictor was coupled to the modulator capillary with a suitable press-fit. All transfer capillaries and connection points were either directly heated to 150 °C by a heating mantle or surrounded by a copper tube, which was then heated by a heating mantle.

The outlet of the TMA device was directly coupled to the TOFMS. This setup was used for detecting amines using benzaldehyde as photo-ionization labelling compound. Reagent and analytes (amine gas standard) were introduced simultaneously for 10 min into the cooled, PDMS, narrow-bore, thick-film capillary trap (inside the modulator steel tube) where the reaction occurred. In this case, the MS vacuum



Chapter 5 – On-line analysis of aldehydes and amines

provided a sampling flow rate of 0.7 mL/min. During modulation, the derivatives were desorbed into the REMPI-TOFMS. Similarly, the derivatization of the aldehydes with phenylhydrazine was demonstrated using only the modulator trap, followed by REMPI-TOFMS detection. The results obtained with the TMA-REMPI-TOFMS setup are given in Table 5.4 and Figures 5.15 and 5.16.

Table 5.4 Gas standard concentrations and calculated detection limits for the aldehydes and amines studied. Permissible Exposure Limits (PEL) as set by the Occupational Safety and Health Administration (OSHA) are also listed [15]. Detection limit values were not directly measured but determined by extrapolation of the larger measured values to a S/N ratio of 2.

Analytes (m/z)	Gas standard	Detection limit	Gas standard	Detection limit	PEL OSHA (ppm)
	Concentration	(s/n = 2 AVG 10)	Concentration	(s/n = 2 AVG 10)	
	EDU - TMA (ppm v/v)	EDU - TMA (ppm v/v)	TMA (ppm v/v)	TMA (ppm v/v)	
Formaldehyde -120	-	-	-	-	0.75
Acetaldehyde -134	-	-	79.4	2.04	200
Acrolein -146	-	-	37.4	0.101	0.1
Crotonal -160	-	-	199	1.52	2
Methylamine -119	34.3	0.257	-	-	10
Ethylamine -133	1.4	0.01	21.7	0.324	10
Propylamine -147	1.8	0.024	27.6	0.138	-
Butylamine -161	2.9	0.1	44.7	0.501	5

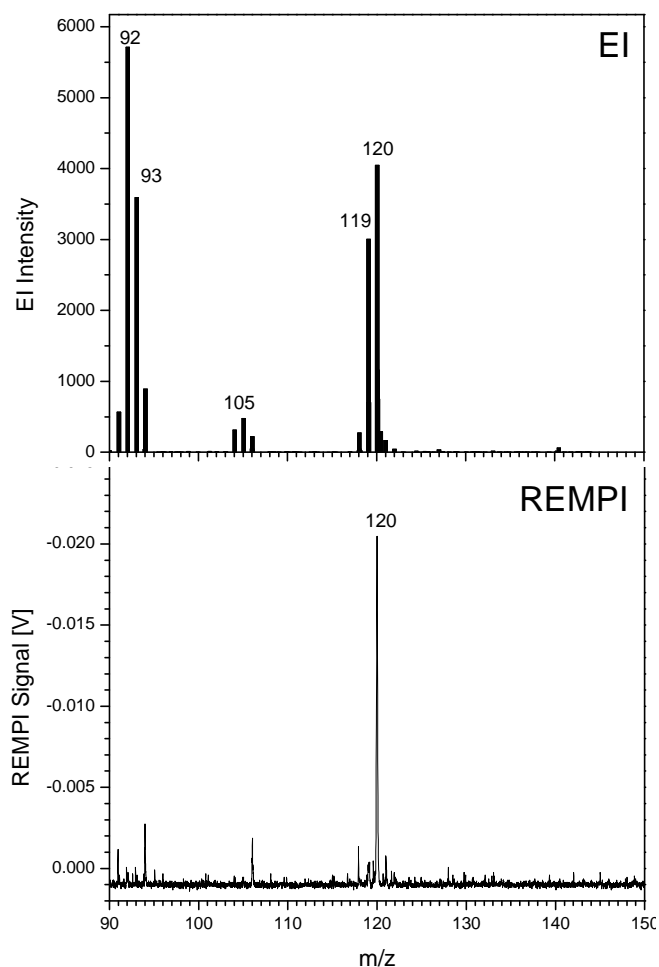


Figure 5.15 Mass spectra obtained for the formaldehyde phenylhydrazone derivative using two different ionization techniques. The Electron Impact (EI) mass spectrum was obtained from a prepared derivative on an accurate mass GC-TOFMS. The Resonance Enhanced Multiphoton Ionization (REMPI) mass spectrum was obtained from the on-line concentration and derivatization experiment.

5.7.3. Second Setup: Supply of Analytes and Reagents to an Enrichment Desorption Unit prior to the TMA (EDU-TMA-REMPI-TOFMS)

The second setup used is as shown in Figure 5.13 (B). Here, the MCT in the enrichment desorption unit (EDU) is used as the concentration-reaction medium, and the TMA is used for subsequent temporal focusing. The MCT is placed within the EDU, which is connected via the TMA to the REMPI-TOFMS



Chapter 5 – On-line analysis of aldehydes and amines

(EDU-TMA REMPI-TOFMS). The principal difference between SPME (or the application of TMA solely) and the MCT is the amount of PDMS available for concentration of analytes, with the MCT having a considerably larger amount of PDMS (approximate PDMS volumes are TMA trap 0.2 mm^3 and the EDU MCT 135 mm^3). As the MCT can concentrate and derivatize more analyte it has the potential to provide lower detection limits. The EDU system is described in chapter 4.

For *in situ* derivatization, the aromatic derivatizing reagent dissolves into the PDMS from the gas phase. Carbonyl compounds (aldehydes and ketones etc.) passing through the trap react selectively with the reagent and remain in the trap until they are thermally desorbed for analysis [60, 61]. In the case of the above-mentioned SPME-GC-FID approach, desorption is performed for some time in the heated GC injector, [49, 60, 61]. The derivatized analytes are refocused in a short band due to the low initial temperature of the GC oven.

For on-line real-time analytical applications, however, analyte focusing can also be important, for time resolution and sensitivity rather than for the enhancement of the chromatographic resolution. As described in the first set-up, analyte focusing can be achieved by repetitive thermal modulation. In this setup, the EDU is used in combination with a segmented TMA, as described above.

Conditions for the EDU used in these experiments were as follows: sampling for 130 s at 6°C with a sampling flow rate of 230 mL/min and thermal desorption for 60 s at 180°C . Injection occurs under reversed flow conditions. During injection, the desorbed compounds are drawn into the REMPI-TOFMS at a flow rate of 15 mL/min , as they are restricted by the capillary jet leading into the ion source. Both the sampling line and the transfer line into the MS are heated at 150°C . Benzaldehyde was sampled for 60 s through the heated sampling line. After 10 s, the amine gas mixture was sampled through the sampling line for 60 s. The sampling flow rate was 230 mL/min . Benzaldehyde accumulates in the PDMS multichannel trap, cooled to 6°C . The introduced amine gas subsequently reacts with the benzaldehyde in the trap. The reaction is further encouraged during desorption at 150°C for 1 min. During the injection phase, the derivatives are transferred to the TMA, which submits timely-focused concentrated pulses to the REMPI-TOFMS system. The results obtained with the EDU-TMA-REMPI-TOFMS setup are given in Table 5.4 and Figure 5.16.

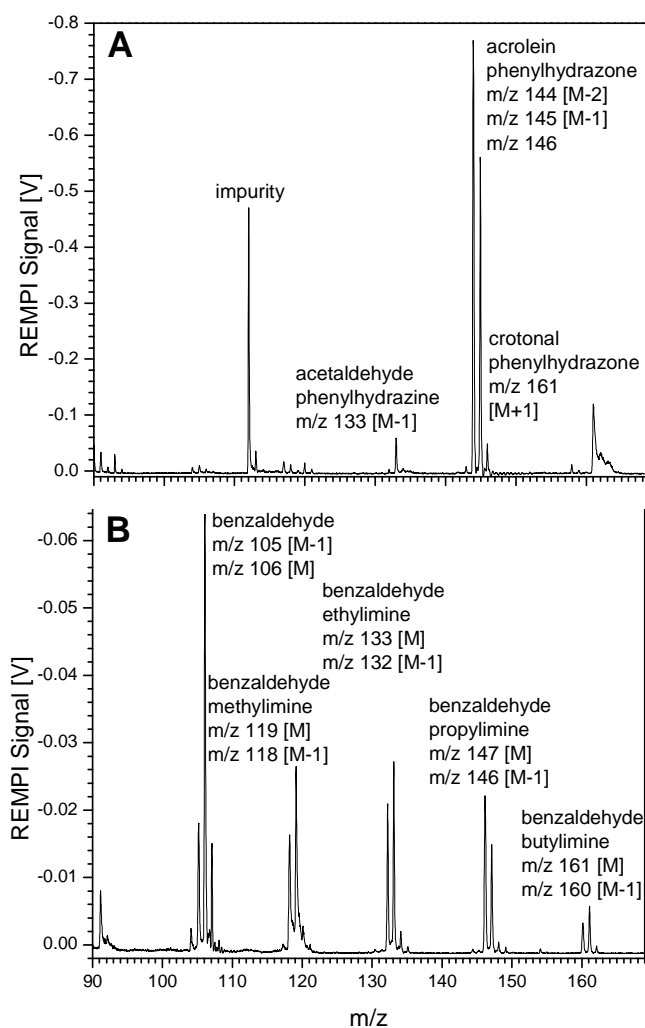


Figure 5.16 REMPI-TOF mass spectra obtained for the on-line concentration and derivatization of **A.** acetaldehyde, acrolein and crotonal with phenylhydrazine at 246 nm, and **B.** methylamine, ethylamine, propylamine and butylamine with benzaldehyde at 240 nm.

5.8. Results and Discussion

Incomplete reaction was confirmed by single photon ionization time-of-flight mass spectrometry (SPI-TOFMS) [32, 232] of the on-line, *in situ* derivatization of propylamine (59 m/z) and butylamine (m/z 73) with benzaldehyde (m/z 106). The presence of both derivatized (161 and 147 m/z) and underivatized analyte (59 and 73 m/z) was observed, as shown in figure 5.17. Although these derivatization reactions are not 100% efficient at room temperature, they still occur readily without the aid of any catalysts. Thus, for quantitation, the use of internal or external standards is required.

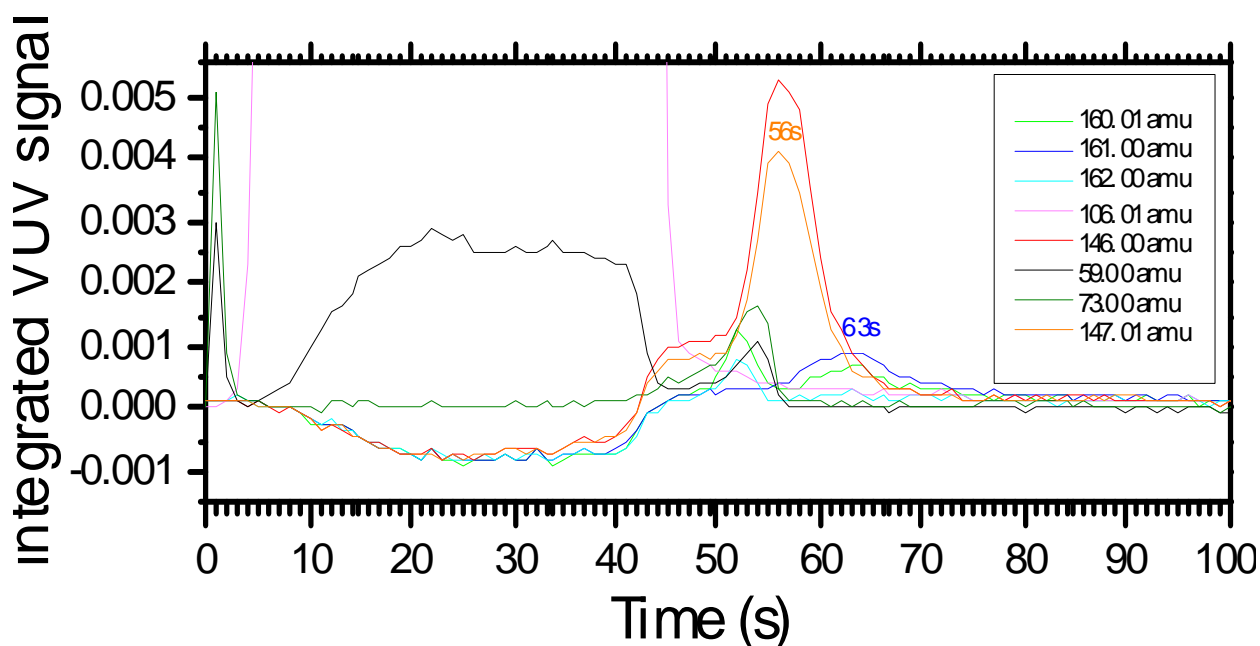


Figure 5.17 Single Photon Ionization (SPI) mass spectrum of the on-line, *in situ* derivatization of Propylamine (m/z 59) and butylamine (m/z 73) with benzaldehyde (m/z 106). The presence of both derivatized (m/z 161 and m/z 147) and underivatized analyte was observed.

The results of the on-line tests with REMPI-TOFMS detection are discussed below. The experiments demonstrated that all investigated amines and aldehydes could be successfully derivatized, desorbed, and identified by REMPI-TOFMS using the on-line setups described above. Figure 5.15 displays the results obtained for formaldehyde. In the upper part (A), a conventional 70-eV EI mass spectrum for the formaldehyde phenylhydrazone derivative is shown. This mass spectrum was obtained from a formaldehyde phenylhydrazone derivative, prepared using the method described by Vogel *et al.* [241] on an accurate mass TOFMS (Micromass, GCT, U.K.). The formaldehyde phenylhydrazone derivative was detected at 120 m/z , together with a H loss of similar intensity (119 m/z). The base peak of the spectrum, however, is due to the $C_6H_5NH^+$ fragment at 92 m/z . The peak at 93 m/z is probably due to $C_6H_5NH_2^+$ formed in a rearrangement.

Figure 5.15 also displays the REMPI mass spectrum (244 nm, averaged over 10 transients) obtained from the equivalent on-line derivatization reaction of formaldehyde using the TMA REMPI-TOFMS setup described above. The soft ionization capability of REMPI provides simple mass spectra with

nearly no fragmentation. The mass peak 94 m/z in the REMPI spectrum is suspected to be due to an impurity in the phenylhydrazine reagent (most likely phenol). Although the emphasis of this study was not on using SPI-TOFMS (since most of the small molecules tested here, excluding formaldehyde, can be detected by SPI), the TMA set-up was also tested using SPI-TOFMS [32], for the detection of formaldehyde only. Figure 5.18 shows the SPI signal over time, obtained from the TMA set-up for m/z 120, the mass of the formaldehyde derivative. Figure 5.18 also displays the mass spectrum for a single transient taken from the SPI-TOFMS signal over time. A clean mass spectrum displaying only the molecular ion m/z 120 for the formaldehyde-phenylhydrazone derivative was observed using SPI. This result is significant as it is demonstrated that formaldehyde can be made visible not only to REMPI-TOFMS but also to SPI-TOFMS.

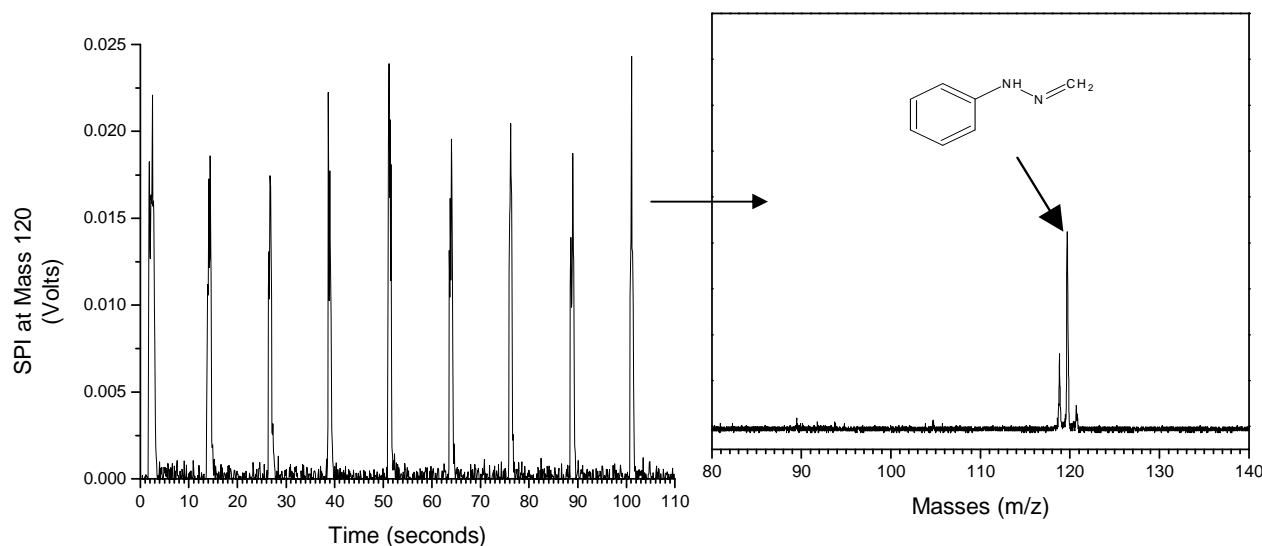


Figure 5.18 SPI signal over time, obtained by applying the on-line *in situ* derivatization TMA setup to the SPI-TOFMS [32] for the analysis of formaldehyde. The insert shows the mass spectrum obtained as a single shot from the time profile, depicting the formaldehyde-phenylhydrazone derivative.

Figure 5.16 shows the REMPI-TOF mass spectra obtained for the TMA and EDU-TMA on-line derivatization of the aldehydes (A) and the amines (B), respectively. The REMPI mass spectrum of the aldehyde derivatives at 246 nm (figure 5.16A) displays the $[M - 1]$ and $[M - 2]$ mass peak for the acrolein-phenylhydrazone derivative (145 and 144 m/z). $[M - 1]$ corresponds to the loss of a hydrogen atom and $[M - 2]$ to the loss of two hydrogen atoms.



The [M - 2] signal is off-scale. These peaks were also observed on the electron impact (EI) mass spectrum of the derivative (not shown here). Only the [M - 1] peak was observed for the acetaldehyde-phenylhydrazone derivative (133 m/z). The crotonal phenylhydrazone was detected as a [M + 1] peak (161 m/z). Additionally, only a very weak [M - 2] peak is visible (158 m/z). [M + 1] adduct peaks are commonly visible in chemical ionization mass spectra, and to a lesser extent in EI mass spectra obtained from ion trap mass spectrometers, when some unintentional chemical ionization can occur. However, [M + 1] peaks do not occur in photo-ionization TOF mass spectra under the chosen conditions (i.e., a pressure of 10^{-4} mbar in the ion source, avoiding protonation *via* ion-molecular reaction). The strong [M + 1] peak for crotonal phenylhydrazone is thus unexpected. It probably indicates that a side reaction has occurred during the derivatization. Because phenylhydrazine, like hydrazine, is a reducing agent, one possible explanation is the hydrogenation of the double bond of crotonal (either before or after the derivatization). The resulting derivative would be butanal phenylhydrazone (162 m/z), which may be detected as an [M - 1] peak (161 m/z), as found for the acetaldehyde and acrolein derivatives. However, it remains unexplained at the current level of research why the same hydrogenation does not take place for acrolein. If we summarize the result for the aldehydes, it can be stated that only formaldehyde can be detected at the unfragmented derivative mass [M] of 120 m/z .

The other aldehyde derivatives, however, were identifiable at either the respective [M - 1] or [M - 2] peak ([M + 1] for crotonal). The molecular ion [M] for acetaldehyde, acrolein, and the crotonal phenylhydrazone were not observed at the applied REMPI wavelength of 246 nm. An EI mass spectrum of the acrolein phenylhydrazone product, however, clearly shows the molecular ion mass peak at m/z 146. (Note that the peak at m/z 146 in Figure 5.16A is due to the ^{13}C isotope peak for the [M - 1] ion, not the molecular ion). This indicates that for higher aldehyde-phenylhydrazone derivatives, a photo-induced fragmentation is observable. This is not, however, a problem for the analytical application because the mass spectra are still very soft; i.e. only one (or two) peak(s) dominate the spectra. Phenylhydrazine itself was not observed at the selected REMPI wavelength. It should be noted that with other REMPI wavelengths or power densities, different relative sensitivities or photo-induced fragmentation activities for the different aldehydes may be observed.



The REMPI mass spectrum (240 nm) of the amine derivatives is shown in Figure 5.16B. Benzaldehyde-methylimine, -ethylimine, -propylimine, and -butylimine display two mass peaks of similar intensities, [M] and [M - 1], corresponding to the molecular ion and the hydrogen atom loss. This trend was also observed on the EI mass spectra. In addition, the derivatizing reagent, benzaldehyde, is also observed in the mass spectrum (Figure 5.16B).

The signal [M] m/z 106 is off-scale. The [M + 1] m/z 107 peak is, therefore, the ^{13}C isotope peak. The presence of m/z 106 confirms that the reagent is present in excess during the on-line reaction. A mass gate is required during on-line derivatization to deflect these ions from the detector when an excessive quantity of reagent, such as benzaldehyde, is present. The mass gate will prevent “blinding” of the detector to masses occurring after 106 mass units (the mass of benzaldehyde).

To summarize, the REMPI detectability of the amine derivatives is as successful as for the aldehydes: all analytes were detected as [M] and [M - 1] with no further fragments.

Detection limits were determined and are summarized in Table 5.4. They were calculated using the combined method of Heger *et al* [33] and Williams *et al* [242] using a S/N of 2 and an average of 10 mass spectra. The results obtained demonstrate the potential of this technique for future applications. The calculated detection limits for the analytes are markedly below permissible exposure limits set by the Occupational Safety and Health Administration (OSHA) [15]. The EDU, constructed specifically for use with the on-line REMPI-TOFMS, allows for the use of a MCT for pre-concentration. Lower detection limits were achieved with this setup, since more PDMS is available for pre-concentration. This is confirmed by the results obtained for the benzaldehyde-methylimine, -ethylimine, -propylimine, and -butylimine derivatives using the EDU-TMA and the TMA, respectively (see Table 5.4). In addition, off-line sampling together with a portable pump is also made possible, since the MCT trap is easily removed from the EDU.



5.9. Conclusions

This work demonstrates that on-line derivatization concepts can be used to expand the unique online analytical properties of the REMPI-TOFMS to aliphatic compound classes. Methods for on-line *in situ* derivatization of alkylamines with benzaldehyde and alkyl aldehydes with phenylhydrazine followed by thermal desorption and detection by the REMPI-TOFMS were successfully tested. The detection limits obtained for all analytes, for which concentration standards were made, are below the permissible exposure limits set by OSHA. Formaldehyde, which is not easily detected by mass spectrometry, can be detected as the phenylhydrazone derivative. In the future, formaldehyde gas standards of known concentration will be needed to determine formaldehyde's detection limit for the on-line reaction.

The potential analytical impact of the concept presented here should not be underestimated. Through the coupling of suitable photo labels to non aromatic compounds, a larger variety of compound classes can now be considered for REMPI-TOFMS detection, including compounds such as sugars, sulphur compounds, organic acids, or alcohols. Fast screening methods, for example for environmental samples, biological samples, or medical applications, may be developed on this basis.

As indicated in the introduction (chapter 1), that it is not possible to concentrate volatile underivatized compounds directly by PDMS. The study presented in this chapter provides an example of the use of derivatization reactions to enable both the collection and the concentration of polar volatile analytes as well as their detection with a selective detector.

The combined use of REMPI (and SPI) and the derivatization strategy provides sufficient selectivity to perform trace analysis of real samples without a lengthy chromatographic separation, allowing for on-line monitoring.

Chapter 6

Determining endocrine disruptors from water by concentration and derivatization in PDMS multichannel traps

6.1. Our approach

The PDMS MCT consists of an open tubular assembly, making it suitable for the concentration of analytes directly from water, without the need for prior filtration. The PDMS MCT has already been utilized to concentrate PAHs from water [63, 67]. Since the analytes had no functional groups which could interfere with the chromatography, no additional sample preparation was required other than the removal of water from the trap before thermal desorption into the GC-MS [63, 67]. In order to extend the range of compounds amenable to PDMS MCT sampling, we decided to extract analytes that would require derivatization before analysis by GC-MS.

As described in chapter 1, there is a need to analyse ultra trace endocrine disruptors from water. Due to their extremely lipophilic nature, estrogens and alkylphenols should, in theory, partition into PDMS MCT traps very easily. However, they possess hydroxyl functional groups, which require derivatization not only to improve the chromatography but also, perhaps simultaneously, to improve the detection properties of these analytes.

It is understood that, due to their lipophilicity, that the estrogens and alkylphenols are more likely to be adsorbed to particulates, sediments and sludge present in water sources. For example, literature indicates that approximately 50-75% of NP is adsorbed on sediment, implying only 25-50% is present in the water [9]. In addition estrogens may also occur as their glucuronide or sulphate conjugates resulting from human excretion [24, 58], the conjugates are not biologically active but are reconverted to free steroids by bacteria in the environment [276]. Thus the estrogens are largely deconjugated in water systems. The scope of this study did not include the investigation of the total content of these analytes in the water source, but to demonstrate the concentration of the free analytes in water in the PDMS MCT.

Ideally, for sampling, the PDMS MCT should be located where it can concentrate the analytes directly from the source, e.g. in a river. Following concentration the trap can be returned to the lab for further treatment without loss/change of the sample. Once in the lab, water can be removed from the trap and the derivatization reaction can be performed *in situ*, followed by thermal desorption and GC/MS analysis.

The first step in this study was to select a suitable derivatization reagent for the analytes and to determine how well the reaction would proceed within the PDMS matrix. Then the completeness of transfer of the derivatives from the trap (i.e. complete thermal desorption) to the column was verified. Once this was known, extraction efficiency of the analytes into the PDMS could be investigated. The steps were carried out in this order since it was impossible to analyse the extracted-undervatized analytes by comparison as their chromatographic performance deteriorates rapidly even when starting with a new GC column. Once concentration and derivatization have been demonstrated, the PDMS MCT could be applied to the analysis of real samples.

Table 6.1 lists the structures of the analytes to be determined in our study.

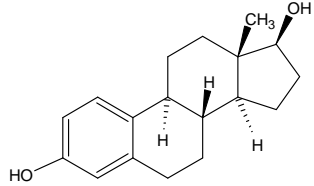
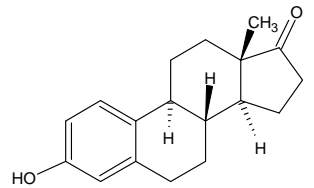
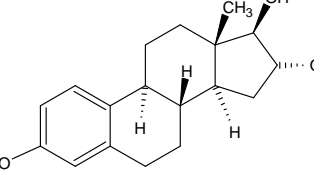
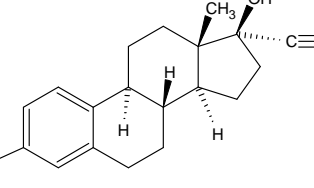
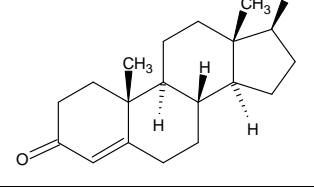
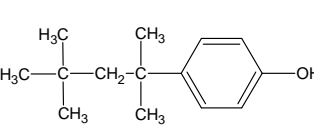
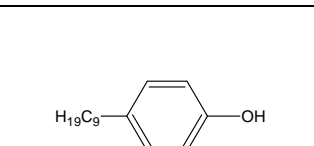
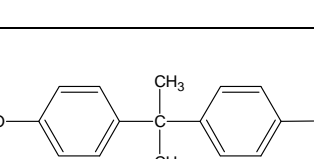
6.2. Derivatization

6.2.1. Initial derivatization reactions involving the estrogens

BSTFA leads the way as the derivatization reagent of choice for the conversion of hydroxyl groups on estrogens and alkylphenols [1-3, 21, 23-25, 243], (see chapter 3 page 63). However, it has been demonstrated that unless the ratio of BSTFA/ 1% TMCS/ pyridine, is not carefully regulated, the β -ethinylestradiol (EE2) derivative readily converts to the estrone (E1) derivative which is often being analysed simultaneously [244, 245].

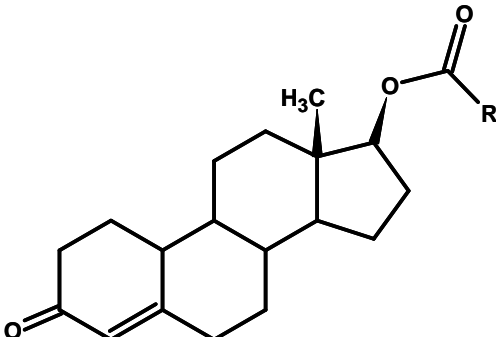
It was therefore decided to rather perform an acylation reaction to convert the EDCs. This has the added advantage that anhydrous conditions are not required (see chapter 3). According to the results obtained by L. Dehennin *et al.* [246], shown in table 6.2, a maximum electron capture detector (ECD) response is obtained when the hydroxyl group on testosterone is substituted to form the heptafluorobutyl (HFB) ester, followed closely by the pentafluorobenzoyl- (PFB) and pentafluorophenyl- (PFP) esters [246]. (See chapter 3 page 60, for derivatization reagents which yield these derivatives).

Table 6.1 Endocrine disrupting compounds to be analysed by concentration and derivatization in the PDMS MCT.

Compound name:	Compound structure:	Molecular Formula:	Molecular Mass:	Abbreviation
17 β -estradiol		C ₁₈ H ₂₄ O ₂	272	E2
estrone		C ₁₈ H ₂₂ O ₂	270	E1
estriol		C ₁₈ H ₂₄ O ₃	288	E3
17 α -ethinylestradiol		C ₂₀ H ₂₄ O ₂	296	EE2
17 β -testosterone		C ₁₉ H ₂₈ O ₂	288	T
<i>tert</i> -octylphenol		C ₁₄ H ₂₂ O	206	TOP
4-n-nonylphenol		C ₁₅ H ₂₄ O	220	NP
bisphenol-A		C ₁₅ H ₁₆ O ₂	228	BPA

From literature it was found that both the HFB and PFBCl reactions occur rapidly and would provide an electron rich derivative suitable for ECD and NCI-MS [62, 190, 192, 193, 247]. Both the HFB and PFBCl reactions required heating to 55°C [62] and 80 °C [191, 192, 247] respectively. However, certain methods have been described where no heating is required for either reaction [62, 193].

Table 6.2 Comparison of electron-capture detector responses for different testosterone acyl-derivatives [246]. With permission from Preston Publications, IL, U.S.A.

Testosterone	R	Relative response
	CH ₃	0.1
	CF ₃	0.4
	CH ₂ Cl	4
	C ₂ F ₅	5
	C ₃ F ₇	19
	CF ₂ Cl	34
		50
	C ₇ F ₁₅	60

[L. Dehennin, A. Reiffstock, R. Scholler; *J. Chromatogr. Sci.* (1972) 10, p 224]

6.2.2. Derivatization of the estrogens with Pentafluorobenzoyl chloride (PFBCl)

Initial tests using PFBCl were attempted. Here the concept was to first derivatize the analytes in the water, then to hydrolyse the excess reagent to the acid (which would remain ionized in the aqueous phase) and extract only the derivatives into the PDMS MCT by pouring the entire sample reaction mixture through the trap. Both Akre, Fedeniuk and MacNeil [191] and Xiao and McCally [192, 247], derivatized the estrogens from water under anhydrous conditions i.e. the sample was first evaporated to dryness. The reaction with PFBCl occurred in organic solvents at elevated temperatures. A more elegant method was presented by Kuch and Ballschmiter [193], where the

reaction between PFBCl and the estrogens occur in water. The derivatives that form immediately, at room temperature, are extracted into hexane [193]. Excess PFBCl remains in the aqueous phase [193]. The latter reaction seemed appropriate for our PDMS MCT experiment. Identical steps could be followed until the final extraction step where the hexane (non-polar solvent) would be replaced by the PDMS MCT (“non-polar” solvent).

Attempts to synthesise the derivatives using the method by Kuch and Ballschmiter [193] were not successful. Only the hydrolyzed reagent was observed, implying that neither the estrogen nor the derivative was extracted into the hexane. It is possible that the reagent was old and already hydrolysed before being opened, thus a new reagent vial was opened but the process still yielded the PFB hydroxide. Figure 6.1 shows a typical chromatogram with mass spectrum of the main reaction product, obtained on a Micromass® GC-TOFMS. The product was confirmed using the NIST library mass spectrum.

Using the methods by Akre *et al* and Xiao *et al*, returned the same result. One of two explanations are possible, the most obvious being: i) the PFBCl reagents have all hydrolysed before the vial is opened; or ii) the reaction conditions, particularly in water or in solvents containing water have caused the PFBCl to hydrolyse, thus preventing the reaction from occurring. Further work with this reagent was abandoned, as time was limited at this stage.

6.2.3. Derivatization of the estrogens with trifluoroacetic acid anhydride (TFAA)

Trifluoroacetic acid anhydride (TFAA) was used to convert both the phenolic and hydroxyl functional groups on the estrogens. The reaction was tested in the PDMS MCT as follows: 50 µl of a 20 ng/µl EDC mixed standard consisting of E1, E2, E3, EE2 and T (defined in table 6.1) in acetone, was inserted into the PDMS trap using a Drummond® Microcap capillary (with plunger). The acetone was removed by gently blowing nitrogen gas through a capillary into the trap until acetone could no longer be detected by smelling the trap outlet (usually less than a minute of purging). 10 µl of TFAA was added to the bottom of the PDMS trap. The PDMS MCT was then sealed at both ends with glass plugs and the reaction allowed to proceed for 10 minutes. The trap was then immediately thermally desorbed in the Chrompack® TDU and analysed by GC-(EI) MS.

The instrument conditions were as follows:

Splitless desorption at 280°C for 20 min with a desorb flow of 100 ml/ min, inject at 280°C for 5 minutes. The GC oven was held at 40°C for 1 min then ramped at 5°/min to 280°C and held for 10 min, then ramped again at 20°/min to 300°C and held for 5 min. A solvent delay of 28 min was set on the MS to avoid the detector being damaged by the excess volatile TFAA entering the MS. A scan range of 40 – 600 amu was used.

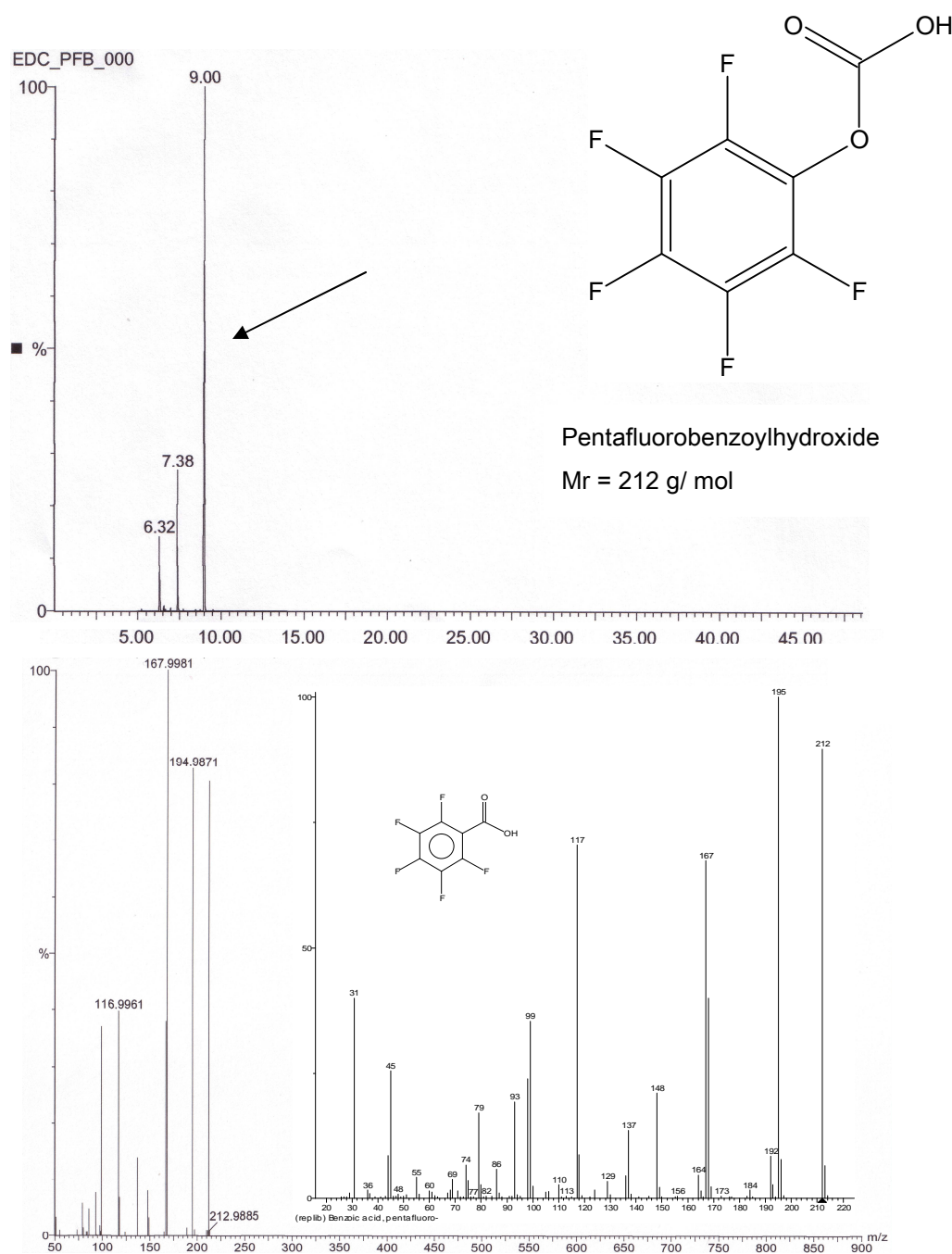


Figure 6.1. Gas chromatogram and time-of-flight mass spectrum of PFBCl hydrolysis product obtained when performing the method introduced by Kuch and Ballschmiter [193].

Figure 6.2 shows the total ion chromatogram (TIC) obtained for this experiment. The TIC for the desorbed PDMS MCT trap shows extremely overloaded and jagged-edged PDMS thermal degradation peaks reflecting the excess TFAA reagent and very high thermal desorption temperature used. It should be noted that the chromatogram using NCI-MS (shown in figure 6.8 below) is significantly cleaner since the PDMS degradation peaks are selectively removed because of poor ionization with the NCI technique.

The reconstructed ion chromatogram (RIC) of the molecular ions of each derivative observed is shown beneath the TIC in figure 6.2. The RIC gives a good indication of how the selectivity of the MS improves when moving to Selected Ion Monitoring (SIM) – where the PDMS thermal degradation peaks are absent.

Figures 6.3 to 6.6 show the EI mass spectra obtained for the E2, E1, E3 and T – TFA derivatives each with an abundant molecular ion. Both hydroxyl and phenol groups were substituted to form the TFA ester. The presence of the TFA moiety in each derivative is confirmed by m/z 69 ($-CF_3$). Out of interest, another peak not shown on the RIC is the enol tautomer of testosterone that is doubly substituted with TFA. Figure 6.7 shows the mass spectrum of the disubstituted derivative together with the keto-enol tautomerism occurring with testosterone. The disubstituted E2 TFA derivative and the T derivative mass spectra agree with the corresponding mass spectra provided by Lerch and Zinn [62]. *Mass spectra for most of the estrogen-TFA derivatives were not available in the NIST or Wiley libraries.* Neither the mono- (M^+ m/z 392) nor the di-TFA (M^+ m/z 488) derivative of EE2 was observed, figure 6.2. The EE2-di-TFA derivative was expected to elute between the E1-TFA and T-TFA derivatives [62].

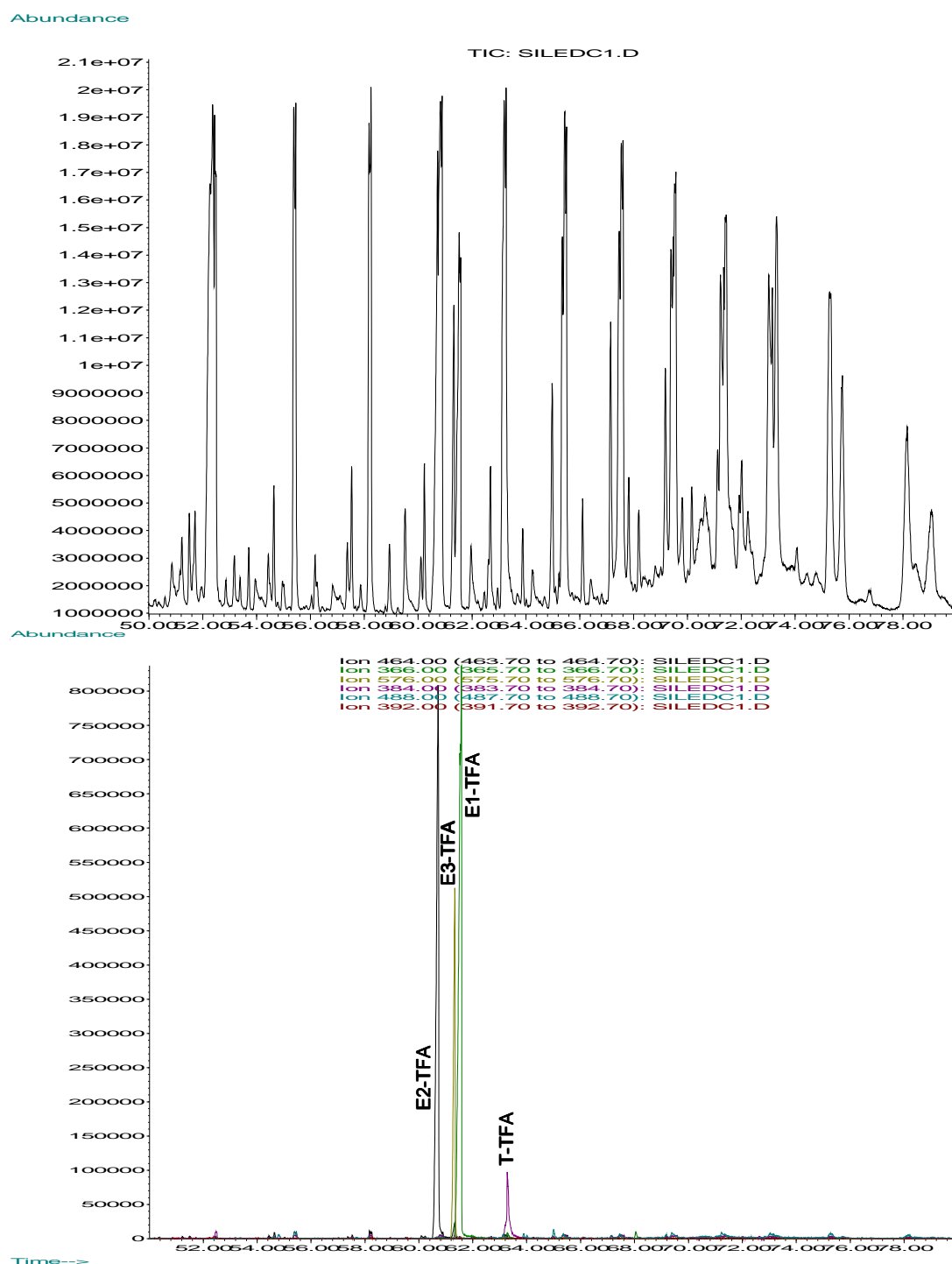


Figure 6.2 GC- (EI) MS: Total ion chromatogram (TIC) of the *in situ* derivatization of estrogens in the PDMS MCT using TFAA. Beneath is the reconstructed ion chromatogram of molecular ions of the derivatives of : estrone (E1-TFA); β -estradiol (E2-di-TFA); estriol (E3-tri-TFA) and testosterone (T-TFA) trifluoroacetate (TFA) derivatives.

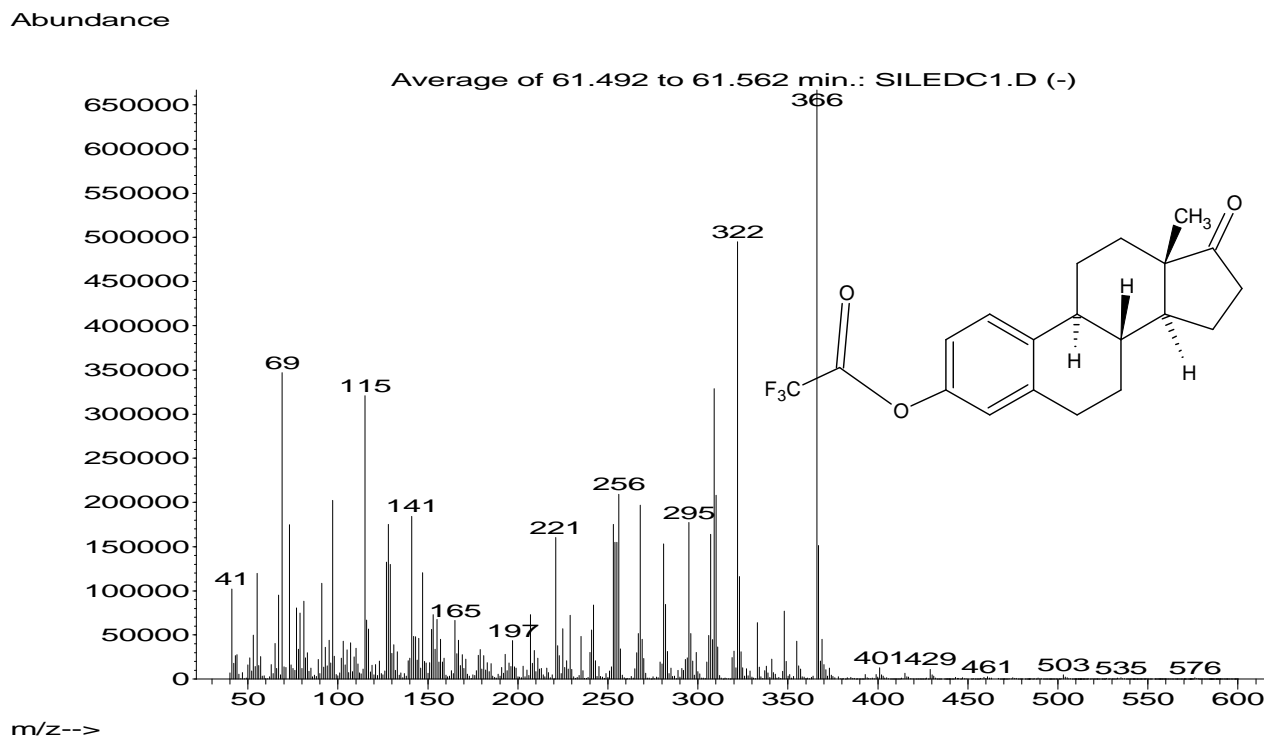


Figure 6.3 Electron impact mass spectrum of the estrone-trifluoroacetate (E1-TFA) derivative. Molecular ion (M^+) m/z 366, ($-CF_3$) m/z 69.

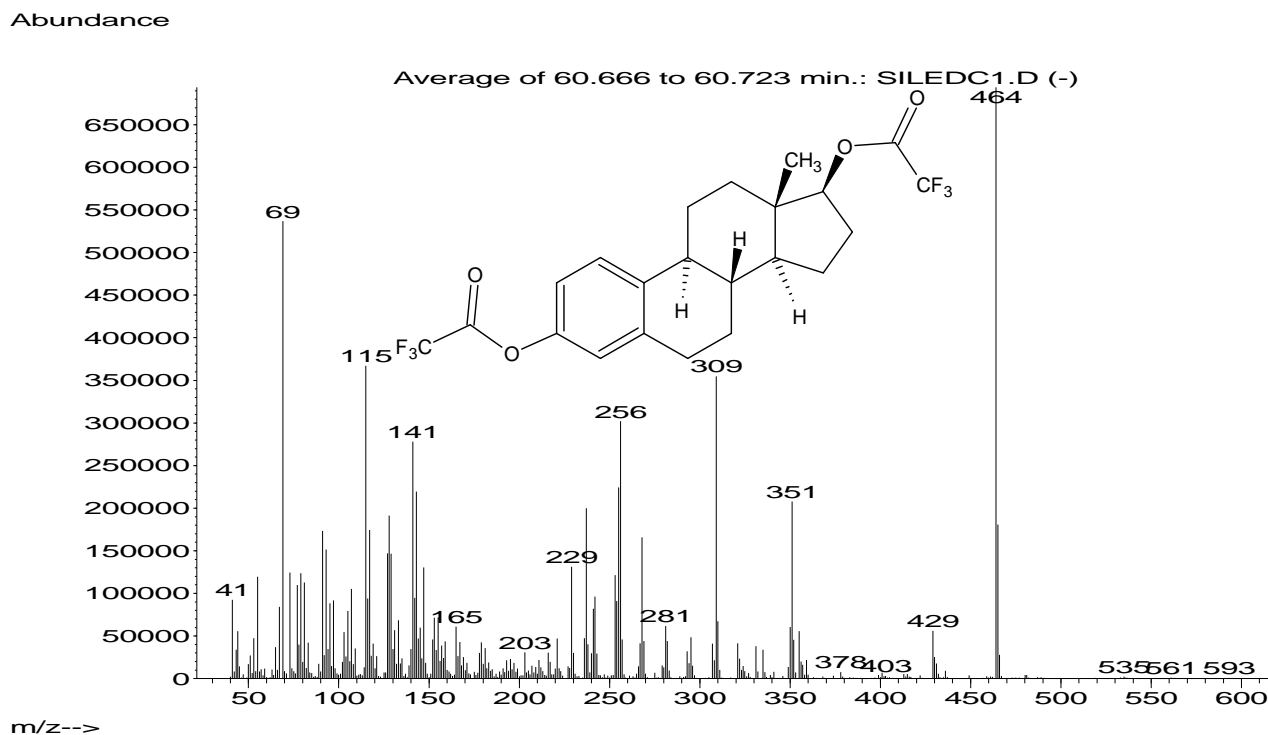


Figure 6.4 Electron impact mass spectrum of the 17 β -estradiol-trifluoroacetate (E2-di-TFA) derivative. Molecular ion (M^+) m/z 464, ($-CF_3$) m/z 69.

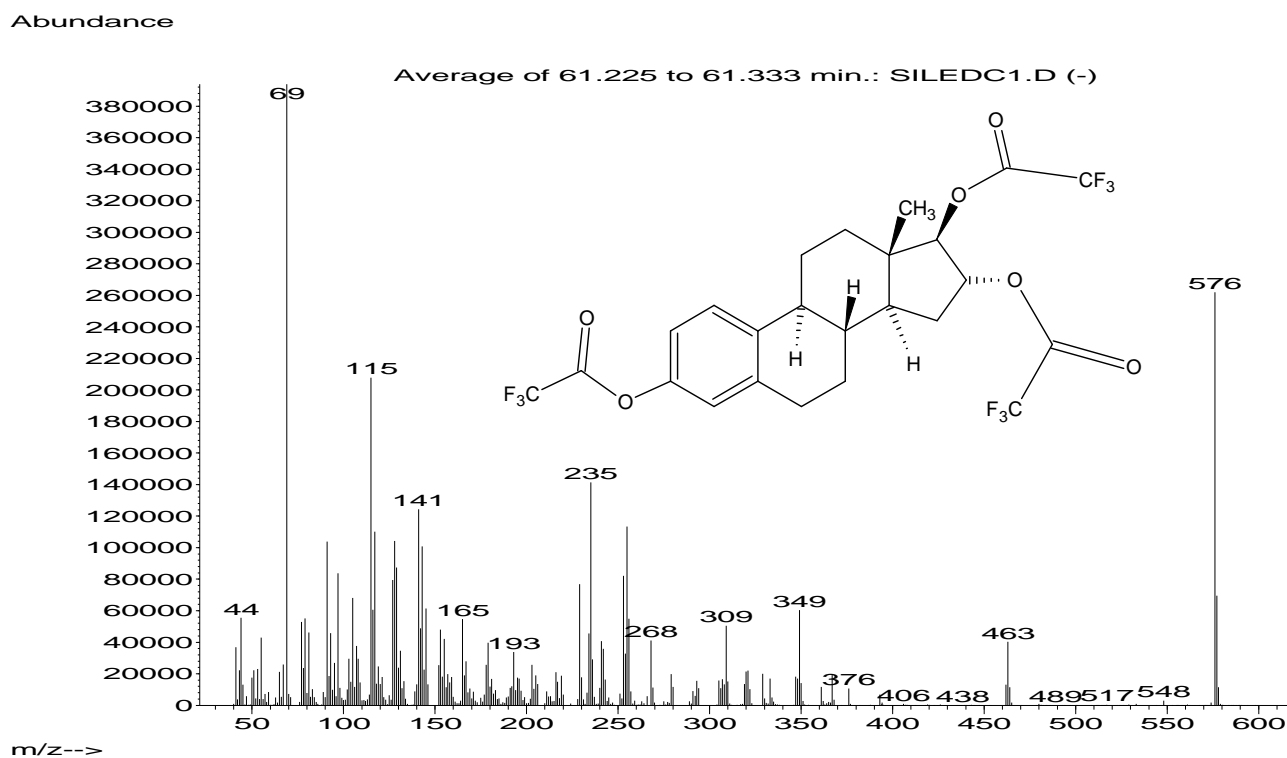


Figure 6.5 Electron impact mass spectrum of the estriol-trifluoroacetate (E3-tri-TFA) derivative. Molecular ion (M^+) m/z 576, ($-CF_3$) m/z 69.

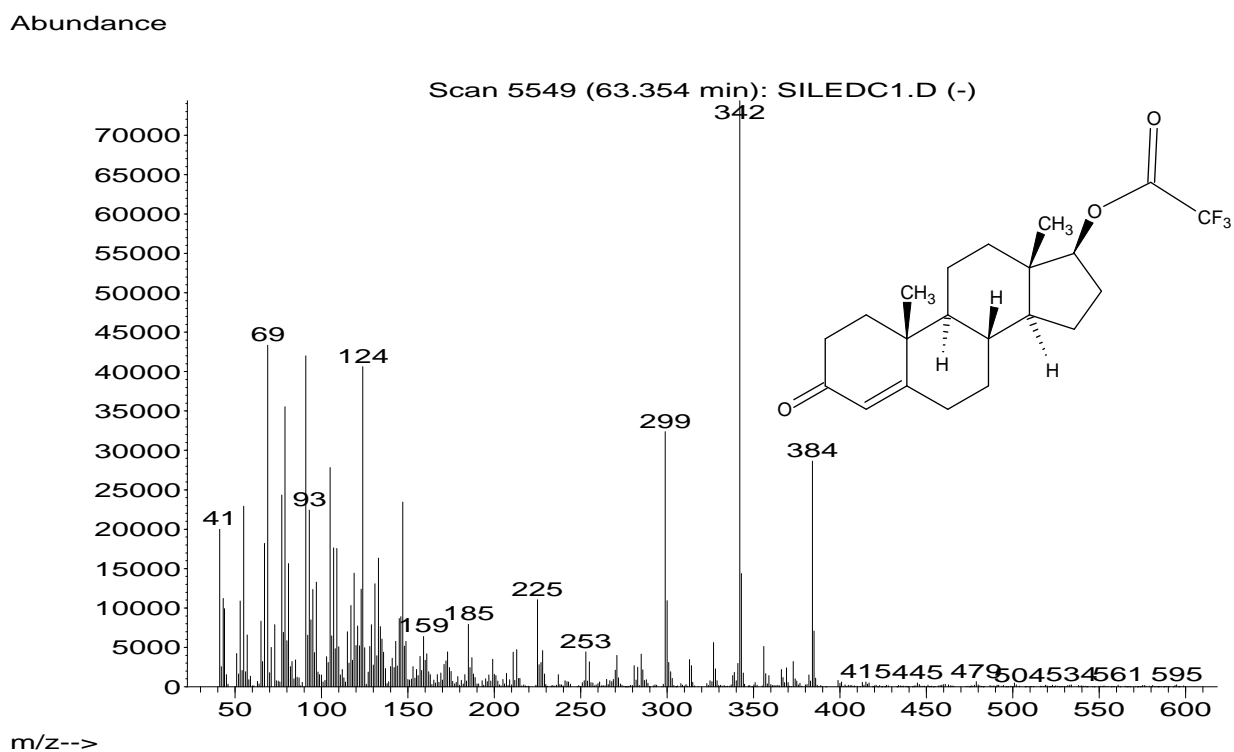


Figure 6.6 Electron impact mass spectrum of the testosterone-trifluoroacetate (T-TFA) derivative. Molecular ion (M^+) m/z 384, ($-CF_3$) m/z 69.

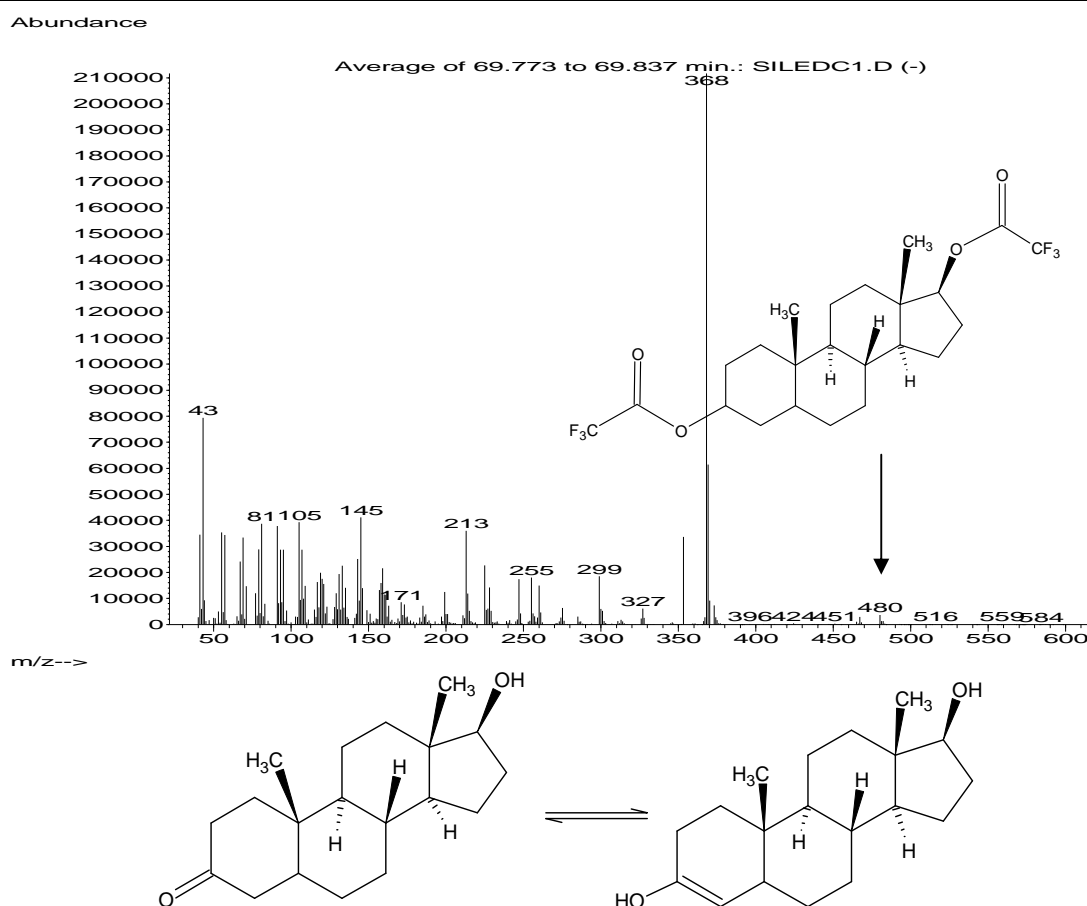


Figure 6.7 Electron impact mass spectrum of the testosterone-ditrifluoroacetate (T-di-TFA) derivative. Molecular ion (M^+) m/z 480, ($-CF_3$) m/z 69. Beneath the mass spectrum is a sketch of the equilibrium between the ketone and enol tautomers of testosterone.

The estrogen TFA derivatives were again synthesised on the trap as described earlier. The trap was then immediately thermally desorbed in the Chrompack ® TDU and analysed by GC-(NCI) MS. Figure 6.8 shows the TIC obtained by GC (NCI) MS. Beneath the TIC is the RIC of m/z 113, which corresponds to the mass of the trifluoroacetate ion $-CF_3CO_2^-$. It appears that several more TFA derivatives are detected by NCI-MS. Most of these chromatographic peaks only have a base mass peak of m/z 113 with no other ion information available to identify them. Peaks having other ions in addition to m/z 113 are m/z 488 and m/z 576 as shown in the subsequent RICs and figure 6.9 below.

Figure 6.9 shows the NCI-Mass Spectra for one of many peaks in the chromatogram with base peak m/z 113, followed by the NCI-mass spectrum for the suspected EE2-TFA derivative and E3-TFA derivative. At the elution time for E3-TFA (~61 min), the molecular ion m/z 576 appears. This is unusual for NCI using methane gas, where ($M-1$) is expected. It is suspected that EE2-TFA (not present in EI-MS) with a base peak of m/z 488 and fragment ion m/z 113 is observed much earlier



in the chromatogram (~37 min). This suggests that the supposedly sterically hindered α - hydroxyl group can be substituted. Several publications and reviews in literature have stated that this hydroxyl group is not substituted by most acylation reagents, due to the hindrance of the alkyne substituent adjacent to the hydroxyl functional group [199]. BSTFA has formed the TMS ester on both aromatic and alkyl substituent, although this was not confirmed by all research groups [199]. The TMS derivatives are also more susceptible to hydrolysis [3, 199]. Notice that m/z 113 is the base peak, when using methane as collision gas [62]. If using water as collision gas, then the molecular ion is expected to be the base peak [62]. This would be a better setup with NCI, since m/z 113 lies very low on the mass scale thus not improving the selectivity of detection. Moving into higher mass ranges would improve the selectivity of the detection technique.

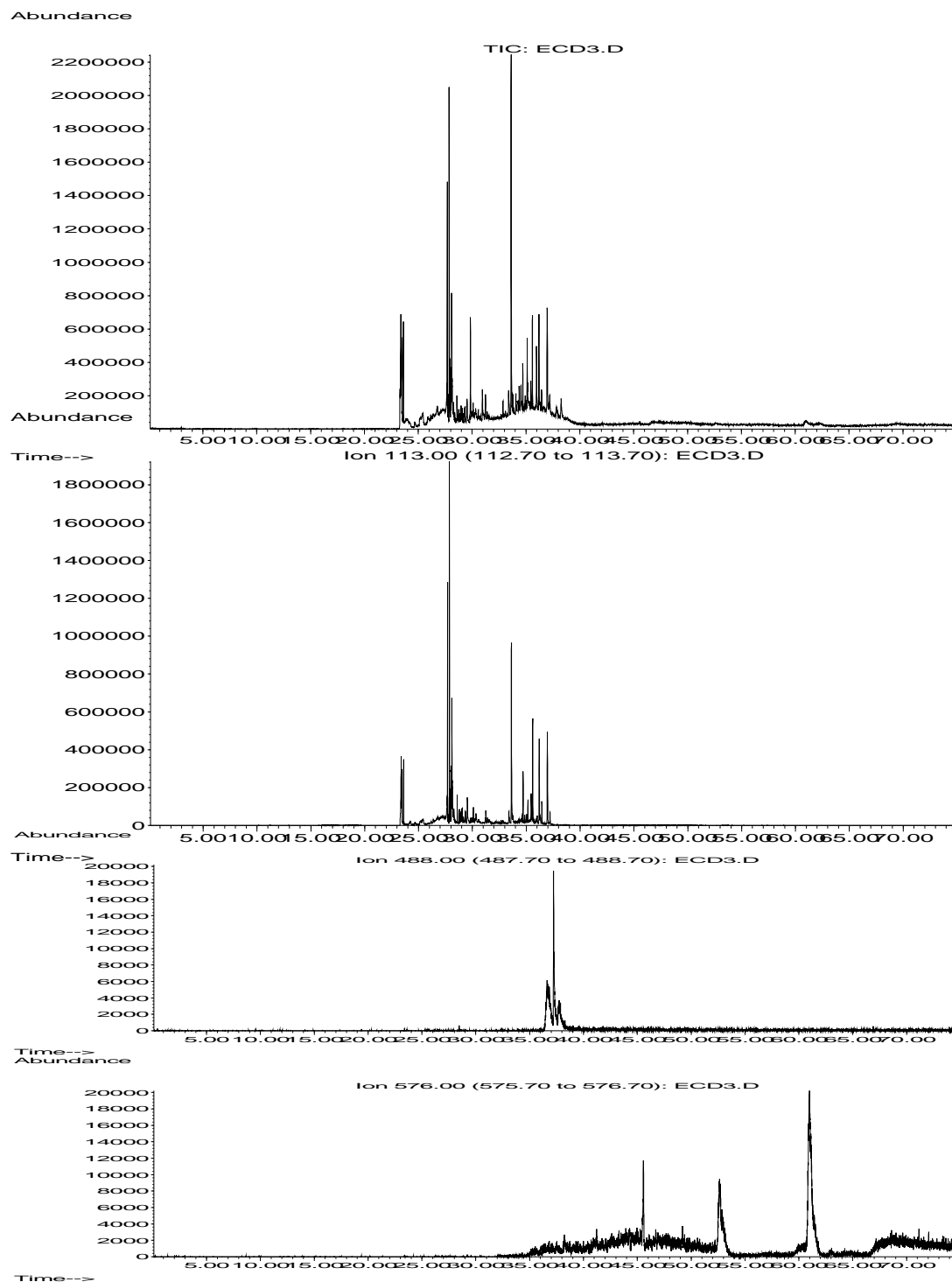


Figure 6.8 The TIC obtained from GC- (NCI) MS of the *in situ* derivatization of estrogens in the PDMS MCT using TFAA, followed by the RIC for m/z 113, indicating all peaks having the trifluoroacetate ion, m/z 488 RIC, indicating the suspected EE2-di-TFA derivative peak eluting at 37 min and m/z 576 RIC indicating the suspected E3-tri-TFA derivative peak eluting at 61 min .

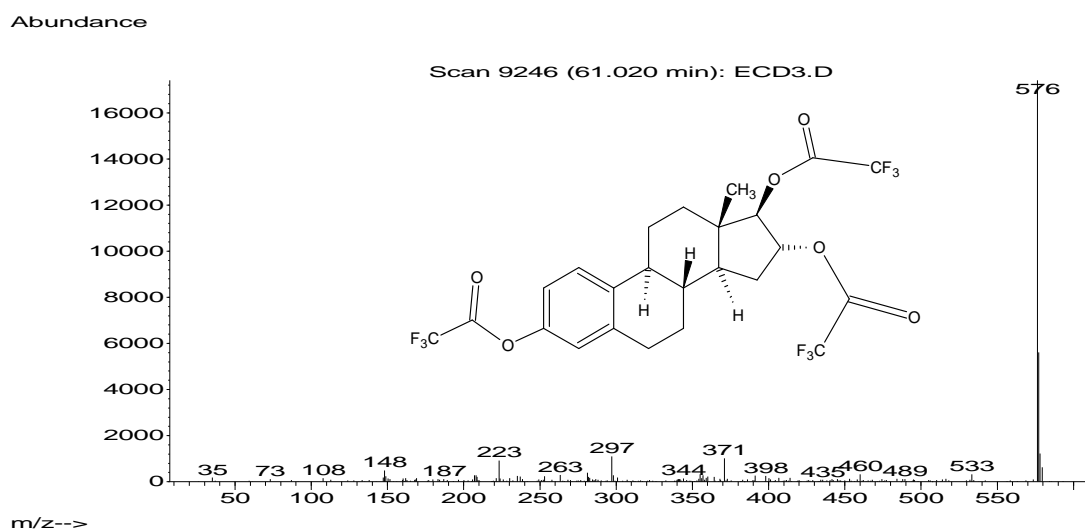
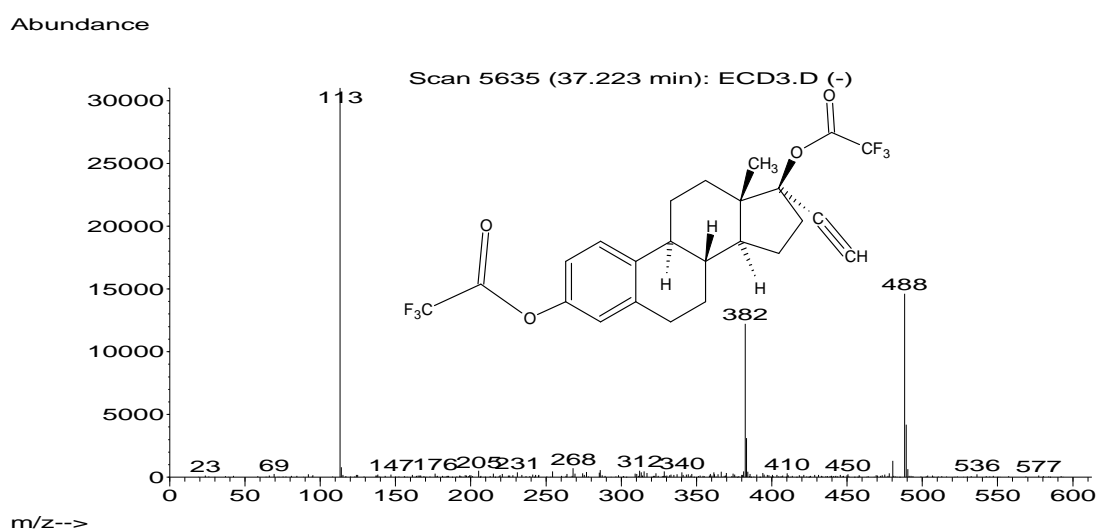
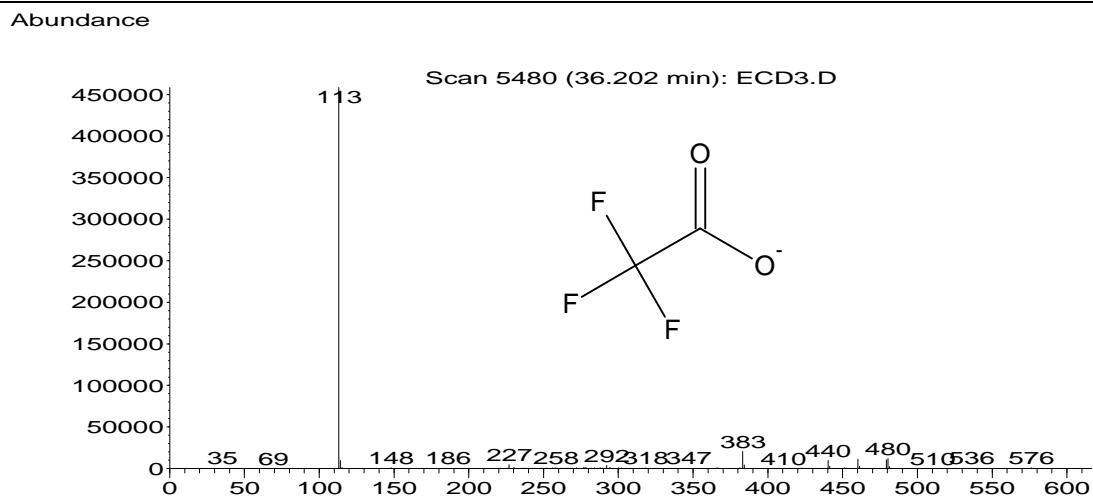


Figure 6.9 The negative chemical ionization-mass spectra (NCI-MS) for one of many peaks in the chromatogram with base peak m/z 113, followed by the NCI-mass spectrum for the suspected EE2-di-TFA derivative (M^- m/z 488) and E3-tri-TFA derivative (M^- m/z 576).

Further investigation of the EE2-di-TFA derivative was performed on the GC-ITD (the instrument available at the time of the study). Here 1 μl of an 8 $\mu\text{g}/\mu\text{l}$ EE2 standard in acetone was placed in an empty glass tube. 1 μl of TFAA was added; the glass tube was sealed with glass caps and allowed to react for 10 min. The tube was then immediately thermally desorbed in the Chrompack® TDU and analysed by GC- (ITD) MS. The instrument conditions were as follows:

Splitless desorption at 280°C for 10 min with a desorb flow of 100 ml/ min, inject at 280°C for 1 minute. The GC oven was held at 40°C for 1 min then ramped at 15°/min to 280°C and held for 10 min. A solvent delay of 16 min was set on the MS to avoid the detector being damaged by the excess volatile TFAA entering the MS. A scan range of 40 – 600 amu was used.

The chromatogram obtained showed the presence of 5 major compounds present for the reaction of TFAA with EE2, figure 6.10. The reaction between TFAA and EE2 occurs in the absence of a basic catalyst resulting in extremely acidic reaction conditions. Under these conditions Wagner-Meerwein rearrangements [248, 249], figure 6.11, and dehydration reactions can occur. Figures 6.12 to 6.16 show the different derivatives of EE2-TFA formed under acidic conditions (in the presence of excess TFAA).

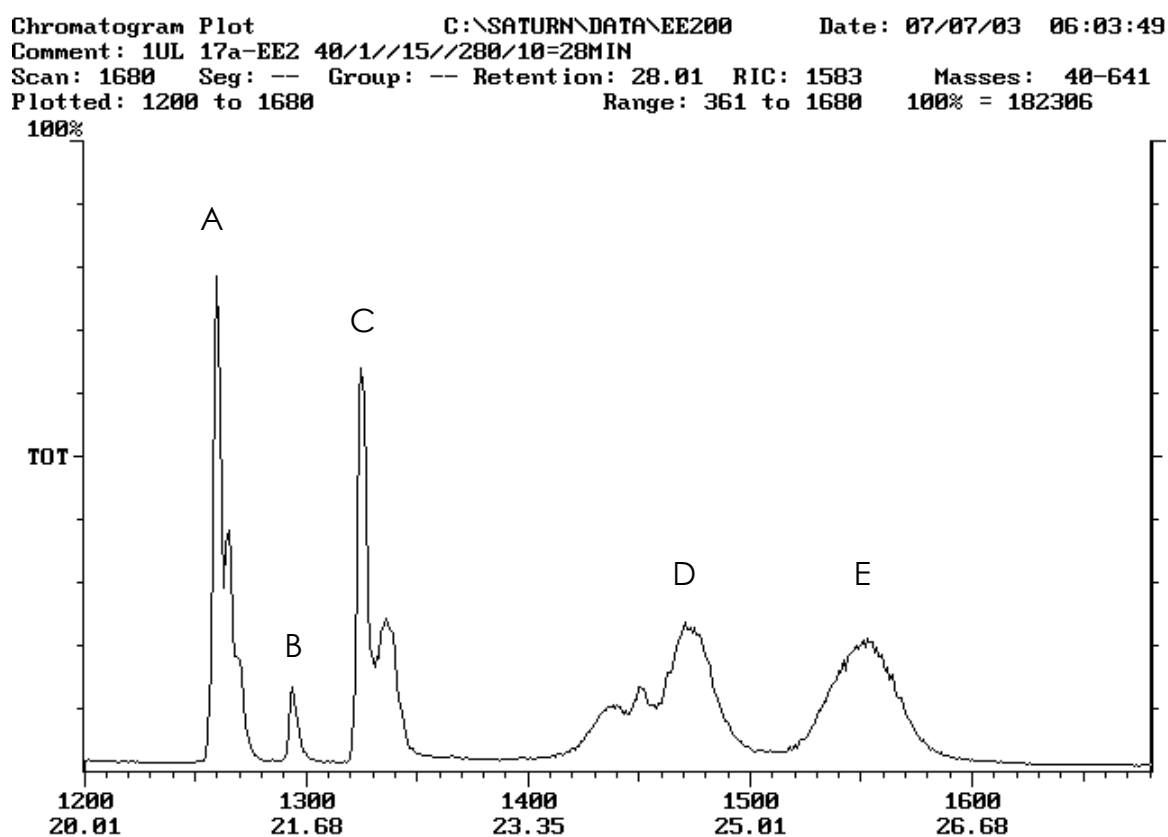


Figure 6.10 The GC- (ITD) MS chromatogram obtained for the reaction of EE2 with TFAA in a glass tube. 5 major compounds, labelled A, B, C, D and E were identified for the derivative.

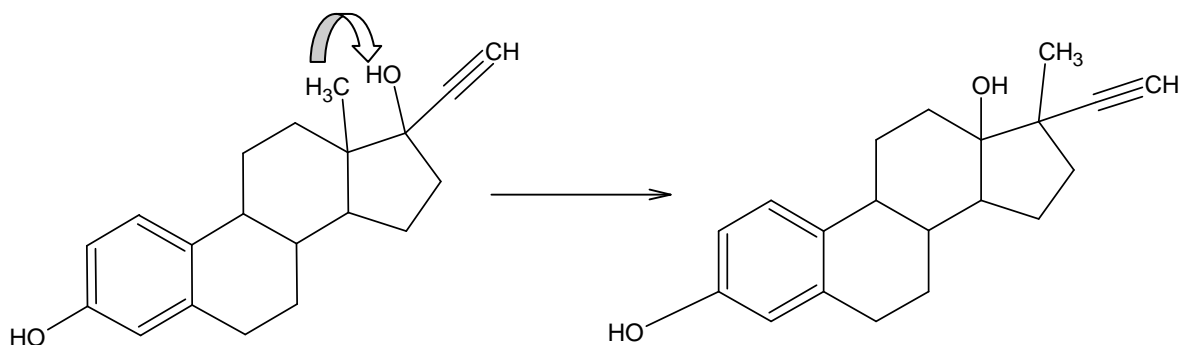


Figure 6.11. 17α -ethinylestradiol (EE2) undergoing a Wagner-Meerwein rearrangement, essentially this is a 1,2- shift between 2 groups on adjacent sp^3 hybridized carbon atoms [248, 249].

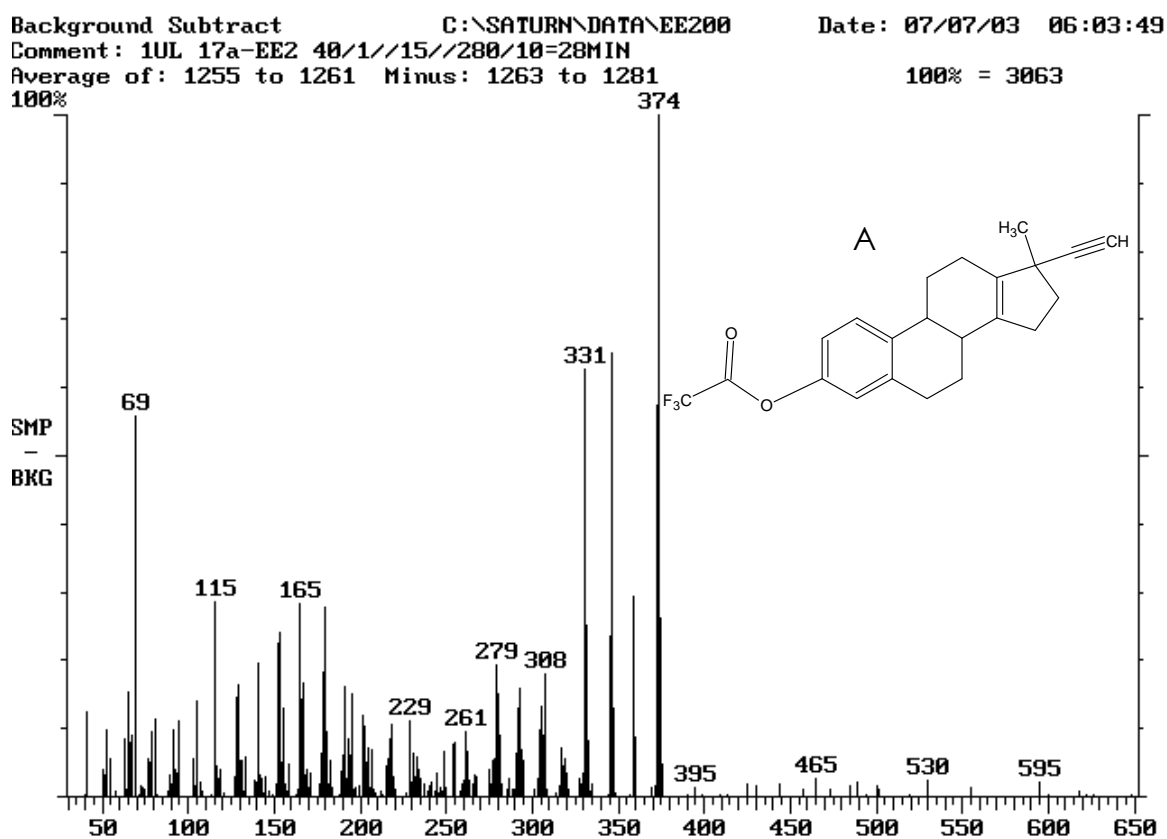


Figure 6.12. The ITD-EI mass spectrum of compound A. The mono-substituted EE2-TFA derivative has undergone a Wagner-Meerwein rearrangement and a water elimination step (dehydration) to form a double bond between the C5 and C6 rings. The base peak m/z 374 is also the molecular ion M^+ .

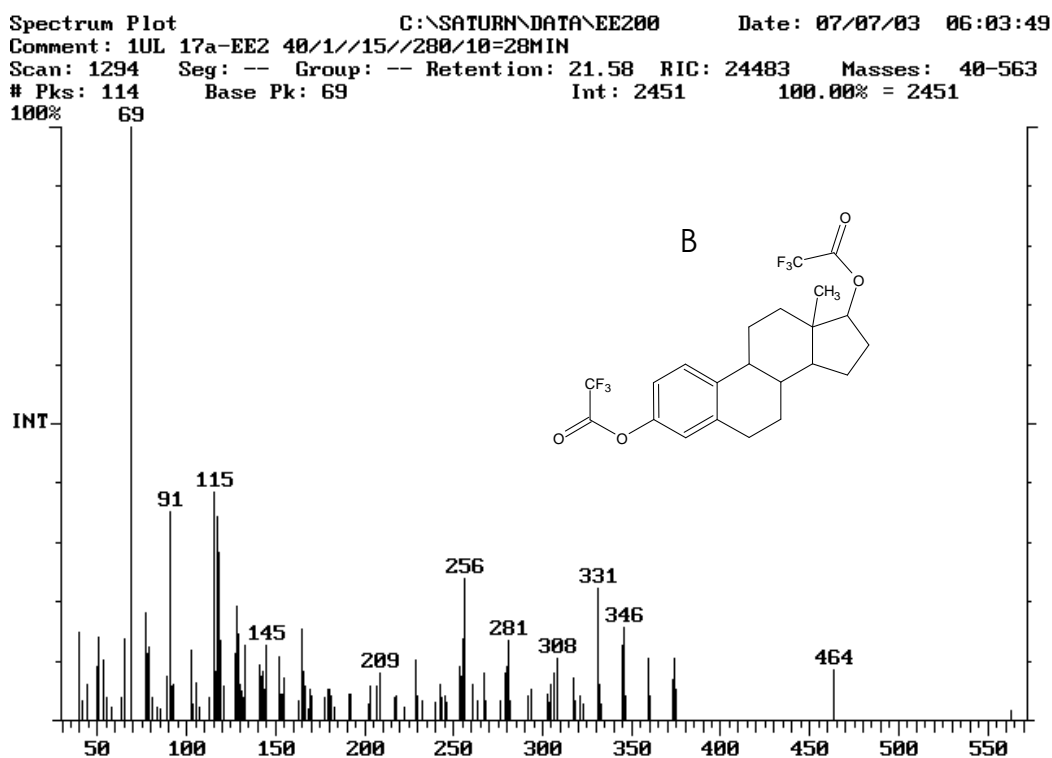


Figure 6.13. The ITD-EI mass spectrum of compound B. The disubstituted EE2-TFA derivative has lost the 17-alkynyl (C-C) group (-24 amu).

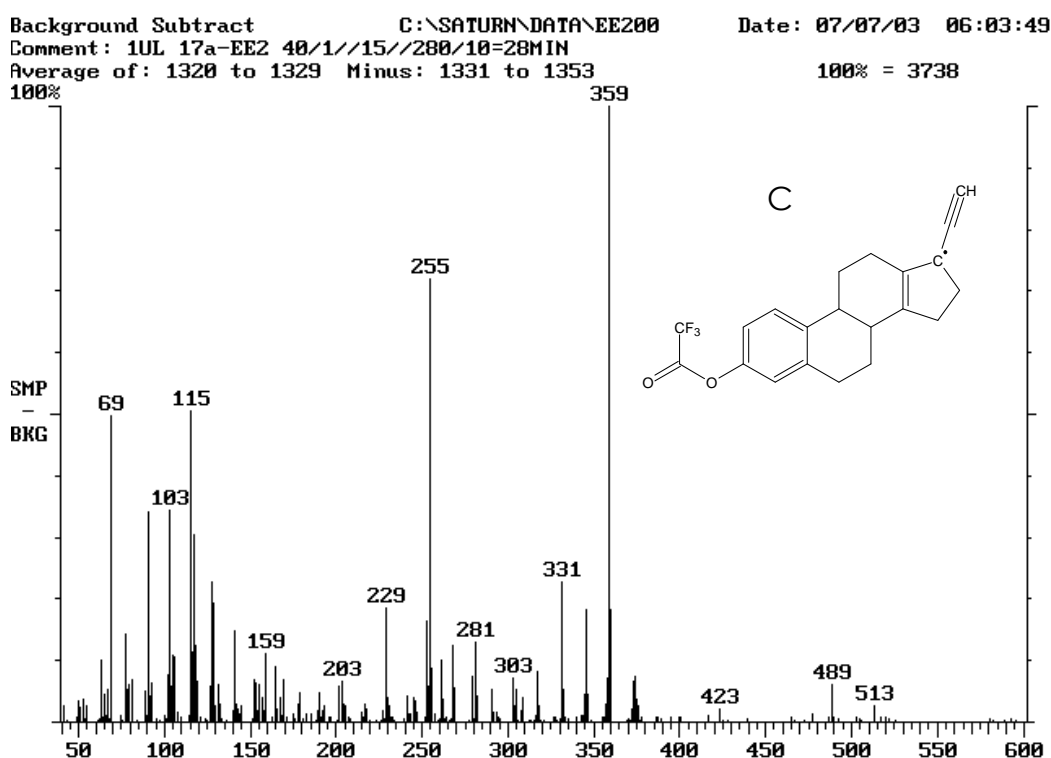
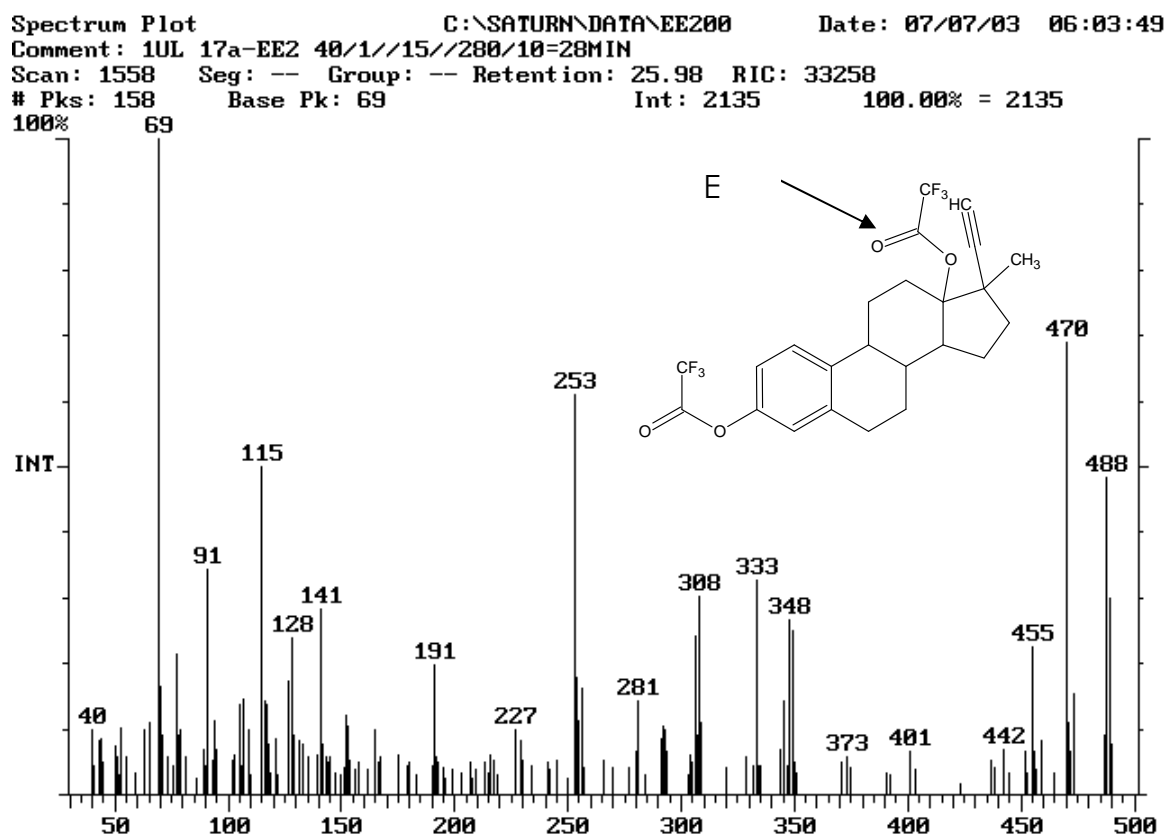
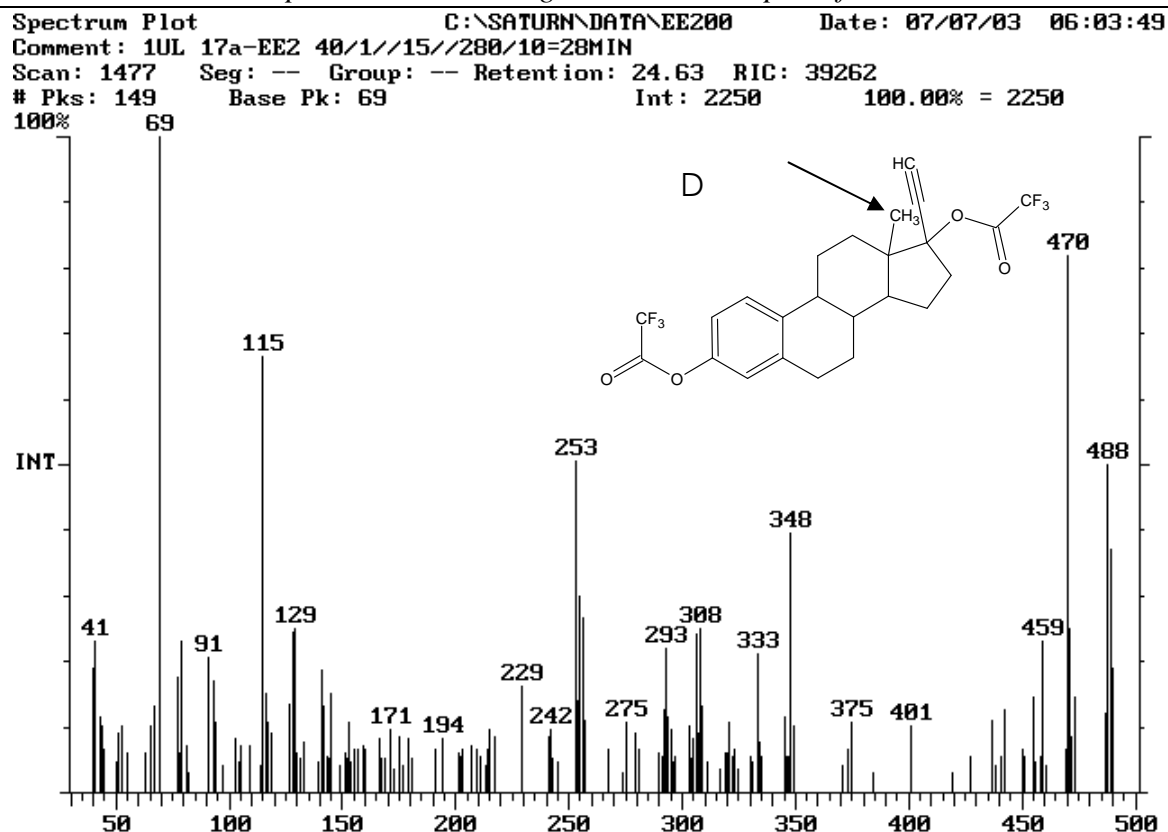


Figure 6.14. The ITD-EI mass spectrum of compound C. The mono-substituted EE2-TFA derivative has undergone a Wagner-Meerwein rearrangement and a water elimination step (dehydration) to form a double bond between the C5 and C6 rings. The methyl group is lost to form base peak m/z 359 and molecular ion at m/z 374.



6.2.4. Dual derivatization of the estrogens with PFBCl and TFAA

In view of the poor results obtained with the PFBCl and TFAA applied separately, as a last resort we decided to combine the reagents. In literature, dual derivatizations are performed to convert functional groups of different reactivity resulting from steric hindrance, as is the case for the hydroxyl group on EE2, which is hindered by the 17-alkynyl group [181].

A simple reaction in a vial with the 20 ng/ μ l EDC standard in acetone, 5 μ l TFAA and 5 μ l PFBCl was performed. 1 μ l of this reaction mixture was injected with a split into the GC- (EI) MS on full scan, with a solvent delay. Figure 6.17 shows the RIC of m/z 195 corresponding to the pentafluorophenyl carbonyl moiety. Although not shown here, the TIC looks similar to the RIC. Figures 6.18 to 6.20 show the 3 derivatives that formed successfully from the dual derivatization; unfortunately 17 α -ethinylestradiol (EE2) was not among them. They are estrone (E1), estriol (E2) and estradiol (E3). It is important to note that the hydrolysed PFBCl (PFBOH) is also present (figure 6.21), as are the derivatives. The presence of both m/z 195 and m/z 69 in the mass spectra of the derivatives indicate that both the PFB and TFA moieties are present. The PFBCl reagent does in fact react with the estrogens. It would appear that it is not entirely hydrolysed in the reagent vial. Further investigation into the methodology required for synthesizing the PFB estrogen derivatives is needed. It remains the model route to follow for the detection of estrogens.

Due to time constraints and the fact that suitable derivatives of the estrogens (with either TFAA or PFBCl) were not achieved, this work was discontinued. The estrogen-TFA derivatives did not yield EE2-TFA on the PDMS MCT either at room temperature or during thermal desorption. The EE2-TFA derivative formed in the glass tube resulted in four products instead of one. The method used for the reaction of PFBCl with the estrogens was not successful. Further work was carried out using the alkylphenols only.

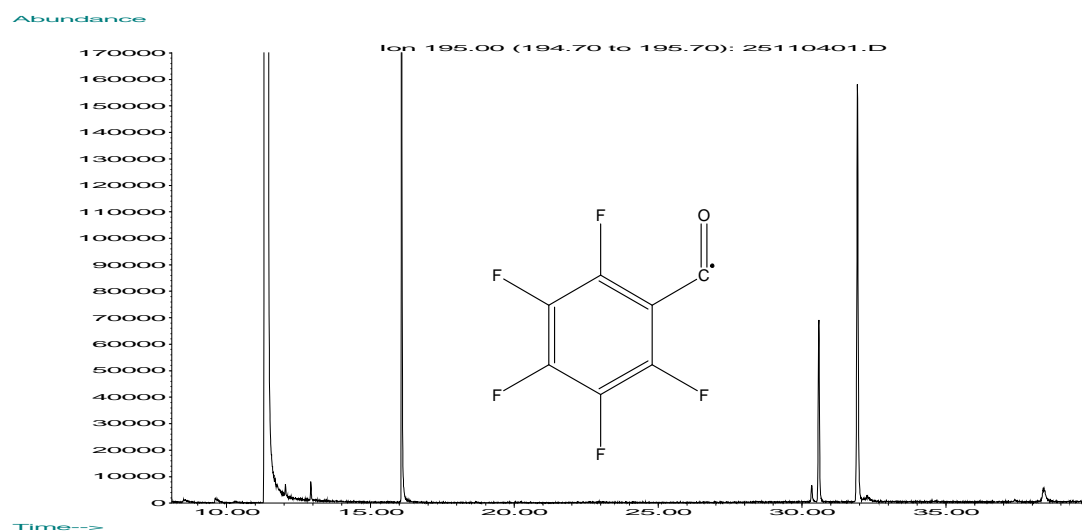


Figure 6.17 The GC- (EI) MS Reconstructed ion chromatogram (RIC) of m/z 195 corresponding to the pentafluorophenyl carbonyl moiety, for the dual derivatization of estrogens with PFBCl and TFAA.

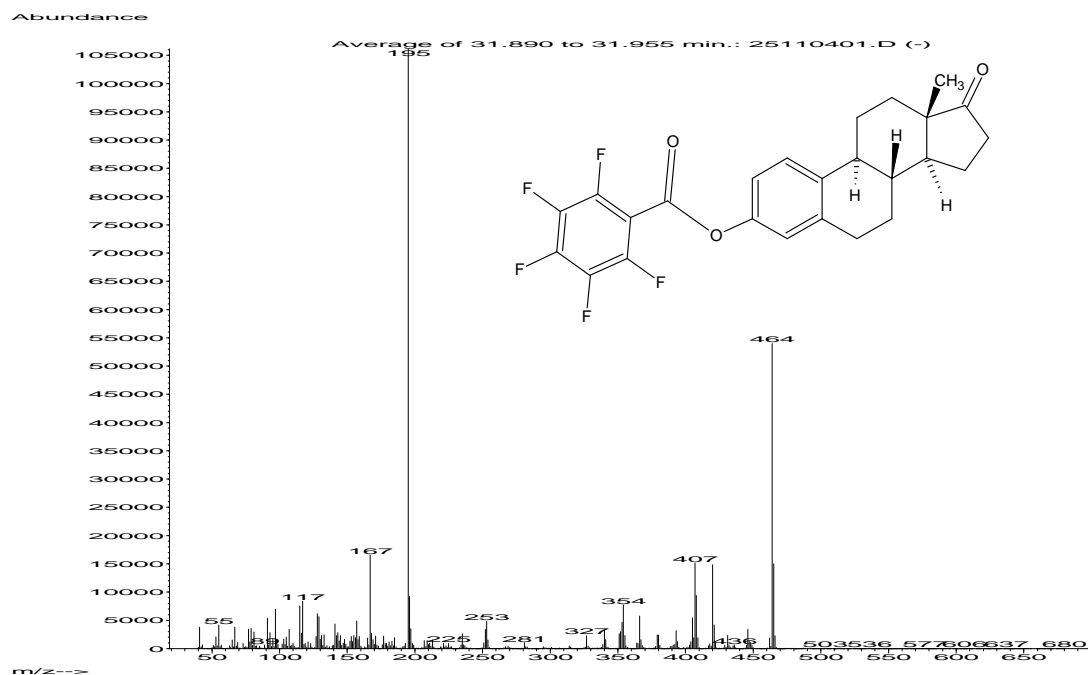


Figure 6.18 The EI mass spectrum obtained for the derivative formed from the reaction of estrone (E1) with PFBCl and TFAA. Base peak m/z 195 (C_7F_5O) and M^+ m/z 464.

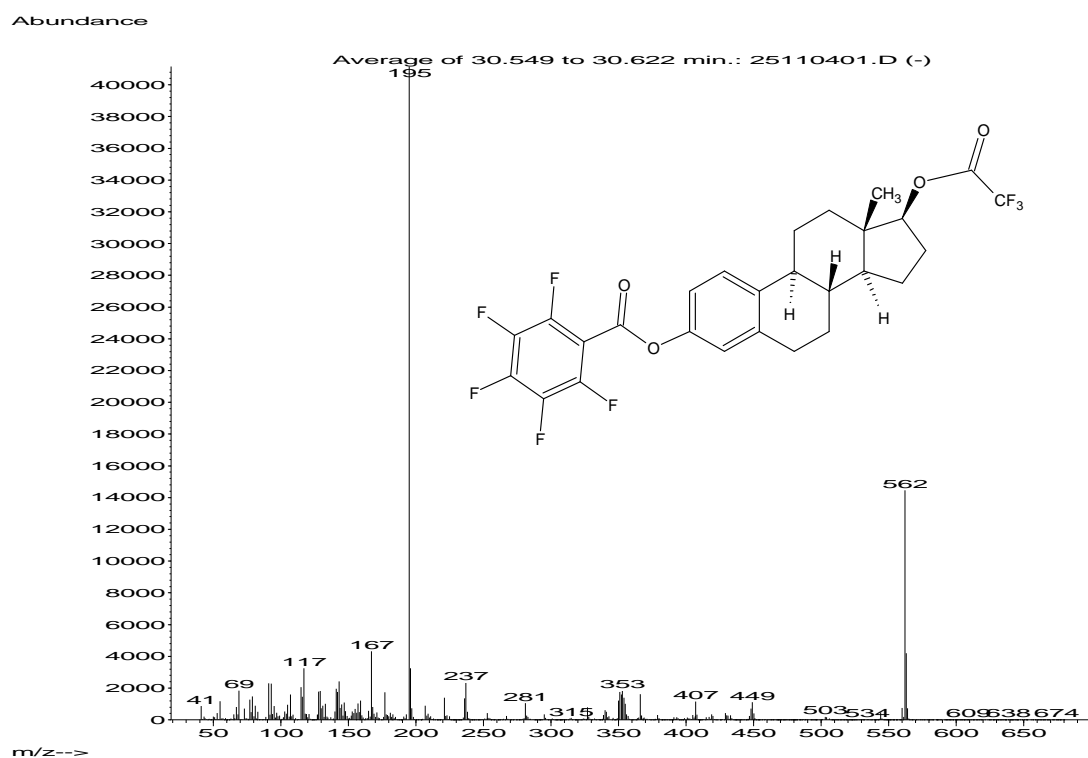


Figure 6.19 The EI Mass Spectrum obtained for the derivative formed from the reaction of 17β-Estradiol (E2) with PFBCl and TFAA. Base peak m/z 195 (C₇F₅O), m/z 69 (CF₃) and M⁺ m/z 562.

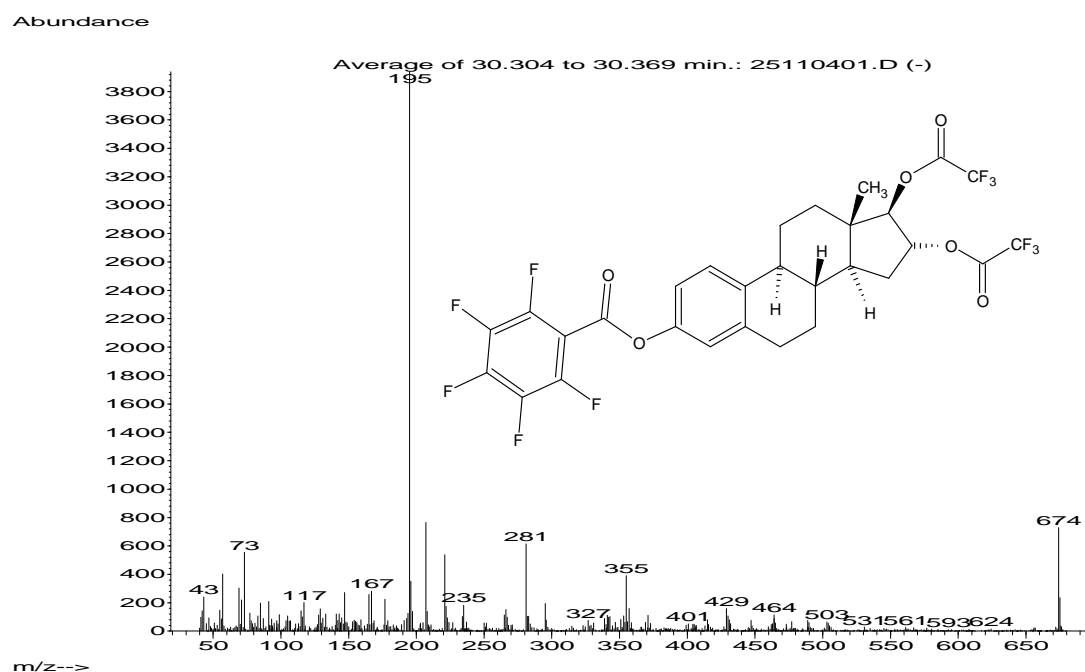


Figure 6.20 The EI mass spectrum obtained for the derivative formed from the reaction of estriol (E3) with PFBCl and TFAA. Base peak m/z 195 (C₇F₅O), m/z 69 (CF₃) and M⁺ m/z 674.

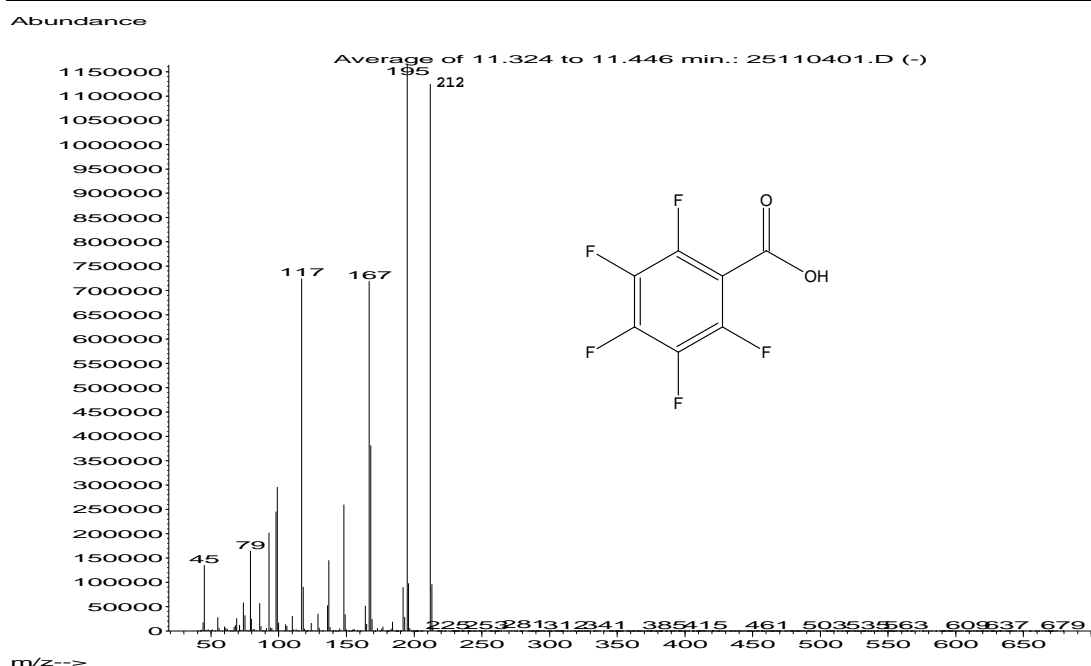


Figure 6.21 The EI mass spectrum obtained for the hydrolysed PFBCl, i.e. Pentafluorobenzoic acid formed from the reaction of the estrogens with PFBCl and TFAA. Base peak m/z 195 (C_7F_5O), and M^+ m/z 212.

6.2.5. Reagent selection for the alkylphenols

From chapter 3, it is clear that acylation with acetic acid anhydride (AAA), prior to extraction, is the preferred derivatization reaction for phenols. The reaction is favoured because it does not require anhydrous reaction conditions and proceeds easily, even in aqueous media. Table 3.2 summarises what has been achieved with other sorptive devices, such as SBSE and SPME using AAA.

In order to decrease the detection limits for the alkylphenols and bisphenol-A, it was decided to form an electron-capturing halogenated derivative suitable for analysis by GC/ECD and GC/NCI-MS. The reaction should proceed with the same ease as for acetic acid anhydride. Trifluoroacetic acid anhydride reacts rapidly with phenols to form the stable trifluoroacetate derivative and trifluoroacetic acid [62]. The reaction mechanism is shown below in figure 6.22. The nucleophilic oxygen on the phenol attacks the electrophilic carbon on the TFA acid anhydride. The trifluoroacetate ion then abstracts a proton to form TFA acid and the corresponding TFA ester. Ordinarily, the acid by-product is removed before instrumental analysis, as the acid would destroy the chromatographic column. The volatile TFA acid however, elutes at low temperatures and does not require prior removal, unlike its related perfluoroacyl anhydrides, PFPAA and HFBA [250].

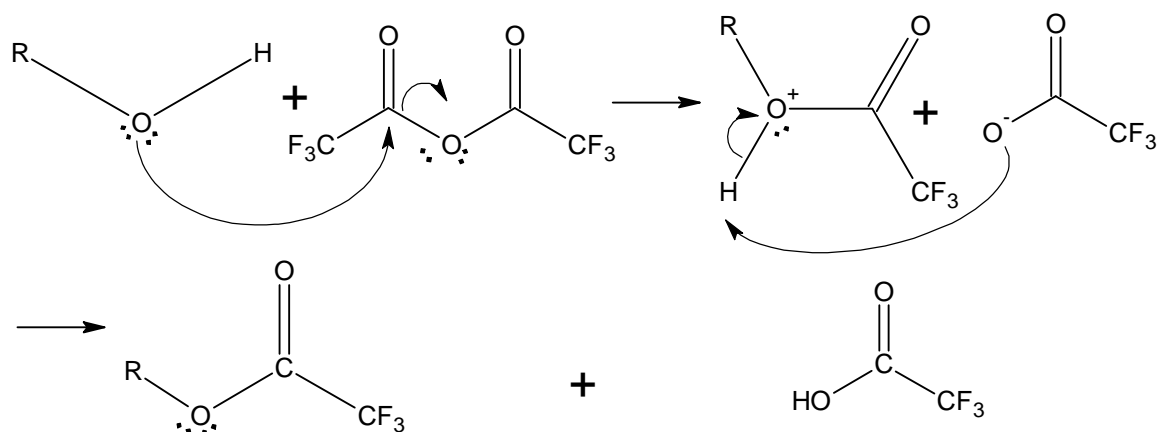


Figure 6.22 Reaction mechanism for the derivatization of a primary alcohol with trifluoroacetic acid anhydride (TFAA) to form the corresponding trifluoroacetate derivative and trifluoroacetic acid by-product.

6.2.6. Derivative confirmation

The trifluoroacetate (TFA) derivatives of TOP, NP and BPA were prepared in acetone using the simple method described by Lerch and Zinn [62]. 10 μ l TFAA is added to the alkylphenol standard in acetone and allowed to react; after 5 min the reaction is complete. An aliquot from this reaction mixture is injected. The synthesized derivative was used for comparison and as an external standard to quantitate the TFA derivatives formed *in situ* in the PDMS traps. Refer to appendix 3 for confirmation chromatograms of the acetone synthesized derivatives.

The electron impact mass spectra, obtained under GC-EI-MS conditions given in section 6.6.1, for each derivative formed is shown below, along with the main fragment formation mechanism. Typically molecular ions of phenyl esters eliminate the neutral ketene after the hydrogen/ atom X on the terminal CX_3 group is transferred to the ether oxygen and the ether oxygen-carbon bond is cleaved (see figure 6.23 and figure 6.24). This is not the case for the trifluoroacetate esters, as the electron rich fluorine atom does not migrate to the ether oxygen. Instead, alpha cleavage at the alkyl chain is observed [62, 251, 252]. The bisphenol-A derivative loses a CH_3 radical to form the abundant base peak m/z 405 [62, 252] (see figure 6.25). Another advantage of the TFA esters is that the most abundant fragments fall in a higher mass range than their corresponding acetate esters.

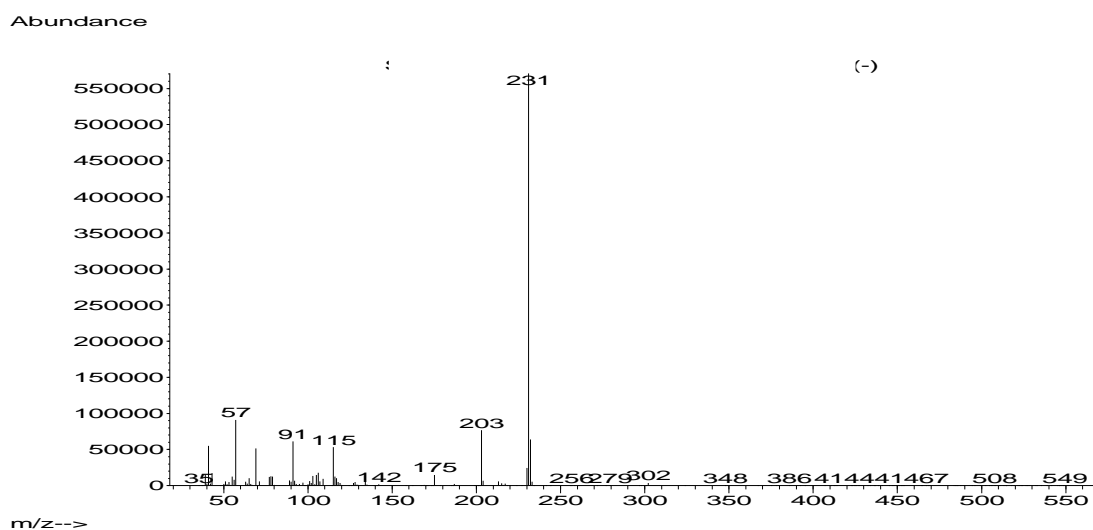
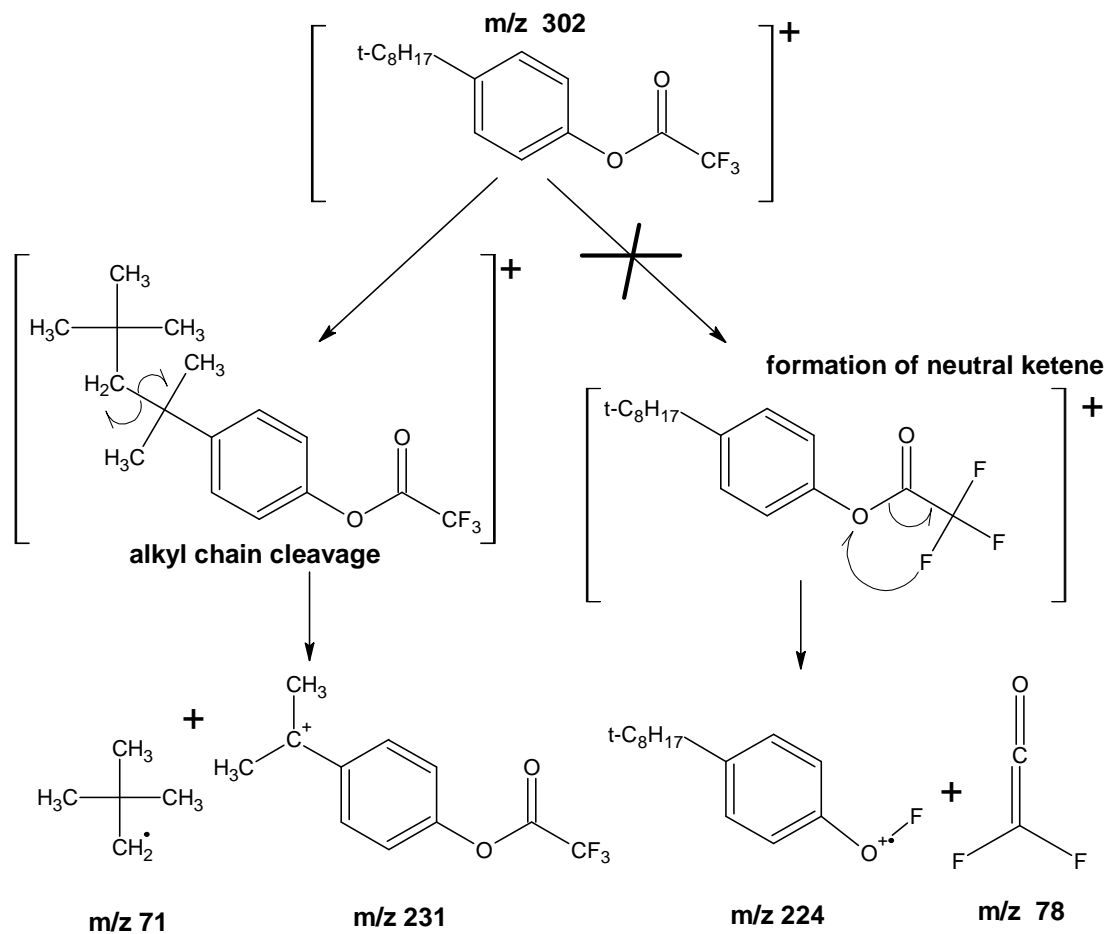


Figure 6.23 Mass spectrum and fragmentation scheme for the main mass spectral fragments obtained for the *tert*-octylphenol TFA derivative. Note the molecular ion (m/z 302) is almost absent.

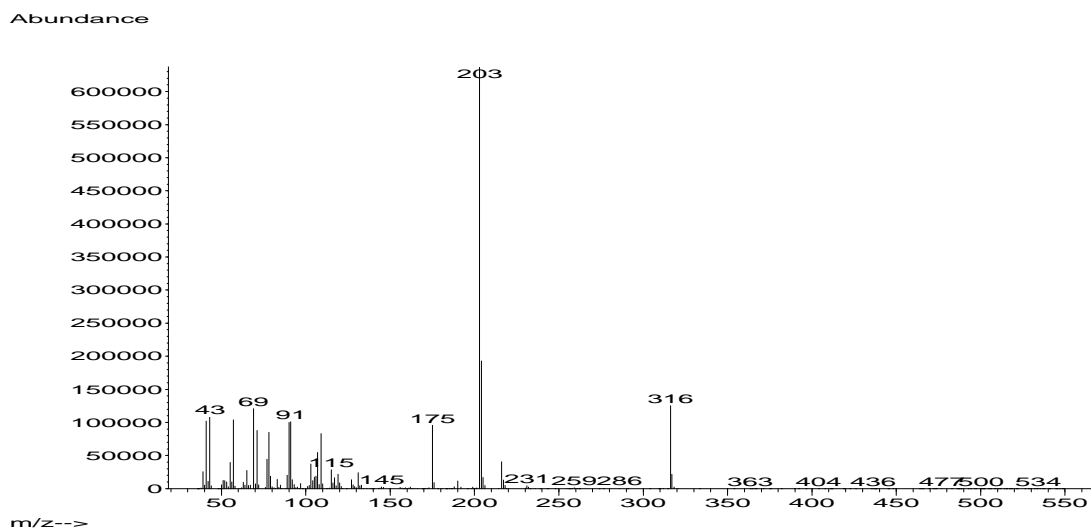
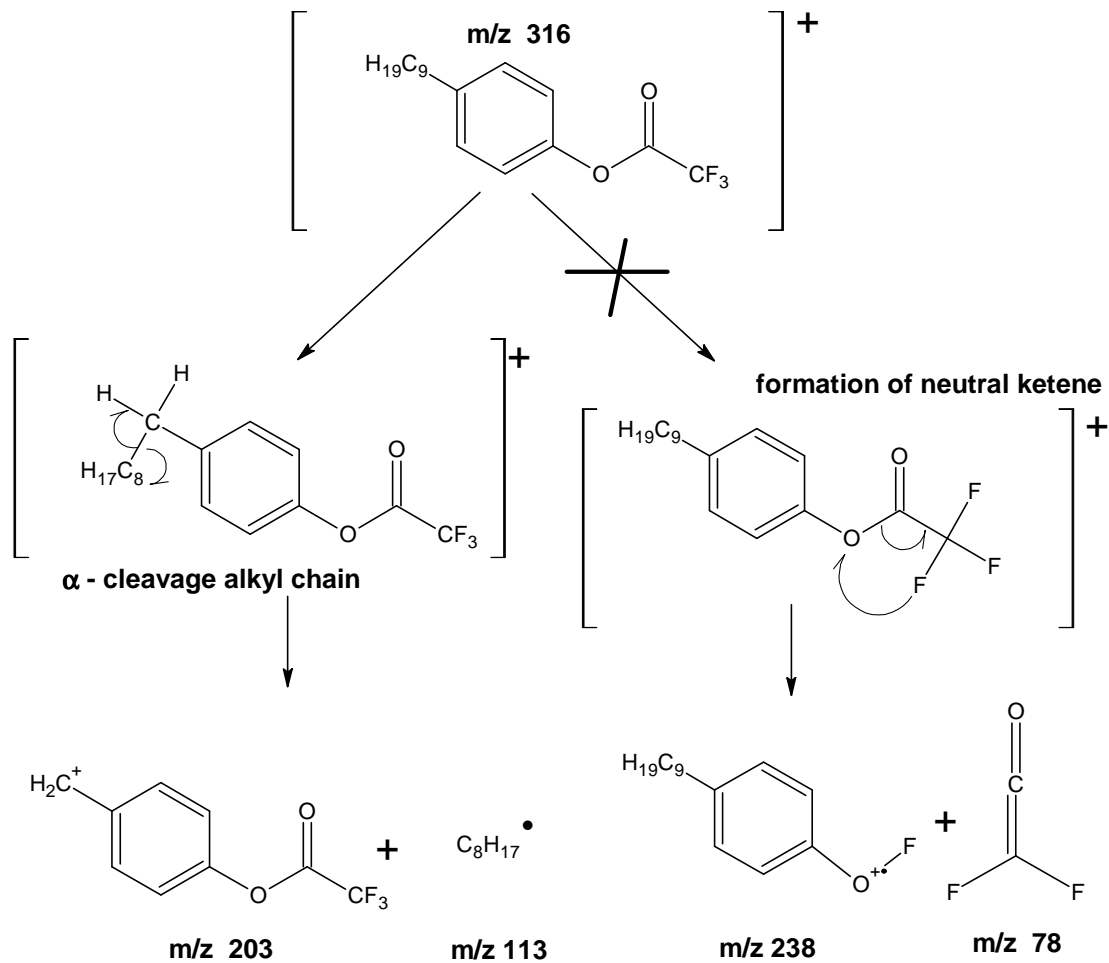


Figure 6.24 Mass spectrum and fragmentation scheme for the main mass spectral fragments obtained for the 4-*n*-nonylphenol TFA derivative.

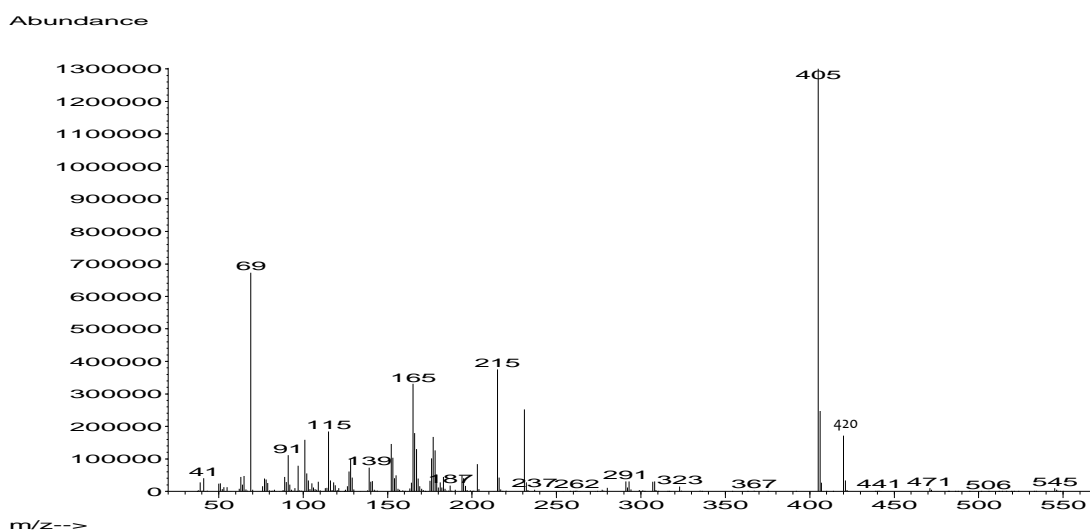
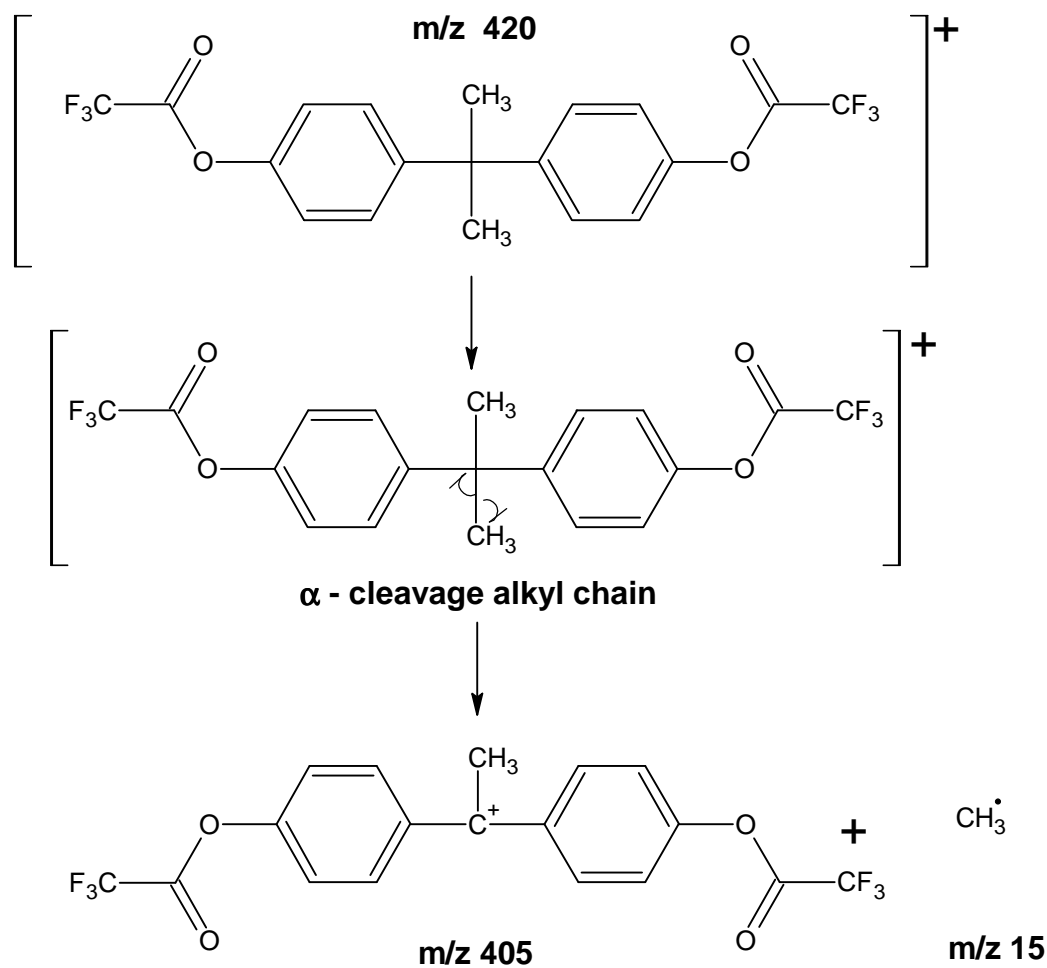


Figure 6.25 Mass spectrum and fragmentation scheme for the main mass spectral fragments obtained for the bisphenol-A TFA derivative.

6.3. Extraction

6.3.1. Predictions based on $K_{o/w}$

Initial calculations to predict the extraction efficiency of the estrogens and alkylphenols (defined in table 6.1) were determined using the phase ratios of the PDMS concentration devices, octanol – water partition coefficients ($K_{o/w}$) for the analytes and equation 2.3 (see chapter 2 section 2.5, page 39). Naturally equation 2.3 is for static equilibrium sampling techniques such as SPME and SBSE. However, as discussed in section 2.4.5 (page 38), dynamic equilibrium sampling (post-breakthrough volumes) should yield similar recoveries. Dynamic equilibrium sampling can be considered the “worst-case scenario” where full breakthrough of all analytes off the trap has occurred and complete equilibrium is reached. It is only appropriate if neither sample volume nor sampling time are not restricted. Predicted recoveries are shown in table 6.3.

$$\frac{m_{PDMS}}{m_0} = \frac{\left(\frac{K_{o/w}}{\beta}\right)}{1 + \left(\frac{K_{o/w}}{\beta}\right)} \quad (2.3)$$

Table 6.3 Prediction of analyte recoveries on 3 different PDMS devices, using equation 2.3.

Analyte	Log $K_{o/w}$ *	% Recovery from a 10 ml water sample		
		MCT ($\beta = 40$)	SBSE ($\beta = 100$)	SPME ($\beta = 20000$)
17 α -ethinylestradiol	4.42	99.96	99.62	56.98
17 β -estradiol	4.48	99.96	99.67	60.27
estriol	3.50	99.65	96.94	13.68
estrone	4.40	99.96	99.60	55.39
testosterone	3.77	99.81	98.31	22.54
<i>tert</i> -octylphenol	4.54	99.88	99.71	63.37
4- <i>n</i> -nonylphenol	5.46	99.99	99.96	93.44
bisphenol-A	3.84	99.43	98.58	25.79

* Values obtained from <http://www.molinspiration.com/cgi-bin/properties> (date: 20 August 2006)

Based on the values presented in table 6.3, it is expected that the analytes will partition very well into the PDMS MCT, without requiring derivatization prior to extraction. Since we did not intend to perform dynamic equilibrium sampling, as this will require extended sampling periods of time, typical retention volumes that could be expected for these analytes on the PDMS MCT by dynamic breakthrough sampling were calculated. This was achieved using Baltussen's equations for aqueous phase dynamic sampling (section 2.4.4 page 37) in determining retention volumes (equation 2.20) and breakthrough volumes (equation 2.21) for a trap.

$$V_r = V_0 \left(1 + \frac{K_{O/W}}{\beta} \right) \quad (2.20)$$

$$V_b = V_r \left(0.9025 + \frac{5.360}{N} + \frac{4.603}{N^2} \right)^{-1/2} \quad (2.21)$$

Table 6.4 shows how the parameters for the PDMS MCT are calculated from geometric considerations. The value for the number of plates is hypothetical for these analytes, and was taken from reference 63 i.e., determined experimentally for benzene on a 32 MCT with similar dimension and flow rate.

Table 6.4. Geometrically calculated parameters for the PDMS MCT.

<i>Parameters for the PDMS MCT:</i>	
No. of PDMS tubes	32
Length (L) (cm)	5
i.d (cm) / i.r (cm)	0.03 / 0.015
o.d (cm) / o.r (cm)	0.065 / 0.0325
Volume of 1 tube (ml) = L [πr^2 (o.d) - πr^2 (i.d)]	0.013
Volume of total tube no. (ml)	0.417
Subtract 40 % (SiO ₂ filler contribution) (ml)	0.167
Volume PDMS (ml)	0.250
Volume sample (ml)	10
Phase ratio β	40
Glass trap tube i.d (cm) / i.r (cm)	0.4 / 0.2
Volume glass trap tube = L [πr^2]	0.628
Void Volume V_0 = Volume (glass tube – PDMS)	0.211
No. of theoretical plates N	11

Table 6.5 Predicted retention (V_r) and breakthrough volumes (V_b) for analytes on the PDMS MCT.

Analytes	Log $K_{O/W}$ *	$K_{O/W}$	V_r (ml)	V_b (ml)
<i>tert</i> -octylphenol	4.54	34 594	183	153
4- <i>n</i> -nonylphenol	5.46	285 102	1 505	1 259
bisphenol-A	3.84	6 950	37	31

For dynamic pre-breakthrough sampling of aqueous analytes through the MCT, table 6.5 predicts that 4-*n*-nonylphenol will have the best retention (1 ½ L) followed by *tert*-octylphenol (180 ml). Bisphenol-A exhibits the poorest retention (37 ml). Breakthrough volumes were calculated at the 5% level. Once mass detection limits are determined, the sample volume can be selected within the required breakthrough volume for that analyte.

6.3.2. pH adjustments

Extraction into the PDMS matrix is based on the octanol-water partition coefficients ($K_{o/w}$) of the neutral analytes, since it is already known that analytes in their ionic form will remain in the aqueous phase. The phenolic analytes are weak acids which have pK_a s well above 10 indicating that they will remain in their non-ionized form at typical environmental pHs [7], although a pH of 7 or less is preferred, to ensure protonation of the weak acids.

In greater detail the influence of pK_a on partitioning can be expressed as follows [253]. The total analyte concentration ratio between the organic and aqueous phases is described by the distribution ratio D_c denoted by:

$$D_c = \frac{[analyte]_{organic}}{[analyte]_{aqueous}} \quad (6.1)$$

The partitioning between the 2 phases is described by the partitioning constant K_p or as in our case $K_{o/w}$:

$$K_p = \frac{[HA]_{organic}}{[HA]_{aqueous}} \approx K_{o/w} \quad (6.2)$$

The acid dissociation constant K_a describes the dissociation of an acid in water (aqueous phase):

$$K_a = \frac{[H^+]_{\text{aqueous}} [A^-]_{\text{aqueous}}}{[HA]_{\text{aqueous}}} \quad (6.3)$$

Assuming that ions are not soluble in the organic phase, D_c can be rewritten to give:

$$D_c = \frac{[HA]_{\text{organic}}}{[HA]_{\text{aqueous}} + [A^-]_{\text{aqueous}}} \quad (6.4)$$

The total concentration of analyte in the aqueous phase is the amount of acid plus the amount of acid that dissociates.

Equation 6.2, 6.3 and 6.4 are combined to yield the following:

$$D_c = \frac{[HA]_{\text{organic}}}{\frac{[HA]_{\text{organic}}}{K_p} + \frac{K_a [HA]_{\text{organic}}}{K_p [H^+]_{\text{aqueous}}}} \quad (6.5)$$

Equation 6.5 simplifies to:

$$D_c = \frac{K_p [H^+]_{\text{aqueous}}}{[H^+]_{\text{aqueous}} + K_a} \quad (6.6)$$

If K_a is much larger than $[H^+]$ then:

$$D_c = \frac{K_p [H^+]_{\text{aqueous}}}{K_a} \quad (6.7)$$

And if $[H^+]$ is much larger than K_a then:

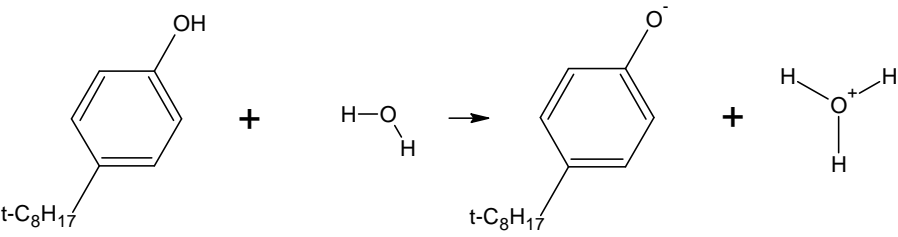
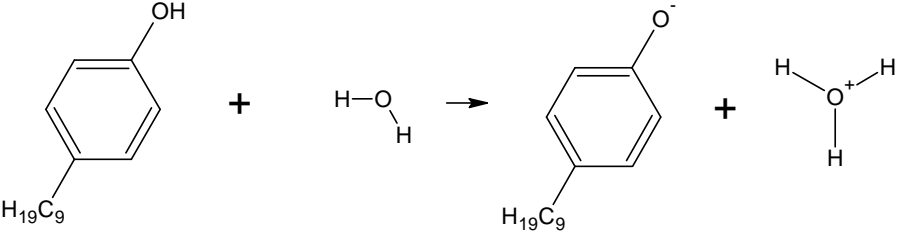
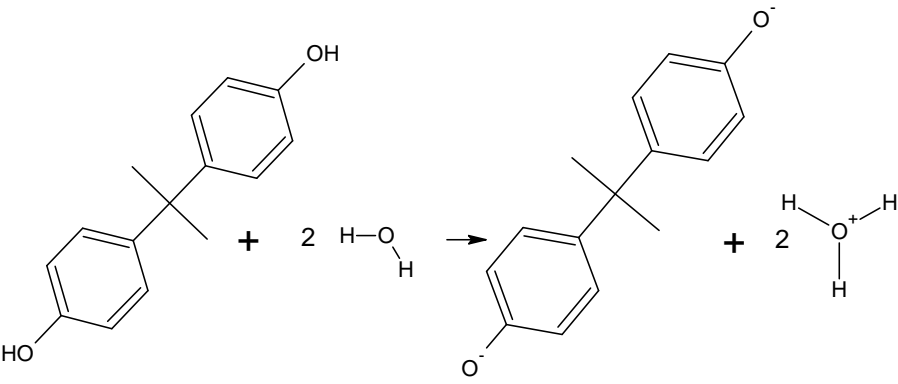
$$D_c = K_p \quad (6.8)$$

The pH of all aqueous samples analysed was determined using universal pH paper. The pH of all samples was in the range of 5-6, including the MilliQ water blanks. No pH adjustments were therefore necessary. The ionization of these analytes analysed from water are depicted in table 6.6, along with their associated pK_a values [254]. The estrogens are not shown in this table, but their pK_a 's are also above 10 [21] as well. For these conditions the acid remains largely non-ionized (from equation 6.3):

$$\frac{[A^-]_{\text{aqueous}}}{[HA]_{\text{aqueous}}} = \frac{K_a}{[H^+]_{\text{aqueous}}} = \frac{10^{-10}}{10^{-6}} = 10^{-4}$$

In addition, the distribution coefficient for a pK_a of 10 and pH of 6 ($K_a = 10^{-10}$ and $[H^+] = 10^{-6}$; $[H^+] \gg K_a$) amounts to $K_{o/w}$ (equation 6.8) as described by equation 6.2.

Table 6.6 Structure of the alkylphenols and bisphenol-A as they ionize in aqueous medium plus their associated ionization constants at 25°C [7, 254].

Analyte ionization in water	pK_a	K_a
 <p><i>tert</i>-octylphenol</p>	10.25	5.62×10^{-11}
 <p>4-<i>n</i>-nonylphenol</p>	10.28	5.25×10^{-11}
 <p>bisphenol-A</p>	9.5 11.3	3.16×10^{-10} 5.01×10^{-12}

6.4. Quantitative Thermal Desorption

6.4.1. Optimising desorption conditions

Several experiments were performed to determine the conditions under which the derivatives would be completely transferred to the GC column i.e. when desorption is complete. As described in chapter 2, the MCT can be compared to a chromatographic column having a PDMS stationary phase. Compounds will elute off the MCT in the same order as compounds elute off a non-polar (PDMS stationary phase) GC column.

Based on previous work in my MSc thesis [61], concerning thermal desorption optimisation, it is convenient to optimise conditions using the alkane that elutes after the analyte of interest. Nonadecane (C19) is the alkane eluting immediately after the BPA-TFA derivative on a PDMS phase GC column. However, several alkanes with increasing boiling points (hence elution temperatures) were used, since this would be useful for future applications. Little additional effort was required to include them. The alkanes selected were C16, C20, C24 and C28. These were placed at the top of the PDMS MCT using a 5 μ L syringe. As desorption flow is from the top to the bottom of the trap, once the alkanes are completely desorbed it is evident that any compound that elutes before that specific alkane on a PDMS phase GC column, has also been completely desorbed from the PDMS MCT. Traps were analysed using the Gerstel ® TDS-CIS HP GC-FID instruments.

Figure 6.26 shows a graph of the various alkane FID peak areas *versus* desorption temperature, for TDS desorption time of 20 minutes, desorption flow rate of 100 ml/min, and CIS injection time of 20 min at 300°C, with a reduced injection flow rate of 5 ml/min. The capillary column limits the CIS injection flow rate. Figure 6.27 shows that more than 10 minutes are required to desorb the alkanes from the CIS at 300°C, as a result of the lower flow rate available for this process. As shown in figure 6.26 all the alkanes have reached a maximum peak area from 180°C onwards. It can be concluded that they have all been completely transferred from the PDMS trap. A temperature of 260°C was chosen for the desorption process, as it was later learned that desorption flow rates greater than 50 ml/min through a glass baffled inlet liner may cause incomplete trapping in the CIS. This is half the flow rate used during desorption temperature

optimisation. A temperature of 260°C also ensured that other non-interesting compounds on the trap would be desorbed. Silicone degradation increases with higher temperatures, which result in increased silicone peak areas (section 2.6), causing additional problems such as peak overlap, column overload and contamination of the MS ion source. For this reason higher temperatures were not chosen. A blank run of the PDMS MCT after this desorption cycle indicated complete transfer of the derivatives and C19; no carry-over was observed. C19 was added, as an internal standard, to all traps just before desorption in the Gerstel® unit. The C19 was used only to check for losses in the desorption unit during the desorption process.

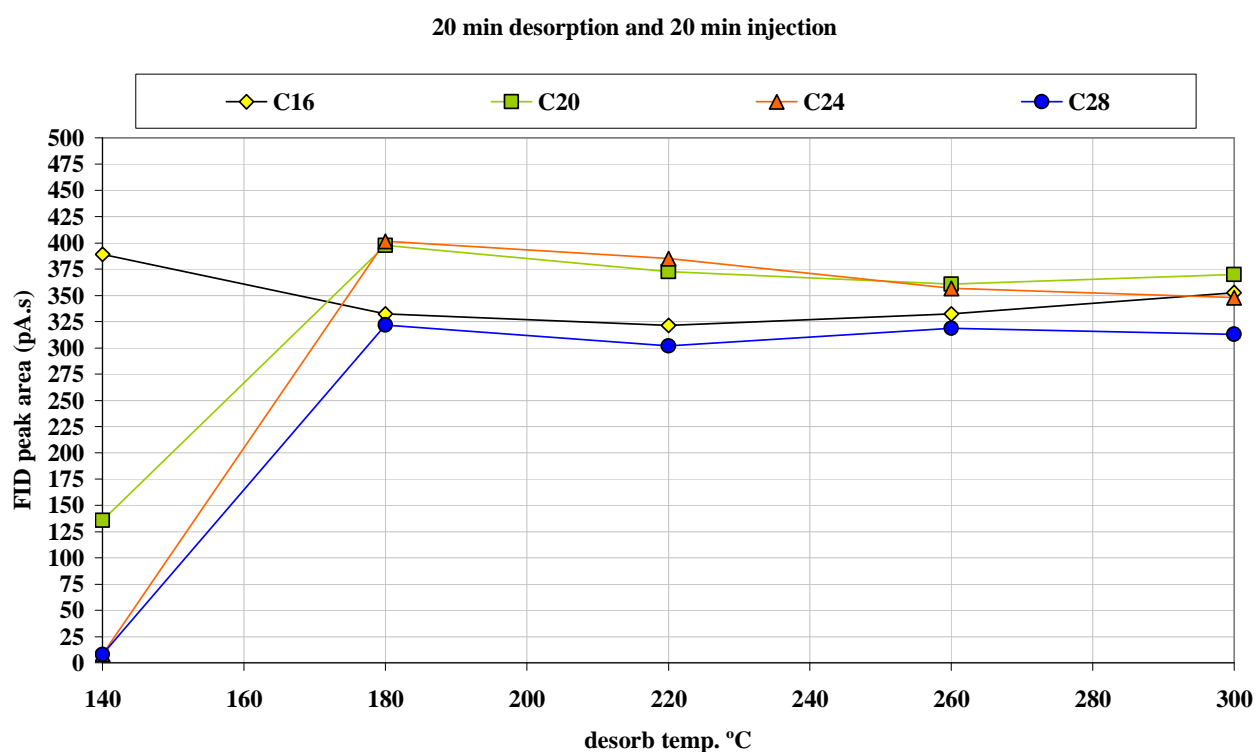


Figure 6.26 Optimisation of thermal desorption temperature of higher boiling alkanes off a 32 PDMS MCT using a Gerstel® TDS-CIS. The injection temperature was maintained at 300°C, while desorption temperature was incremented by 40°C per desorption run. The measurement values are depicted as an x-y scatter plot with data points connected by lines. The optimum desorption temperature was visually determined to be 180°C where the peak areas of the analytes appear to reach a plateau.

Optimisation of 30 ng alkane desorption from PDMS trap Gerstel TDS-CIS

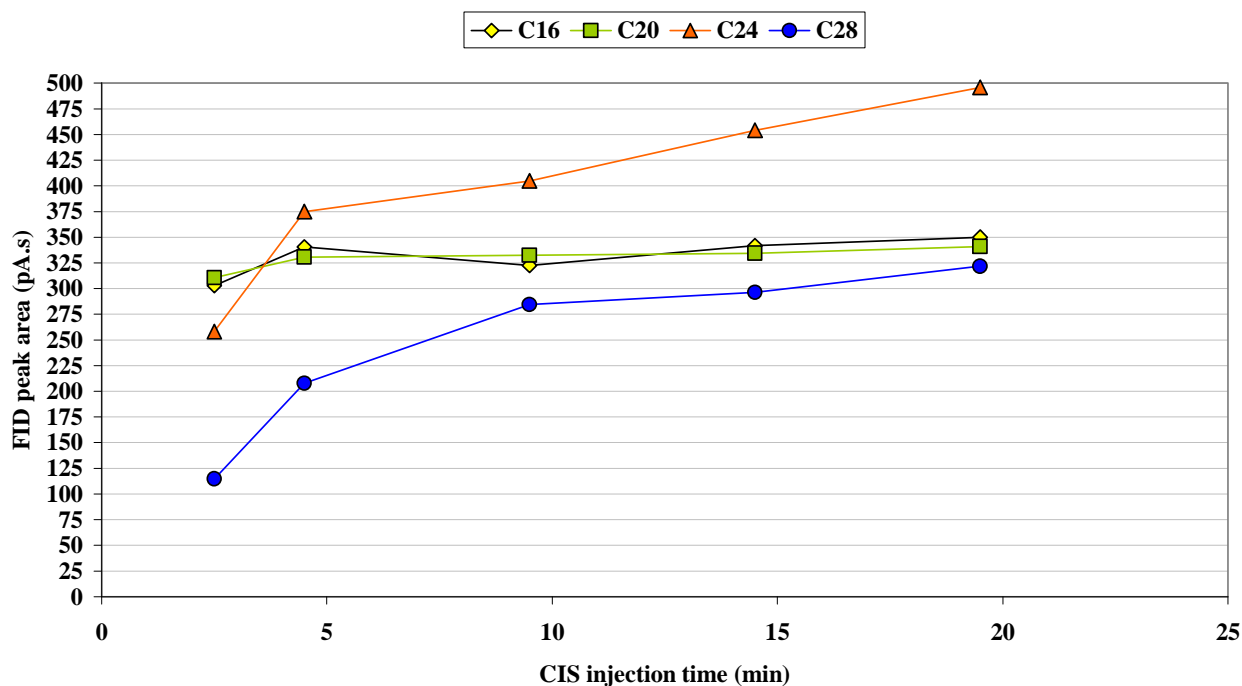


Figure 6.27 Optimisation of CIS injection time of higher boiling alkanes off a glass baffled inlet liner using a Gerstel® TDS-CIS at 300°C. The measurement values are depicted as an x-y scatter plot with data points connected by lines. The optimum CIS injection time was visually determined to be 5 min for alkanes from C16 to C20, as the peak areas of these analytes appear to reach a plateau at this time. Higher boiling alkanes (C24 to C28) require more than 20 minutes to be desorbed completely off the CIS. A midpoint of 10 min was selected for injection time in this study.

6.4.2. The “Christmas tree effect”

During thermal desorption the excess derivatization reagent, derivatives and by-product, as well as the PDMS thermal degradation products, are injected onto the GC column. Under ideal conditions, the solvent forms a homogenous film that wets the stationary phase allowing the analytes to partition into the phase and begin the chromatographic process, producing the standard Gaussian chromatographic peaks, figure 6.28 (A). This only occurs if the polarities of the solvent and stationary phase are matched. In our case, however, the TFAA and TFA are polar solvents, which are present in a quantity that exceeds 1-2 μ l. Thus, instead of forming a homogenous wetting film on the PDMS stationary phase, droplets are formed inside the column. Each droplet gives rise to its own “solvent effect” i.e. analytes partition into the PDMS once the droplet of solvent has evaporated. This can occur at various points along the column. As a result the peaks that elute are

no longer gaussian but broader “Christmas tree-like” peaks, figure 6.28 (B). This is a typical occurrence in large volume splitless injections, and the problem can normally be overcome by inserting a retention gap before the GC column [255]. In our study an alternative to the retention gap is suggested. This is made possible through the use of a PTV injector or CIS in this case.

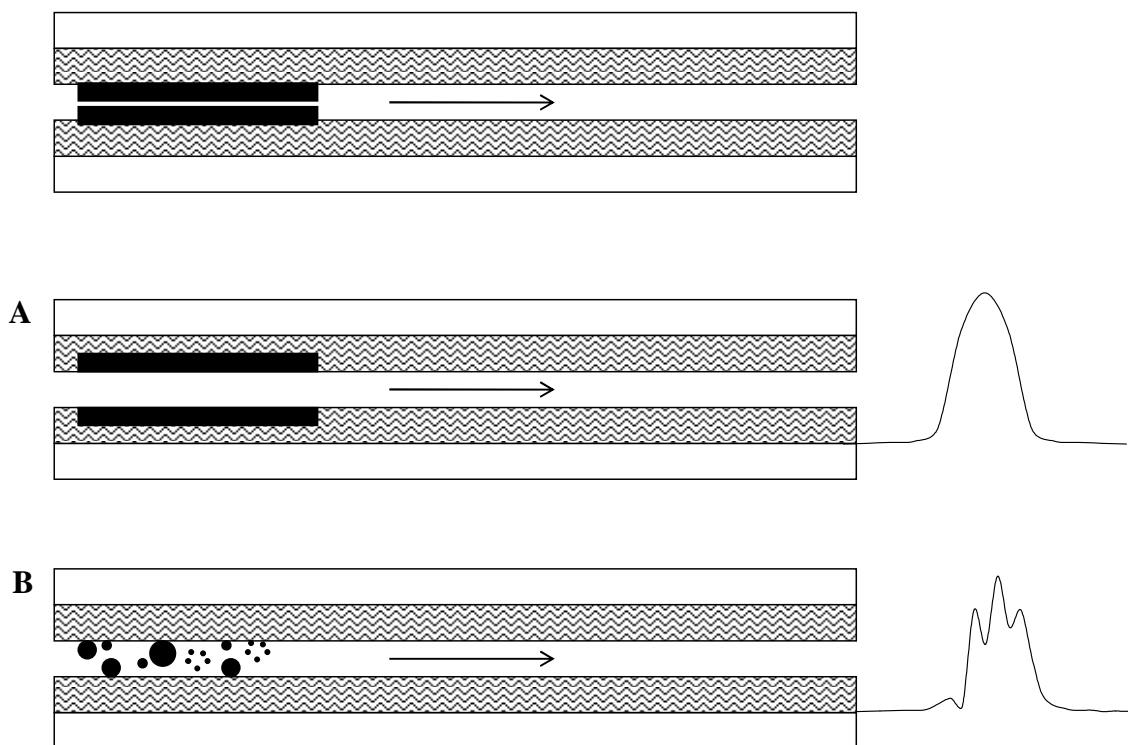


Figure 6.28 Cross-section of a non-polar capillary column showing a large volume splitless injection using (A) a non-polar solvent and (B) a polar solvent. The top figure shows the injection plug entering the column in the mobile phase. Figure A shows how the non-polar solvent “wets” the stationary phase as “like-dissolves-like”. The analytes in the plug begin to partition into the stationary phase and start the chromatographic process resulting in Gaussian peaks eluting from the column. Figure B shows how the polar solvent forms droplets as it does not wet the stationary phase. Each droplet gives rise to its own solvent effect resulting in broad split peaks eluting from the column [255].

Initial injection conditions from the cooled inlet onto the GC column were as follows:

The CIS is ballistically heated from -100°C to 260°C where it is held for 20 min, while the analytes move onto the column, then held at 40°C for 20 min, at an approximate flow rate of 5 ml/min.

Since the TFA can cause damage to the column at higher temperatures the aim is to remove it prior to raising the column temperature. However, this should not be at the expense of creating “Christmas trees”. By altering the injection conditions so that the solvent is selectively desorbed

(based on boiling point) from the CIS prior to desorption of the analytes, it is possible to remove the excess TFA such that the “Christmas tree” effect is avoided.

The CIS desorption conditions were altered as follows:

The CIS was heated from -100°C to 35°C , where it was maintained for 10 min. During this period, the TFA moved off the CIS onto the column. However, since the column was maintained at 40°C for 20 min, the “solvent” could not recondense, but moved straight through the column unretained. At this point the CIS was heated to 260°C and held for 10 min, while the analytes were focussed onto the column at 40°C . Figure 6.29 shows a section of two overlaid chromatograms indicating the improvement in chromatography as a result of the changed injection parameters.

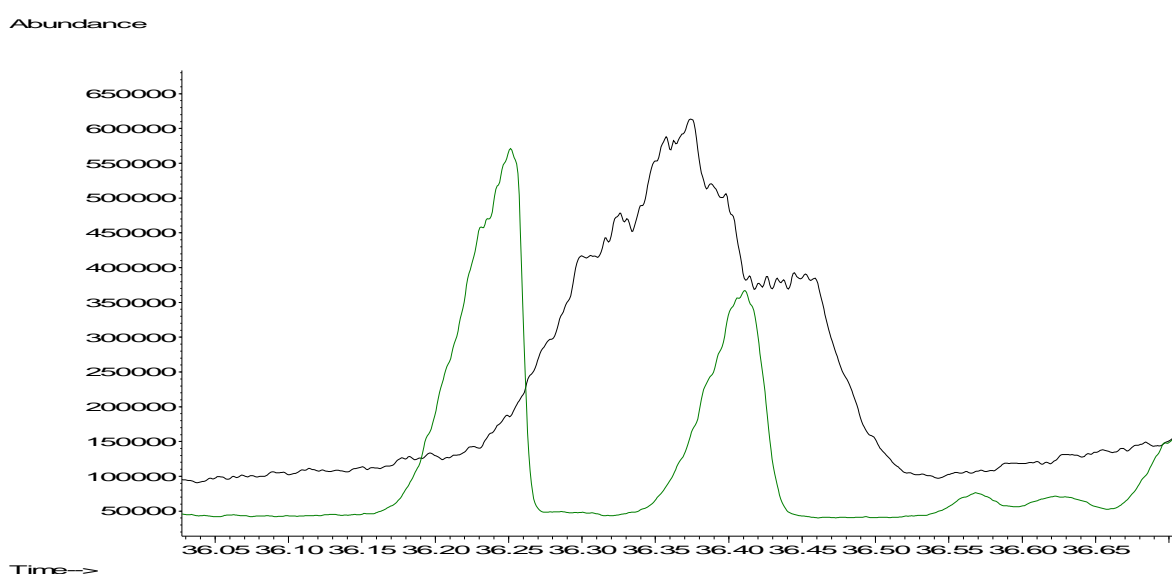


Figure 6.29 Section of two overlaid chromatograms depicting the improvement of chromatographic conditions for a large volume splitless injection. The “Christmas tree effect” of the larger co-eluting peak is replaced by 2 separated, smooth, peaks.

6.5. Sampling

6.5.1. Sampling setup and procedure

Figure 6.30 shows the simple setup used for sampling water through the PDMS MCT in the lab. A glass funnel was used as the water sample reservoir at the top of the PDMS MCT. It was connected to the MCT via a piece of Teflon® tubing. At the outlet of the MCT, a length of fused silica capillary was again connected with Teflon® tubing (fitted in a Swagelok ® reducing union $\frac{1}{4}$ ” to

1/16”) which acted as a flow restrictor. By adjusting the height of the restrictor outlet relative to the height of the water sample meniscus, (i.e. the pressure drop), it was possible to regulate the flow rate through the trap. Similar flow rates through the MCT could be obtained for all sampling arrangements using this setup. A sampling flow rate of approximately 50 $\mu\text{l}/\text{min}$ was used throughout this study. Based on previous work by Ortner, 11 plates can be obtained on the 32 channel PDMS MCT at 75 $\mu\text{l}/\text{min}$ for benzene in aqueous samples [63].

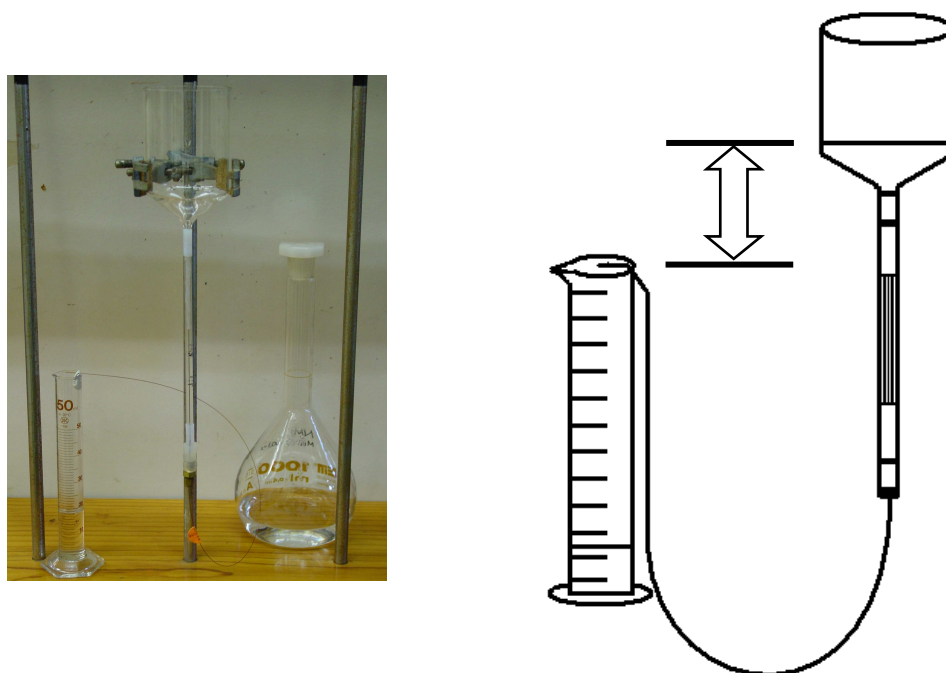


Figure 6.30 The simple setup used in the lab to sample water through the PDMS MCT.

The PDMS MCT trap must be conditioned with water before sampling, to ensure that no air bubbles are present as this affects the sampling flow rate through the channels in the trap. From Henry's Law for gases [256] we know that the solubility of a gas is inversely related to the temperature of the solvent, i.e. the warmer the solvent the less gas is dissolved in it. Thus pouring water at a temperature of approximately 60°C, through the trap was sufficient to remove any air bubbles that formed in the process. Tapping the PDMS MCT with a rubber tube during the conditioning step decreased the time required for degassing the trap. The water was allowed to reach just above the start of the PDMS at which point the sample was added. The water sample could only be added to the PDMS MCT once the trap had reached room temperature again. A Pasteur pipette was used to suck out the bubble that formed in between the two water levels.

The risk of losing analytes through adsorption onto active sites on the glassware was possible at this stage. It was assumed that the amount of time that the sample spent in the sampling funnel was short enough such that adsorption would not occur. Usually an organic modifier such as methanol could be added to the sample to prevent adsorption from occurring [47].

6.6. *Experimental*

6.6.1. *Instrumentation*

The analyses were performed on an Agilent 6890 GC system equipped with an FID or a 5973 Mass Selective Detector (Agilent Technologies, Palo Alto, CA, U.S.A) coupled to a Gerstel TDS-CIS4 thermal desorption unit (Gerstel, Mülheim an der Ruhr, Germany). An empty glass-baffled inlet liner was fitted in the CIS4; liquid nitrogen was used as the cryogen.

The thermal desorption conditions were as follows:

Desorption temperature 260°C; desorption time 20 min; helium desorption flow rate 50 ml/min (solvent vent mode); transfer line temperature 280°C.

The cold inlet conditions were as follows:

CIS trap temperature during thermal desorption -100°C; inject splitless for 10 min; 1st heating rate 10°C/s, initial injection temperature 35°C hold time 5 min, 2nd heating rate 10°C/s, final injection temperature 280°C hold time 5 min.

The GC oven was fitted with an HP-5 capillary column (30 m length, 0.25 mm i.d. and 0.25 µm film thickness). The oven was programmed as follows: 40°C (hold for 10 min during the splitless injection) to 160°C at a rate of 12°C/min (hold 3 min) and to 220°C at a rate of 12°C/min. The oven was then heated to 300°C (hold for 2 min). Helium was used as carrier gas with an average linear velocity of 40 cm/s. The FID temperature was set to 300°C. The GC-MSD transfer line was set to 280°C.

The MSD was programmed either for total ion scan from 40-500 amu or for SIM: m/z 231, 203, 245, 216, 405, 420, the 3 most abundant ions for each derivative.

6.6.2. Reagents and Materials

Trifluoroacetic acid anhydride (TFAA) was obtained from Supelco (Bellefonte, U.S.A.), 4-*tert*-octylphenol (TOP) from Aldrich (Steinheim, Germany), 4-*n*-nonylphenol (NP) from Riedel-de Haën (Steinheim, Germany) and bisphenol A (BPA) from Fluka (Steinheim, Germany). Medical grade PDMS tubing was obtained from Sil-Tech technical products (Georgia, USA). The method adopted for preparing PDMS MCTs is described in the literature [65].

6.6.3. Extraction Efficiency

2 ml MilliQ water was spiked with 1 μl of a 40 ng/ μl solution of alkylphenols and bisphenol-A in methanol. The water was sampled by pouring it through a funnel connected to the PDMS trap with Teflon® tubing. The flow through the trap was regulated using a capillary restrictor connected at the PDMS trap outlet. The sampling flow rate was set at approximately 50 $\mu\text{l}/\text{min}$. After sampling, residual water was removed by physically tapping it out, then purging (1 minute) with a fast stream (approximately 1 L/min) of hydrogen gas introduced through a capillary. The traps were then plugged with silica gel to remove any further water vapour before derivatization. The silica gel was baked in an oven at 100°C when not in use. The plugs were prepared using glass tubes of the same dimension as the PDMS MCT. Each tube has one side sealed off. The silica gel is packed into the tube which is then pressed onto the PDMS trap using a tightly fitting Teflon® sleeve. The silica gel does not come into physical contact with the PDMS. No signs of contamination originating from this operation was observed in the resulting chromatograms. Recoveries were compared to a 40 ng standard in acetone, placed on the PDMS trap, reacted and desorbed.

This extraction efficiency experiment was repeated twice. The first series of extractions was performed using a set of traps prepared from the same batch of silicone. The extracted analytes from this first set of traps were analysed by GC-FID. The second series of extractions was performed using a set of traps prepared from a different batch of silicone to the first series. The extracted analytes from these traps were analysed by GC-MS (using reconstructed ions).

6.6.4. Reaction efficiency

The optimum reagent volume was determined by placing 1 μl of a 40 ng/ μl alkylphenol standard in acetone onto the PDMS and allowing the acetone to evaporate. Different volumes ranging from 2 μl to 10 μl of TFAA was added using a 10 μl syringe. The trap was capped on both ends with glass plugs for 10 minutes.

The reaction efficiency was tested by placing 1 μl of a 40 ng/ μl alkylphenol standard in acetone onto the PDMS and allowing it to evaporate. 5 μl TFAA was added using a 10 μl syringe. The trap was capped on both ends with glass plugs for the duration of the reaction. This experiment was repeated for different reaction times. Structures of the derivatives were confirmed by EI mass spectrometry (figure 6.23 – 6.25) [62]. The derivative masses were obtained by comparison to the synthesized derivatives in acetone (refer to section 6.2.6).

6.6.5. Reaction Calibration Curves

Calibration curves for the derivatives were obtained after the *in situ* reaction with the standards of the target analytes. The underivatized alkylphenols were prepared in acetone in concentrations ranging from 5 to 80 ng/ μl . 1 μl of the standard mixture was placed on the trap and allowed to evaporate. 5 μl TFAA was added to the trap and allowed to react for 10 minutes. The trap was then thermally desorbed. The quantity of derivative formed was determined by comparison with the synthesized derivatives in acetone (refer to section 6.2.6).

6.7. Results and Discussion

6.7.1. Extraction efficiency

The extraction efficiencies, obtained on different PDMS MCTs (made from 2 different PDMS batches), are summarized in table 6.7. The *tert*-octylphenol (TOP) displays good recoveries (~70-79%) on both trap batches with similar extraction efficiencies. On the first PDMS batch nonylphenol (NP) was 80% extracted. However, the second PDMS batch only extracted half that amount. In both cases the variation was large. Bisphenol-A (BPA), was poorly extracted (between

10-26%) on both PDMS batches. The poor extraction confirmed previous work performed by Nakamura *et al.* [54] using SBSE. The results of a two-tailed t-test ($P=0.05$) indicated that the means of the results of the 2 batches for each analyte differ significantly. The significance test can be found in appendix 4.

Extraction of analytes into PDMS can loosely be predicted by the octanol-water partition coefficient of the analyte. Typically, high extraction efficiencies are obtained for compounds with large octanol-water partition coefficients [257, 258]. BPA, despite having a relatively large octanol-water partition coefficient, does not partition well into PDMS. Extraction only improves once hydroxyl groups have been derivatized. Although designed to operate under dynamic pre-breakthrough sampling conditions (100% extraction expected) i.e. a 5 ml water sample is less than the calculated breakthrough volumes of any of the analytes, shown in table 6.5, extraction efficiencies are even less than those expected for dynamic equilibrium sampling conditions shown in table 6.3. Further work is required to investigate the reason for the low extraction efficiency observed.

In addition, table 6.7 indicates a poor reproducibility between different batches of PDMS tubing, which will require further investigation. This can be due to differences in the PDMS polymer material or to particulates in the trap. It is unlikely that particulates larger than $0.45\ \mu\text{m}$ are present in the filtered MilliQ water. Other particulates may arise from dust in the laboratory.

As noted in section 6.7.2 below, the reaction efficiency data indicates that constant derivatization efficiency can be expected. We therefore assume that it too does not contribute to the observed variation. A reconstructed ion chromatogram of the raw alkylphenols' most abundant ions m/z 135 and 213 from the extraction analyses does not indicate the presence of unreacted TOP or NP, see appendix 3. As for BPA, the chromatographic run was stopped before the unreacted analyte could be detected. However, as discussed below, we would expect to see BPA since it does not convert efficiently.

Table 6.7 Extraction efficiencies obtained for TOP, NP and BPA on 2 different PDMS MCT batches.

		<i>tert-octylphenol</i> TFA	<i>4-n-nonylphenol</i> TFA	<i>Bisphenol-A</i> TFA
PDMS 1	% extraction	70	84	10
	% RSD	4	26	15
	n	7	8	8
PDMS 2	% extraction	79	43	26
	% RSD	3	22	8
	n	5	5	5

6.7.2. Reaction efficiency

Acetic acid anhydride is often used to convert alcoholic and phenolic functional groups into their corresponding acetates, in the presence of a base [54, 180]. The reaction is fairly quick and can take place in an aqueous medium. However, the final extraction medium is very acidic (pH 2) and causes degradation of the PDMS absorbent as observed by an increase in the siloxane degradation peaks in the chromatogram [180].

Trifluoroacetic acid anhydride (TFAA) converts the alcoholic and phenolic functional groups into their corresponding trifluoroacetate esters, with the added advantage of moving the derivatives out of the lower mass ranges and opening up detection possibilities to include electron capture and negative chemical ionization mass spectrometry. TFAA does not require a catalyst and derivatization is rapid. However, it is not suitable for use in an aqueous medium [62]. In the PDMS medium (when dry), TFAA will also form the trifluoroacetic acid by-product, however, as TFA is so volatile and unretained by the PDMS, the bulk is easily removed from the trap before thermal desorption begins.

Results obtained for the optimum reaction volume for TFAA are plotted in figure 6.31. A maximum peak area was observed when using 5 μl TFAA. It is not clear at this stage why the efficiency drops with larger volumes of reagent.

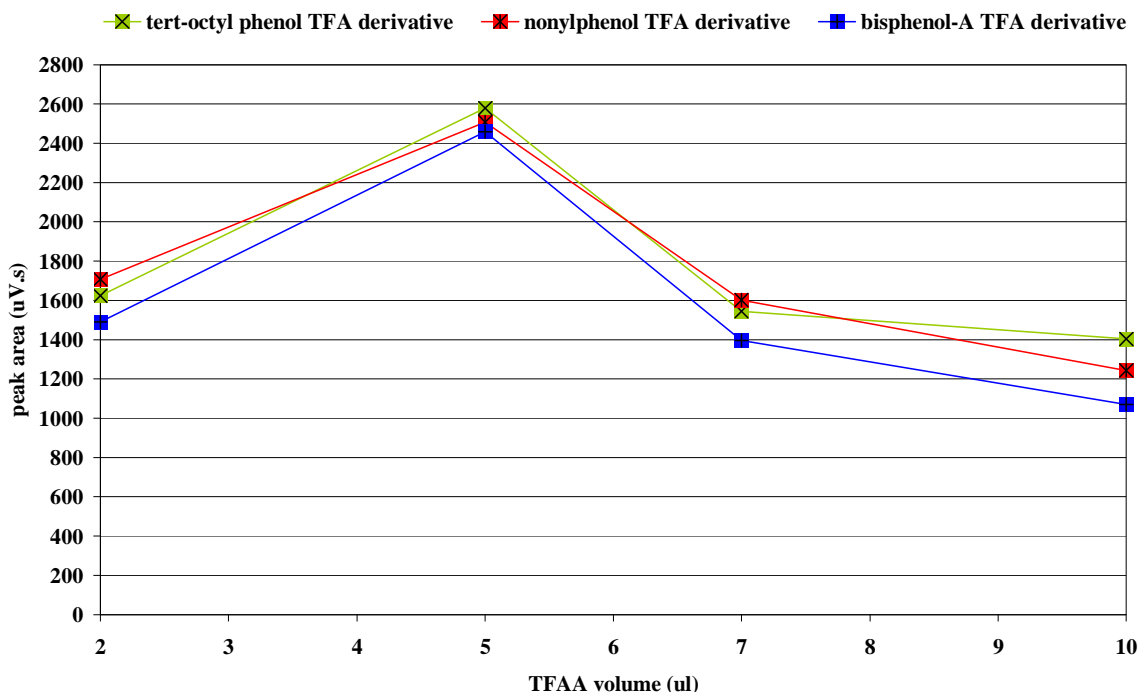


Figure 6.31 Optimum TFAA reagent volume, determined by placing 1 μl 42 ng/ μl TOP, 44 ng/ μl NP and 54 ng/ μl BPA in acetone on the PDMS trap; the corresponding reagent volumes are added after the solvent has evaporated. The trap is then sealed with glass caps for 10 minutes before thermal desorption and analysis. The optimum TFAA volume of 5 μl was visually determined from the x-y scatter plot as the point where maximum derivative peak area is observed.

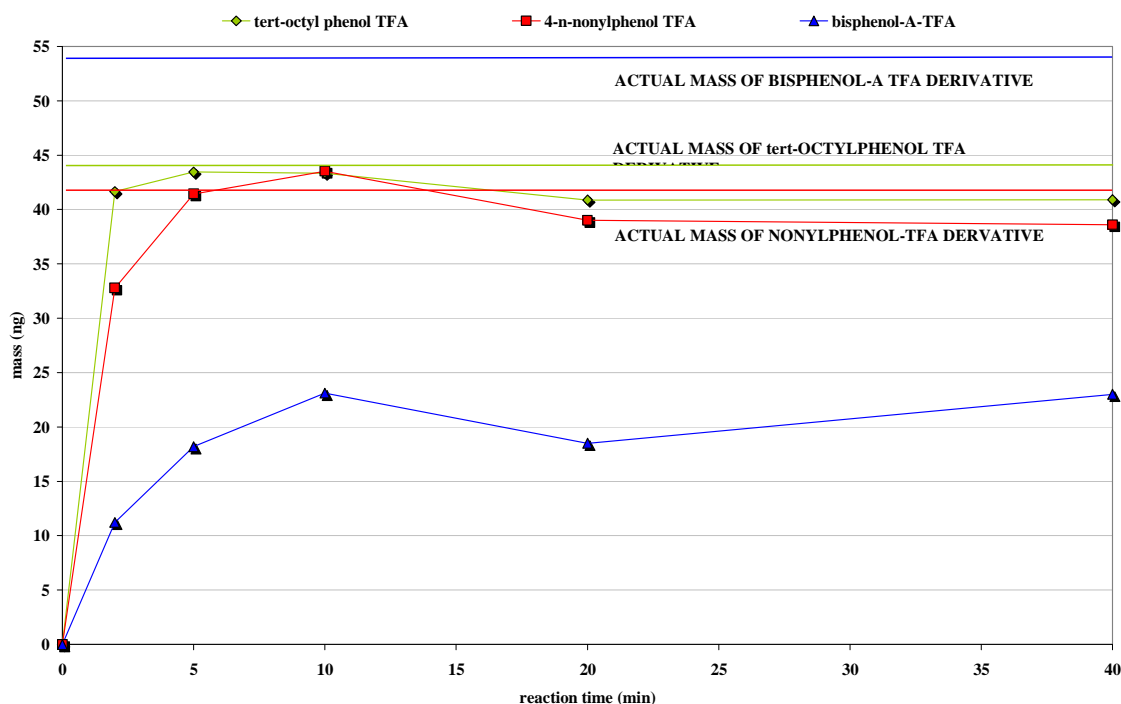


Figure 6.32 Reaction efficiencies, determined by placing 1 μ l 42 ng/ μ l TOP, 44 ng/ μ l NP and 54 ng/ μ l BPA in acetone on the PDMS trap. 5 μ l TFAA is added after the solvent has evaporated. The trap is then sealed with glass caps for the duration of the reaction. The measurement values are depicted as an x-y scatter plot with data points connected by lines. The optimum reaction time was visually determined to be 5 min, where the peak areas of the TFA-derivatives appear to reach a plateau.

Reaction efficiencies are shown in figure 6.32. All three derivatives appear to reach a plateau after 5 minutes reaction time. This normally indicates that the reaction is complete [62]. However, a comparison of the plateau amount with the actual amount of derivative expected to form indicates that only TOP and NP have reacted completely (100%). BPA shows less than 50% reaction efficiency. Despite this the BPA-TFA derivative amount remains stable after 10 minutes and as such can still be deemed a viable reaction for the purposes of this study. The experiment was repeated and similar results were obtained as shown in appendix 3, figure A3.6. The reaction appeared complete after 5 minutes. The quantity of derivative formed was determined by comparison with the synthesized derivatives in acetone (refer to section 6.2.6).

6.7.3. Reaction calibration curves

Figure 6.33 shows a typical calibration curve obtained after *in situ* derivatization, using a GC-FID and one PDMS trap. Calibration using the MSD involved the confirmation with 3 ions and quantitation of the base peak ion. Table 6.8 summarises the detection limits possible with the instrumental setup used. An unexpected problem of carry-over from the thermal desorber presently limits the quantitation levels for these analytes, particularly BPA, which already suffers from poor recovery and reaction conversion. Further work in reducing the desorber contamination would be required to lower the detection limits.

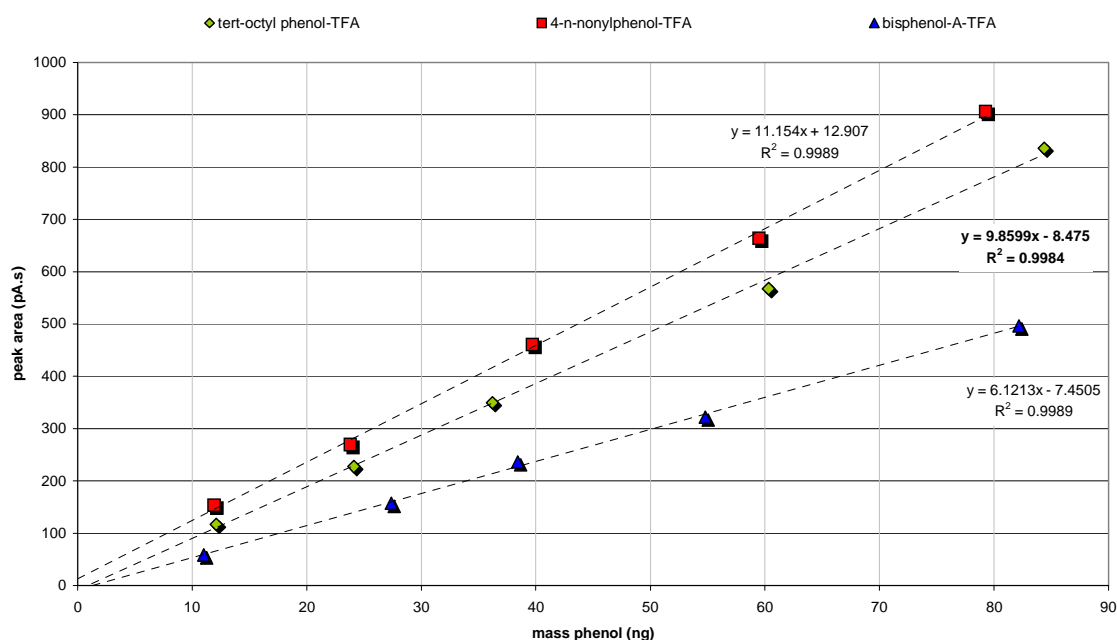


Figure 6.33 GC-FID calibration curves obtained by the *in situ* reaction of alkylphenols on the PDMS trap.

6.7.4. Minimum Detection Levels of accumulated mass

Table 6.8 lists the Minimum Detection Levels (MDL) possible for the analytes concerned once collected on the trap. The MDLs were calculated using 1) Regression line analysis of the calibration curves [277] and 2) The instrumental signal-to-noise (s/n) ratio. The s/n detection limits are generally lower as they do not take the variability of a series of measurements into account.

As expected, the LOD ($s/n = 5$) improves when moving from the FID to reconstructed single ion data from full scan EI-MS to selected ion monitoring EI-MS. The LOQ, using regression line analysis, for FID and full scan MS is similar as this analysis gives a better indication of the spread of measurements resulting from derivative formation and thermal desorption. The SIM LOQ is lower than the RIC LOQ, not only because of the improved s/n ratio expected from SIM but also because the thermal desorption unit was cleaned prior to measurements using SIM. Due to the number of problems experienced during this study, the final set of measurements made were those using SIM only to obtain an indication of what the best detection levels could be using a clean system. Once the underlying problems of this method are resolved, further work would be to repeat these measurements using full scan MS and SIM under consistent conditions.

The levels at which the alkylphenols and bisphenol-A can be measured using this technique are similar to the levels mentioned in the literature (see the summary presented in table 3.2.). For example, derivatization and concentration of TOP, NP and BPA in 10 ml of river water sample using acetic acid anhydride and SBSE yielded a LOD of 0.5, 5 and 2 ppt respectively by GC-SIM-MS [177]. The LOQ for TOP, NP and BPA from a 10 ml river water sample was 2, 20 and 10 ppt respectively [177]. Working with a 10 ml spiked water sample our technique can reach a LOD of 3.2, 7.1 and 20 ppt for TOP, NP and BPA respectively. However, as we are limited by background contamination our LOQ is 40, 21 and 110 ppt respectively using GC-SIM-MS. These values are based on the assumption of 100% reaction and extraction efficiencies. With the removal of background contamination detection limits can be even lower. Furthermore this technique has the added selectivity advantage of using GC-NCI-MS or GC-ECD for the detection of the electron-rich trifluoroacetate derivative as opposed to the non-halogenated acetate derivatives. The sensitivity of response of GC-NCI-MS or GC-ECD with respect to the trifluoroacetate derivatives has not been determined in this project, hence it cannot yet be established whether the increased selectivity will have a positive influence on the LOD and LOQ for these compounds.

Table 6.8 Minimum Detection Levels. (FID = flame ionization detection, EI-RIC=electron impact reconstructed single ion, EI-SIM=electron impact selected ion monitoring, LOD=limit of detection, LOQ= limit of quantitation, LOC= level of confidence from regression line analysis, LOQ from reagent blanks (5 µl TFAA on PDMS MCT) obtained by taking the average plus three times the standard deviation of the series of measurements). The LOD (s/n =5) was determined by extrapolation from a larger signal and not from actual measurements.

	<i>mass (ng)</i>			
	4- <i>tert</i> -octylphenol	4- <i>n</i> -nonylphenol	bisphenol-A	
FID	3.5	5.2	4.7	LOD (s/n = 5)
FID	4.1	3.1	3.1	LOD (95% LOC)
FID	14	10	10	LOQ (95% LOC)
EI-RIC	0.17	0.10	0.42	LOD (s/n = 5)
EI-RIC	0.22	0.16	0.54	LOD (95% LOC)
EI-RIC	1.6	5.2	6.7	<i>LOQ (blanks n = 4)</i>
EI-RIC	9.0	18	10	LOQ (95% LOC)
EI-SIM	0.032	0.071	0.20	LOD (s/n = 5)
EI-SIM	0.40	0.21	1.1	<i>LOQ (blanks n = 4)</i>

6.8. Limitations of this method

6.8.1. PDMS degradation

Initial water sampling experiments indicated that the PDMS MCT was severely degraded after *in situ* derivatization with the TFAA. It was found that without complete removal of water from the PDMS trap, the PDMS degradation would be significant. Figure 6.34 shows an overlaid chromatogram of two analysed PDMS MCTs that underwent *in situ* derivatization under “wet” and “dry” PDMS conditions.

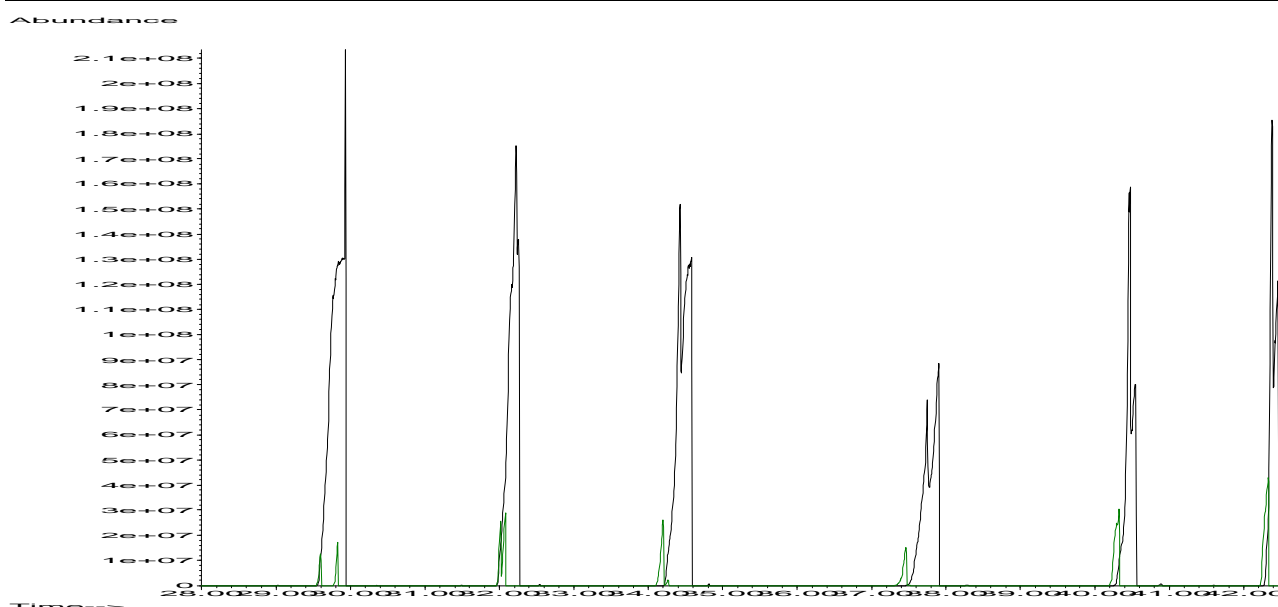


Figure 6.34 Overlaid chromatogram of 2 PDMS MCTs. The green chromatogram is obtained after the *in situ* derivatization reaction on a “dried” trap. The black chromatogram is obtained after the *in situ* derivatization reaction on a “wet” trap.

Under “dry” PDMS conditions, the TFA acid by-product that forms during the *in situ* derivatization reaction (figure 6.22) remains un-ionized in the gas phase; the bulk is removed from the PDMS MCT before thermal desorption occurs.

It is suspected that when the trap is “wet”, the TFA acid is ionized, in the aqueous phase, to form the extremely acidic hydronium ion (H_3O^+) shown in figure 6.35. This hydronium ion triggers the chemical degradation of the PDMS polymer. It is suggested that this degradation, along with the usual thermal degradation of the PDMS, leads to the increased siloxane peaks observed in figure 6.34.



Figure 6.35 Reaction equation for the TFA acid by-product in the presence of water.

Purging the trap with nitrogen gas after centrifuging (the method suggested by Ortner [63]) did not remove all the water. However, in Ortner’s [63] case removal of all the water was not critical. Physically tapping water out of the trap by dropping it several times down a 1.5 m long tube, helped to remove the water droplets that were trapped through capillary action inside the PDMS channels.

Followed by a 1 min high flow (approximately 1L/min) purge with hydrogen gas, this process removed most of the water from the trap. See appendix 5 for the trap drying investigation results.

The best results were obtained when the trap was capped with dried silica gel for approximately 2 hours or left overnight. This last step removed any residual vapour caught in the PDMS matrix. Removal of the residual water vapour could not be determined gravimetrically, see appendix 5. The only indication that all the water vapour had been removed was through the *in situ* derivatization in the PDMS. When the size of the PDMS degradation peaks resulting from a PDMS MCT having undergone *in situ* derivatization did not differ much from the PDMS degradation peaks resulting from a PDMS MCT blank desorption run, we assumed that all the water had been removed. As discussed in chapter 2 (Section 2.6), the PDMS matrix is not 100% pure PDMS, but contains up to 40% fumed silica (SiO_2) as filler. It is possible that the SiO_2 holds the residual water vapour in the PDMS matrix, since it is known that pure PDMS is a hydrophobic polymer.

It should also be noted that analytes, with boiling points in the C16 to C20 range, are not volatile enough to be removed from the trap during the high-speed gas-purging step at room temperature. This step should be of concern only when working with analytes that have low retention volumes or high volatilities.

6.8.2. Desorber contamination

As can be seen in figure 6.36, from the system blank chromatogram obtained from desorption of an empty glass tube that desorber contamination has occurred as a result of sample carry-over. This persistent carry-over limits the minimum possible levels of detection for the analytes being determined, see table 6.8.

After the thermal desorption phase in the Gerstel® desorption unit (see figure 4.3), the tube desorption chamber is cooled down from 260°C to the initial temperature of 40°C, before the CIS is ramped to desorb the cryogenically trapped analytes from the baffled glass inlet.

It is suspected that sample carry-over occurs inside the TDS tube desorption chamber (see figure 4.3) during this cooling phase. Despite a permanent carrier gas purge flow of 3 ml/min around the desorption tube, the underivatized analytes and particularly the TFA acid by-product can condense onto the metal surfaces inside the chamber where they are desorbed during future desorption cycles. An improvement in background levels was observed when this chamber was cleaned out with

methanol. Another possible solution to this problem is to increase the purge flow around the tube manually.

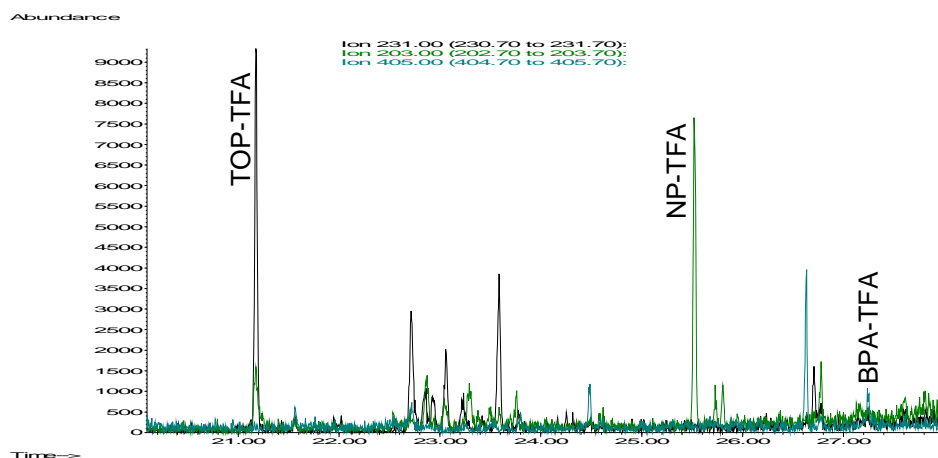


Figure 6.36 System blank reconstructed ion chromatogram obtained from desorption of an empty glass tube. *Tert*-octylphenol trifluoroacetate derivative (TOP-TFA) m/z 231, $t_R = 21.2$ min; 4-*n*-nonylphenol trifluoroacetate derivative (NP-TFA) m/z 203, $t_R = 25.6$ min; bisphenol-A trifluoroacetate derivative (BPA-TFA) m/z 405, $t_R = 27.2$ min.

6.9. Spiked water samples

Figure 6.37 depicts the TFAA reagent blank (A) and a 5 ml water sample spiked with $1\mu\text{l}$ of a 25 $\text{ng}/\mu\text{l}$ of the alkylphenols and bisphenol-A in methanol (B). Figure 6.37 (C) shows the extracted ion chromatogram for the base peak ions of each derivative, namely: m/z 231 (TOP-TFA), m/z 203 (NP-TFA) and m/z 405 (BPA-TFA). The procedures for extraction and reaction are as described above in sections 6.6.3 and 6.6.4.

6.10. Real water samples

Water samples were brought to the lab for preliminary testing. Once the method has been improved upon, further work would include on-site extraction of water samples using the PDMS MCT.

All water samples analysed used the same procedure (described in sections 6.6.3 and 6.6.4 above) for testing the extraction and reaction efficiencies. However, a sample size of 20 ml was used instead of 5 ml. This still falls within the expected breakthrough volumes of the analytes under test (see table 6.5.).

The first 5 L sample was taken from the Apies River, downstream from a sewage treatment plant. The second 5 L sample was taken from the river at the LC de Villiers Sports Centre at the University of Pretoria. In both cases, the bottle openings were covered with aluminium foil before sealing with screw-on caps. Upon reaching the lab, methanol (100 ml) was added to the bottle to prevent adsorption of phenolic compounds on any active glass surfaces. Methanol, often 5 % of the sample volume, is added to water samples to prevent adsorption of analytes on active glass surfaces [47, 63, 278]. However, Lee *et.al*, found that adding methanol to the sample reduced the extraction yield of 4-nonylphenol using SBSE. As a point of departure, we opted for adding 2% methanol as modifier to the water sample, as a precautionary measure against larger losses due to adsorption. 20 ml aliquots were taken, using a glass pipette, for PDMS concentration. Both samples were analysed within 48 hours. The quantitative results are summarised in table 6.9.

Figures 6.38 and 6.40 show the results obtained for 2 aliquots of the Apies river water sample extracted and derivatized on 2 different PDMS MCTs. Figure 6.39 shows the reagent blank. All 3 figures show the total ion chromatogram, followed by the extracted PDMS degradation peaks (note the repeatable retention times) and the extracted derivative ions. It is obvious that the reagent blank is not “blank” since the system is contaminated. What is also of concern is that 2 aliquots analysed on 2 different traps gave 2 different sets of results. Interestingly, only the amounts determined for bisphenol-A fall below the limits of quantification (LOQ) (see table 6.9.). Both TOP and NP are detected in the sample above levels detected in the blank. This can be observed visually by inspection of the respective peaks on the blank and sample chromatograms and quantitatively by comparison with external standard calibration curves.

Figures 6.41 and 6.42 present the results obtained for the reagent blank and a 20 ml aliquot of the second sample taken from the Sports Centre river site. These results were obtained by operating the mass spectrometer in selected ion mode (SIM) using the base peaks and more abundant ions for each derivative. Masses 231, 203, 245, 316, 405, 420 were selected for SIM. Once again, only the quantities obtained for bisphenol-A fall below the LOQ.

Note the LOQ(RIC) values were determined before the TDS was cleaned. The LOQ(SIM) values are still limited by carry-over but were determined after the TDS was cleaned, hence the lower value. The process of determining LOQs must be determined under identical conditions once the continuous sample carry-over problem is resolved. It is not practical to keep cleaning the TDS chamber after each measurement.

It was also observed that with continued use and degradation of the PDMS traps, more peaks would appear in the chromatograms that contained ions related to PDMS and to the derivatives, probably indicating that side products were starting to form with the PDMS degradation products and the TFAA reagent. This is particularly noticeable in SIM where peaks with the selected ion masses were eluting at the PDMS peak retention times. Bisphenol-A, for example, has a peak eluting before and after its own peak at 27.2 min. It can be assumed that these are isomers of BPA. However, the presence of siloxane masses in the mass spectrum indicates that it is not the case. In addition, the ratios of the ions m/z 405 to m/z 420 (the base peak and molecular ions) are different from the BPA-TFA derivative. Peak one (ratio 10:1) BPA-TFA peak (ratio 7:1) and peak 2 (ratio 13:1).

Table 6.9 Quantitative results obtained for 20 ml real samples by external standard calibration, after subtraction of the blank value. Concentration values based on 100% reaction and extraction efficiencies. Corrected concentration values obtained through inclusion of extraction and reaction efficiency factors (PDMS batch 2). TOP (100% reaction, 79 % extraction); NP (100% reaction, 43% extraction) and BPA (37% reaction, 26% extraction). Analyte concentrations below LOQ are not listed.

		TOP	NP	BPA	
		231	203	405	
		LOQ (RIC)	0.079	0.26	0.33
					ppb
RIC	APIES river - sample 1	1.3	0.93	-	conc.
		1.7	2.2	-	<i>corrected conc.</i>
	APIES river - sample 2	0.63	1.7	-	conc.
		0.80	3.9	-	<i>corrected conc.</i>
LOQ (SIM)		0.020	0.011	0.054	ppb
SIM	LC river - sample 1	0.091	0.19	-	conc.
		0.12	0.45	-	<i>corrected conc.</i>
	LC river - sample 2	0.26	0.025	-	conc.
		0.33	0.058	-	<i>corrected conc.</i>

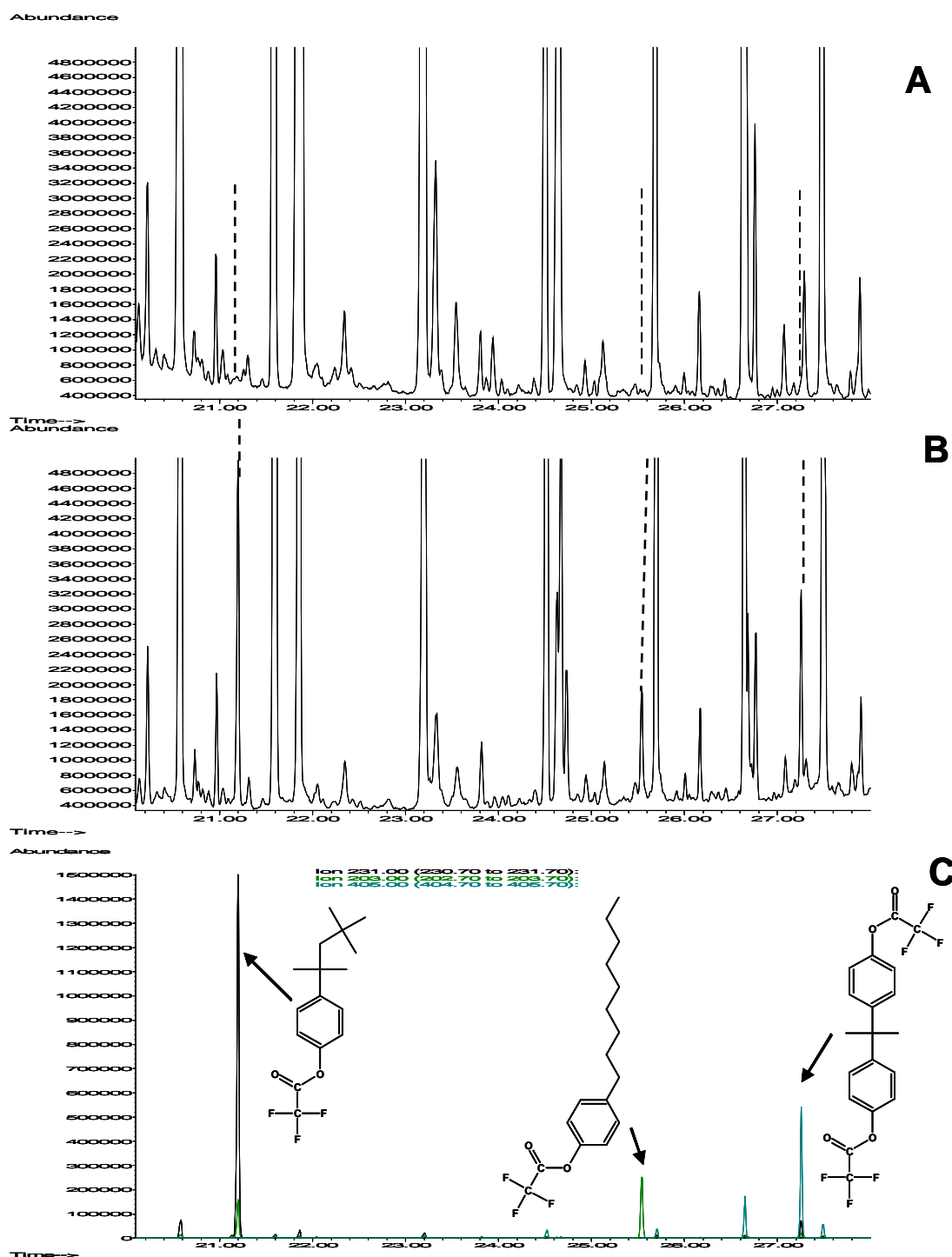


Figure 6.37 (A) Total ion chromatogram of the reagent blank.

Figure 6.37 (B) Total ion chromatogram of a 5 ml MilliQ water sample spiked with 25 ng alkylphenol standard in methanol, sampled through the PDMS MCT (50 μ l/min), dried and allowed to react with 5 μ l trifluoroacetic acid anhydride for 10 min, followed by thermal desorption. Figure 6.37 (C) The extracted ion chromatogram of the base peak ions used for quantitation. *Tert*-octylphenol trifluoroacetate derivative (TOP-TFA) m/z 231, $t_R = 21.2$ min; 4-*n*-nonylphenol trifluoroacetate derivative (NP-TFA) m/z 203, $t_R = 25.6$ min; bisphenol-A trifluoroacetate derivative (BPA-TFA) m/z 405, $t_R = 27.2$ min.

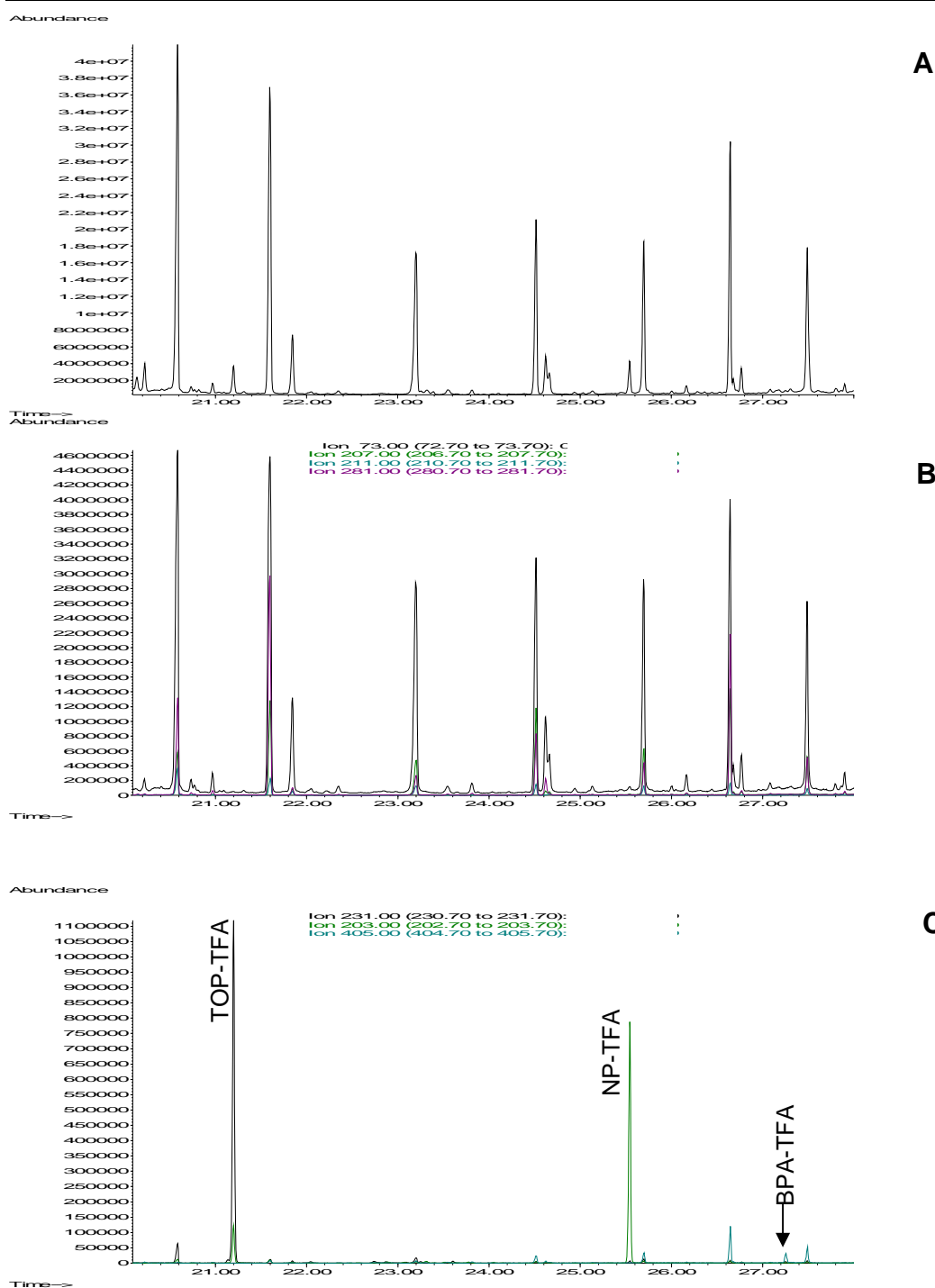


Figure 6.38 (A) Total ion chromatogram of the 20 ml Apies River water sample on PDMS MCT M1. Sample extracted at a flow rate of 50 $\mu\text{l}/\text{min}$, dried and allowed to react with 5 μl trifluoroacetic acid anhydride for 10 min, followed by thermal desorption.

Figure 6.38 (B) Extracted ion chromatogram of PDMS degradation peaks m/z 73, 207, 211 and 281. Figure 6.38 (C) Extracted ion chromatogram of the base peak ions used for quantitation. *Tert*-octylphenol trifluoroacetate derivative (TOP-TFA) m/z 231, $t_R = 21.2$ min; 4-*n*-nonylphenol trifluoroacetate derivative (NP-TFA) m/z 203, $t_R = 25.6$ min; bisphenol-A trifluoroacetate derivative (BPA-TFA) m/z 405, $t_R = 27.2$ min.

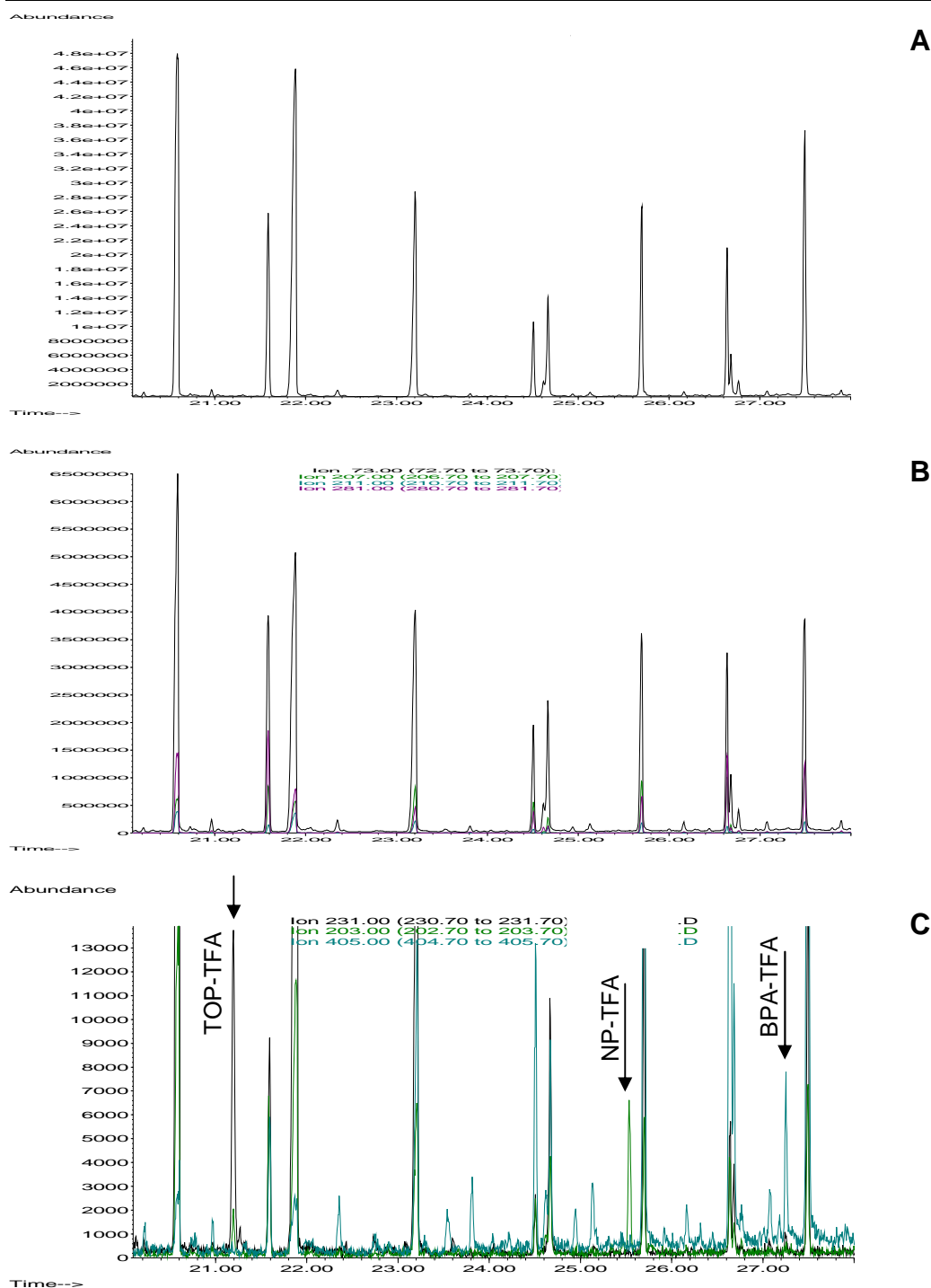


Figure 6.39 (A) Total ion chromatogram of the TFAA reagent blank on PDMS MCT M1.

5 μ l trifluoroacetic acid anhydride placed on trap for 10 min, followed by thermal desorption.

Figure 6.39 (B) Extracted ion chromatogram of PDMS degradation peaks m/z 73, 207, 211 and 281.

Figure 6.39 (C) Extracted ion chromatogram of the base peak ions used for quantitation. *Tert*-octylphenol trifluoroacetate derivative (TOP-TFA) m/z 231, $t_R = 21.2$ min; 4-*n*-nonylphenol trifluoroacetate derivative (NP-TFA) m/z 203, $t_R = 25.6$ min; bisphenol-A trifluoroacetate derivative (BPA-TFA) m/z 405, $t_R = 27.2$ min.

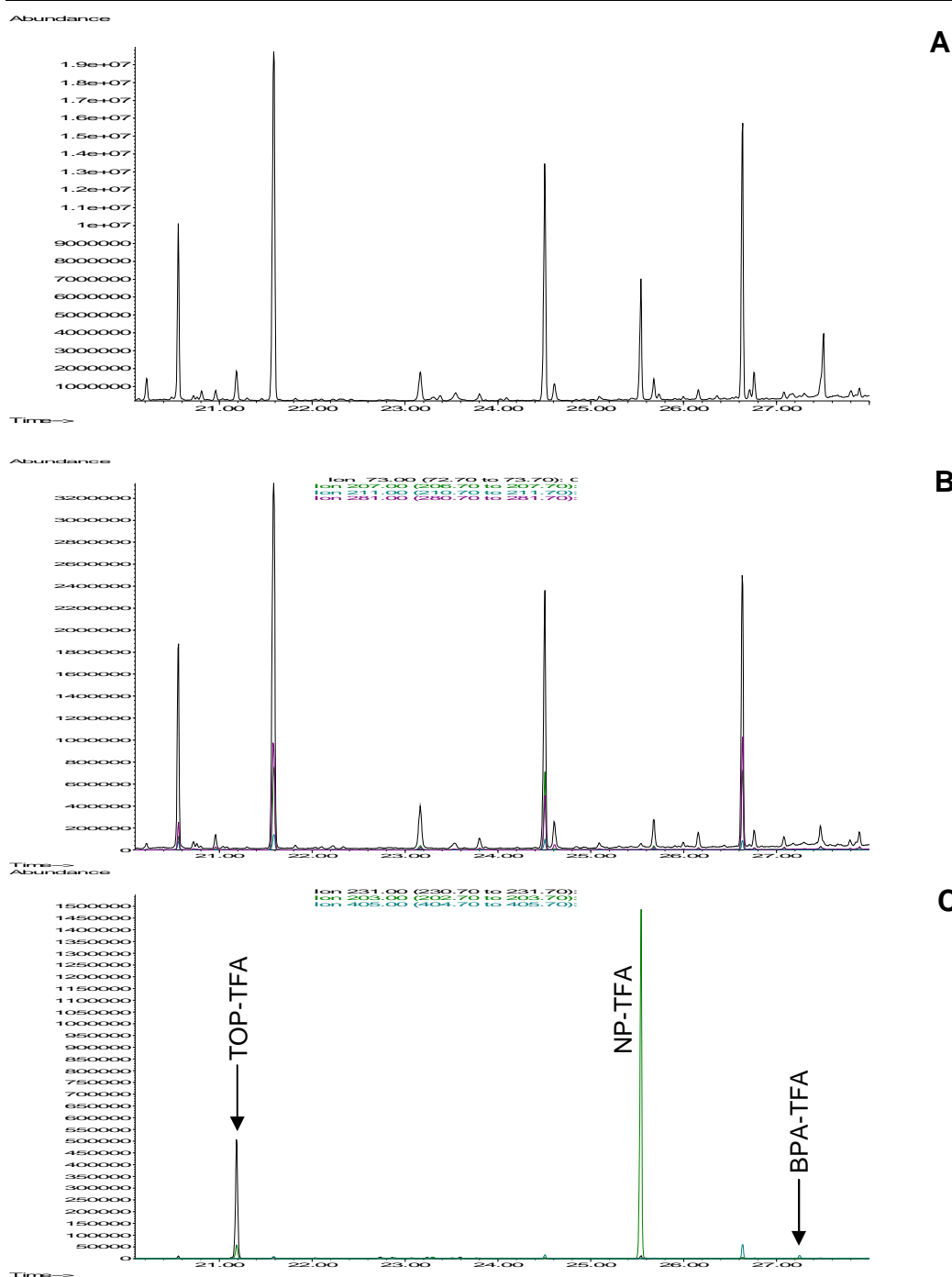


Figure 6.40 (A) Total ion chromatogram of the 20 ml Apies River water sample on PDMS MCT M2.

Sample extracted at a flow rate of 50 $\mu\text{l}/\text{min}$, dried and allowed to react with 5 μl trifluoroacetic acid anhydride for 10 min, followed by thermal desorption.

Figure 6.40 (B) Extracted ion chromatogram of PDMS degradation peaks m/z 73, 207, 211 and 281.

Figure 6.40 (C) Extracted ion chromatogram of the base peak ions used for quantitation. *Tert*-octylphenol trifluoroacetate derivative (TOP-TFA) m/z 231, $t_R = 21.2$ min; 4-*n*-nonylphenol trifluoroacetate derivative (NP-TFA) m/z 203, $t_R = 25.6$ min; bisphenol-A trifluoroacetate derivative (BPA-TFA) m/z 405, $t_R = 27.2$ min.

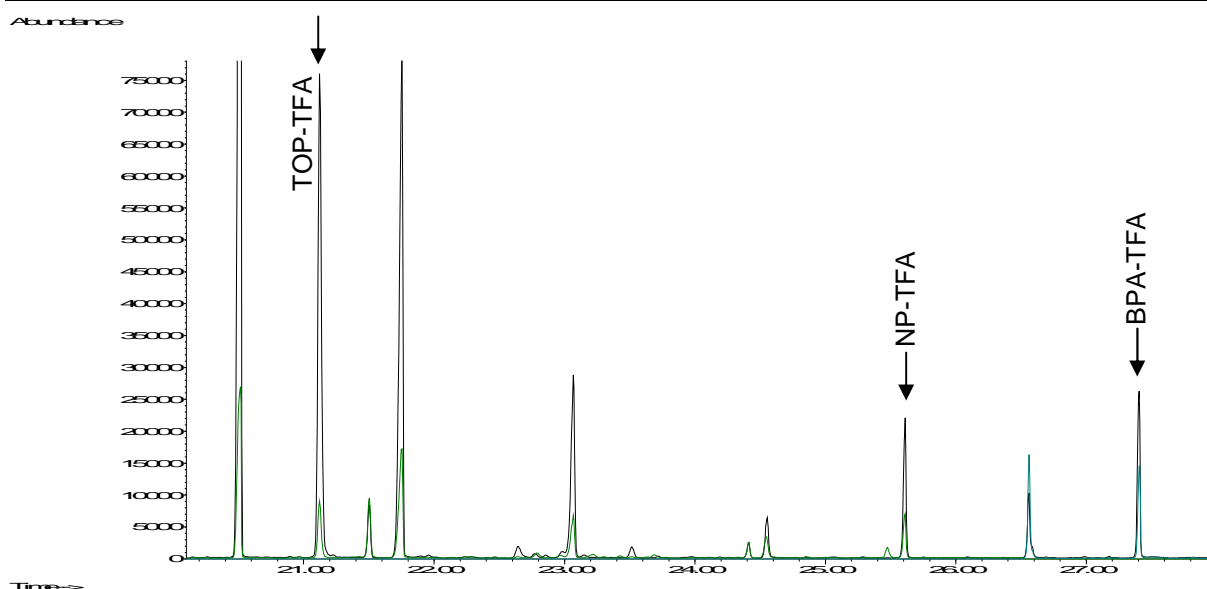


Figure 6.41 Selected Ion Mode (SIM) chromatogram of the TFAA reagent blank on PDMS MCT M3. Selected ions were m/z 231, 203, 245, 316, 405, 420. 5 μ l trifluoroacetic acid anhydride placed on trap for 10 min, followed by thermal desorption. *Tert*-octylphenol trifluoroacetate derivative (TOP-TFA) m/z 231, $t_R = 21.2$ min; 4-*n*-nonylphenol trifluoroacetate derivative (NP-TFA) m/z 203, $t_R = 25.6$ min; bisphenol-A trifluoroacetate derivative (BPA-TFA) m/z 405, $t_R = 27.2$ min.

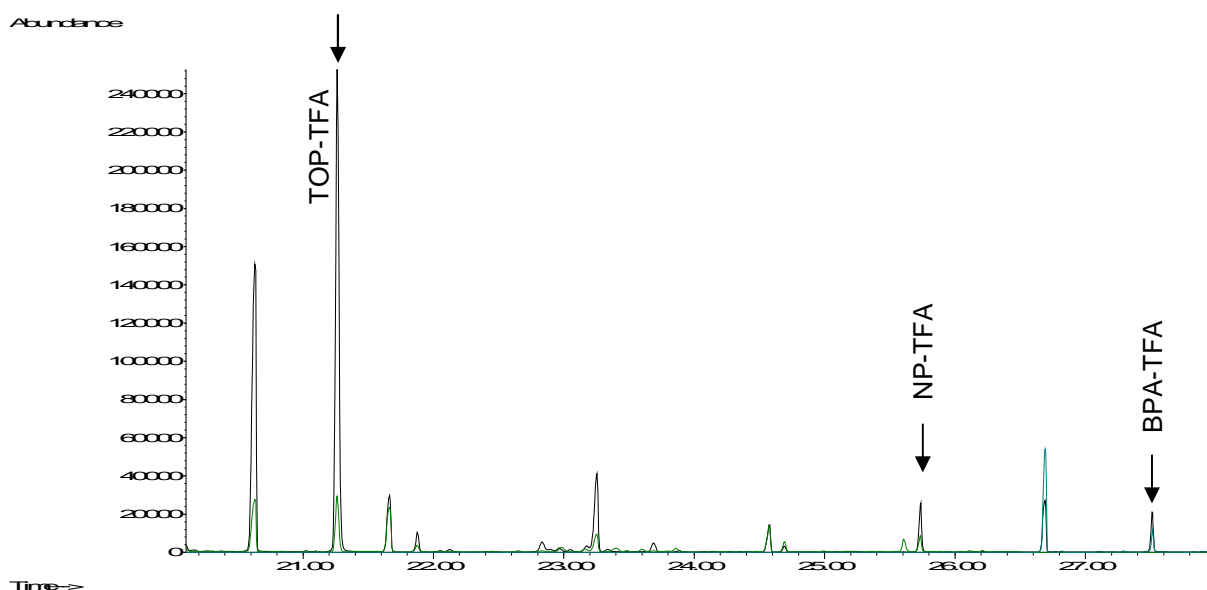


Figure 6.42 Selected Ion Mode (SIM) chromatogram of the 20 ml UP Sports Centre river water sample on PDMS MCT M3. Sample extracted at a flow rate of 50 μ l/min, dried and allowed to react with 5 μ l trifluoroacetic acid anhydride for 10 min, followed by thermal desorption. Selected ions were m/z 231, 203, 245, 316, 405, 420. *Tert*-octylphenol trifluoroacetate derivative (TOP-TFA) m/z 231, $t_R = 21.2$ min; 4-*n*-nonylphenol trifluoroacetate derivative (NP-TFA) m/z 203, $t_R = 25.6$ min; bisphenol-A trifluoroacetate derivative (BPA-TFA) m/z 405, $t_R = 27.2$ min.

6.11. Conclusion

The multichannel PDMS trap can be used to extract the moderately polar *tert*-octyl phenol and nonylphenol directly from water and can serve as a “one-pot” concentration, transport, derivatization and desorption vessel.

An extraction efficiency of over 70% is obtained for *tert*-octylphenol. However, extraction of nonylphenol and bisphenol-A is not as reproducible between different PDMS batches. A deviation from the expected partitioning of these lipophilic compounds, based on calculations using their octanol-water partitioning coefficients, is evident. Only ~40% nonylphenol and ~20% bisphenol-A partitions into the PDMS, while 99% partitioning is expected.

The *in situ* derivatization reaction, using only 5 μ l of trifluoroacetic acid anhydride, is convenient as it occurs at room temperature in the PDMS trap and is 100% complete within 10 minutes for *tert*-octylphenol and nonylphenol. Bisphenol-A demonstrates a modest reaction efficiency of approximately 37%, however, this appears to be constant over time.

Analyte carry-over from the thermal desorber presently prevents the achievement of further reduction in detection levels expected when moving from GC-EI-MS to GC-NCI-MS. Despite this, minimum detectable levels are similar to those achieved in the literature. The limit of quantitation (determined by the reagent blank) for this technique using GC-SIM-MS are 20, 11 and 54 ppt for *tert*-octylphenol, nonylphenol and bisphenol-A respectively.

The ability of the PDMS MCT to concentrate alkylphenols directly from water followed by *in situ* derivatization using TFAA, was demonstrated on real samples brought into the laboratory. Both *tert*-octylphenol and nonylphenol were detected in all samples at the low ppb level, while bisphenol-A fell below the level of quantitation. Once background levels are reduced, on-site sampling with the PDMS MCT would still need to be tested.

Chapter 7

Conclusions

Two approaches for concentrating analytes in PDMS were investigated in this study, namely, 1) the on-line concentration and *in-situ* derivatization of volatile polar analytes from air followed by resonance-enhanced multiphoton ionization time-of-flight mass spectrometric (REMPI-TOFMS) detection, and 2) the concentration of phenolic lipophilic analytes from water requiring derivatization prior to analysis by GC/MS. The study has demonstrated that the PDMS MCT is versatile and has the ability to concentrate volatile aldehydes and amines at the low ppb level from the gas phase, and alkylphenols at the low ppt level from the aqueous phase.

In this study we set out to (1) reduce the complexity and cost of the sampling system involved (2) reduce the experimental uncertainties/errors (3) lower the limit of detection.

7.1. *On-line analysis of volatile aldehydes and amines from air using PDMS traps*

This study is a novel investigation of on-line *in-situ* derivatization of volatile aldehydes and amines in silicone rubber traps in order to pre-concentrate and render them visible to a REMPI-TOFMS. Formaldehyde was detected for the first time in an on-line study by single photon ionization time-of-flight mass spectrometry (SPI-TOFMS).

Unlike most other pre-concentration devices used to determine aldehydes and amines, the silicone rubber trap is inert, rugged, simple and inexpensive.

In the study, recovery of the derivatives was achieved by thermal desorption which (1) reduced the time required for on-line analysis (2) removed the need for expensive, toxic solvents and (3) rendered the silicone trap immediately reusable. No thermal degradation products from the silicone rubber trap were detected with this technique. No deterioration in the performance of the traps was observed.

Permeation tubes were successfully prepared and calibrated to provide reliable aldehyde and amine gas standards in the ppm range. The thermal depolymerization of paraformaldehyde yielded a stable formaldehyde gas standard.

Phenylhydrazine and benzaldehyde were selected as the most suitable derivatizing reagents for the on-line study. Simultaneous introduction of the analyte and headspace vapour of the derivatization reagents into the silicone rubber was successfully achieved. This reduced sample preparation time and allowed for the rapid introduction of reagent and analyte into the system.

SPME was used to determine reaction efficiencies for the analytes, in a PDMS matrix, with the selected reagents. The results were satisfactory, especially considering that the reactions occurred at room temperature without the assistance of a catalyst. Formaldehyde yielded a low reaction/concentration efficiency of 41% with phenylhydrazine in PDMS, while acetaldehyde, acrolein and crotonal displayed improved values of 92%, 61% and 74% respectively. Both propylamine and butylamine yielded 28% reaction/concentration efficiency with benzaldehyde in the PDMS matrix.

The analytes were successfully converted in the on-line *in-situ* derivatization set-up. The derivatives were detected by the REMPI-TOFMS and identities confirmed by GC/MS. Analytes that were previously undetectable by REMPI-TOFMS could now be detected. Using this concept other compounds should now also be amenable to REMPI-TOFMS analysis.

Testing two different types of PDMS concentrators proved that larger PDMS volumes provide increased analyte capacity. Larger quantities of derivatives were concentrated on the combined OTT-PDMS MCT than on the open tubular PDMS trap alone. However, thermal desorption from the thermal modulator array, used to desorb the OTT, provided shorter desorption times than the enrichment desorption unit used to desorb the PDMS MCT.

Both PDMS concentration devices provided detection limits that were significantly lower than the permissible exposure limits (PELs) for the volatile aldehydes and amines investigated, set by the Occupational Safety and Health Administration (OSHA).

7.1.1. Further work

Further testing using a stable formaldehyde gas standard is recommended. Obtaining external calibration curves using permeation gas standards would then allow for quantification of real samples. Testing the method on-line in industrial factories or the office workplace would be required to emphasise the concentration ability of PDMS and the selectivity of the detection technique.

7.2. Determining endocrine disruptors from water by concentration and derivatization in PDMS traps

Trifluoroacetate derivatives of bisphenol-A, the alkylphenols: *tert*-octylphenol, 4-*n*-nonylphenol, and the estrogens: estrone, estriol and 17 β -estradiol were successfully formed in the PDMS MCT and detected by GC-(EI) MS. However, 17 α -ethinylestradiol, the crucial estrogen urgently requiring detection, could not be converted. In addition, to reach the mandatory ultra trace detection levels needed for estrogens, it would be better to convert them into their pentafluorobenzoyl derivatives and analyse these by GC- (NCI) MS. Although methods used to derivatize the estrogens with PFBCl alone were not successful, dual derivatization using PFBCl and TFAA showed promising results. Further investigation of these reactions is recommended.

The gravity sampling procedure for the analysis of water using the PDMS MCT was very simple. Water was allowed to run through the trap at a flow rate determined by the restrictor at the exit end of the trap. During this process the analytes partitioned into the trap. Thereafter the water was purged from the trap and derivatizing reagent was added to the trap using a syringe. The trap was capped and the reaction was allowed to occur at room temperature. The PDMS MCT was then thermally desorbed and analysed by GC- (EI) MS.

At room temperature and without the presence of a catalyst, the reaction of the alkylphenols with trifluoroacetic acid anhydride in the PDMS matrix was 100% complete after 5 minutes. Bisphenol-A reacted to less than 50% completion during this period, however, the amount of derivative formed remained constant.

Complete transfer of the formed derivatives off the PDMS MCT was achieved through optimization of thermal desorption and injection conditions.

Determination of the extraction efficiencies of the alkylphenols and bisphenol-A revealed a problem with the PDMS MCTs. Poor batch-to-batch repeatability in extraction efficiency indicated that the PDMS matrix is not homogenous. For two different PDMS batches: *tert*-octylphenol displayed extraction efficiencies of 70% and 79%, nonylphenol 84% and 43% and bisphenol-A 10% and 26% respectively. A t-test confirmed that the mean results obtained between batches for each analyte were significantly different.

Our study has revealed that although the PDMS MCT has potential as a pre-concentration device for aqueous samples using *in-situ* derivatization it has several limitations. Persistent carry-over problems inside the desorption unit restricted the limits of detection for the alkylphenols and bisphenol-A. In addition poor reproducibility between PDMS batches decreased the reliability of the extraction technique. The silicone proved inert and reusable only when all the water had been removed. Removal of water from the PDMS MCT was a time-consuming step.

7.2.1. Recommendations

Placing an excess of sample, reagent or analyte on the MCT for thermal desorption should be avoided as it leads to contamination of the desorption unit. Regardless of the presence of a permanent purge flow in the desorption unit, carry over does occur, causing memory effects and compromising detection limits.

Only derivatization reagents that produce neutral by-products should be used directly in the PDMS matrix. Examples would be diazomethane reagents, which release harmless nitrogen gas and phenylhydrazine or benzaldehyde that form water as a by-product. In all other cases, derivatization should be performed in the sample matrix, followed by extraction into the PDMS. The extraction step should also selectively exclude the absorption of excess reagent.

Unless working with 100 % pure PDMS, it cannot be assumed the PDMS matrix is inert and hydrophobic. It was observed in this study that the trifluoroacetic acid by-product forms hydronium ions (H_3O^+) in the presence of water retained by the fumed silica (SiO_2) filler in the PDMS. The hydronium ions catalysed the degradation of the PDMS matrix.

7.2.2. Further work

The possibility of manufacturing a pure PDMS matrix for further studies needs to be explored, particularly for extraction of analytes from aqueous matrices.

The extraction efficiencies for the analytes were not repeatable. The reason for this will need to be investigated further. The entire process for repeat extraction-derivatization-thermal desorption is lengthy. In addition, the EI MS source becomes contaminated with PDMS degradation product deposits and large quantities of liquid nitrogen are consumed in the process. A more cost-effective and efficient manner to investigate the analyte partitioning into the PDMS would be to use a syringe pump and UV detector setup as applied by Ortner [63].

Extraction efficiency tests should also be conducted on new and used traps as it is suspected that *damage to the traps caused by H_3O^+ ions may contribute to differences in partitioning between new and old traps*. The setup as applied by Ortner [63], can also be used to determine the optimum sampling flow rate for the analytes through the MCT. A sampling flow rate of 50 $\mu\text{l}/\text{min}$ was used in our study. This selection was based on results obtained by Ortner [63] where benzene in water yielded 11 plates on a 32 MCT at a flow rate of 75 $\mu\text{l}/\text{min}$.

Since it remains desirable to use the MCT for on-site concentration followed by derivatization, the use of derivatization reagents, yielding neutral by products, such as the fluoroacylimidazoles instead of the acyl acid anhydrides should be investigated. The reaction may not proceed to completion as rapidly as for the acid anhydrides, but the by-product is the relatively inert imidazole. Thus the need to remove every last bit of water vapour may be reduced and sample preparation further simplified.

From the theory discussed in chapter 2, it appears that the PDMS MCT has potential as a concentrating device, due to its open tubular nature and very large analyte capacity. Provided the above limitations are resolved the trap could be tested in the field.

It would also be interesting to examine the extraction and derivatization of ultra trace-level analytes, for example the estrogens, using electron-capturing derivatives analysed by GC-NCI-MS, GC-ECD and even GCxGC-ECD or GCxGC-TOFMS to obtain improved detection levels and simplicity in sample preparation.

REFERENCES

1. PETROVIC, M., Eljarret, E., Lopez de Alda, M.J., Barcelo, D., 2002. REVIEW: Recent advances in the mass spectrometric analysis related to endocrine disrupting compounds in aquatic environmental samples. *J.Chromatogr. A*, 974, 23-51.
2. LOPEZ de ALDA, M.J., Barcelo, D., 2001. Review of analytical methods for the determination of estrogens and progestogens in waste water. *Fresenius J. Anal. Chem.*, 371, 437-447.
3. SILVIA DIAZ-CRUZ, M., Lopez de Alda, M.J., Lopez, R., Barcelo, D., 2003. Determination of estrogens and progestogens by mass spectrometric techniques (GC/MS, LC/MS and LC/MS/MS). *J. Mass Spectrom.*, 38, 917-923.
4. VIDAEFF, A.C., Sever, L.E., 2005. REVIEW: In utero exposure to environmental estrogens and male reproductive health: a systematic review of biological and epidemiologic evidence. *Reproductive Toxicology*, 20, 5-20.
5. GWRC: Global Water Research Coalition, London, U.K., Sept. 2003. Endocrine Disrupting Compounds - Priority list of EDCs. <http://www.globalwaterresearchcoalition.net>. Access 5 April 2006.
6. CADBURY, D., 1997. The feminization of nature - our future at risk, *Penguin books*, London, England. ISBN 0-14-026205-9.
7. ET AL, Schenectady International, 2 April 2003. Alkylphenols Category - Section 1: Development of categories and test plans / Chemical right-to-know initiative HPV challenge program. <http://www.epa.gov/hpv/pubs/summaries/alkylphn/c13007rt.pdf>. Access 5 Oct 2007.
8. COUSINS, I.T., Staples, C.A., Klečka, G.M., Mackay, D., 2002. A Multimedia Assessment of the Environmental Fate of Bisphenol A. *Human and Ecological Risk Assessment*, 8, 1107-1135.
9. PORTER, A.J., Hayden, N. J., Nonylphenol in the Environment: A Critical Review, Department of Civil and Environmental Engineering University of Vermont Burlington, VT 05405.
10. de VOOGT, P., de Beer, K., van der Wielen, F., 1997. Determination of alkylphenol ethoxylates in industrial and environmental samples. *Trends in analytical chemistry*, 16, 584-595.
11. VOM SAAL, F., 16 February 2007. Oral presentation, American Association for the Advancement of Science (AAAS), San Francisco, California, U.S.A.
12. CORNWELL, T., Cohick, W., Raskin, I., 2004. REVIEW: Dietary phytoestrogens and health. *Phytochemistry*, 65, 995-1016.
13. HENLEY, D.V., Lipson, N., Korach, K.S., Bloch, C.A., 2007. Prepubertal Gynecomastia linked to lavender and tea tree oils. *N. Engl. J. Med.*, 356, 479-485.
14. Et Al, Chemical, Toxicity, Safety and Environmental Analysis Information for Formaldehyde, <http://www.instantref.com/formald.htm>, access: 27 Aug 1999.
15. OSHA, Occupational Safety and Health Administration U.S. Department of Labor, OSHA Regulations - Formaldehyde. 1910.1048. <http://www.osha-slc.gov>, access: 2 Feb 2004.

16. NIOSH Manual of Analytical Methods, Method 2016, 1998. Formaldehyde by HPLC-UV. 4th Edition.
17. CRUMP, D.R. in Volatile Organic Compounds in the Atmosphere, editors Hester, R.E., Harrison, R.M., 1995. Volatile organic Compounds in Indoor air. *Issues in Environmental Science and Technology*, The Royal Society of Chemistry, U.K, 4, 109-124.
18. Occupational Safety and Health Administration U.S. Department of Labor, OSHA Fact Sheets - 01/01/1995 - Occupational Exposure to formaldehyde. <http://www.osha-slc.gov>, access: 2 Feb 2004.
19. McNAUGHT, A.D., Wilkinson, A., 1997. *Compendium of chemical terminology IUPAC recommendations*, 2nd edition, Blackwell Science Ltd. Oxford. ISBN 0865426848.
20. WILLOUGHBY, R., Sheenan, E., Mitrovich, S., 1998. *A global view of LC/MS - how to solve your most challenging analytical problems*, First Edition, Global view publishing, Pittsburgh, Pennsylvania. ISBN 09660813-0-7.
21. INGERSLEV, F., Halling-Sørensen, B., APS Danish Environmental Protection Agency, 2003. "Evaluation of Analytical Chemical Methods for Detection of Estrogens in the Environment Working Report No. 44, 2003"
22. OOSTERKAMP, A.J., Hock, B., Seifert, M., Irth, H., 1997. Novel Monitoring strategies for xenoestrogens. *Trends in analytical chemistry*, 16, 544.
23. RICHARDSON, S.D., 2004. Environmental Mass Spectrometry: Emerging Contaminants and Current Issues. *Anal. Chem.*, 76, 3337-3364.
24. KUSTER, M., Lopez de Alda, M.J., Barcelo, D., 2004. Analysis and distribution of estrogens and progestogens in sewage sludge, soils and sediments. *Trends in analytical chemistry*, 23, 790.
25. SHIMADA, K., Mitamura, K., Higashi, T., 2001. Gas chromatography and high-performance liquid chromatography of natural steroids. *J. Chromatogr. A*, 935, 141-172.
26. SCHNEIDER, C., Schöler, H.F., Schneider, R.J., 2005. Direct sub-ppt detection of the endocrine disruptor ethinylestradiol in water with a chemiluminescence enzyme-linked immunosorbent assay. *Anal. Chim. Acta*, 551, 92-97.
27. LI, Z., Wang, S., Lee, N.A., Allan, R.D., Kennedy, I.R., 2004. Development of a solid-phase extraction—enzyme-linked immunosorbent assay method for the determination of estrone in water. *J. Chromatogr. A*, 503, 171-177.
28. GOMES, R.L.; Avcioglu, E.; Scrimshaw, M.D.; Lester, J.N., 2004. Steroid estrogen determination in sediment and sewage sludge: a critique of sample preparation and chromatographic/mass spectrometry considerations, incorporating a case study in method development. *Trends in analytical chemistry*, 23, 737-744.
29. SANTOS, F.J., Galceran, M.T., 2003. Review: Modern developments in gas chromatography—mass spectrometry based environmental analysis. *J. Chromatogr. A*, 1000(27), 125-151.

30. NAKAMURA, S., Sian, T.H., Daishima, S., 2001. Determination of estrogens in river water by gas chromatography– negative-ion chemical-ionization mass spectrometry. *J.Chromatogr. A*, 919, 275-282.
31. BOESL, U., Heger, HJ., Zimmermann, R., Nagel, H., Püffel, P., 2000. Laser Mass Spectrometry in Trace Analysis, *Encyclopedia of Analytical Chemistry*, R.A. Meyers (Ed.), John Wiley & Sons Ltd, Chichester, 2087-2118.
32. MÜHLBERGER, F.; Zimmermann, R.; Kettrup, A., 2001. A mobile mass spectrometer for comprehensive on-line analysis of trace and bulk components of complex gas mixtures. *Anal. Chem.*, 73, 3590-3604.
33. HEGER, H. J.; Zimmermann, R.; Dorfner, R.; Beckmann, M.; Griebel, H.; Kettrup, A.; Boesl, U., 1999. On-Line Emission Analysis of Polycyclic Aromatic Hydrocarbons down to pptv Concentration Levels in the Flue Gas of an Incineration Pilot Plant with a Mobile Resonance-Enhanced Multiphoton Ionization Time-of-Flight Mass Spectrometer. *Anal. Chem.*, 71, 46-57.
34. DORFNER, R.; Ferge, T.; Yeretian, C.; Kettrup, A.; Zimmermann, R., 2004. Laser Mass Spectrometry as On-Line Sensor for Industrial Process Analysis: Process Control of Coffee Roasting. *Anal. Chem.*, 76 (5), 1386-1402.
35. DORFNER, R.; Ferge, T.; Kettrup, A.; Zimmermann, R.; Yeretian, C., 2003. *J. Agric.Food Chem.*, 51 (19), 5768-5773.
36. ZIMMERMANN, R.; Heger, H. J.; Kettrup, A., 1999. On-line Monitoring of Traces of Aromatic-, Phenolic- and Chlorinated Components in the Flue Gases of Industrial Incinerators, Mineral Oil Headspace and Cigarette Smoke by Direct-Inlet Laser Ionization-Mass Spectrometry (REMPI-TOFMS). *Fresenius' J. Anal. Chem.*, 363, 720-730.
37. HAULER, T. E.; Boesl, U.; Kaesdorf, S.; Zimmermann, R., 2004. Mobile resonance enhanced multiphoton ionisation–time-of-flight mass spectrometer with a novel hybrid laser desorption/molecular beam ion source for rapid detection of aromatic trace compounds from gas phase and solid samples. *J. Chromatogr. A*, 1058, 39-49.
38. OTSON, R., Fellin, P., 1988. Determination of airborne aldehydes - literature Review. *Science of the Total Environment*, 77, 95.
39. KENNEDY, E.R., Teass, A.W., Gagnon, Y.T. in Formaldehyde - Analytical chemistry and toxicology, Editor Turoski, V., 1985. Industrial Hygiene Sampling and analytical methods for formaldehyde - Past and present. *Advances in chemistry and toxicology series*, 210, 1-11.
40. BEREZKIN, V. G.; Drugov, Y. S., 1991. Gas chromatography in air pollution analysis. *J. Chromatogr. Libr.*, 49, 190-194.
41. MUNSON, B., 1977. Chemical Ionization Mass Spectrometry. *Anal. Chem.*, 49, 772-778A.
42. LUBMAN, D. M., Ed., 1990. Lasers and Mass Spectrometry; Oxford University Press: New York, ISBN 0195059298.
43. COOL, T. A.; Williams, B. A., 1992. Ultrasensitive Detection of Chlorinated Hydrocarbons by Resonance Ionization. *Combust. Sci. Technol.*, 82, 67.

44. BOESL, U.; Zimmermann, R.; Weickhardt, C.; Lenoir, D.; Schramm, K.-W.; Kettrup, A.; Schlag, E.W., 1994. Resonance Enhanced Laser Ionisation as a Compound-Selective Ion Source for Mass Spectrometry: Technique and Experimental Setup, *Chemosphere*, 29, 1429-1440.
45. MILLER, J. C.; Compton, R. N., Cooper, C.D., 1982. Vacuum Ultraviolet Spectroscopy of Molecules Using Third-Harmonic Generation in Rare Gases. *J. Chem. Phys.*, 76 (8), 3967.
46. NOMAYO, M.; Thanner, R.; Pokorny, H.; Grotheer, H.-H.; Stütze, R., 2001. Measurements in the raw gas of a full scale municipal waste incinerator using a wavelength resolved REMPI mass spectrometer. *Chemosphere*, 43, 461-467.
47. BALTUSSEN, H.A., 2000. New Concepts in Sorption Based Sample Preparation for Chromatography. D.Phil. Thesis, Technical University Eindhoven, Eindhoven.
48. BEREZKIN, V.G., Drugov, Y.S, 1991. Gas chromatography in air pollution analysis. *Journal of Chromatography Library* -Elsevier, Germany, 49, 35-119.
49. PAWLISZYN, J., 1997. Solid Phase Microextraction - Theory and Practice. Wiley-VCH, Canada, ISBN 0471190349.
50. BASHEER, C., Parthiban, A., Jayaraman, A., Kee Lee, H., Valiyaveetil, S., 2005. Determination of alkylphenols and bisphenol-A. A comparative investigation of functional polymer-coated membrane microextraction and solid-phase microextraction techniques. *J.Chromatogr. A*, 1087, 274-282.
51. KAWAGUCHI, M., Sakui, N., Okanouchi, N., Ito, R., Saito, K., Izumi, SI., Makino, T., Nakazawa, H., 2005. Stir bar sorptive extraction with in situ derivatization and thermal desorption-gas chromatography-mass spectrometry for measurement of phenolic xenoestrogens in human urine samples. *J.Chromatogr. B.*, 820, 49-57.
52. CHANG, CM., Chou, CC., Lee, MR., 2005. Determining leaching of bisphenol A from plastic containers by solid-phase microextraction and gas chromatography-mass spectrometry. *Anal. Chim. Acta*, 539, 41-47.
53. LATORREA, A., Lacorteb, S., Barceló, D., Monturya, M., 2005. Determination of nonylphenol and octylphenol in paper by microwave-assisted extraction coupled to headspace solid-phase microextraction and gas chromatography-mass spectrometry. *J.Chromatogr. A*, 1065, 251-256.
54. NAKAMURA, S., Daishima, S., 2004. Simultaneous determination of alkylphenols and bisphenol A in river water by stir bar sorptive extraction with in situ acetylation and thermal desorption-gas chromatography-mass spectrometry. *J.Chromatogr. A*, 1038, 291-294.
55. KAWAGUCHIA, M., Sakuia, N., Okanouchi, N., Ito, R., Saito, K., Nakazawa, H., 2005. Stir bar sorptive extraction and trace analysis of alkylphenols in water samples by thermal desorption with in tube silylation and gas chromatography-mass spectrometry. *J.Chromatogr. A*, 1062, 23-29.
56. KAWAGUCHI, M.; Inoue, K.; Yoshimura, M.; Sakui, N.; Ito, R.; Izumi, S-I.; Makino, T.; Okanouchi, N.; Nakazawa, H., 2004. Stir bar sorptive extraction and thermal desorption-gas chromatography-mass spectrometry for the measurement of 4-nonylphenol and 4-tert-octylphenol in human biological samples. *J.Chromatogr. B.*, 799, 119-125.

57. BROWN, L., du Preez, J.L., Meintjies, E., 1997. The qualitative and quantitative evaluation of estrogen and estrogen-mimicking substances in the South African water environment: a 1996-1997 perspective. *Report on WRC project*.
58. PETROVICÈ, M., Eljarrat, E., Lopez de Alda, M.J., Barcelo, D., 2001. Analysis and environmental levels of endocrine disrupting compounds in freshwater sediments. *Trends in analytical chemistry*, 20, 637.
59. PAWLISZYN, J., 2006. Why move analysis from laboratory to on-site? *Trends in analytical chemistry*, 25, 633-634.
60. MARTOS, P.A., Pawliszyn, J., 1998. Sampling and determination of formaldehyde using solid phase microextraction with on-fibre derivitization. *Anal. Chem.*, 70, 2311-2320.
61. FERNANDES, M.J., 2001. Concentration and derivatisation in silicone rubber traps for gas chromatographic trace analysis of aldehydes. *MSc thesis*, University of Pretoria, Pretoria, South Africa.
62. LERCH, O., Zinn, P., 2003. Derivatisation and Gas chromatography-chemical ionisation mass spectrometry of selected synthetic and natural endocrine disruptive chemicals. *J. Chromatogr. A*, 991, 77-97.
63. ORTNER, E.K., 1999. Analysis of aqueous samples with the multichannel silicone rubber trap and capillary gas chromatography. *D.Phil. Thesis*, University of Pretoria, Pretoria, South Africa.
64. ORTNER, E.K., 1994. Alternative concentration techniques for the trace analysis of semi-volatile organic air pollutants by capillary gas chromatography. *MSc thesis*, University of Pretoria, Pretoria, South Africa.
65. ORTNER, E.K., Rohwer, E.R., 1996. Trace analysis of semi-volatile organic air pollutants using thick film silicone rubber traps with capillary gas chromatography. *J. High Resolut. Chromatogr.*, 19, 339-344.
66. ORTNER, E.K., Rohwer, E.R., 1999. Trapping efficiency of aqueous pollutants using multichannel thick film silicone rubber traps with capillary gas chromatography. *J. Chromatogr. A*, 863, 57-68.
67. ORTNER, E.K.; Rohwer, E.R., 1999. Trace determination of organic compounds in water by direct enrichment in multichannel thick film silicone rubber traps with capillary gas chromatography. *J. High Resolut. Chromatogr.*, 22 (9), 521-526.
68. HASSET, A.J.; Rohwer, E.R., 1999. Analysis of odorous compounds in water by isolation by closed-loop stripping with a multichannel silicone rubber trap followed by GC-MS. *J. Chromatogr. A*, 849, 521-528.
69. HARPER, M., 2000. Review: Sorbent trapping of volatile organic compounds from air. *J. Chromatogr. A*, 885, 129-151.
70. NAMIESNIK, J., 1988. Preconcentration of gaseous organic pollutants in the atmosphere. *Talanta*, 35, 567-587.

71. GRIMALT, J.O., Flesca, N.G., Castellnou, A., 1997. Refridgerated multibed adsorption in sampling and analysis of atmospheric light hydrocarbons at ppb(v/v) and sub ppb(v/v) concentrations. *J.Chromatogr. A.*, 778, 269-277.
72. MASTROGIACOMO, A.R., Pierini, E., Sampaulo, L., 1995. A comparison of the critical parameters of some adsorbents employed in trapping and thermal desorption of organic pollutants. *Chromatographia*, 41(11), 599-604.
73. ET AL, 1999. SUPELCO Product catalogue, http://www.sigmaaldrich.com/Brands/Supelco_Home.html.
74. HUCK, C.W., Bonn, G.K., 2000. Review: Recent developments in polymer - based sorbents for solid phase extraction. *J.Chromatogr. A.*, 885, 51-72.
75. SCHMIED, W., Przewosnik, M., Bachmann, K., 1989. Determination of traces of aldehydes and ketones in the troposphere via solid phase derivatisation with DNSH. *Fresenius J. Anal. Chem.*, 335, 464-468.
76. LEMPUHL, D.W., Birks, J.W., 1996. New gas chromatographic-electron-capture detection method for the determination of atmospheric aldehydes and ketones based on cartridge sampling and derivatisation with 2,4,6-trichlorophenylhydrazine. *J.Chromatogr. A.*, 740A, 71-81.
77. LAHANIATI, M., Calogirou, A., Duane, M., Larsen, B., Kotzias, D., 1998. Identification of biogenic carbonyls in air with O-(2,3,4,5,6-pentafluorobenzyl)hydroxylamine hydrochloride (PFBHA) coated C18-silica gel cartridges. *Fresenius. Environ. Bull.*, 7, 302-307.
78. STASHENKO, E.E., Ferreira, M.C., Sequeda, L.G., Martinez, J.R.; Wong, J.W., 1997. Comparison of extraction methods and detection systems in the gas chromatographic analysis of volatile carbonyl compounds. *J.Chromatogr. A*, 779, 360-369.
79. DUNEMANN, L., Begerow, J., Bucholski, A. Executive editor Gerhartz W., 1988. Sample preparation for trace analysis *Ullmann's Encyclopedia of Industrial Chemistry*. VCH, vol B5, 84-89.
80. STILES, R., Yang, I., Lippincott, R.L., Murphy, E., Buckley, B., 2007. Identifying Potential Sources of Background Contaminants Resulting From Solid Phase Extraction and Solid Phase Microextraction. *J.Sep.Sci*, 30, 1029-1036.
81. POOLE, C.F., Poole, S.K., 1991. *Chromatography Today*, 5th Edition, Elsevier, Amsterdam, The Netherlands, 735-840. ISBN 0444891617.
82. BALTUSSEN, E., David, F., Sandra, P., Janssen, H.G., Cramers, C.A., 1997. A new method for sorptive enrichment of gaseous samples: Application in air analysis and natural gas characterization. *J. High Resolut. Chromatogr.*, 20(7), 385-393.
83. BALTUSSEN, E., David, F., Sandra, P., Janssen, H.G., Cramers, C.A., 1998. Capillary GC determination of amines in aqueous samples using sorptive preconcentration on polydimethylsiloxane and polyacrylate phases. *J. High Resolut. Chromatogr.*, 21, 645-648.
84. BURGER, B.V., le Roux, M., 1992. Headspace gas analysis: Comparison of the efficiency of thick film, ultra thick film, and activated charcoal Open tubular capillary traps for the

- concentration of volatile, airborne, organic compounds. *J. High Resolut. Chromatogr.*, 15 (6), 373-376.
85. BLOMBERG, S., Roeraade, J., 1987. Preparative capillary gas chromatography II. Fraction collection on traps coated with a very thick film of immobilized stationary phase. *J. Chromatogr. A.*, 394, 443-453.
86. BLOMBERG, S., Roeraade, J., 1988. A technique for coating capillary columns with a very thick film cross-linked stationary phase. *J. High Resolut. Chromatogr.*, 11(6), 457-461.
87. BURGER, B.V., le Roux, M., Burger, W.J.G., 1990. Headspace analysis: A novel method for the production of capillary traps with ultra-thick stationary phase layers. *J. High Resolut. Chromatogr.*, 13(11), 777-779.
88. BALTUSSEN, E., David, F., Sandra, P., Janssen, H.G., Cramers, C.A., 1998. Sorption Tubes packed with polydimethylsiloxane: A new and promising technique for the preconcentration of volatiles and semi-volatiles from air and gaseous samples. *J. High Resolut. Chromatogr.*, 21(6), 332-340.
89. BALTUSSEN, E., David, F., Sandra, P., Janssen, H.G., Cramers, C.A., 1998. Retention model for sorptive extraction-thermal desorption of aqueous samples: application to the automated analysis of pesticides and polyaromatic hydrocarbons in water samples. *J. Chromatogr. A.*, 805, 237-247.
90. BALTUSSEN, E., den Boer, A., Sandra, P., Janssen, H.G., Cramers, C.A., 1999. Monitoring of nicotine in air using sorptive enrichment on polydimethylsiloxane and TD-CGC-NPD. *Chromatographia*, 49, 520-524.
91. MOL, H.G.J., Janssen, H.G., Cramers, C.A., 1993. Use of open tubular trapping columns for on-line extraction-capillary gas chromatography of aqueous samples. *J. High Resolut. Chromatogr.*, 16, 413-418.
92. WELSCH, T., Teichmann, U., 1991. The Thermal immobilization of hydroxy-terminated Silicone phases in high-temperature-Silylated glass capillaries. A study of reaction mechanisms. *J. High Resolut. Chromatogr.*, 14(3), 153-159.
93. LORD, H., Pawliszyn, J., 2000. Review: Evolution of Solid Phase Microextraction technology. *J. Chromatogr. A*, 885, 153-193.
94. COLAS, A., Curtis, J., (DOW CORNING), 2005. Silicone Biomaterials: History and Chemistry & Medical applications of silicones, Reprinted from Biomaterials Science - An introduction to materials in medicine, 2nd Edition, Elsevier.
95. BALTUSSEN, E., Sandra, P., David, F., Cramers, C., 1999. Stir Bar Sorptive Extraction (SBSE), a novel extraction technique for aqueous samples: Theory and Principles. *J. Microcolumn Separations*, 11, 737-747.
96. LOVKVIST, P., Jonsson, J.A., 1987. Capacity of sampling and preconcentration columns with a low number of theoretical plates. *Anal. Chem.*, 59(3), 818-821.
97. GROB, K., Habich, A., 1985. Headspace gas analysis: the role and design of concentration traps specifically suitable for capillary GC. *J. Chromatogr. A*, 321, 45-58.

98. BURGER, B.V., Munroe, Z., 1986. Headspace gas analysis: Quantitative trapping and thermal desorption of volatiles using fused silica open tubular capillary traps. *J.Chromatogr. A*, 370, 449-464.
99. BURGER, B.V., le Roux, M., Munroe, Z.M., Wilken, M.E., 1991. Production and use of capillary traps for headspace gas chromatography of airborne volatile organic compounds. *J.Chromatogr. A*, 552, 137-151.
100. EISERT, R., Pawliszyn, J., 1997. Automated In-Tube Solid-Phase Microextraction Coupled to High-Performance Liquid Chromatography. *Anal. Chem.*, 69, 3140-3147.
101. MITANI, K., Kataoka, H., 2004. Online Concentration by In-Tube Solid Phase Microextraction and Its Application to Food Analysis. *Foods Food Ingredients J. Jpn.*, 209.
102. NARDI, L., 2002. Coupled in-tube SPME-HRGC: A complementary SPME technique to analyze aqueous samples by GC. *American Laboratory*, 30-37.
103. WU, J., Tragas, C., Lord, H., Pawliszyn, J., 2002. Analysis of polar pesticides in water and wine samples by automated in-tube solid-phase microextraction coupled with high-performance liquid chromatography-mass spectrometry. *J.Chromatogr. A*, 976, 357-367.
104. FERNANDES-WHALEY, M., Mühlberger, F., Whaley, A., Adam, T., Zimmermann, R., Rohwer, E., Walte, A., 2005. On-Line Derivatization for Resonance-Enhanced Multiphoton Ionization Time-of-Flight Mass Spectrometry: Detection of Aliphatic Aldehydes and Amines via Reactive Coupling of Aromatic Photo Ionization Labels. *Anal. Chem.*, 77, 1-10.
105. ET AL, 1998. Supelco Bulletin 923 - Solid Phase Microextraction: Theory and Optimization of Conditions Sigma-Aldrich Co, 1-8.
106. MARSEL, J., Velikonja Bolta, S., Zupancic Kralji, L., 1998. Gas chromatographic determination of formaldehyde in air using SPME sampling. *Chromatographia*, 48, 95-99.
107. STASHENKO, E.E.; Martinez, J.R., 2004. Derivatization and solid-phase microextraction. *Trends in analytical chemistry*, 23, 553-561.
108. TIENPONT, B., David, F., Bicchi, C., Sandra, P., 2000. Headspace Sorptive extraction, Riva Del Garda Chromatography Conference Poster, 1-11.
109. BICCHI, C., Corderoa, C., Libertoa, E., Rubioloa, P., Sgorbinia, B., Sandra, P., 2005. Impact of phase ratio, polydimethylsiloxane volume and size, and sampling temperature and time on headspace sorptive extraction recovery of some volatile compounds in the essential oil field. *J.Chromatogr. A*, 1071, 111-118.
110. BURGER, B.V., Marx, B., le Roux, M., Burger, W.J.G., 2006. Simplified analysis of organic compounds in headspace and aqueous samples by high-capacity sample enrichment probe. *J.Chromatogr. A*, 1121, 259-267.
111. SANDRA, P., Baltussen, E., David, F., Hoffmann, A., 2000. A novel extraction technique for aqueous samples: Stir bar sorptive extraction, *Gerstel Application Note 1*, www.gerstel.de/application.htm.

112. TIENPONT, B.; David, F.; Desmet, K.; Sandra, P., 2002. Stir bar sorptive extraction-thermal desorption-capillary GC-MS applied to biological fluids. *Anal. Bioanal. Chem.*, 373, 46-55.
113. BICCHI, C., Cordero, C., Rubiolo, P., Sandra, P., 2003. SBSE in food matrices. *European Food Research and Technology*, 216, 449.
114. BALTUSSEN, E., Cramers, C.A., Sandra, P.J.F., 2002. Sorptive sample preparation - a review. *Anal. Bioanal. Chem.*, 373, 3-22.
115. RAYMOND, A., Guiochon, G., 1975. The use of graphitized carbon black as a trapping material for organic compounds in light gases before a GC-analysis. *J. Chromatogr. Sci*, 13, 173-177.
116. POOLE, C.F., Schuette, S.A., 1983. Isolation and concentration techniques for Capillary column GC analysis. *J. High Resolut. Chromatogr*, 6 (10), 526-549.
117. FLUKA, 2002. "Derivatization reagents ANALYTIX Advances in Analytical Chemistry", Sigma-Aldrich Co. <http://www.sigmaaldrich.com>.
118. ROSENFELD, J.M., 2003. Derivatization in the current practice of analytical chemistry. *Trends in analytical chemistry*, 22, 785-798.
119. SUPELCO, 1997. Guide to Derivatization Reagents for GC. *Bulletin 909A*, Sigma-Aldrich Co. <http://www.sigmaaldrich.com>.
120. MARTINEZ, D., Borrull, F., Calull, M., Ruana, J., Colom, A., 1998. Application of solid phase extraction membrane discs in the determination of haloacetic acids in water by gas chromatography-mass spectrometry. *Chromatographia*, 48, 811-816.
121. KATAOKA, H., 1996. REVIEW: Derivatization reactions for the determination of amines by gas chromatography and their applications in environmental analysis. *J.Chromatogr. A*, 733, 19-34.
122. SEGURA, J., Ventura, R., Jurado, C., 1998. REVIEW: Derivatization procedures for gas chromatographic - mass spectrometric determination of xenobiotics in biological samples, with special attention to drugs of abuse and doping agents. *J.Chromatogr. B*, 713, 61-90.
123. XIE, Y., 2001. Technical note: Analyzing haloacetic acids using gas chromatography/mass spectrometry. *Wat. Res.*, 35, 1599-1602.
124. SARRION, M.N., Santos, F.J., Galceran, M.T., 1999. Solid phase microextraction coupled with gas chromatography-ion trap mass spectrometry for the analysis of haloacetic acids in water. *J.Chromatogr. A*, 859, 159-171.
125. NIKOLAOU, A.D., Golfopoulos, S.K., Kostopoulou, M.N., Lekkas, T.D., 2002. Technical note: Determination of haloacetic acids in water by acidic methanol esterification-GC-ECD method. *Wat. Res.*, 36, 1089-1094.
126. PIERCE®, 1998. Acylation Derivatization Reagents, Pierce Chemical Company. www.piercenet.com.

127. LITTLE, J.L., 1999. Artifacts in Trimethylsilyl Derivatization Reactions and Ways to Avoid Them. *J.Chromatogr. A*, 844, 1-22.
128. SCHLITT, H., 1997. Impinger sampling coupled to HPLC by a modified autoinjector interface. *J.Chromatogr. A*, 762, 187-192.
129. RUTTEN, G.A., Burtner, C.W.J., Rijks, J.A., Visser, H., 1988. The determination of aldehydes in exhaust gases of LPG fuelled engines. *Chromatographia*, 26, 274-280.
130. BEASLEY, R.K., Hoffmann, C.E., Rueppel, M.L., Worley, J.W., 1980. Sampling of formaldehyde in air with coated solid sorbent and determination by high Performance liquid chromatography. *Anal. Chem.*, 52, 1110-1114.
131. GUENIER, J.P., Simon, P., Delcourt, J., Didierjean, M.F., Lefevre, C., Muller, J., 1984. Air Sampling of aldehydes - application to chromatographic determination of formaldehyde and acetaldehyde. *Chromatographia*, 18(3), 137-144.
132. SAKURAGAWA, A., Yoneno, T., Inoue, K., Okutani, T., 1999. Trace analysis of carbonyl compounds by liquid chromatography-mass spectrometry after collection as 2,4-dinitrophenylhydrazine derivatives. *J.Chromatogr. A*, 844, 403-408.
133. DALENE, M., Persson, P., Skarping, G., 1992. Determination of formaldehyde in air by chemisorption on glass filters impregnated with 2,4-dinitrophenylhydrazine using gas chromatography with thermionic specific detection. *J.Chromatogr. A*, 626, 284-288.
134. SESANA, G., Nano, G., Baj, A., Balestreri, S., 1991. New sampling tool for airborne volatile aldehydes. *Fresenius J. Anal. Chem.*, 339(7), 485-487.
135. OTSON, R., Fellin, P., Tran, Q., Stoyanoff, R., 1993. Examination of sampling methods for assessment of personal exposures to airborne aldehydes. *Analyst*, 118(10), 1253-1259.
136. NISHIKAWA, H., Sakai, T., 1995. REVIEW: Derivatization and chromatographic determination of aldehydes in gaseous and air samples. *J.Chromatogr. A*, 710(1), 159-165.
137. GROSJEAN, E., Green, P.G., Grosjean, D., 1999. Liquid chromatography analysis of carbonyl (2,4-Dinitrophenyl)hydrazones with detection by diode array Ultraviolet spectroscopy and by atmospheric pressure negative chemical ionization mass spectrometry. *Anal. Chem.*, 71, 1851-1861.
138. DYE, C., Oehme, M., 1992. Comments concerning the HPLC separation of Acrolein from other C3 carbonyl compounds as 2,4-Dinitrophenylhydrazones: A proposal for improvement. *J. High Resolut. Chromatogr.*, 15(1), 5-8.
139. STASHENKO, E.E., Puertas, M.A., Salgar, W., Delgado, W., Martinez, J.R., 2000. Solid-Phase Microextraction with on-fibre derivatization applied to the analysis of volatile carbonyl compounds, Riva Del Garda Chromatography Conference Poster, 1-7.
140. CANCELLA, D.A., Chou, C., Barthel, R., Que Hee, S.S., 1992. Characterization of the O-(2,3,4,5,6-pentafluorobenzyl)-hydroxylamine hydrochloride (PFBOA) derivatives of some aliphatic mono- and dialdehydes and quantitative water analysis of these aldehydes. *JAOAC International*, 75, 842-854.

141. NAWROCKI, J., Kalkowska, I., Dabrowska, A., 1996. Optimisation of solid phase extraction method for analysis of low ppb amounts of aldehydes-ozonation by-products. *J.Chromatogr. A*, 749A, 157-163.
142. OJALA, M., Kotiaho, T., Siirila, J., Sihvonen, M., 1994. Analysis of aldehydes and ketones from beer as O-(2,3,4,5,6-pentafluorobenzyl)hydroxylamine derivatives. *Talanta*, 41, 1297-1309.
143. VIDAL, J.P., Estreguil, S., Cantagrel, R., 1993. Quantitative analysis of Cognac carbonyl compounds at the ppb level by GC-MS of their O - (pentafluorobenzyl amine) derivatives. *Chromatographia*, 36, 183-186.
144. STRASSNIG, S., Wenzl, T., Lankmayr, E.P., 2000. Microwave-assisted derivatization of volatile carbonyl compounds with O-(2,3,4,5,6-pentafluorobenzyl)hydroxylamine. *J.Chromatogr. A*, 891, 267-273.
145. WUE, L.J., Que Hee, S.S., 1995. A solid sorbent personal air sampling method for aldehydes. *Am. Ind. Hyg. Assoc. J.*, 56(4), 362-367.
146. TSAI, S.W., Que Hee, S.S., 1999. A new passive sampler for aldehydes. *Am. Ind. Hyg. Assoc. J.*, 60, 463-473.
147. MARTOS, P.A., Pawliszyn, J., 1999. Time - weighted average sampling with solid-phase microextraction device: Implications for enhanced personal exposure monitoring to airborne pollutants. *Anal. Chem.*, 71, 1513-1520.
148. KENNEDY, E.R., O'Connor, P.F., Gagnon, Y.T., 1984. Determination of Acrolein in air as an oxazolidine derivative by gas chromatography. *Anal. Chem.*, 56, 2120-2123.
149. THOMAS, P., McGill, C.L., Towill, C.D., 1997. Determination of formaldehyde by conversion to hexahydroazolo[3,4-a]pyridine in a denuder tube with recovery by thermal desorption and analysis by GC-MS. *Analyst*, 122, 1471-1476.
150. NIOSH Method 2541, 1994. Formaldehyde by GC. *NIOSH Manual of Analytical Methods*. www.cdc.gov/niosh/nmam.
151. NIOSH Method 2539, 1994. Aldehydes, screening. *NIOSH Manual of Analytical Methods*. www.cdc.gov/niosh/nmam.
152. MIYAKE, T., Shibamoto, T., 1995. Quantitative analysis by GC of volatile carbonyl compounds in cigarette smoke. *J.Chromatogr. A*, 693, 376-381.
153. YASUHARA, A., Shibamoto, T., 1994. Gas chromatographic determination of trace amounts of aldehydes in automobile exhaust by cysteamine derivatisation methods. *J.Chromatogr. A*, 672, 261-266.
154. KARTSOVA, L.A., Makarova, Y.L., Stolyarov, B.V., 1997. Selective gas chromatographic determination of formaldehyde in air. *J.Anal.Chem*, 52(4), 337-340.
155. PELTONEN, K., Pfaffli, P., Itkonen, A., 1984. Determination of aldehydes in air as dimethone derivatives by gas chromatography with electron capture detection. *J.Chromatogr. A*, 315, 412-416.

156. RECHE, F., Garrigos, M.C., Sanchez, A., Jimenez, A., 2000. Simultaneous supercritical fluid derivatization and extraction of formaldehyde by the Hantzsch reaction. *J.Chromatogr. A*, 896, 51-59.
157. ZUREK, G., Karst, U., 1999. Liquid Chromatography - mass Spectrometry method for the determination of aldehydes derivatized by the Hantzsch reaction. *J.Chromatogr. A*, 864, 191-197.
158. BLAU, K., King, G.S., 1977. Handbook of derivatives for Chromatography. Heyden & Son Ltd, London, U.K.
159. PAN, L., Chong, M., Pawliszyn, J., 1997. Determination of amines in air and water using derivatization combined with solid-phase microextraction. *J.Chromatogr. A*, 773, 249-260.
160. GYLLENHAAL, O.; Hoffmann, K-J.; Lamm, B.; Simonsson, R.; Vessman, J., 1986. Degradation of perfluoroacyl derivatives of tocainide and some of its analogues in the presence of an excess of anhydride reagent. *J.Chromatogr. A*, 355, 127-140.
161. MASUDA, Y.; Hoffmann, D., 1969. A method for the determination of primary amines of polynuclear aromatic hydrocarbons. *J. Chromatogr. Sci*, 7, 694-697.
162. CHIA, K-J.; Huang, S-D., 2005. Simultaneous derivatization and extraction of amphetamine-like drugs in urine with headspace solid-phase microextraction followed by gas chromatography-mass spectrometry. *Anal. Chim. Acta*, 539, 49-54.
163. KOSTER, E.H.M.; Bruins, C.H.P.; de Jong, G.H., 2002. On-fiber derivatization for direct immersion solid-phase microextraction. Part II. Acylation of amphetamine with pentafluorobenzoylchloride for urine analysis. *Analyst*, 127, 598-602.
164. ZHAO, YY., Cai, LS., Jing, ZZ., Wang, H., Yu, JX., Zhang, HS., 2003. Determination of aliphatic amines using N-succinimidyl benzoate as a new derivatization reagent in gas chromatography combined with solid-phase microextraction. *J.Chromatogr. A*, 1021, 175-181.
165. SACHET, F., Lenz, S., Brauch, HJ., 1997. Analysis of primary and secondary aliphatic amines in waste water and surface water by gas chromatography-mass spectrometry after derivatization with 2,4-dinitrofluorobenzene or benzenesulfonyl chloride. *J.Chromatogr. A*, 764, 85-93.
166. LU, J., Cwik, M., Kanyok, T., 1997. Determination of paromomycin in human plasma and urine by reversed phase HPLC using 2,4-dinitrofluorobenzene derivatization. *J.Chromatogr. B*, 695, 329-335.
167. HEGEDU, H., Gergely, A., Veress, T., Horváth, P., 1999. Novel derivatization with Sanger's reagent (2,4-dinitrofluorobenzene [DNFB]) and related methodological developments for improved detection of amphetamine enantiomers by circular dichroism spectroscopy. *Analisis*, 27, 458-463.
168. BJORKLUND, J., Einarsson, S., Engstrom, A., Grzegorzcyk, A., Becker, H.D., Josefsson, B., 1998. Automated amino acid determination by high-performance liquid chromatography with 2-(9-anthryl)ethyl chloroformate as precolumn reagent. *J.Chromatogr. A*, 798, 1-8.

169. HUSEK, P., 1998. REVIEW: Chloroformates in gas chromatography as general purpose derivatizing agents. *J.Chromatogr. B.*, 717, 57-91.
170. ROSENFELD, J.M., 1999. REVIEW: Solid-phase analytical derivatization: enhancement of sensitivity and selectivity of analysis. *J.Chromatogr. A*, 843, 19-27.
171. RODRIGUEZ, I., Turnes, M.I., Mejuto, C., Cela, R., 1996. Determination of chlorophenols at the sub-ppb level in tap water using derivatization, solid-phase extraction and gas chromatography with plasma atomic emission detection. *J.Chromatogr. A*, 721, 297-304.
172. MEYER, A., Kleiboumlhmer, W., 1995. Determination of pentachlorophenol in leather using supercritical fluid extraction with in situ derivatization. *J.Chromatogr. A*, 718, 131-139.
173. LLOMPART, M.P., Lorenzo, R.A., Cela, R., Jocelyn Par, J.R., Brlanger, J.M.R., Li, K., 1997. Phenol and methylphenol isomers determination in soils by in-situ microwave-assisted extraction and derivatization. *J.Chromatogr. A*, 757, 157-164.
174. KAWAGUCHI, M., Ito, R., Endo, N., Okanouchi, N., Sakui, N., Saito, K., Nakazawa, H., 2006. Liquid phase microextraction with in situ derivatization for measurement of bisphenol A in river water sample by gas chromatography–mass spectrometry. *J.Chromatogr. A*, 1110, 1-5.
175. ALBERICI, R.M.; Sparrapan, R.; Jardim, W.F.; Eberlin, M.N., 2001. Selective trace level analysis of phenolic compounds in water by flow injection analysis-membrane introduction mass spectrometry. *Environ. Sci. Technol.*, 35, 2084-2088.
176. KAWAGUCHI, M., Ishii, Y., Sakui, N., Okanouchi, N., Ito, R., Inoue, K., Saito, K., Nakazawa, H., 2004. Stir bar sorptive extraction with in situ derivatization and thermal desorption–gas chromatography–mass spectrometry in the multi-shot mode for determination of estrogens in river water samples. *J.Chromatogr. A*, 1049, 1-8.
177. KAWAGUCHI, M., Inoue, K., Yoshimura, M., Sakui, N., Okanouchi, N., Ito, R., Yoshimura, Y., Nakazawa, H., 2004. Trace analysis of phenolic xenoestrogens in water samples by stir bar sorptive extraction with in situ derivatization and thermal desorption–gas chromatography–mass spectrometry. *J.Chromatogr. A*, 1041, 19-26.
178. KAWAGUCHI, M.; Ishii, Y.; Sakui, N.; Okanouchi, N.; Ito, R.; Saito, K.; Nakazawa, H., 2005. Stir bar sorptive extraction with in-situ derivatization and thermal desorption-gas chromatography-mass spectrometry for determination of chlorophenols in water and body fluid samples. *Anal. Chim. Acta*, 533, 57-65.
179. ITOH, N.; Tao, H.; Ibusuki, T., 2005. Optimization of aqueous acetylation for determination of hydroxy polycyclic aromatic hydrocarbons in water by stirbar sorptive extraction and thermal desorption - gas chromatography - mass spectrometry. *Anal. Chim. Acta*, 535, 243-250.
180. MONTERO, L.; Conradi, S.; Weiss, H.; Popp, P., 2005. Determination of phenols in lake and ground water samples by stir bar sorptive extraction-thermal desorption -gas chromatography-mass spectrometry. *J.Chromatogr. A*, 1071, 163.
181. KAWAGUCHI, M., Ito, R., Sakui, N., Okanouchi, N., Saito, K., Nakazawa, H., 2005. Dual derivatization–stir bar sorptive extraction–thermal desorption–gas chromatography–mass spectrometry for determination of 17 β -estradiol in water sample. *J.Chromatogr. A*, 1105, 140-147.

182. STACH, J.; Zimmer, D.; Moder, M.; Herzsuh, R., 1989. Determination of hydroxyaromatic compounds in complex mixtures by tandem mass spectrometry. *Org. Mass Spectrom.*, 24, 946-952.
183. LEE, H.B., Peart, T.E., 1998. Determination of 17 beta-estradiol and its metabolites in sewage effluent by solid-phase extraction and gas chromatography mass spectrometry. *J. AOAC Int.*, 81, 1209-1216.
184. PENG, X., Wang, Z., Yang, C., Chen, F., Mai, B., 2006. Simultaneous determination of endocrine-disrupting phenols and steroid estrogens in sediment by gas chromatography–mass spectrometry. *J.Chromatogr. A*, 1116, 51-56.
185. WAHLBERG, C.; Renberg, L.; Wideqvist, U., 1990. Determination of nonylphenol and nonylphenol ethoxylates as their pentafluorobenzoates in water, sewage sludge and biota. *Chemosphere*, 20, 179-195.
186. McCALLUM, N.K.; Armstrong, R.J., 1973. The derivatisation of phenols for gas chromatography using electron capture detection. *J.Chromatogr. A*, 78, 303-307.
187. BUISSON, R.S.K.; Kirk, P.W.W.; Lester, J.N., 1984. Determination of chlorinated phenols in water, wastewater, and wastewater sludge by capillary GC/ECD. *J. Chromatogr. Sci.*, 22, 339-342.
188. BIANCHI, F.; Careri, M.; Mucchino, C.; Musci, M., 2002. Improved determination of chlorophenols in water by solid-phase microextraction followed by benzylation and gas chromatography with electron capture detection. *Chromatographia*, 55, 595-600.
189. MEIER, S., Klungsoyr, J., Boitsov, S., Eide, T., Svardal, A., 2005. Gas chromatography–mass spectrometry analysis of alkylphenols in cod (*Gadus morhua*) tissues as pentafluorobenzoate derivatives. *J.Chromatogr. A*, 1062, 255-268.
190. BOITSOV, S.; Meier, S.; Klungsoyr, J.; Svardal, A., 2004. Gas chromatography-mass spectrometry analysis of alkylphenols in produced water from offshore oil installations as pentafluorobenzoate derivatives. *J.Chromatogr. A*, 1059, 131-141.
191. AKRE, C.; Fedeniul, R.; MacNeil, J.D., 2004. Validation of a simple, sensitive method for the determination of β -estradiol in bovine urine using gas-chromatography negative-ion chemical ionization mass spectrometry. *Analyst*, 129, 145-149.
192. XIAO, XY., McCalley, D., McEvoy, J., 2001. Analysis of estrogens in river water and effluents using solid-phase extraction and gas chromatography-negative chemical ionisation mass spectrometry of the pentafluorobenzoyl derivatives. *J.Chromatogr. A*, 923, 195-204.
193. KUCH, H.M.; Ballschmiter, K., 2001. Determination of Endocrine-disrupting phenolic compounds and estrogens in surface and drinking water by HRGC-(NCI)-MS in the picogram per liter range. *Environ. Sci. Technol.*, 35, 3201-3206.
194. DASGUPTA, A.; Thompson, W.C.; Malik, S., 1994. Use of microwave irradiation for rapid synthesis of perfluorooctanoyl derivatives of fatty alcohols, a new derivative for gas chromatography - mass spectrometric and fast atom bombardment mass spectrometric study. *J.Chromatogr. A*, 685, 279-285.
195. SHAREEF, A., Angove, M.J., Wells, J.D., 2006. Optimization of silylation using N-methyl-N-(trimethylsilyl)-trifluoroacetamide, N,O-bis-(trimethylsilyl)-trifluoroacetamide and N-(tert-

- butyldimethylsilyl)-N-ethyltrifluoroacetamide for the determination of the estrogens estrone and ethinylestradiol. *J.Chromatogr. A*, 1108, 121-128.
196. DING, W.H., Chiang, CC., 2003. Derivatization procedures for the determination of estrogenic chemicals by GC/MS. *Rapid Commun. Mass Spectrom*, 17, 56-63.
197. MURAD, I.H., Helaleh, A., Fujii, S., Korenaga, T., 2001. Column silylation method for determining endocrine disruptors from environmental water samples by solid phase micro-extraction. *Talanta*, 54, 1039-1047.
198. CARPINTEIRO, J., Quintana, J.B., Rodriguez, I., Carro, A.M., Lorenzo, R.A., Cela, R., 2004. Applicability of solid-phase microextraction followed by on-fiber silylation for the determination of estrogens in water samples by gas chromatography–tandem mass spectrometry. *J.Chromatogr. A*, 1056, 179-185.
199. QUINTANA, J.B., Carpinteiro, J., Rodriguez, I., Lorenzo, R.A., Carro, A.M., Cela, R., 2004. Determination of natural and synthetic estrogens in water by gas chromatography with mass spectrometric detection. *J.Chromatogr. A*, 1024, 177-185.
200. LI, D., Park, J., Oh, J.R., 2001. Silyl Derivatization of Alkylphenols, Chlorophenols, and Bisphenol A for Simultaneous GC/MS Determination. *Anal. Chem.*, 73, 3089-3095.
201. OKEYO, P., Rentz, S.M., Snow, N.H., 1997. Analysis of steroids from human serum by SPME with headspace derivatization and GC/MS. *J. High Resolut. Chromatogr*, 20, 171-173.
202. YANG, L., Luan, T., Lan, C., 2006. Solid-phase microextraction with on-fiber silylation for simultaneous determinations of endocrine disrupting chemicals and steroid hormones by gas chromatography–mass spectrometry. *J.Chromatogr. A*, 1104, 23-32.
203. HONGA, J.E., Pyoa, H., Park, S.J., Lee, W., 2005. Solid-phase microextraction with on-fiber derivatization for the determination of hydroxy-polychlorinated biphenyl compounds in urine. *Anal. Chim. Acta*, 539, 55-60.
204. WOO, K.L., Kim, J.I., 1999. New hydrolysis method for extremely small amounts of lipids and capillary gas chromatographic analysis as N(O)-tert-butyldimethylsilyl fatty acid derivatives compared with methyl ester derivatives. *J.Chromatogr. A*, 862, 199-208.
205. LE BIZEC, B., Monteau, F., Gaudin, I., Andre, F., 1999. Evidence for the presence of endogenous 19-norandosterone in human urine. *J.Chromatogr. B.*, 723, 157-172.
206. HERBERER, T., Stan, H.J., 1997. Detection of more than 50 substituted phenols as their t-butyldimethylsilyl derivatives using gas chromatography-mass spectrometry. *Anal. Chim. Acta*, 341, 21-34.
207. KELLY, C., 2000. Analysis of steroids in environmental water samples using solid-phase extraction and ion-trap gas chromatography-mass spectrometry and gas chromatography-tandem mass spectrometry. *J.Chromatogr. A*, 872, 309-314.
208. MOL, H.G.J., Sunarto, S., Steijger, O.M., 2000. Determination of Endocrine Disruptors in water after derivatization with N-methyl-N-(tert-butyldimethylsilyl)trifluoroacetamide) using gas chromatography with mass spectrometric detection. *J.Chromatogr. A*, 879, 97-112.

209. FINE, D.D., Breidenbach, G.B., Price, T.L., Hutchins, S.R., 2003. Quantitation of estrogens in ground water and swine lagoon samples using solid-phase extraction, pentafluorobenzyl/trimethylsilyl derivatizations and gas chromatography–negative ion chemical ionization tandem mass spectrometry. *J.Chromatogr. A*, 1017, 167-185.
210. GALCERAN, M.T., Moyano, E., Poza, J.M., 1995. Pentafluorobenzyl derivatives for the gas chromatographic determination of hydroxy-polycyclic aromatic hydrocarbons in urban aerosols. *J.Chromatogr. A*, 710, 139-147.
211. SANDRA, P.J.F., 1994. Gas Chromatography in *Ullmann's Encyclopedia of Industrial Chemistry*, Hans-Jürgen Arpe (Editor), 5th Edition, VCH, vol B5, 181-236. ISBN 3527201351.
212. GROB, K., 2001. *Split and Splitless Injection for Quantitative Gas Chromatography- Concepts, processes, Practical guidelines, Sources of Error*, 4th Edition, Wiley-VCH Verlag GmbH & Co., Weinheim, Germany. ISBN 33527298797.
213. ET AL, ChromPack - Thermal desorption Cryo-Trapping unit 4020 User Manual.
214. ET AL, ThermoDesorptionSystem (TDS) Global Analytical Solutions-Gerstel Application Note (Flyer), www.gerstel.de/application.htm.
215. ET AL, 2001. Dilution, Enrichment & Desorption Unit Handbook, Version 1.0, WMA Airsense Analysentechnik GmbH.
216. BURGER, B. V.; Snyman, T.; Burger, V. J. G.; van Rooyen, W. F., 2003. Thermal modulator array. *J.Sep.Sci*, 26, 123-128.
217. PHILLIPS, J. B; Beens, J., 1999. REVIEW: Comprehensive two-dimensional gas chromatography: a hyphenated method with strong coupling between the two dimensions. *J.Chromatogr. A*, 856, 331-347.
218. LIU, Z.; Phillips, J. B., 1994. Sensitivity and Detection Limit Enhancement of Gas Chromatographic Detection by Thermal Modulation. *J.Microcolumn Separations*, 6, 229-235.
219. PHILLIPS, J. B, Xu, J., 1995. REVIEW: Comprehensive multi-dimensional gas Chromatography. *J.Chromatogr. A*, 703, 327-334.
220. de GEUS, H. J.; de Boer, J.; Phillips, J. B.; Brinkman, U. Th., 1997. Development of a thermal desorption modulator for gas chromatography. *J.Chromatogr. A*, 767, 137-151.
221. PHILLIPS, J. B.; Ledford, E. B., 1996. Thermal Modulation: A Chemical Instrumentation Component of Potential Value in Improving Portability. *Field Anal. Chem. Technol.*, 23-29.
222. KINGHORN, R. M.; Marriot, P. J., 1997. Longitudinally Modulated Cryogenic System. A Generally Applicable Approach to Solute Trapping and Mobilization in Gas Chromatography. *Anal. Chem.*, 69, 2582-2588.
223. KINGHORN, R. M.; Marriot, P. J.; Dawes, P. A., 1998. Longitudinal Modulation Studies for Augmentation of Injection and Detection in Capillary Gas Chromatography. *J.Microcolumn Separations*, 10(7), 611-616.

224. GHOOS, Y., Hiele, M., Rutgeerts, P., Vantrappen, G., 1989. Porous -layer open-tubular gas chromatography in combination with an ion trap detector to assess volatile metabolites in human breath. *Biomedical and environmental MS*, 18, 613-616.
225. CANCELLA, D.A., Que-Hee, S.S., 1992. REVIEW: O-(2,3,4,5,6-Pentafluorophenyl)methylhydroxylamine hydrochloride: a versatile reagent for the determination of carbonyl-containing compounds. *J.Chromatogr. A*, 627, 1-16.
226. MUNCH, J.W., Munch, D.J., Winslow, S.D., 1998. A User's guide to aldehyde analysis using PFBHA derivatisation and GC-ECD detection : Avoiding the pitfalls. *Proc-Water Qual.Technol.Conf.[computer optical disk]*, 898-913.
227. VOGEL, A.I., 1989. Aldehyde and amine derivatization reactions with phenylhydrazine and benzaldehyde respectively. *Vogel's Textbook of practical organic chemistry*, 5th Ed revised, Editors Brian Ed Furniss [et al], Longman group, Essex, UK.
228. NAMIESNIK, J., 1984. Generation of standard gaseous mixtures. *J.Chromatogr. A*, 300, 79-108.
229. SCARANGELLI, F.P., O'Keefe, A.E., Rosenberg, E., Bell, J.P., 1970. Preparation of known concentrations of gases and vapours with permeation devices calibrated gravimetrically. *Anal. Chem.*, 42, 871-876.
230. ROHWER, E. R.; Pretorius, V.; Apps, P. J., 1983. Simple press-fit connectors for flexible fused silica tubing in gas-liquid chromatography. *J. High Resolut. Chromatogr*, 9, 295-297.
231. FRANK, H., Renschen, D., Klein, A., Scholl, H., 1995. Trace analysis of airborne haloacetates. *J. High Resolut. Chromatogr*, 18, 83-88.
232. TONG, H.Y., Karasek, F.W., 1984. Flame Ionisation Detector response factors for compound classes in quantitative analysis of complex organic mixtures. *Anal. Chem.*, 56, 2124-2128.
233. SCANLON, J.T., Willis, D.E., 1985. Calculation of flame ionization detector relative response factors using the effective carbon number concept. *J. Chromatogr. Sci*, 23, 333-340.
234. Walte, A., 2001. Airsense Analytics Dilution, Enrichment and Desorption Unit Handbook, WMA Airsense Analysentechnik, GmbH: Schwerin, Germany.
235. BOESL, U., Heger, H.J., Zimmermann,R., Nagel,H., Püffel,P., 2000. Laser Mass Spectrometry in Trace Analysis. *Encyclopedia of Analytical Chemistry*, R.A. Meyers (Ed.), John Wiley & Sons Ltd, Chichester, 2087-2118.
236. ENGELKE, F.; Hahn, J. H.; Henke, W.; Zare, R. N.,1987. Determination of phenylthiohydantoin-amino acids by two-step laser desorption/multiphoton ionization. *Anal. Chem.*, 59, 909-912.
237. CLEMETT, S. J.; Maechling, C. R.; Zare, R. N.; Swan, P. D.; Walker, R. M., 1993. Identification of complex aromatic molecules in individual interplanetary dust particles. *Science*, 262, 721-725.

238. DALE, M. J.; Jones, A. C.; Pollard, S. J. T.; Langridge-Smith, P. R. R.; Rowley, A. G., 1993. Trace analysis of polyaromatic hydrocarbons in water using multiphoton ionization-membrane introduction mass spectrometry. *Environ. Sci. Technol.*, 8, 1693-1695.
239. DALE, M. J.; Downs, O. H. J.; Costello, K. F.; Wright, S. J.; Langridge-Smith, P. R. R.; Cape, J. N., 1995. Direct analysis of polycyclic aromatic hydrocarbons in cloud-water aerosol filtrates using laser desorption mass spectrometry. *Environ. Pollut.*, 89, 123-129.
240. HAEFLIGER, O. P.; Bachel, T. D.; Zenobi, R., 1999. *Analusis*, 27, 337-340.
241. FURNISS, B. S.; Hannaford, A. J.; Smith, P. W. G.; Tatchell, A. R., 1989. Vogel's Textbook of Practical Organic Chemistry, 5th ed.; Longman Scientific and Technical: Essex, England., 1258.
242. WILLIAMS, B. A.; Tanada, T. N.; Cool, T. A., 1992. In Twenty-Fourth International Symposium on Combustion; The Combustion Institute: Pittsburgh, 1587-1596.
243. OOSTERKAMP, A.J., Hock, B., Seifert, M., Irth, H., 1997. Novel Monitoring strategies for xenoestrogens. *Trends in analytical chemistry*, 16, 544.
244. ZUO, Y., Zhang, K., 2005. Discussion Suitability of N,O-bis(trimethylsilyl)trifluoroacetamide as derivatization reagent for the determination of the estrogens estrone and 17 β -ethinylestradiol by gas chromatography-mass spectrometry. *J.Chromatogr. A*, 1095, 201-202.
245. ZHANG, K., Zuo, Y., 2005. Pitfalls and solution for simultaneous determination of estrone and 17 β -ethinylestradiol by gas chromatography-mass spectrometry after derivatization with N,O-bis(trimethylsilyl)trifluoroacetamide. *Anal. Chim. Acta*, 554, 190-196.
246. DEHENNIN, L., Reiffstock, A., Scholler, R., 1972. *J. Chromatogr. Sci.*, 10, 224.
247. XIAO, XY., McCalley, D., 2000. Quantitative analysis of estrogens in human urine using gas chromatography/negative chemical ionisation mass spectrometry. *Rapid Commun. Mass Spectrom.*, 14, 1991-2001.
248. STOCKL, D., Thienpont, L.M., de Brabandere, V.I., de Leenheer, A.P., 1995. Novel Perfluoroacyl derivatives of corticosteroids. *J. Am. Soc. Mass Spectrom.*, 6, 264-276.
249. De BRABANDERE, V.I., Thienpont, L.M., Stockl, D., De Leenheerzy, A.P., 1997. ¹³C-NMR and mass spectral data of steroids with a 17,17-dialkyl-18-nor-13(14)-ene substructure. *Journal of Lipid Research*, 38, 780.
250. SUPELCO®, 1997. Supelco - Product Specification Perfluoroacyl anhydrides, Sigma-Aldrich Co., http://www.sigmaaldrich.com/Brands/Supelco_Home.html.
251. CROLEY, T.R., Lynn, Jr B.C., 1998. Molecular Ion Stabilization for Enhanced Tandem Mass Spectrometry Through Derivatization for Alkylphenols. *Rapid Commun. Mass Spectrom.*, 12, 171-175.
252. STEHMANN, A., Schröder, H.Fr., 2004. Derivatisation of 4-nonylphenol and bisphenol A with halogenated anhydrides. *Water Science and Technology*, 50, 115-118.

253. PETERS, D.G., Hayes, J.M., Hieftje, G.M., 1974. Chemical separations and measurements, Theory and practise of analytical chemistry, W.B.Saunders company, P.A., U.S.A.
254. MACKAY, D., Varhannickova, D., Ma, Kuo-Ching, Shiu, Wan-Ying, 1994. Chlorophenols and alkylphenols: A review and correlation of environmentally relevant properties and fate in an evaluative environment. *Chemosphere*, 29, 1155-1224.
255. JANSSEN, HG., 1998. GERSTEL Sample Introduction Techniques For Capillary Gas Chromatography, Global Analytical Solutions-Gerstel Technical Note Version 3, www.gerstel.de/application.htm.
256. SKOOG, D.A., West, D.M., Holler, F.J., 1994. Analytical chemistry - An introduction, Saunders College Publishing, Sixth edition, ISBN 003097285X.
257. SHURMER, B., Pawliszyn, J., 2000. Determination of Distribution Constants between a Liquid Polymeric Coating and Water by a Solid-Phase Microextraction Technique with a Flow-Through Standard Water System. *Anal. Chem.*, 72, 3660-3664.
258. BALTUSSEN, E., Sandra, P., David, F., Janssen, HG., Cramers, C., 1999. Study into the Equilibrium Mechanism between Water and Poly(dimethylsiloxane) for Very Apolar Solutes: Adsorption or Sorption? *Anal. Chem.*, 71, 5213-5216.
259. HUNT, G., Pangaro, N., 1982. Potential contamination from the use of synthetic adsorbents in air sampling procedures. *Anal. Chem.*, 54, 369-372.
260. MORGAN, E.D., Bradley, N., 1989. Method for analysis of dilute vapours in flue gases and working atmospheres. *J.Chromatogr. A*, 40, 339-344.
261. KRUSCEL, B.D.; Bell, R.W.; Chapman, R.E.; Spencer, M.J.; Smith, K.V., 1994. Analysis of ambient polar and non-polar volatile organic compounds(VOC's) by thermal desorption, high resolution gas chromatography-mass spectrometry(TD/HRGC-MS). *J. High Resolut. Chromatogr.*, 17(3), 187-190.
262. HERNANDO, M.D.; Mezcua, M.; Gomez, M.J.; Malato, O.; Aguera, A.; Fernandez-Alba, A.R., 2004. Comparative study of analytical methods involving gas chromatography-mass spectrometry after derivatization and gas chromatography-tandem mass spectrometry for the determination of selected endocrine disrupting compounds in wastewaters. *J.Chromatogr. A*, 1047, 129-135.
263. BELFROID, A.C., Van Der Horst, A., Vethaak, A.D., Schafer, A.J., Rijs, G.B.J., Wegener, J., Cofino, W.P., 1999. Analysis and occurrence of estrogenic hormones and their glucuronides in surface water and waste water in The Netherlands. *Science of the Total Environment*, 225, 101-108.
264. DIAZ, A., Ventura, F., Galceran, M.T., 2002. Simultaneous Determination of Estrogenic Short Ethoxy Chain Nonylphenols and Their Acidic Metabolites in Water by an In-Sample Derivatization/Solid-Phase Microextraction Method. *Anal. Chem.*, 74, 3869-3876.
265. RODGERS-GRAY, T.P., Jobling, S., Morris, S., Kelly, C., Kirby, S., Janbakhsh, A., Harries, J.E., Waldock, M., Sumpter, J.P., Tyler, C.R., 2001. Long-Term Temporal Changes in the Estrogenic Composition of Treated Sewage Effluent and Its Biological Effects on Fish. *Environ. Sci. Technol.*, 34, 1521-1528.

266. MULLER, S., Moder, M., Schrader, S., Popp, P., 2003. Semi-automated hollow-fibre membrane extraction, a novel enrichment technique for the determination of biologically active compounds in water samples. *J.Chromatogr. A*, 985, 99-106.
267. BRAUN, P., Moeder, M., Schrader, S., Popp, P., Kusch, P., Engewald, W., 2003. Trace analysis of technical nonylphenol, bisphenol A and 17 α -ethinylestradiol in wastewater using solid-phase microextraction and gas chromatography-mass spectrometry. *J.Chromatogr. A*, 988, 41-51.
268. ROUTLEDGE, E.J., Brighty, G.C., Sumpter, J.P., Waldock, M., 1998. Identification of Estrogenic Chemicals in STW Effluent. 1. Chemical Fractionation and in Vitro Biological Screening. *Environ. Sci. Technol.*, 32, 1549-1557.
269. WATABE, Y., Kubo, T., Nishikawa, T., Fujita, T., Kaya, K., Hosoya, K., 2006. Fully automated liquid chromatography-mass spectrometry determination of 17 β -estradiol in river water. *J.Chromatogr. A*, 1120, 252-259.
270. HU, J., Zhang, H., Chang, H., 2005. Improved method for analyzing estrogens in water by liquid chromatography-electrospray mass spectrometry. *J.Chromatogr. A*, 1070, 221-224.
271. PENALVER, A., Pocurull, E., Borrull, F., Marce, R.M., 2002. Method based on solid-phase microextraction-high-performance liquid chromatography with UV and electrochemical detection to determine estrogenic compounds in water samples. *J.Chromatogr. A*, 964, 153-160.
272. LOPEZ de ALDA, M.J., Barcelo, D., 2000. Determination of steroid sex hormones and related synthetic compounds considered as endocrine disrupters in water by liquid chromatography-diode array detection-mass spectrometry. *J.Chromatogr. A*, 892, 391-406.
273. LOPEZ de ALDA, M.J., Barcelo, D., 2001. Use of solid-phase extraction in various of its modalities for sample preparation in the determination of estrogens and progestogens in sediment and water. *J.Chromatogr. A*, 938, 145-153.
274. MITANI, K., Fujioka, M., Kataoka, H., 2005. Fully automated analysis of estrogens in environmental waters by in-tube solid-phase microextraction coupled with liquid chromatography-tandem mass spectrometry. *J.Chromatogr. A*, 1081, 218-224.
275. RODRIGUEZ-MOZAZ, S.; Lopez de Alda, M.J.; Barcelo, D., 2004. Picogram per liter level determination of estrogens in natural waters and waterworks by a fully automated on-line solid-phase extraction-liquid chromatography-electrospray tandem mass spectrometry. *Anal. Chem.*, 76, 6998-7006.
276. CHIARABARONTI, R. A., D'Ascenzo, G., Dicorcia, A., Gentili, A., Samperi, R., 2000. Monitoring Natural and Synthetic Estrogens at Activated Sludge Sewage Treatment Plants and in a Receiving River Water. *Environ. Sci. Technol.*, 34, 5059.
277. MILLER, J.N.; Miller, J.C., 2000. Statistics and chemometrics for analytical chemistry, Fourth edition, Prentice Hall. ISBN 0130228885.
278. LEE, W-Y.; Barud-Zubillaga, A., 2005. A Baseline Study on the Occurrence of Organic Wastewater Compounds in the Paso del Norte. Project number: W-04-08, University of Texas at El Paso.

APPENDIX 1: Table 1. A comparison of various adsorbents [48, 69, 70-72, 82, 115, 116]

	ADSORBENT	COMPOSITION	SURFACE AREA (m ² /g)	PORE DIAMETER (nm)	APPLICATIONS	ADVANTAGES	DISDAVANTAGES
CARBON – BASED	Activated carbon Anasorb 747	Coconut/ petroleum based charcoal	800-1000	2.0 / 1.8-2.2	Non-specific i.e. Most organic and inorganic compounds. Non-polar, polar, reactive and/or volatile. Mercury-vapour.	Cheap, efficient, permanent gases not adsorbed – H ₂ , N ₂ , O ₂ , CO, CH ₄ . Anasorb absorbs less H ₂ O and desorption efficiencies for polar compounds are improved.	Polar compounds irreversibly adsorbed. Incomplete desorption. H ₂ O reduces sorption of other compounds. Catalytic activity. Reacts with oxygen or sulphur derivatives.
	Graphitised carbon black Carbotraps	Pre-treated carbon black under vacuum and inert gas/ reductive atmosphere at 3000°C			Non-specific, as above.	No irreversible adsorption sites. No retention of H ₂ O and low molecular mass compounds (CO _x , CH ₄)	High desorption temperatures (400°C) required. Tiny particles of carbon can enter desorption unit.

APPENDIX 1: Table 1. A comparison of various adsorbents [48, 69, 70-72, 82, 115, 116]

	ADSORBENT	COMPOSITION	SURFACE AREA (m ² /g)	PORE DIAMETER (nm)	APPLICATIONS	ADVANTAGES	DISDAVANTAGES
CARBON – BASED	Carbon molecular sieves Carbosieves	Thermally decomposed polymer e.g. polyvinyl chloride			Adsorption of hydrocarbons and low-boiling C1-C4 hydrocarbons, methyl formate and alkyl mercury compounds.	High capacity for small volatile molecules. Suitable for thermal desorption.	Inefficient retention of polar compounds. Solvent with high heat of adsorption required for displacement of adsorbates. H ₂ O can block cryotrap.
INORGANIC	Silica gel	Si-OH groups on surface	100-800	2-4	Polar compounds from air. Amines, halogens, oxygen derivatives, organo-metallics, MeOH, HCHO and DMF. Silica gel is often used as a substrate for coating with derivatizing reagents.	Cooling the sorbent allows trapping of C1-C4 hydrocarbons	Hydrophilicity decreases sorption capacity. Thermal desorption difficult. Silica gel retains H ₂ O and CO ₂
	Aluminium oxide	Al ₂ O ₃					

APPENDIX 1: Table 1. A comparison of various adsorbents [48, 69, 70-72, 82, 115, 116]

	ADSORBENT	COMPOSITION	SURFACE AREA (m ² /g)	PORE DIAMETER (nm)	APPLICATIONS	ADVANTAGES	DISDAVANTAGES
INORGANIC	Molecular sieves	Zeolites	Varied	Varied	Toxic inorganic compounds. Small conc. of H ₂ S	Thermally desorbed at 240°C/extract with ice H ₂ O	Organic compounds are irreversibly adsorbed excl. HCHO, acrolein and certain S-compounds. H ₂ O block cryotrap
POROUS POLYMERS	Tenax	Poly-2,6-diphenyl-p-phenylene oxide	19	140	Organic bases, neutral and high boiling compounds. Chlorohydrocarbons. Support for derivatising reagents. Broad trapping range of compounds of varied molecular mass and polarity.	Tenax has a high thermal limit 350-400°C. Ideal for thermal desorption.	Not suited to solvent extraction due to low capacity for volatiles and is incompatible with many solvent systems.

APPENDIX 1: Table 1. A comparison of various adsorbents [48, 69, 70-72, 82, 115, 116]

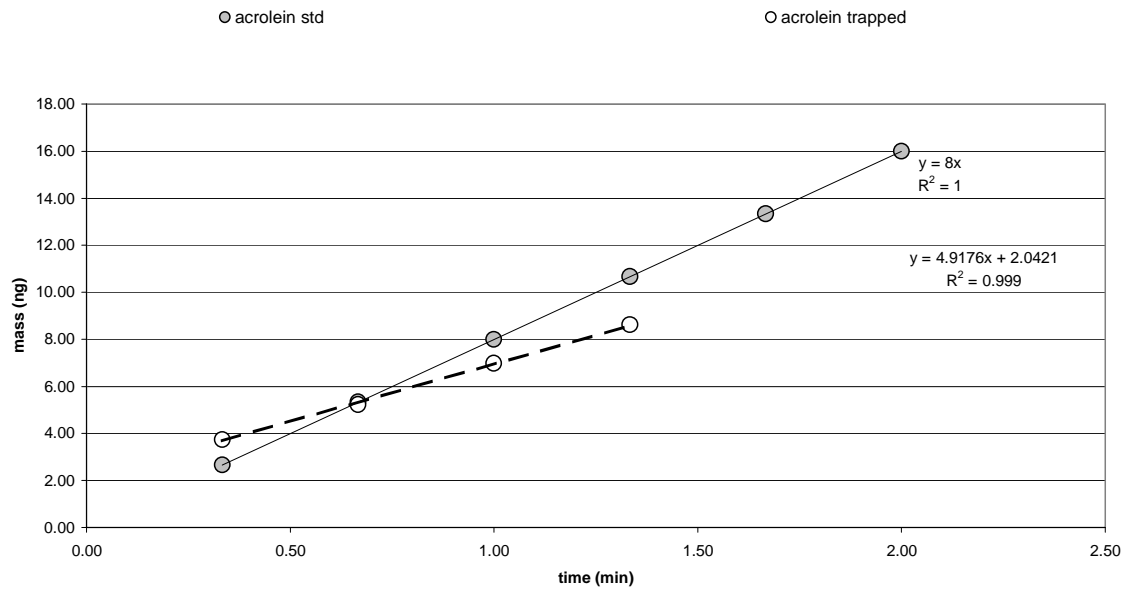
	ADSORBENT	COMPOSITION	SURFACE AREA (m ² /g)	PORE DIAMETER (nm)	APPLICATIONS	ADVANTAGES	DISDAVANTAGES
POROUS POLYMERS	XAD-2 (Amberlite, Chromosorb 102)	Copolymer in which one moiety is styrene or ethylvinylbenzene and the other monomer a polar vinyl compound.	300-400	8.5	Nitroso-compounds and polychlorinated biphenyls, aromatic, aliphatic nitro-compounds.	XAD's, Porapaks and Chromosorbs come in wide ranges of polarity. Chromosorb 106 greater capacity than Tenax, suited to thermal desorption.	
	Porapak		600-650	7.5	Depending on polarity. Non-polar to polar compounds can be adsorbed. Chromosorbs adsorb inorganic compounds		Polar Porapaks retain H ₂ O and require great amount of energy to remove sorbates. Can't withstand the high temperature.
	Chromosorb101, 103, 104, 106, 108.		50 varied	300-400 varied			

Appendix 2

Reaction efficiency data

Additional experimental data obtained for results discussed in section 5. 4.

Acrolein Reaction Efficiency



Crotonal Reaction Efficiency

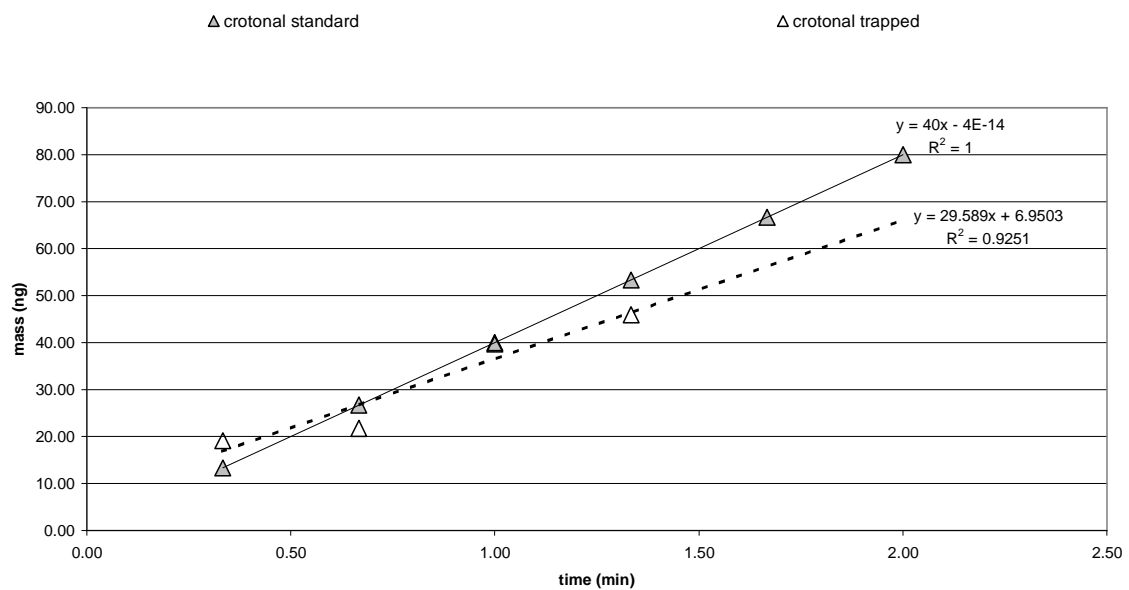


Figure A2.1 Reaction efficiency graphs for the on-line derivatization of acrolein and crotonal with phenylhydrazine. The graph displays i) the amount of gas standard released over that time interval as determined by their permeation rate and ii) the amount of analyte gas trapped using *in-situ* derivatization on the SPME fibre as calculated using the internal standard and effective carbon number response for the signal obtained from the GC-FID for the derivative. A comparison of the gradients obtained from the standard and the actual amount of analyte trapped gives an approximation of the reaction/trapping efficiency for this reaction.

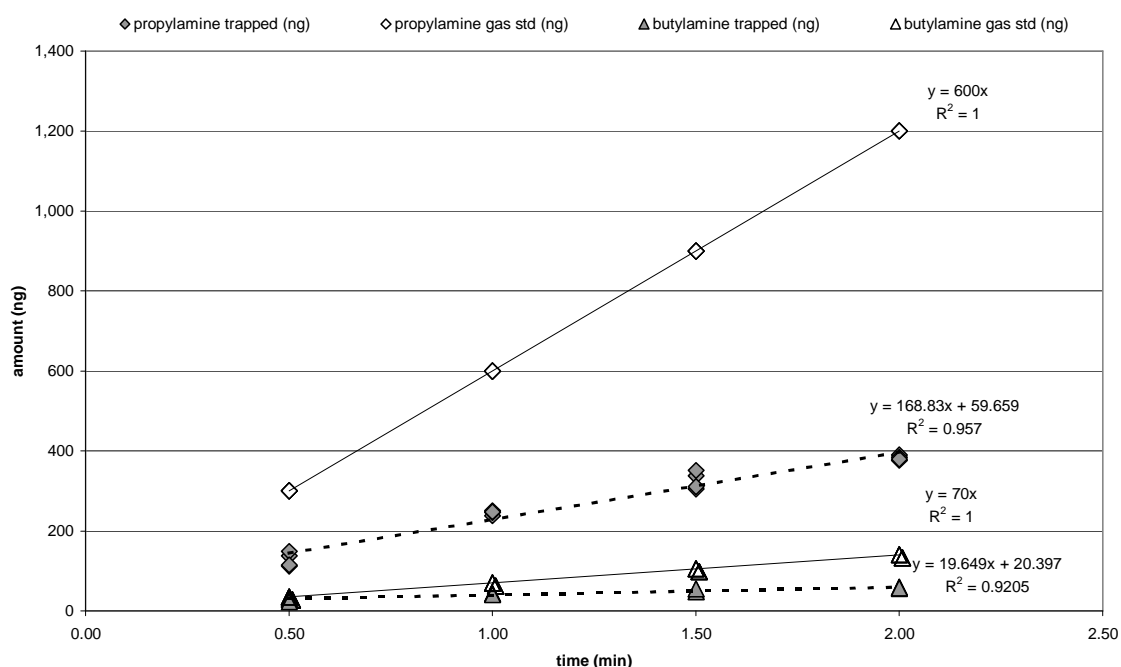


Figure A2.2 Reaction efficiency graphs for the on-line derivatization of propylamine and butylamine with benzaldehyde. The graph displays i) the amount of gas standard released over that time interval as determined by their permeation rate and ii) the amount of analyte gas trapped using *in-situ* derivatization on the SPME fibre as calculated using the internal standard and effective carbon number response for the signal obtained from the GC-FID for the derivative. A comparison of the gradients obtained from the standard and the actual amount of analyte trapped gives an approximation of the reaction/trapping efficiency for this reaction.

Appendix 3

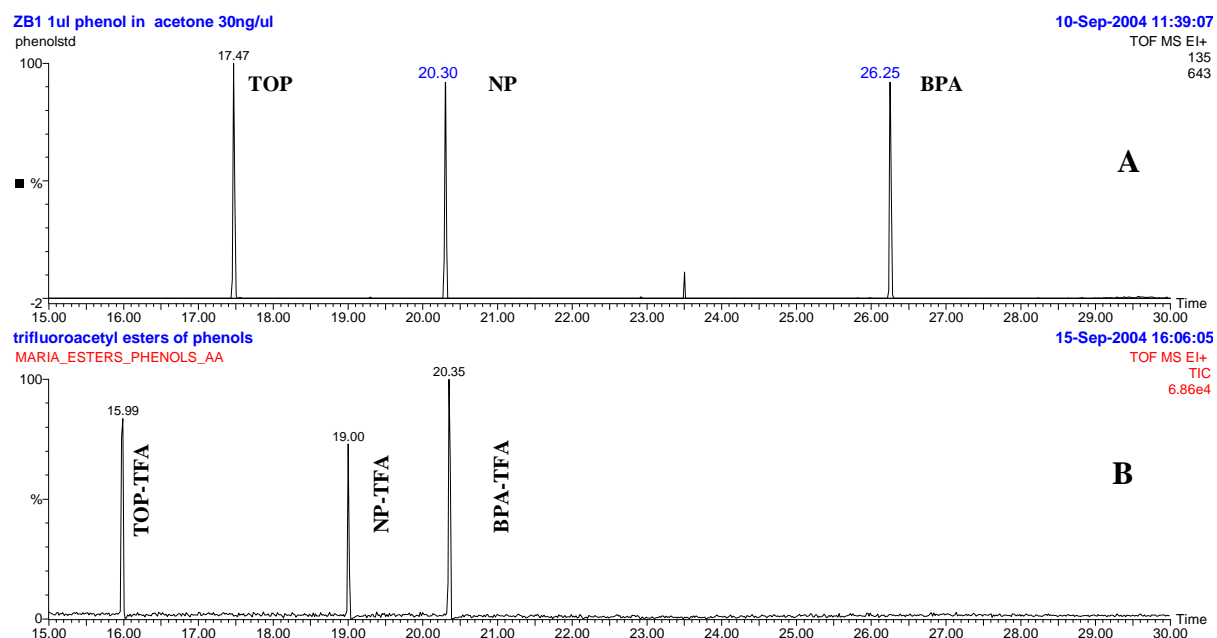
Confirmation of the alkylphenol-TFA derivatives

Figure A3.1

A) GC-TOFMS chromatogram obtained for the underivatized phenols, TOP $t_R = 17.47$ min, NP $t_R = 20.30$ min and BPA $t_R = 26.25$ min.

B) GC-TOFMS confirmation chromatogram for the trifluoroacetate derivatives prepared in a vial in acetone as described in section 6.2.6. TOP-TFA $t_R = 15.99$ min, NP-TFA $t_R = 19.00$ min and BPA-TFA $t_R = 20.35$ min. Notice the absence of underivatized phenols.

The TFA derivatives elute earlier than the underivatized phenols allowing for shorter chromatographic runs, while the mass spectra yields masses higher up in the mass range allowing for improved selectivity during analysis.

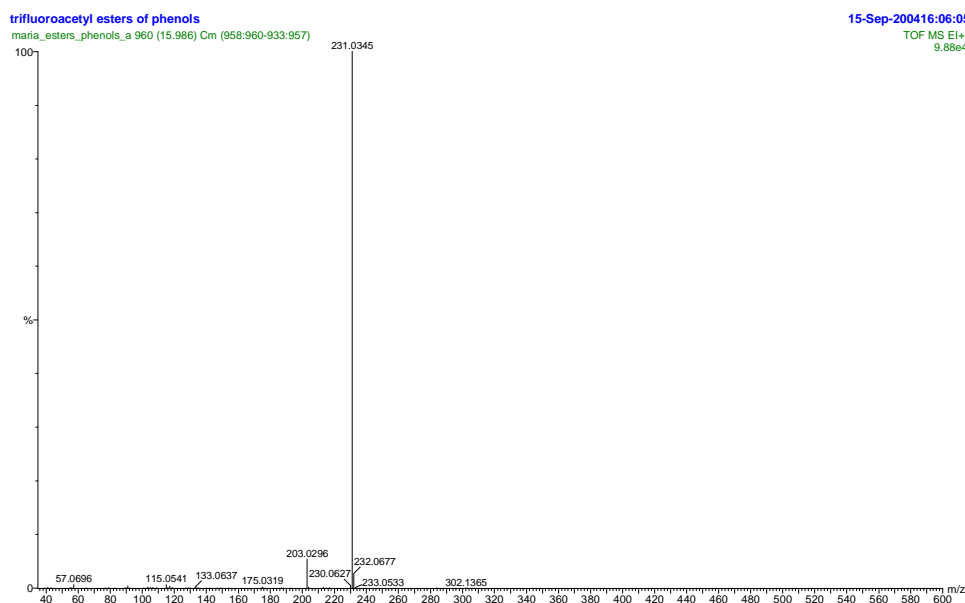


Figure A3.2 GC-TOFMS mass spectrum obtained for the TOP-TFA derivative $t_R = 15.99$ min. M^+ m/z 302, base peak m/z 231.

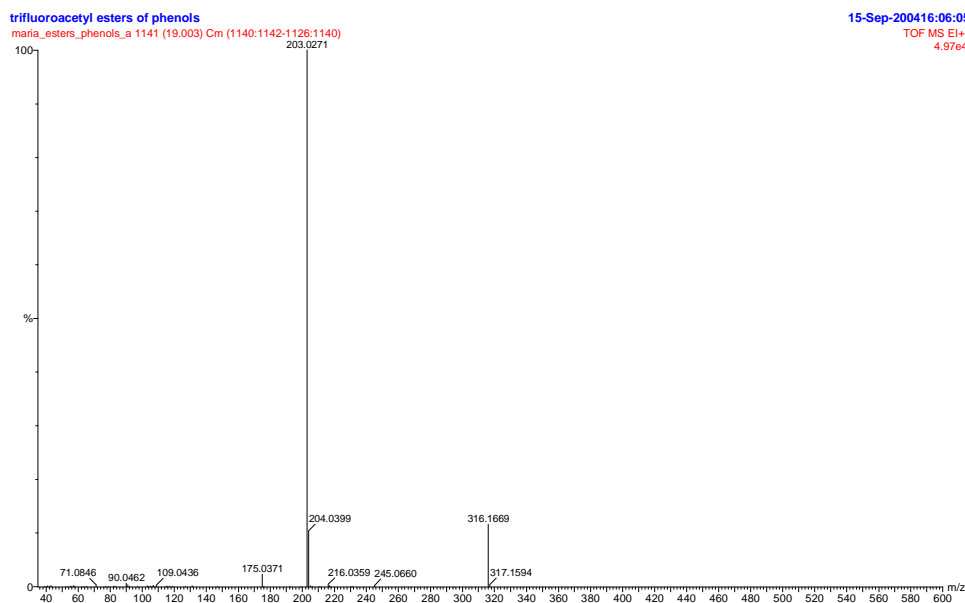


Figure A3.3 GC-TOFMS mass spectrum obtained for the NP-TFA derivative $t_R = 19.00$ min. M^+ m/z 316, base peak m/z 203.

trifluoroacetyl esters of phenols

maria_esters_phenols_a_1222 (20.352) Cm (1222:1223-1154:1213)

15-Sep-200416:06:05

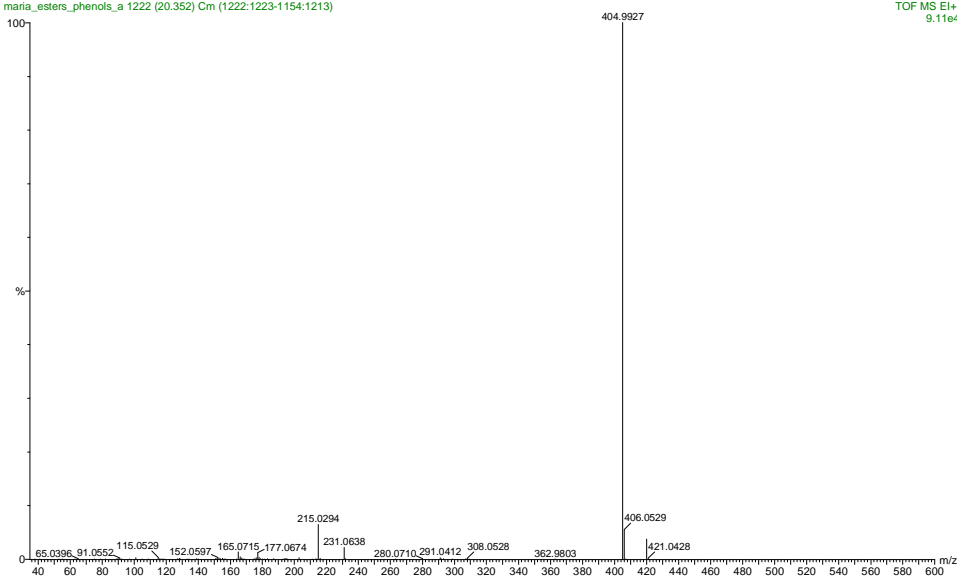
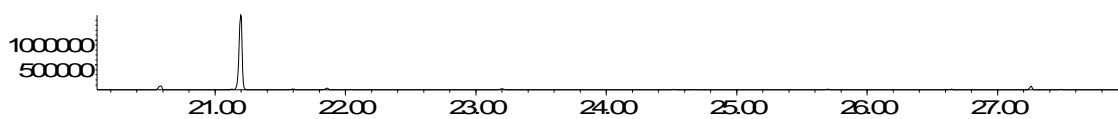
TOF MS EI+
9.11e4

Figure A3.4 GC-TOFMS mass spectrum obtained for the BPA-TFA derivative $t_R = 20.35$ min. M^+ m/z 420, base peak m/z 405.

Abundance

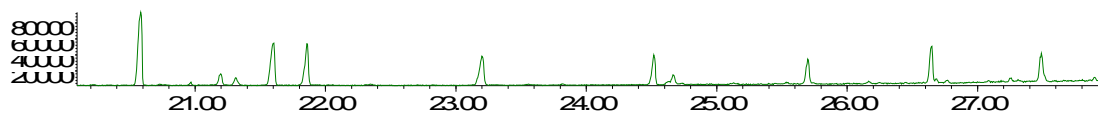
Ion 231.00 (230.70 to 231.70): 08050604.D



Time-->

Abundance

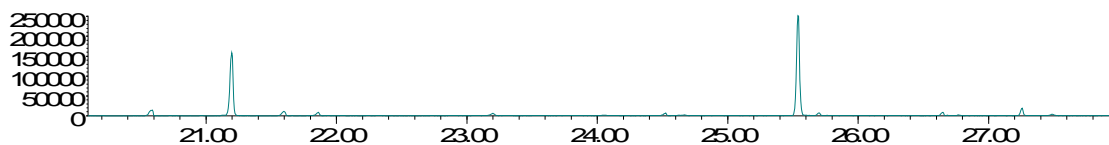
Ion 135.00 (134.70 to 135.70): 08050604.D



Time-->

Abundance

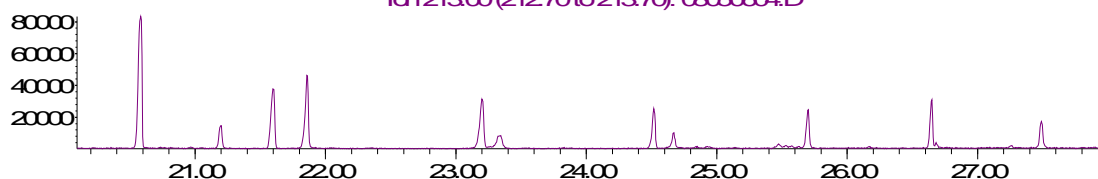
Ion 203.00 (202.70 to 203.70): 08050604.D



Time-->

Abundance

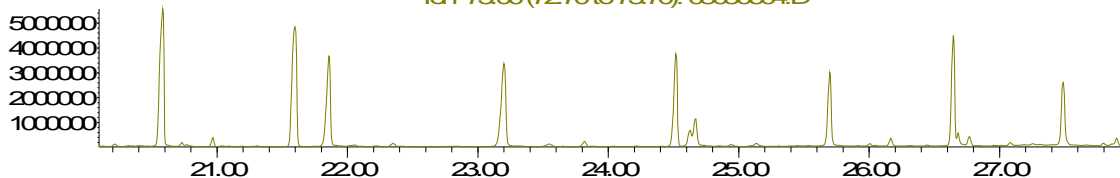
Ion 213.00 (212.70 to 213.70): 08050604.D



Time-->

Abundance

Ion 73.00 (72.70 to 73.70): 08050604.D



Time-->

Figure A3.5 Reconstructed ion chromatograms for m/z 231 and m/z 203 representing the TFA derivatives of TOP and NP respectively, along with m/z 135 and m/z 213 representing ions for the corresponding underivatized alkylphenols. The PDMS degradation peaks are indicated by the m/z 73 ion trace.

From figure A3.1, the unreacted phenols are expected to elute after the TFA derivatives. There is no clear evidence from the RICs that the underivatized phenols are present. Ions 213 and 135 that are present appear to originate from the PDMS thermal degradation peaks. See section 6.7.1.

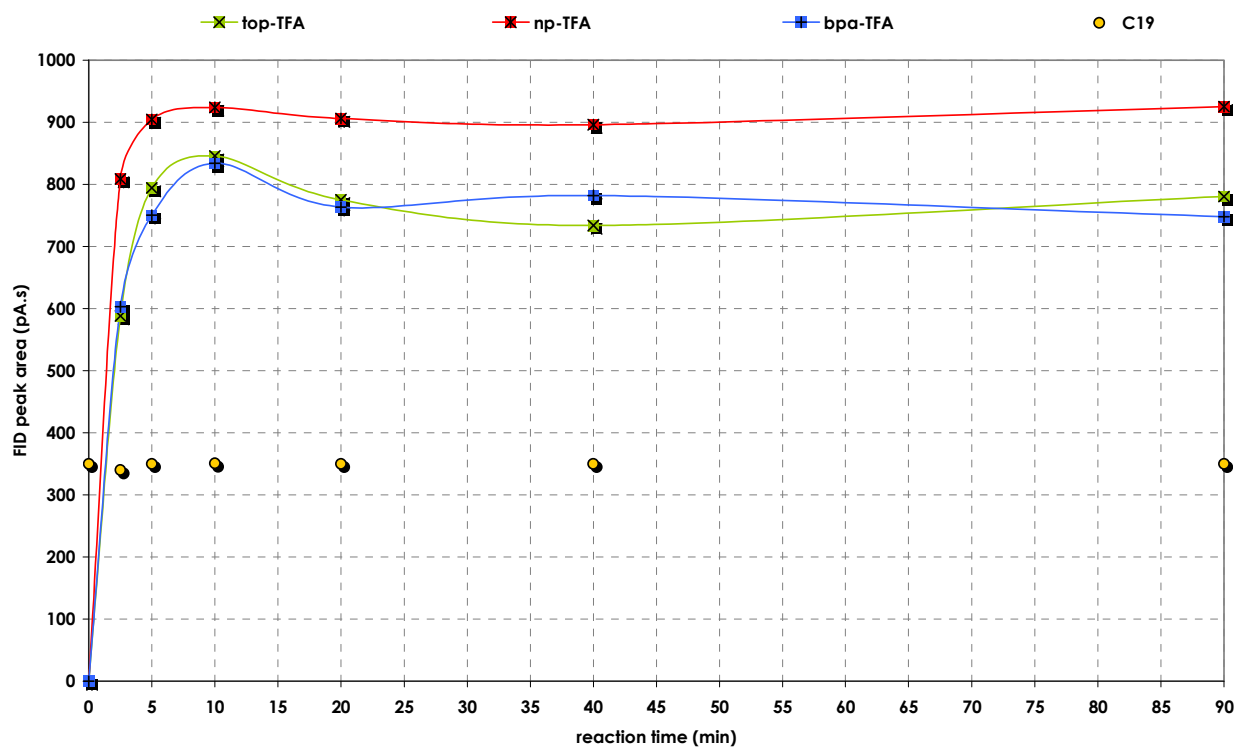


Figure A3.6 Reaction efficiencies, determined by placing 1 μ l 42 ng/ μ l TOP, 44 ng/ μ l NP and 54 ng/ μ l BPA in acetone on the PDMS trap, 5 μ l TFAA is added after the solvent has evaporated. The trap is then sealed with glass caps for the duration of the reaction. The reaction appears to be complete after 5 minutes. See section 6.7.2.

Appendix 4

Significance test for comparing extraction efficiency from two different PDMS batches

1. An F-test is used to compare the population standard deviations between the two batches of PDMS. These need to be the same in order to perform a t-test to compare the two mean results between the batches. The equation used to determine F is shown below [276]:

$$F = \frac{s_1^2}{s_2^2} \quad \text{A.4.1}$$

Where s_1 and s_2 are the standard deviations for the measurement series and are arranged so that $F > 1$.

Critical values of F for a two-tailed test ($P=0.05$) are obtained from table A.4, page 256 [276]. Where v_1 and v_2 are the degrees of freedom ($n-1$) for the number of measurements made (n) in the respective measurement series.

2. A t-test can now be used to compare the two mean results between the batches. The variance (s^2) needs to be calculated as shown in equation A.4.2, in order to determine t from equation A.4.3 [276].

$$s^2 = \frac{(n_1 - 1)s_1^2 + (n_2 - 1)s_2^2}{n_1 + n_2 - 2} \quad \text{A.4.2}$$

$$t = \frac{(\bar{x}_1 - \bar{x}_2)}{s \sqrt{\frac{1}{n_1} + \frac{1}{n_2}}} \quad \text{A.4.3}$$

Where n is the number of measurements performed in each measurement series and x the average measurement result obtained.

Critical values of t for a two-tailed test ($P=0.05$) obtained from table A.2, page 254 [276], where t has $(n_1 + n_2 - 2)$ degrees of freedom (v).

Summary of results obtained using the equations as described above:

Table A.4 Summary of significance test results

	TOP batch 1	TOP batch 2	NP batch 1	NP batch 2	BPA batch 1	BPA batch 2
x	70	79	84	43	10	26
s	2.8	2.37	21.8	9.5	1.5	2.08
n	7	5	8	5	8	5
F_{crit}	9.197		9.074		9.074	
F	1.396		5.330		1.923	
$F < F_{crit}$	Population standard deviation of the two batches are equal		Population standard deviation of the two batches are equal		Population standard deviation of the two batches are equal	
t_{crit}	2.23		2.20		2.20	
t	5.83		3.92		16.19	
$t > t_{crit}$	Means of the two batches differ significantly		Means of the two batches differ significantly		Means of the two batches differ significantly	

Appendix 5

PDMS MCT trap drying investigation

A few drops of bromothymol blue indicator was added to a 5 ml Milli-Q water sample. The water was sampled at a flow rate of $\sim 50 \mu\text{l}/\text{min}$ through the PDMS MCT. The presence of the bromothymol blue gave a visual indication of water still trapped inside the PDMS channels. These drops of water were best removed by mechanical dropping of the trap, as opposed to purging with gas. Dropping the trap down a 1.5 m length of tube provided enough force to break the capillary action occurring between the water and PDMS walls.

After sampling the PDMS MCT was weighed on a 4 decimal place balance. The trap was weighed after each drying step. A summary of the results obtained for the drying steps performed in series are shown in the graph below. The trap appears to reach a constant mass after purging with hydrogen gas for 2 minutes at a flow rate of 500 ml/min. An equivalent result is obtained by purging for 1 min at 1L/min. The mass difference between the last drying step and thermal desorption of the trap is 0.2 mg. The mass balance performance was not monitored and this mass difference could easily fall within the uncertainty of the balance. However, this mass difference was later assumed to be residual water vapour, even though no water could be visually observed after the last drying step, degradation on the PDMS trap was still observed.

Weighing the trap after plugging with the silica gel caps was not performed as such a small mass cannot be determined accurately on the available mass balance.

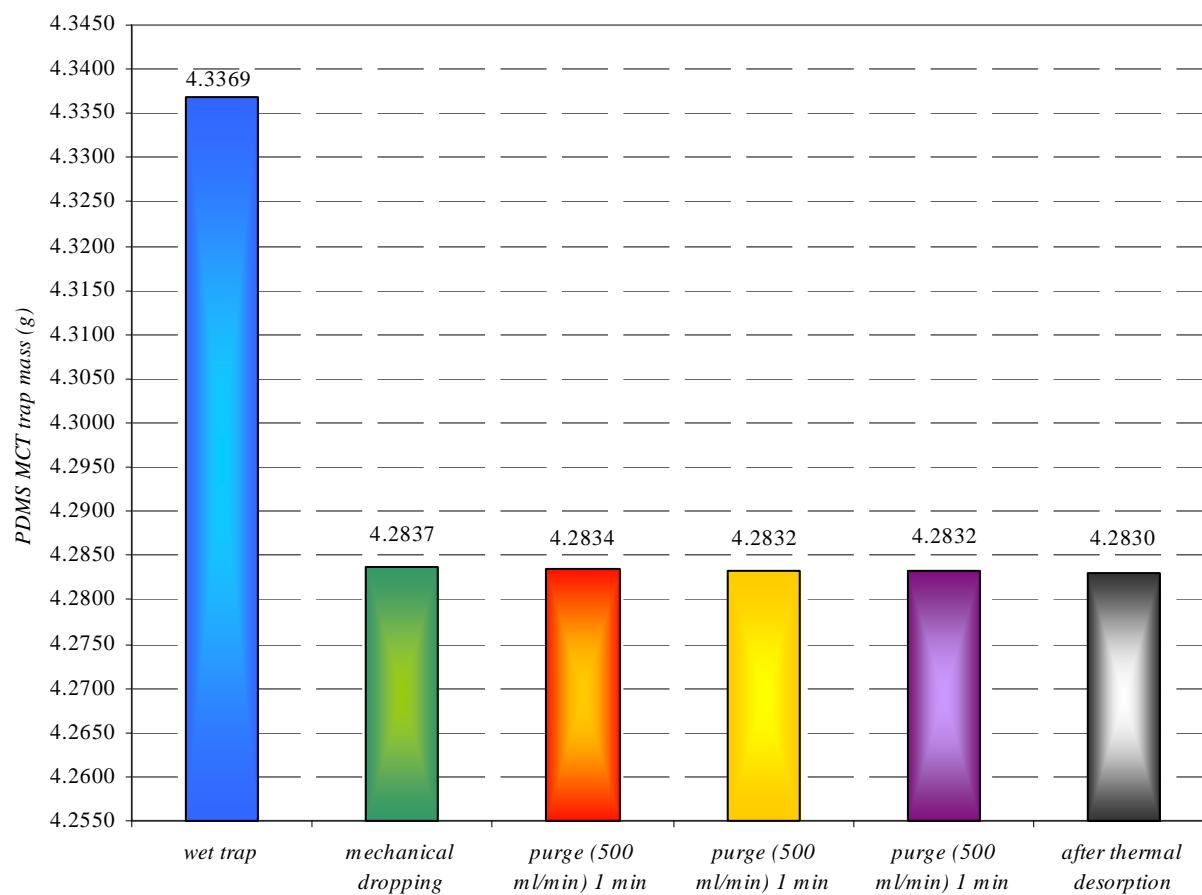


Figure A.5 Summary of the drying steps performed in series with the resulting PDMS MCT mass loss achieved from each drying step.



Appendix 6

Published article

Anal. Chem. **2005**, *77*, 1–10

Accelerated Articles

On-Line Derivatization for Resonance-Enhanced Multiphoton Ionization Time-of-Flight Mass Spectrometry: Detection of Aliphatic Aldehydes and Amines via Reactive Coupling of Aromatic Photo Ionization Labels

Maria Fernandes-Whaley,[†] Fabian Mühlberger,[‡] Alexander Whaley,[†] Thomas Adam,[‡]
Ralf Zimmermann,^{*,‡,§,||} Egmont Rohwer,^{*,†} and Andreas Walte^{||}

Department of Chemistry, University of Pretoria, Pretoria, 0002, South Africa, Institute for Ecological Chemistry, GSF Research Centre, 85764 Oberschleissheim, Germany, Analytische Chemie, Institut für Physik, Universität Augsburg, D-86159 Augsburg, Germany, BfA-Bayerisches Institut für Angewandte Umweltforschung und -technik GmbH, Abteilung für Umwelt- und Prozesschemie, D-86167 Augsburg, Germany, and Airsense Analytics, Hagenower Str. 73, 19061 Schwerin, Germany.

Resonance-enhanced multiphoton ionization time-of-flight mass spectrometry (REMPI-TOFMS) is a powerful technique for the on-line analysis of aromatic compounds with unique features regarding selectivity and sensitivity. Aliphatic compounds, however, are difficult to address by REMPI due to their unfavorable photo ionization properties. This paper describes the proof of concept for an on-line derivatization approach for converting nonaromatic target analytes into specific, photoionizable aromatic derivatives that are readily detectable by REMPI-TOFMS. A multichannel silicone trap or poly(dimethylsiloxane) (PDMS) open tubular capillary was used as a reaction medium for the derivatization of volatile alkyl aldehydes and alkylamines with aromatic “photoionization labels” and to concentrate the resulting aromatic derivatives. The aldehydes formaldehyde, acetaldehyde, acrolein, and crotonal, which when underivatized are poorly detectable by REMPI, were converted into their easily photoionizable phenylhydrazone derivatives by the on-line reaction with phenylhydrazine as reagent. Similarly, the methyl-, ethyl-, propyl-, and butylamines were converted into their REMPI-ionizable benzaldehyde alkylimine derivatives by the on-line reaction with benzaldehyde as reagent. The derivatives were thermally desorbed from the PDMS matrix and transferred into the REMPI-TOFMS for detection. The REMPI-TOFMS detection limits obtained for acetalde-

hyde; acrolein; crotonal; and methyl-, ethyl-, propyl-, and butylamine using this photo ionization labeling method were in the sub-parts-per-million range and, thus, readily below the permissible exposure limits set by OSHA.

There is an increasing awareness of the harmful effects that volatile aldehydes and amines, particularly formaldehyde, can have on human health. Formaldehyde is classified as a probable human carcinogen by the EPA, OSHA, NIOSH, and the ACGIH.^{1–3} Low-molecular-mass aldehydes and amines are typically eye, nose, and throat irritants.^{3–5} As volatile polar compounds, they are notoriously difficult to analyze. Real time monitoring of these trace

* Direct correspondence to either author. E-mails: erohwer@postino.up.ac.za, ralf.zimmermann@gsf.de.

[†] University of Pretoria.

[‡] GSF Research Centre.

[§] Universität Augsburg.

^{||} BfA-Bayerisches Institut für Angewandte Umweltforschung und -technik GmbH, Abteilung für Umwelt- und Prozesschemie.

^{||} Airsense Analytics.

- (1) *Chemical, Toxicity, Safety and Environmental Analysis Information for Formaldehyde*. <http://www.instantref.com/formald.htm>; Accessed Feb. 2, 2004.
- (2) Occupational Safety and Health Administration, U.S. Department of Labor. *OSHA Permissible Exposure Limits*; <http://www.osha-slc.gov/pls/oshaweb/>; Accessed Feb. 2, 2004.
- (3) Brabec, M. J. Aldehydes and Acetals. In *Patty's Industrial Hygiene and Toxicology*, 3rd rev. ed.; Clayton, G. D., Clayton, F. E., Eds.; John Wiley & Sons: New York, 1981; Vol 2A, pp 2692–2669.



organic compounds in air or process gases is not easily achieved. Measurement usually requires extended sample preconcentration, cleanup, and instrumental analysis, for example, by gas chromatography/mass spectrometry (GC/MS) in a well-equipped analytical laboratory.^{6–8} It involves a time-consuming and labor-intensive process that prevents the timely data generation required, for example, for effective pollution control measures.

Recently, several on-line monitoring methods based on direct inlet mass spectrometry (MS) with soft and selective ionization methods were established. This includes chemical ionization MS⁹ as well as photoionization MS techniques.^{10–19} One particularly powerful approach for real time monitoring of aromatic compounds is resonance-enhanced multiphoton ionization time-of-flight mass spectrometry (REMPI-TOFMS). The REMPI-TOFMS method, for example, has been used for the on-line monitoring of dioxin surrogates and other aromatic trace species in waste incinerator emissions,^{15,16} characterization of the formation of phenolic compounds during coffee roasting,^{17,18} and puff-resolved analysis of toxic aromatic compound release during the cigarette smoking process¹⁹ as well as the characterization of wood combustion.²⁰ In addition to the analysis of gaseous matrixes, solid matrixes can be handled as well in a two-step process using laser desorption followed by REMPI of the volatilized compounds.^{21–25} The REMPI process is based on a two-UV-photon absorption/ionization utilizing excited intermediate states (i.e., UV absorption bands) for resonance enhancement. Most aromatic compounds exhibit strong

absorption bands in the region is easily accessible by commercial laser systems. The combination of selectivity and immediate availability of mass spectral information eliminates the time-consuming separation step of gas chromatography. Unfortunately, many compounds not possessing an aromatic chromophore, such as aliphatic aldehydes and amines, cannot be easily detected by the rather simple one-color two-photon REMPI process. For example, many aldehydes require complicated REMPI schemes, which are based either on multilaser wavelength excitation or the inclusion of nonresonant multiphoton absorption steps. In other cases, as for many amines, the suitable REMPI wavelengths for the various compound homologues are different, preventing a simultaneous detection of the homologue profile.

A fast method for the on-line detection of aldehydes and amines, however, would have several potential applications in the field of process gas analysis, ambient air monitoring, or emission analysis. Furthermore, it would be desirable to also make use of the advantages of the REMPI-TOFMS method (i.e., selectivity, sensitivity, and measurement speed) for the detection of these aliphatic compounds. To make aldehydes and amines accessible to REMPI-TOFMS detection, a concept to convert the nonaromatic analytes into specific aromatic derivatives, which would then be detectable by the REMPI-TOFMS, was developed (“photoionization labeling”). Derivatization reactions which in principle can be used for “photoionization labeling” usually are performed in liquid solutions or, as recently demonstrated, in a poly(dimethylsiloxane) (PDMS) matrix as reaction medium. PDMS, for example, has been used for in situ derivatization of low-molecular-mass aldehydes for GC/MS analysis.^{26,27} The work presented here describes the development of a PDMS-based on-line “photoionization labeling” derivatization technique which can be directly hyphenated to the REMPI-TOFMS system. The PDMS devices are shown in Figure 1A. The principle of the “photoionization labeling” derivatization is as follows (depicted in Figure 1B).

The analytes from the sample gas current (i.e., containing traces of amines or aldehydes to be analyzed) as well as the derivatization reagent are coabsorbed in a PDMS trap. After a short enrichment phase, the trap is heated. The heating induces both the derivatization reaction itself and the thermal desorption of the formed derivatives. The desorbed derivatives are subsequently transferred to the REMPI-TOFMS spectrometer for analysis. This procedure can be repeated rapidly for a (quasi) on-line analysis.

At first, potential derivatization reactions were selected (derivatization of aldehydes with phenylhydrazine to form the respective phenylhydrazone derivatives and derivatization of amines with benzaldehyde to form the respective benzaldehyde alkylimine derivatives). The proof of principle (i.e., of efficient PDMS-mediated derivatization) was tested in a solid-phase microextraction (SPME) approach with GC/MS and GC-FID detection. Subsequently, an experimental on-line derivatization setup was built and coupled to the REMPI-TOFMS system. Two different setup variants were used for the derivatization procedure. In the first setup, a thermal modulator array²⁸ with a fused-silica capillary

- (4) Occupational Safety and Health Administration, U.S. Department of Labor. *OSHA Permissible Organic Method #36 Ethylamine*; <http://www.osha-slc.gov/dts/sltc/methods/organic/org036/org036.html>; Accessed Feb. 2, 2004.
- (5) Occupational Safety and Health Administration, U.S. Department of Labor. *OSHA Permissible Organic method #40 methylamine*; <http://www.osha-slc.gov/dts/sltc/methods/organic/org040/org040.html>; Accessed Feb. 2, 2004.
- (6) Otson, R.; Fellin, P. *Sci. Total Environ.* **1988**, *77*, 95–131.
- (7) Kennedy, E. R.; Teass, A. W.; Gagnon, Y. T. *Formaldehyde – Analytical chemistry and toxicology*; Turoski, V., Ed.; *Advances in chemistry and toxicology series*, 1985, *210*, 1–11.
- (8) Berezkin, V. G.; Drugov, Y. S. *J. Chromatogr. Libr.* **1991**, *49*, 190–194.
- (9) Munson, B. *Anal. Chem.* **1977**, *49*, 772–778A.
- (10) Lubman, D. M., Ed. *Lasers and Mass Spectrometry*; Oxford University Press: New York, 1990.
- (11) Cool, T. A.; Williams, B. A. *Combust. Sci. Technol.* **1992**, *82*, 67.
- (12) Boesl, U.; Zimmermann, R.; Weickhardt, C.; Lenoir, D.; Schramm, K.-W.; Kettrup, A.; Schlag, E. W. *Chemosphere* **1994**, *29*, 1429.
- (13) Miller, J. C.; Compton, R. N. *J. Chem. Phys.* **1982**, *76* (8), 3967.
- (14) Nomayo, M.; Thanner, R.; Pokorny, H.; Grotheer, H.-H.; Stützel, R. *Chemosphere* **2001**, *43*, 461–467.
- (15) Mühlberger, F.; Zimmermann, R.; Kettrup, A. *Anal. Chem.* **2001**, *73*, 3590–3604.
- (16) Heger, H. J.; Zimmermann, R.; Dorfner, R.; Beckmann, M.; Griebel, H.; Kettrup, A.; Boesl, U. *Anal. Chem.* **1999**, *71*, 46–57.
- (17) Dorfner, R.; Ferge, T.; Yerezian, C.; Kettrup, A.; Zimmermann, R. *Anal. Chem.* **2004**, *76* (5), 1386–1402.
- (18) Dorfner, R.; Ferge, T.; Kettrup, A.; Zimmermann, R.; Yerezian, C. *J. Agric. Food Chem.* **2003**, *51* (19), 5768–5773.
- (19) Zimmermann, R.; Heger, H. J.; Kettrup, A. *Fresenius' J. Anal. Chem.* **1999**, *363*, 720–730.
- (20) Hauler, T. E.; Boesl, U.; Kaesdorf, S.; Zimmermann, R. *J. Chromatogr., A* **2004**, in press.
- (21) Engelke, F.; Hahn, J. H.; Henke, W.; Zare, R. N. *Anal. Chem.* **1987**, *59*, 909–912.
- (22) Clemett, S. J.; Maechling, C. R.; Zare, R. N.; Swan, P. D.; Walker, R. M. *Science* **1993**, *262*, 721–725.
- (23) Dale, M. J.; Jones, A. C.; Pollard, S. J. T.; Langridge-Smith, P. R. R.; Rowley, A. G. *Environ. Sci. Technol.* **1993**, *8*, 1693–1695.
- (24) Dale, M. J.; Downs, O. H. J.; Costello, K. F.; Wright, S. J.; Langridge-Smith, P. R. R.; Cape, J. N. *Environ. Pollut.* **1995**, *89*, 123–129.
- (25) Haefliger, O. P.; Bachel, T. D.; Zenobi, R. *Analyst* **1999**, *27*, 337–340.

(26) Martos, P. A.; Pawliszyn, J. *Anal. Chem.* **1998**, *70*, 2311–2320.

(27) Fernandes, M. J. M.Sc. thesis, University of Pretoria, Pretoria, 2001.

(28) Burger, B. V.; Snyman, T.; Burger, V. J. G.; van Rooyen, W. F. *J. Sep. Sci.* **2003**, *26*, 123–128.

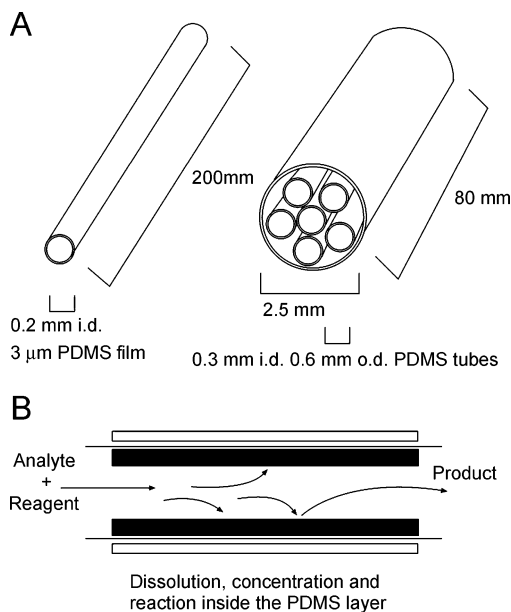


Figure 1. Two variations of silicone (PDMS) concentrators are shown in A, namely, the thick film capillary trap, used in the thermal modulator array (TMA), and the multichannel silicone rubber trap (MCSRT) used in the EDU. B Cross section of a capillary trap, which demonstrates the concentration and reaction within these concentrating devices.

column ($3\text{-}\mu\text{m}$ silicone film, DB-1 equivalent) is used to absorb, derivatize, desorb, and refocus the analytes. The second setup consists of an enrichment desorption unit (EDU; Airsense Analytics, Schwerin, Germany)²⁹ with a multichannel silicone rubber trap^{27,30,31} as PDMS medium for derivatization followed by the above-mentioned arrangement with the thermal modulator array.²⁸ These experimental setups are shown in Figure 2A, B, and C, respectively.

EXPERIMENTAL SECTION

(A) Derivatization Reaction for “Photoionization Labeling” of Amines and Aldehydes. Phenylhydrazine^{32,33} and benzaldehyde³³ were selected as “photoionization labeling compounds” and were used to derivatize the aldehydes (formaldehyde, acetaldehyde, acrolein, and crotonal) and amines (methylamine, ethylamine, propylamine, butylamine), respectively. Methylamine, ethylamine, propylamine, benzaldehyde, formaldehyde (36.5% in water), and phenylhydrazine were purchased from Aldrich (Taufkirchen, Germany). Acetaldehyde, acrolein, and crotonal were obtained from Merck (Darmstadt, Germany). Butylamine was obtained from ChemService (Johannesburg, S. A.). *Caution: Because phenylhydrazine is highly poisonous and formaldehyde is a potential carcinogen, it is essential always to wear gloves and avoid inhalation when working with these reagents.*

Schemes for the deriva formed are shown in Figure 3A and B. These reagents were selected to introduce a REMPI-active chromophore to the analyte structure. Substituted rings, such as pentafluorinated benzaldehyde, were discarded because they pose the risk of reducing the REMPI efficiency. In addition, in order for the reaction to occur efficiently, both reagents had to possess a significant vapor pressure to ensure that the reagent would be present in excess in the gas phase. Stable gaseous concentrations of the analytes were obtained by preparing permeation and diffusion gas standards of the respective aldehydes and amines. Gas standard preparation and measurement has been described in the literature.^{34,35} Concentrations provided by the gas standards are listed in Table 1. Headspace from formaldehyde (stabilized with methanol in water) was used as the formaldehyde gas source. This concentration is rather high and could not be determined in the framework of the experiments presented here.

(B) Setup for SPME GC-FID-Based Testing of the PDMS-Mediated Derivatization Reactions. Simple reaction tests were performed to determine whether the selected derivatization reaction would take place in the PDMS and to estimate how efficiently the arrangement would trap the analyte. Figure 2A shows the on-line setup used to determine the approximate reaction efficiency for the various derivatization reactions. The gas standards were purged with nitrogen gas at a flow rate of 4 mL/min. The gas standards provide a known concentration of analyte gas into the glass Y press-fit connector³⁶ (obtained from Chromatography Research Supplies, Inc., Louisville, KY) via an uncoated length of fused-silica capillary. Similarly, the derivatizing reagent, also being purged with nitrogen gas at 4 mL/min, was introduced at the other end of the Y press-fit connector. A 1-mL portion of the derivatizing reagent was placed in a 2-mL vial and sealed with a crimp cap. Two holes were pierced into the septum of the vial. A length of uncoated fused-silica capillary was pushed through each hole in the septum. One capillary was connected to the nitrogen gas, the other to the Y press-fit connector. Leading from the combined exit of the Y press-fit connector was another length of uncoated fused-silica capillary. The measured flow rate at this point was 8 mL/min, similar to the flows obtained from the REMPI-TOFMS vacuum. The exiting capillary was sealed into another glass press-fit connector, the opposite end of which was modified to house the exposed SPME fiber.

Current concentration methods are mainly off-line.^{37–39} Solid-phase microextraction (SPME)^{26,40} and the multichannel silicone rubber trap (MCSRT)²⁷ are two examples of a novel technique that uses poly(dimethylsiloxane) as the concentration and reaction medium, eliminating problems experienced with earlier concentration methods.^{27,37–39} In situ derivatization in PDMS has been used to trap low-molecular-mass aldehydes for GC-FID and GC/MS analysis.^{26,27} The PDMS concentrators used in this study are

(29) Walte, A. *Airsense Analytics Dilution, Enrichment and Desorption Unit Handbook*, WMA Airsense Analysentechnik, GmbH: Schwerin, Germany, 2001.
(30) Ortner, E. K.; Rohwer, E. R. *J. High Resolut. Chromatogr.* **1996**, *19*, 339–344.
(31) Ortner, E. K.; Rohwer, E. R. *J. Chromatogr., A* **1999**, *863*, 57–68.
(32) Vogel, M.; Büldt, A.; Karst, U. *Fresenius' J. Anal. Chem.* **2000**, *366*, 781–791.
(33) Blau, K.; King, G. S. *Handbook of derivatives for chromatography*; Heyden & Son Ltd.: London, U.K., 1979.

(34) Namiesnik, J. *J. Chromatogr., A* **1984**, *300*, 79–108.
(35) Scarangelli, F. P.; O'Keefe, A. E.; Rosenberg, E.; Bell, J. P. *Anal. Chem.* **1970**, *42*, 871–876.
(36) Rohwer, E. R.; Pretorius, V.; Apps, P. J. *J. High Resolut. Chromatogr.* **1983**, *9*, 295–297.
(37) Berezkin, V. G.; Drugov, Y. S. *J. Chromatogr. Libr.* **1991**, *49*, 35–119.
(38) Namiesnik, J. *Talanta* **1988**, *35*, 567–587.
(39) Stashenko, E. E.; Ferreira, M. C.; Sequeda, L. G.; Martinez, J. R.; Wong, J. W. *J. Chromatogr., A* **1997**, *779*, 360–369.
(40) Pawliszyn, J. *Solid-Phase Microextraction – Theory and Practice*; Wiley-VCH: Canada, 1997.

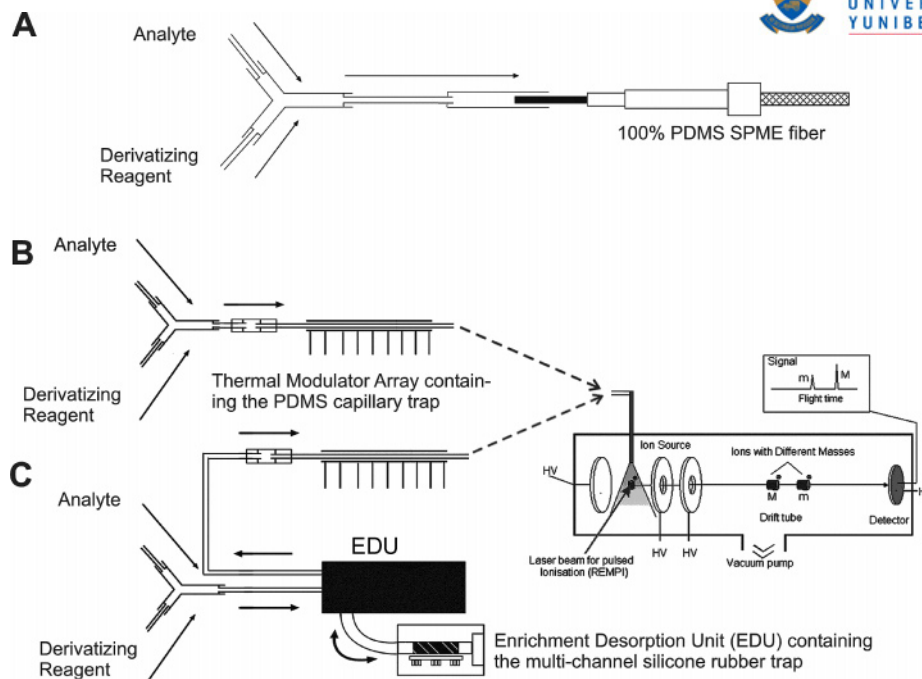


Figure 2. Experimental setup used for (A) determining the reaction efficiencies for the on-line derivatization reactions, (B) on-line concentration and derivatization for REMPI-TOFMS using the thermal modulator array (TMA) with a thick-film capillary as enrichment and reaction medium, and (C) on-line concentration and derivatization for REMPI-TOFMS using a MCSRT in an EDU as enrichment and reaction medium and the TMA with a thick film capillary for analyte modulation.

Table 1. Gas Standard Concentrations and Calculated Detection Limits for the Aldehydes and Amines Studied^a

analytes (<i>m/z</i>)	gas std concn EDU-TMA (ppm v/v)	detection limit (S/N = 2 av 10) EDU-TMA (ppm v/v)	gas std concn TMA (ppm v/v)	detection limit (S/N = 2 av 10) TMA (ppm v/v)	PEL OSHA (ppm)
formaldehyde (120)					0.75
acetaldehyde (134)			79.4	2.04	200
acrolein (146)			37.4	0.101	0.1
crotonal (160)			199	1.52	2
methylamine (119)	34.3	0.257			10
ethylamine (133)	1.4	0.010	21.7	0.324	10
propylamine (147)	1.8	0.024	27.6	0.138	
butylamine (161)	2.9	0.100	44.7	0.501	5

^a Permissible exposure limits (PEL) as set by OSHA are also listed (see ref 2).

depicted in Figure 1A. The SPME device consists of a 100- μ m PDMS-coated fiber mounted on the tip of a syringe needle, which is housed within the syringe barrel when not exposed during sampling.⁴⁰ A 100- μ m PDMS SPME fiber was exposed over increasing time intervals to a similar on-line arrangement used for the REMPI-TOFMS shown in Figure 2B. The SPME assembly and 100- μ m PDMS fibers were obtained from Supelco (Bellefonte, PA). The fiber was desorbed in the heated inlet of a Varian 3300 GC at 150°C for 1 min. Quantitation was performed by flame ionization detection (FID) using undecane as internal standard and relative effective carbon number responses of the derivatives.^{27,41,42} Thermal desorption of the SPME fiber is performed simply and quickly in the heated inlet of the GC oven; however, desorption of the silicone trap requires a desorption unit with some form of cooling in order to focus the desorbed contents onto the GC column. This is usually a longer process.²⁷ When the above

procedure is carried out in GC-FID or GC/MS, the low initial temperature of the GC oven also acts to focus or concentrate the derivatized analyte in a short band. For real-time on-line applications, in the absence of such a focusing mechanism in the direct coupling of the trap to the TOFMS, another concentration device is required to enhance detectability. The results for this experiment are shown in Figure 4.

(C) REMPI-TOFMS. The resonance-enhanced multiphoton ionization time-of-flight mass spectrometer used for this application is a home-built system containing a pulsed Nd:YAG laser (Quanta-Ray INDI 50; Spectra Physics, Stratford, CT). The initial 1064-nm laser beam (repetition rate 10 Hz, pulse duration 10 ns) is frequency tripled, and the resulting wavelength of 355 nm is used to pump a β -BBO crystal of a thermally stabilized type II OPO-laser system (GWU-Lasertechnik, Germany) to generate wavelength-tuneable laser pulses in the range of 220 nm to 2.5 μ m. The generated laser pulses ($\sim 10^6$ W cm⁻²) are directed into the ionization chamber of the TOF (Kaessdorf Instruments, Germany)

(41) Scanlon, J. T.; Willis, D. E. *J. Chromatogr. Sci.* **1985**, *23*, 333–340.

(42) Tong, H. Y.; Karasek, F. W. *Anal. Chem.* **1984**, *56*, 2124–2128.

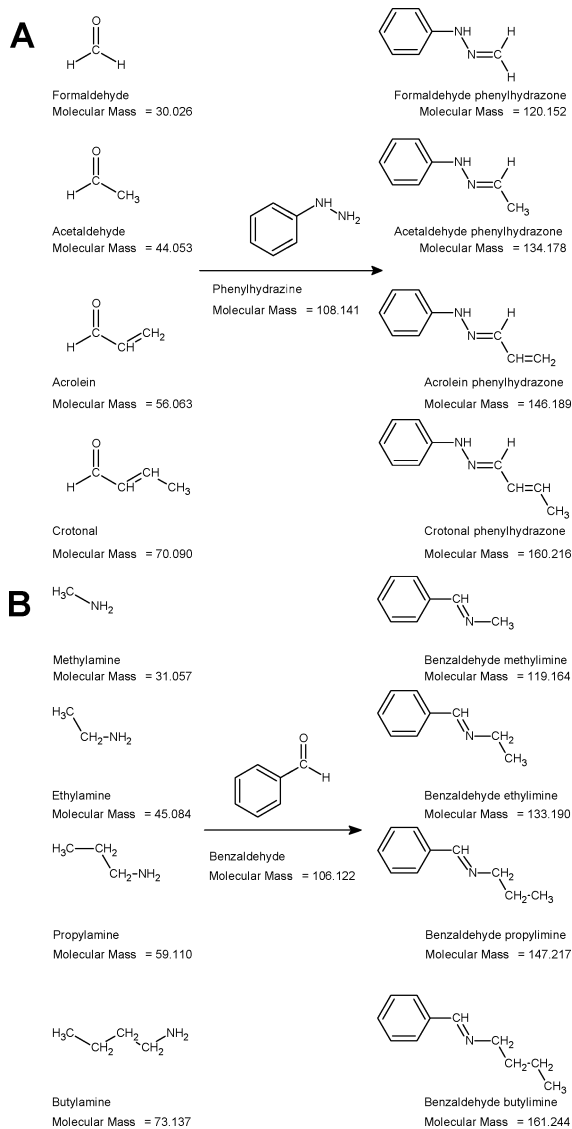


Figure 3. Reaction schemes for the derivatization of (A) the aldehydes with phenylhydrazine and (B) the alkylamines with benzaldehyde.

underneath the jet capillary inlet by optical elements. Molecular ions formed are accelerated and extracted into the flight tube of the reflectron TOFMS. Mass spectra are recorded via a transient recorder PC card (Aquiris, Switzerland, 250 MHz, 1 GS/s, 128 k) whereby data processing is done by LabView (National Instruments, Austin, TX)-based home-written software. Wavelengths of 244 and 246 nm were selected for REMPI-TOFMS analysis of the formaldehyde- and acrolein-phenylhydrazone derivatives, respectively, and 240 nm for the benzaldehyde alkylimine derivatives. Spectroscopic investigations showed that for the REMPI-TOFMS setup used, these wavelengths are very efficient.

(D) On-Line Derivatization Setup for REMPI-TOFMS.

Figure 2B and C shows the on-line derivatization REMPI-TOFMS setups. Unlike the arrangement for principal testing (SPME), the gas standards and reagents were not purged with nitrogen gas. In this case, the mass spectrometer vacuum provides the flow into the REMPI-TOFMS. On-line in situ derivatization was investigated using two different enrichment desorption devices:

(i) a thermal modulator ϵ trap (TMA) and (ii) an enrichment desorption unit with a multichannel PDMS rubber trap. Two setup variants were tested. In the first setup, only the thermal modulator array (i) with a PDMS thick-film capillary trap was used, whereas in the second setup, the enrichment desorption unit with a multichannel PDMS rubber trap (ii) was applied in combination with the thermal modulator array with a PDMS thick-film capillary trap (i).

In the following, the two experimental setups are described in more detail.

First Setup: Direct Supply of Analytes and Reagents through the Thermal Modulator Array (TMA-REMPI-TOFMS). The centerpiece of the derivatization setup is the segmented thermal modulator array.²⁸ The modulator houses a narrow bore capillary coated on the inside with a thick film of PDMS (capillary trap). This capillary represents the concentrating/derivatizing device. The amount of PDMS within the capillary is comparable to the amount of PDMS forming the SPME fiber. In detail, the modulator capillary consisted of a fused-silica capillary column (0.2-mm i.d.) coated with nonpolar phase PS-255 (3- μ m film, DB-1 equivalent). A capillary of 20-cm length was used with 5 cm of the stationary phase stripped off on either end, as described in reference 28.

A stainless steel capillary (105 mm \times 0.6 mm o.d. \times 0.35 mm i.d.) was converted to a modulator.²⁸ An electronic sequencer was used to provide current to the modulator in steps from 1 to 10 A at 5 V with a time duration of 10–2500 ms. To maintain reasonable flow rates and operate at atmospheric pressure, jet restrictors yielding a flow rate of between 0.6 and 1.0 mL/min were prepared according to the method described in reference 43 from an uncoated capillary (30 cm \times 0.32 mm i.d.). The restrictor was coupled to the modulator capillary with a suitable press-fit. All transfer capillaries and connection points were either directly heated to 150 °C, by a heating mantle or surrounded by a copper tube, which was then heated by a heating mantle.

Modulators have predominantly been developed for use as an interface between two columns in comprehensive two-dimensional gas chromatography.⁴⁴ Its function is to rapidly focus fractions of effluent from the first column onto the head of the second column. In this work, a modulator is used to transfer and focus the effluent from the capillary trap into the REMPI-TOFMS.

In principle, the sorption and desorption of effluent from the stationary phase in the modulator capillary can be controlled by careful manipulation of the capillary temperature. This was originally achieved by painting a segment of the modulator capillary with an electrically conductive paint, thus allowing the capillary to be resistively heated.^{45,46} This modulator was tedious to prepare and did not prove robust. Alternatively, a copper wire could be coiled around the modulator capillary.⁴⁷ A mechanically driven thermal sweeper was developed to eliminate the high thermal inertia experienced by the metal painted modulator.⁴⁸ A moveable slotted heating element was used to “sweep” periodically over the modulator capillary. This design demonstrates good

(43) Hafner, K.; Zimmermann, R.; Rohwer, E. R.; Dorfner, R.; Kettrup, A. *Anal. Chem.* **2001**, *73*, 4171–4180.

(44) Phillips, J. B.; Beens, J. *J. Chromatogr., A* **1999**, *856*, 331.

(45) Liu, Z.; Phillips, J. B. *J. Microcolumn Sep.* **1994**, *6*, 229.

(46) Phillips, J. B.; Xu, J. *J. Chromatogr., A* **1995**, *703*, 327.

(47) de Geus, H. J.; de Boer, J.; Phillips, J. B.; Brinkman, U. Th. *J. Chromatogr., A* **1997**, *767*, 137.

(48) Phillips, J. B.; Ledford, E. B. *Field Anal. Chem. Technol.* **1996**, *1*, 23.

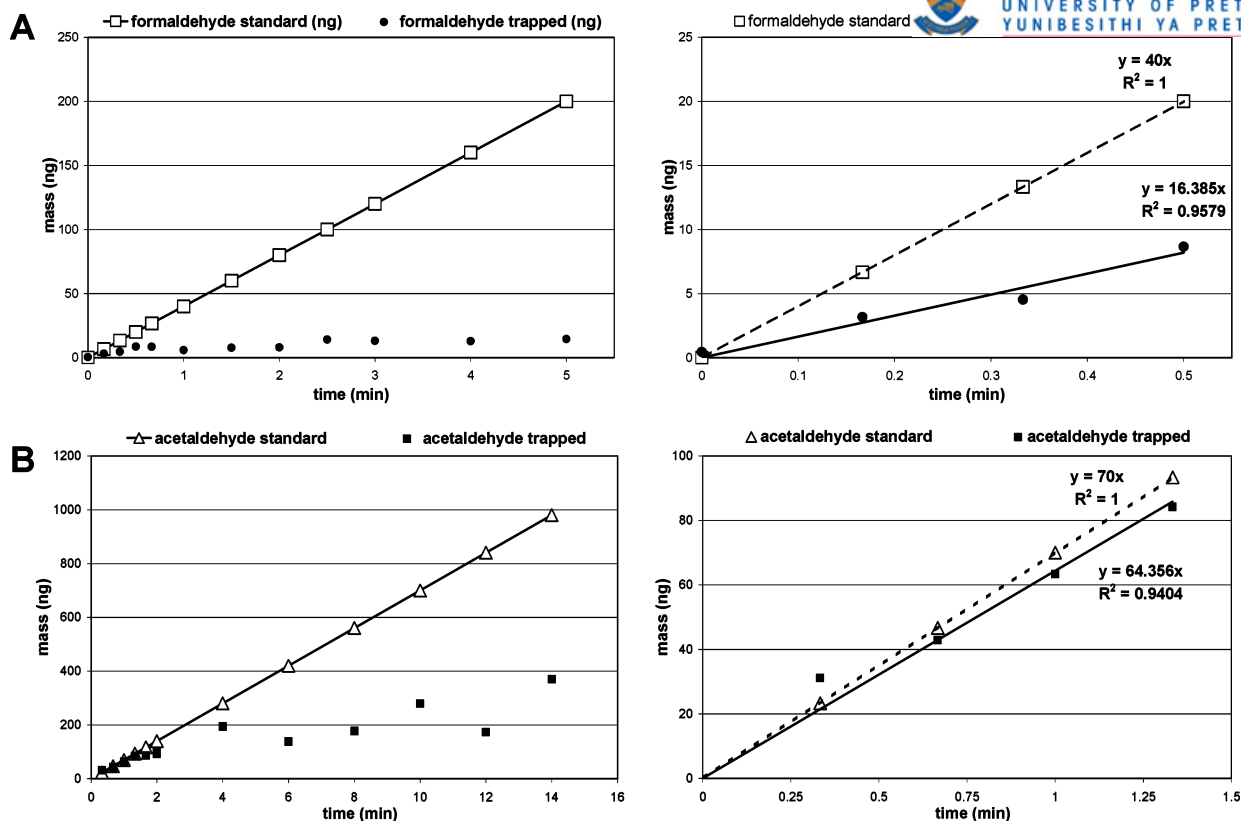


Figure 4. Reaction efficiency results for the on-line derivatization of (A) formaldehyde and (B) acetaldehyde with phenylhydrazine. Both graphs display (i) the amount of gas standard released over that time interval, as determined by their permeation rate, and (ii) the amount of analyte gas trapped using in situ derivatization on the SPME fiber as calculated using the internal standard and effective carbon number response for the signal obtained from the GC-FID for the derivative. The graphs on the right-hand side represent an enlargement of the left-hand side graphs, where the initial accumulation on the SPME fiber appears linear. A comparison of the gradients obtained from the standard and the actual amount of analyte trapped gives an approximation of the reaction/trapping efficiency for this reaction.

temperature control and focusing, but is too bulky and complex, requiring the heating element to be at least 100°C higher in temperature than the capillary to effectively focus the effluent.⁴⁵ Thus, much attention has been given to cryogenic modulators. A longitudinal modulating cryogenic system^{49,50} consists of a moveable steel sleeve, which surrounds the capillary. Liquid CO₂ is supplied at timed intervals into the sleeve to cool the capillary. The GC oven provides heating to the capillary segments not being cooled by the moving sleeve. A similar approach in which the CO₂ is sprayed directly onto the capillary⁵¹ was also used; however, contact of the moving modulator with the second column often causes column breakage. Therefore, a nonmoving dual jet cooling modulator was developed. Two different types exist: the first uses two nonmoveable CO₂ jets to cool the capillary trap while the GC oven is used for heating.⁵² The second, from the ZOEX Corporation, uses two cold and two warm nonmoveable nitrogen jets to cool and reinject the effluent from the capillary into the second column.⁵³ Although the cryomodulators provide excellent refocus-

ing of effluent, they require expensive cryogenics that require attention when in use.

The thermal modulator array²⁸ is an improved combination of the metal-painted and “sweep” modulators described above. Rapid resistive heating of consecutive segments of a stainless steel tube surrounding the capillary focuses the effluent inside the modulator capillary. This provides the “sweeping” heat motion without the disadvantageous cold spots or moveable parts. The segmented heating of the effluent in the capillary speeds up the chromatographic process in the capillary column, “compressing” zones from the rear and providing a focused chromatographic band that enters the REMPI-TOFMS. Although not providing the shortest injection pulse widths, the TMA is simple and compact; it does not require cryogenic cooling and can operate unattended, making it suitable for on-line analysis with the REMPI-TOFMS.

The outlet of the TMA device was directly coupled to the TOFMS. This setup was tested for detecting amines using benzaldehyde as photoionization labeling compound. Reagent and analytes (amine gas standard) were introduced simultaneously for 10 min into the cooled, PDMS, narrow bore, thick-film capillary trap (inside the modulator steel tube) where the reaction occurred. In this case, the MS vacuum provided a sampling flow rate of 0.7 mL/min. During modulation, the derivatives were desorbed into the REMPI-TOFMS. Similarly, the derivatization of the aldehydes

(49) Kinghorn, R. M.; Marriot, P. J. *Anal. Chem.* **1997**, *69*, 2582.
 (50) Kinghorn, R. M.; Marriot, P. J.; Dawes, P. A. *J. Microcolumn Sep.* **1998**, *10* (7), 611.
 (51) Beens, J.; Delluge, J.; Adachour, M.; Vreuls, R. J. J.; Brinkman, U. Th. *J. Microcolumn Sep.* **2001**, *13* (3) 134.
 (52) Beens, J.; Adachour, M.; Vreuls, R. J. J.; van Alena, K.; Brinkman, U. Th. *J. Chromatogr., A* **2001**, *919*, 127.
 (53) Ledford, E. B., Jr.; Billesbach, C. J. *High Resolut. Chromatogr.* **2000**, *23*, 202.

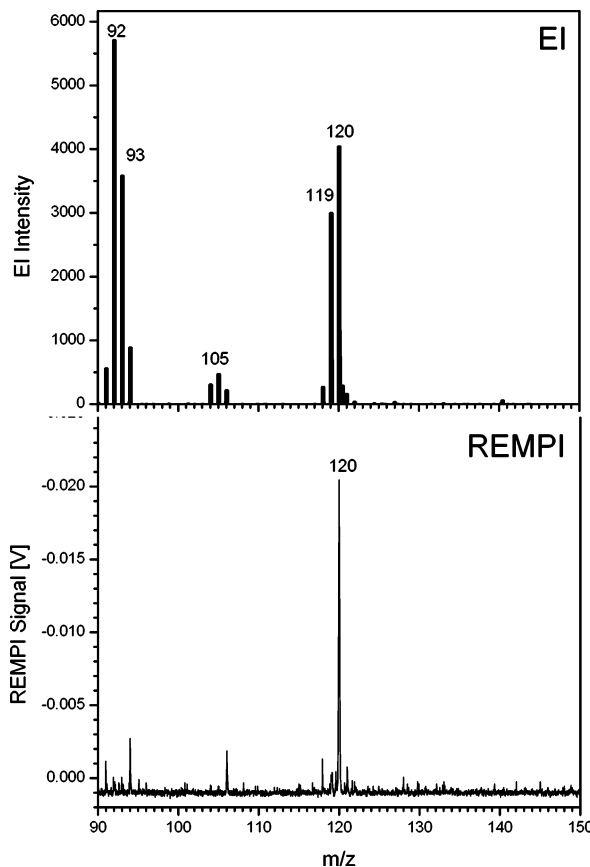


Figure 5. Mass spectra obtained for the formaldehyde–phenylhydrazone derivative using two different ionization techniques. The EI mass spectrum was obtained from a prepared derivative on an accurate mass GC/TOFMS. The REMPI mass spectrum at 244 nm was obtained from the on-line concentration and derivatization experiment (using the TMA setup).

with phenylhydrazine was demonstrated using only the modulator trap, followed by REMPI-TOFMS detection. The results obtained with the TMA-REMPI-TOFMS setup are given in Table 1 and Figures 5 and 6.

Second Setup: Supply of Analytes and Reagents to an Enrichment Desorption Unit prior to the TMA (EDU-TMA-REMPI-TOFMS). The second setup used is as shown in Figure 2 C. Here, the multichannel silicone rubber trap in the enrichment desorption unit is used as concentration–reaction medium, and the TMA is used for subsequent temporal focusing. The multichannel silicone rubber trap consists of a glass tube containing several smaller silicone rubber tubes, each 10 cm long, arranged in parallel,^{27,30,31} as shown in Figure 1A. SIL-TEC medical grade silicone tubing for the silicone rubber trap was obtained from Technical Products Inc. (Georgia, U.S.A). It has been shown that the MCSRT can be used as an *inert* absorptive (off-line) concentrator^{27,30,31} having a very low pressure drop (or flow resistance) with properties similar to the packed PDMS trap,^{54–56} which has demonstrated better properties than other current off-line concentration methods.

The MCSRT is placed within the enrichment desorption unit that is connected via the TMA to the REMPI-TOFMS (EDU-TMA-REMPI-TOFMS). The EDU is an automated stand-alone sampling

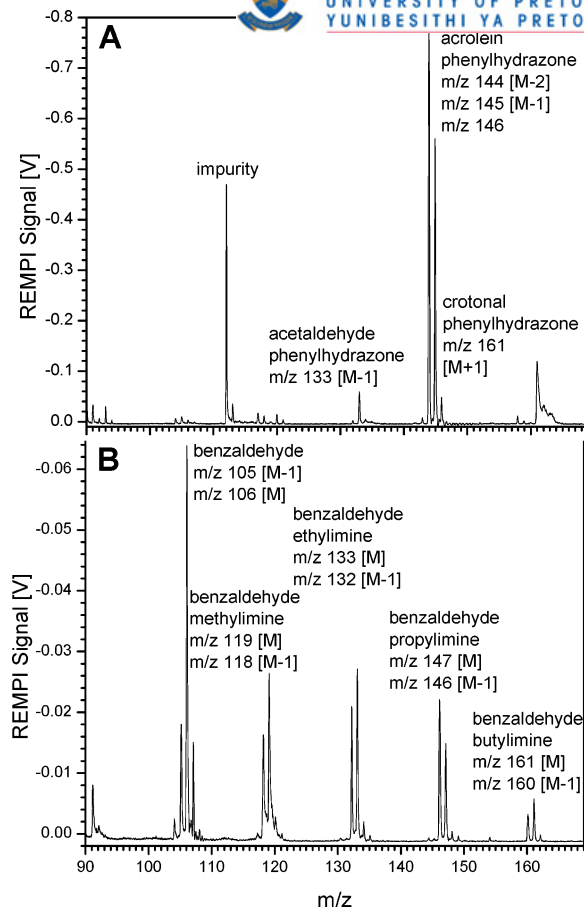


Figure 6. REMPI-TOF mass spectra obtained for the on-line concentration and derivatization of (A) acetaldehyde, acrolein, and crotonal with phenylhydrazine at 246 nm (using the TMA setup) and (B) methylamine, ethylamine, propylamine, and butylamine with benzaldehyde at 240 nm (using the EDU-TMA setup).

and desorption device (Airsense Analytics, Schwerin, Germany). The principal difference between SPME (or the application of TMA solely) and MCSRT is the amount of PDMS available for concentration of analytes, with the MCSRT having a considerably larger amount of PDMS (approximate PDMS volumes are TMA trap 0.2 mm³ and the MCSRT 135 mm³). Thus, the MCSRT can concentrate and derivatize more analyte and, therefore, has the potential to provide lower detection limits.

The EDU system used in this work is a unique trap and thermal desorption system developed by Airsense Analytics for the Institute of Ecological Chemistry, GSF. Gaseous substances are trapped at sampling temperatures (ambient or less) on, for example, Tenax adsorption tubes and analyzed after thermal desorption. The enrichment factor is related to many different physical and sampling parameters. It can be calculated on the basis of breakthrough volumes known from common tables. Typically, the detection limit can be reduced by a factor of 20 with volatile compounds and up to 1000 with low volatiles. Temperatures of the adsorbent during sampling and desorption phases can be adjusted via settings within the related software EDU.

(55) Baltussen, E.; David, F.; Sandra, P.; Janssen, H. G.; Cramers, C. A. J. *High Resolut. Chromatogr.* **1998**, *21*, 332–340.

(56) Baltussen, E.; den Boer, A.; Sandra, P.; Janssen, H. G.; Cramers, C. A. *Chromatographia* **1999**, *49*, 520–524.

(54) Baltussen, E.; David, F.; Sandra, P.; Janssen, H. G.; Cramers, C. A. J. *High Resolut. Chromatogr.* **1997**, *20*, 385–393.



For increasing the speed of analysis, very small tubes with inner diameters of 1.5 mm filled with Tenax-TA can be used. With applications in very damp environments, this hydrophobic polymer is advantageous because it eliminates the negative influence of humidity on the analysis.

Peltier cooling is used in order to achieve sampling temperatures of 4 °C. After sampling, the tubes are desorbed by resistive heating. With this flash desorption, temperature increments of 200 °C are possible in just 4 s. The complete system is controlled by a microprocessor unit, which is programmed through a serial port.

By sucking air through a cold adsorption tube, the analytes are trapped. In the case of sampling hot gases, it is also possible to dilute the sampling gas to reduce the temperature of the gas. After sampling, a postsampling step is possible to sweep away noninteresting gases and vapors (e.g., humidity).

To extract analytes off the trap, thermal desorption is performed. For injection, the gas flow is reversed and leads into the detection system. Afterward, the tube is cleaned by heating it to a higher temperature than the desorption temperature and flushing the tube with cleaned air. After cooling to near ambient temperatures, the trap is ready for the next measurement. All analytical steps, sampling, postsampling, desorbing, injecting, cleaning, and cooling are performed automatically.

For in situ derivatization, illustrated in Figure 1B, the aromatic derivatizing reagent, in the gas phase, dissolves into the PDMS. Carbonyl compounds (aldehydes and ketones etc.), which pass through the trap, react selectively with the reagent and remain in the trap until they are thermally desorbed for analysis.^{26,27} In the case of the above-mentioned SPME-GC-FID approach, the desorption is performed for some time in the heated GC injector,^{26,27,40} and the derivatized analytes are refocused in a short band due to low initial temperature of the GC oven. For on-line real-time analytical applications, however, analyte focusing can also be important, although not for the enhancement of the chromatographic resolution, but for time resolution and sensitivity. Analyte focusing can be achieved, as described in the first setup, by repetitive thermal modulation. Therefore, in this setup, the EDU is used in combination with a segmented thermal modulator array, as described above. Conditions for the EDU used in these experiments were as follows: sampling for 130 s at 6 °C with a sampling flow rate of 230 mL/min and thermal desorption for 60 s at 180 °C. Injection occurs under reversed flow conditions. During injection, the desorbed compounds are drawn into the REMPI-TOFMS at a flow rate of 15 mL/min, as restricted by the capillary jet leading into the ion source. Both the sampling line and the transfer line into the MS are heated at 150 °C. Benzaldehyde was sampled for 60 s through the heated sampling line. After 10 s, the amine gas mixture was sampled through the sampling line for 60 s. The sampling flow rate was 230 mL/min. Benzaldehyde accumulates in the PDMS multichannel trap, cooled to 6 °C. The introduced amine gas subsequently reacts with the benzaldehyde in the trap. The reaction is further encouraged during desorption at 150 °C for 1 min. During the injection phase, the derivatives are transferred to the TMA, which submits timely focused concentrated pulses to the REMPI-TOFMS system. The results obtained with the EDU-TMA-REMPI-TOFMS setup are given in Table 1 and Figure 6.

Table 2. Approximation of Reaction Efficiency of On-Line Derivatization Reaction Efficiencies at Room Temperature without Catalyst, as Determined by SPME Setup (see Figure 2A)

compound	reagent	% reaction efficiency	R^2 (n)
formaldehyde	phenylhydrazine	41	0.9579 (4)
acetaldehyde	phenylhydrazine	92	0.9404 (4)
acrolein	phenylhydrazine	61	0.9990 (4)
crotonal	phenylhydrazine	74	0.9251 (4)
propylamine	benzaldehyde	28	0.9570 (4)
butylamine	benzaldehyde	28	0.9205 (4)

RESULTS AND DISCUSSION

In the first experiments, the reaction efficiency of the selected derivatization reagents with the selected analytes was tested with the SPME GC-FID approach. The reaction efficiency graphs shown in Figure 4 for the on-line derivatization of formaldehyde and acetaldehyde with phenylhydrazine display the increasing mass accumulation of derivative on the SPME fiber over time. Both graphs display (i) the amount of gas standard released over that time interval, as determined by their permeation rate, and (ii) the amount of analyte gas trapped using in situ derivatization on the SPME fiber, as calculated using an internal standard and the effective carbon number response for the signals obtained from the GC-FID for the desorbed derivatives.^{27,41,42} The graphs on the right represent an enlargement of the graphs on the left, where the initial accumulation on the SPME fiber appears linear. A comparison of the initial gradients obtained from the analyte standard and the actual amount of analyte trapped gives an approximation of the reaction/trapping efficiency for this reaction.²⁷ The flattening off of the accumulation curves over time is the result of increased loss or “breakthrough” of the reaction product from the SPME fiber concentrator. The reaction efficiency data, shown in Table 2, were obtained at room temperature using the arrangement in Figure 2A. In Table 2, approximate reaction efficiencies of 28% for the reaction of propylamine and butylamine with benzaldehyde, 30% for the formaldehyde reaction with phenylhydrazine, and around 70% for the aldehydes with phenylhydrazine are indicated.

Incomplete reaction was confirmed by single photon ionization time-of-flight mass spectrometry (SPI-TOFMS)^{15,42} of the on-line, in situ derivatization of propylamine (59 m/z) and butylamine (m/z 73) with benzaldehyde (m/z 106). The presence of both derivatized (161 and 147 m/z) and underivatized analyte (59 and 73 m/z) was observed. Although these derivatization reactions are not 100% efficient at room temperature, they still occur readily without the aid of any catalysts. Thus, for quantitation, the use of internal or external standards is required. The results of the on-line tests with REMPI-TOFMS detection are given below. The experiments demonstrated that all investigated amines and aldehydes could be successfully derivatized, desorbed, and identified by REMPI-TOFMS using the on-line setups described above. Figure 5 displays the results obtained for formaldehyde. In the upper part (A), a conventional 70-eV EI mass spectrum for the formaldehyde–phenylhydrazone derivative is shown. This mass spectrum was obtained from a formaldehyde–phenylhydrazone derivative, pre-



pared using the method described by Vogel et al.,⁵⁸ on an accurate mass TOFMS (Micromass, GCT, U.K.). The formaldehyde–phenylhydrazone derivative is detected at 120 m/z , together with its H loss of similar intensity (119 m/z). The base peak of the spectrum, however, is due to the $C_6H_5NH^+$ fragment at 92 m/z . The peak at 93 m/z is probably due to $C_6H_5NH_2^+$ formed in a rearrangement. Figure 5 also displays the REMPI mass spectrum (244 nm, averaged over 10 transients) obtained from the equivalent on-line derivatization reaction of formaldehyde using the TMA-REMPI-TOFMS setup described above. The soft ionization capability of REMPI provides simple mass spectra with nearly no fragmentation. The mass peak 94 m/z in the REMPI spectrum is suspected to be due to an impurity in the phenylhydrazine reagent (most likely phenol).

Figure 6 shows the REMPI-TOF mass spectra obtained for the TMA and EDU-TMA on-line derivatization of the aldehydes (A) and the amines (B), respectively. The REMPI mass spectrum of the aldehyde derivatives at 246 nm, Figure 6A, displays the $[M - 1]$ and $[M - 2]$ mass peak for the acrolein–phenylhydrazone derivative (145 and 144 m/z). $[M - 1]$ corresponds to the loss of a hydrogen atom and $[M - 2]$ to the loss of two hydrogen atoms. The $[M - 2]$ signal is off-scale. These peaks were also observed on the electron impact (EI) mass spectrum of the derivative (not shown here). Only the $[M - 1]$ peak was observed for the acetaldehyde–phenylhydrazone derivative (133 m/z). The crotonal phenylhydrazone was detected as a $[M + 1]$ peak (161 m/z). Additionally, only a very weak $[M - 2]$ peak is visible (158 m/z). $[M + 1]$ adduct peaks commonly are visible in chemical ionization mass spectra, also to a lesser extent in EI mass spectra obtained from ion trap mass spectrometers, when some unintentional chemical ionization can occur. However, $[M + 1]$ peaks do not occur in photoionization TOF mass spectra under the chosen conditions (i.e., a pressure of 10^{-4} mbar in the ion source, avoiding protonation via ion–molecular reaction). The strong $[M + 1]$ peak for crotonal phenylhydrazone, thus, is unexpected and indicates that most likely a side reaction has occurred during the derivatization. Because phenylhydrazine, like hydrazine, is a reducing agent, one possible explanation is the hydrogenation of the double bond of crotonal (either before or after the derivatization). The resulting derivative would be butanal phenylhydrazone (162 m/z), which may be detected as an $[M - 1]$ peak (161 m/z), as found for the acetaldehyde and acrolein derivatives. However, it remains unexplained at the current level of research why the same hydrogenation does not take place for acrolein. If we summarize the result for the aldehydes, it can be stated that only formaldehyde can be detected at the unfragmented derivative mass $[M]$ of 120 m/z . The other aldehyde derivatives, however, were identifiable at either the respective $[M - 1]$ or $[M - 2]$ peak ($[M + 1]$ for crotonal). The molecular ion $[M]$ for acetaldehyde, acrolein, and the crotonal phenylhydrazone were not observed at the applied REMPI wavelength of 246 nm. An EI mass spectrum of the acrolein phenylhydrazone product, however, clearly shows the

molecular ion mass peak 146 in Figure 6A is due to the ^{13}C isotope peak for the $[M - 1]$ ion, not the molecular ion). This indicates that for higher aldehyde–phenylhydrazone derivatives, a photoinduced fragmentation is observable, which is, however, not a problem for the analytical application because the mass spectra are still very soft; i.e., only one (or two) peak(s) dominate the spectra. Phenylhydrazine itself was not observed at the used REMPI wavelength. Note, with other REMPI wavelengths or power densities, different relative sensitivities or photoinduced fragmentation activities for the different aldehydes may be observed.

The REMPI mass spectrum (240 nm) of the amine derivatives is shown in Figure 6B. Benzaldehyde–methylimine, –ethylimine, –propylimine, and –butylimine display two mass peaks of similar intensities, $[M]$ and $[M - 1]$, corresponding to the molecular ion and the hydrogen atom loss. This trend was also observed on the EI mass spectra. In addition, the derivatizing reagent, benzaldehyde, is also observed in the mass spectrum (Figure 6B). The signal $[M] m/z$ 106 is off-scale. The $[M + 1] m/z$ 107 peak is, therefore, the ^{13}C isotope peak. The presence of m/z 106 confirms that the reagent is present in excess during the on-line reaction. A mass gate is required during on-line derivatization when an excessive quantity of reagent, such as benzaldehyde, is present to deflect these ions from the detector. The mass gate will prevent “blinding” of the detector to masses occurring after 106 mass units (the mass of benzaldehyde).

To summarize, the REMPI detectability of the amine derivatives is as successful as for the aldehydes: all analytes were detected as $[M]$ and $[M - 1]$ with no further fragments.

Detection limits were determined and are summarized in Table 1. They were calculated using the combined method of Heger et al.¹⁶ and Williams et al.,⁵⁹ using a S/N of 2 and an average of 10 mass spectra. These results demonstrate the potential of this technique in future applications. The calculated detection limits for the analytes are markedly below permissible exposure limits set by the Occupational Safety and Health Administration (OSHA).²

The EDU, constructed specifically for use with the on-line REMPI-TOFMS, allows for the use of a multichannel silicone rubber trap for preconcentration. Lower detection limits were achieved with this setup, since more PDMS is available for preconcentration. This is confirmed by the results obtained for the benzaldehyde–methylimine, –ethylimine, –propylimine, and –butylimine derivatives using the EDU-TMA and the TMA, respectively (see Table 1). In addition, off-line sampling together with a portable pump is also made possible, since the MCSRT trap is easily removed from the EDU.

CONCLUSIONS

The work presented here, on one hand, demonstrates that on-line derivatization concepts can be used to expand the unique on-line analytical properties of the resonance-enhanced multiphoton ionization time-of-flight mass spectrometer to aliphatic compound classes. In detail, a method for on-line in situ derivatization of alkylamines with benzaldehyde and alkyl aldehydes with phenylhydrazine followed by thermal desorption and detection by the REMPI-TOFMS was successfully tested. The detection limits obtained for all analytes, for which concentration standards were made, are below the permissible exposure limits set by OSHA. Formaldehyde, which is not easily detected by mass spectrometry,

(57) Pallix, J. B.; Schuhle, U.; Becker, C. H.; Huestis, D. L. *Anal. Chem.* **1989**, *61*, 805–811.

(58) Furniss, B. S.; Hannaford, A. J.; Smith, P. W. G.; Tatchell, A. R. *Vogel's Textbook of Practical Organic Chemistry*, 5th ed.; Longman Scientific and Technical: Essex, England, 1989; p 1258.

(59) Williams, B. A.; Tanada, T. N.; Cool, T. A. In *Twenty-Fourth Symposium (International) on Combustion*; The Combustion Institute: Pittsburgh, 1992; p 1587–1596.

can be detected as the phenylhydrazone derivative. In the future, formaldehyde gas standards of known concentration must be prepared to determine formaldehyde's detection limit for the on-line reaction.

The potential analytical impact of the concept presented here should not be underestimated. Through coupling of suitable photolabels to nonaromatic compounds, a larger variety of compound classes can now be considered for REMPI-TOFMS detection, including compounds such as sugars, sulfur compounds, organic acids, or alcohols. Fast screening methods, for example, for environmental samples, biological samples, or medical applications, may be developed on this basis.



UNIVERSITEIT VAN PRETORIA
UNIVERSITY OF PRETORIA
YUNIBESITHI YA PRETORIA

ACKNOWLEDGMENT

We thank Professor Ben Burger for the supply of one of his thermal modulator systems and the useful discussions regarding its application. Financial support from the National Research Foundations in South Africa (NRF), the GSF Research Center, the Federal German Ministry of Education and Scientific Research (BMBF, WTZ program), and the German Environmental Foundation (DBU-Deutsche Bundesstiftung Umwelt) is acknowledged.

Received for review August 11, 2004. Accepted October 21, 2004.

AC040151A